The hydrogen atom QUANTUM wave function or probability density graphs match exactly with the shapes of the CMB, black hole physics, star formation rates and many other MACRO phenomenon graphs.

Harsimran Singh Dhaliwal

Abstract:

Graphs of the hydrogen atom's wave function or probability density were compared to observational data of cosmic macro phenomena such as photons orbits around black holes, black hole masses, LIGO detected gravitational waves, the CMB, quasars distributions , galaxy rotation curves, galaxy distributions, supernova events and numerous other cosmic graphs. There is an identical symmetry between graphs of cosmic macro phenomena and the graphs of the hydrogen wave function or its probability density. The hydrogen atom's wave function or probability density describes macro phenomena, or macro phenomena describes hydrogen atom's wave function or probability density, or both.

Methods:

The hydrogen atom's wave function or probability density was super imposed upon observational graphs of macro phenomena. The hydrogen graphs were enlarged with the height and width ratios locked until its shape matched the observational graph of macro phenomena. In other instances, the hydrogen graph was stretched on the X axis and or Y axis to account for differing scales or units of related parameters between the two graphs. Rarely, a macro phenomenon graph may have been flipped on the x and or y axis, which may be due to a related parameter. In a few instances, a graph may have been rotated slightly. The hydrogen graph in each example had its opacity lowered until both graphs were easily visible. For each comparison, the Hydrogen Graph will be shown first, then the graph of the macro phenomena, than the two graphs will be shown with the hydrogen graph super imposed on top. Below are a few examples of how the super imposed graphs will appear:

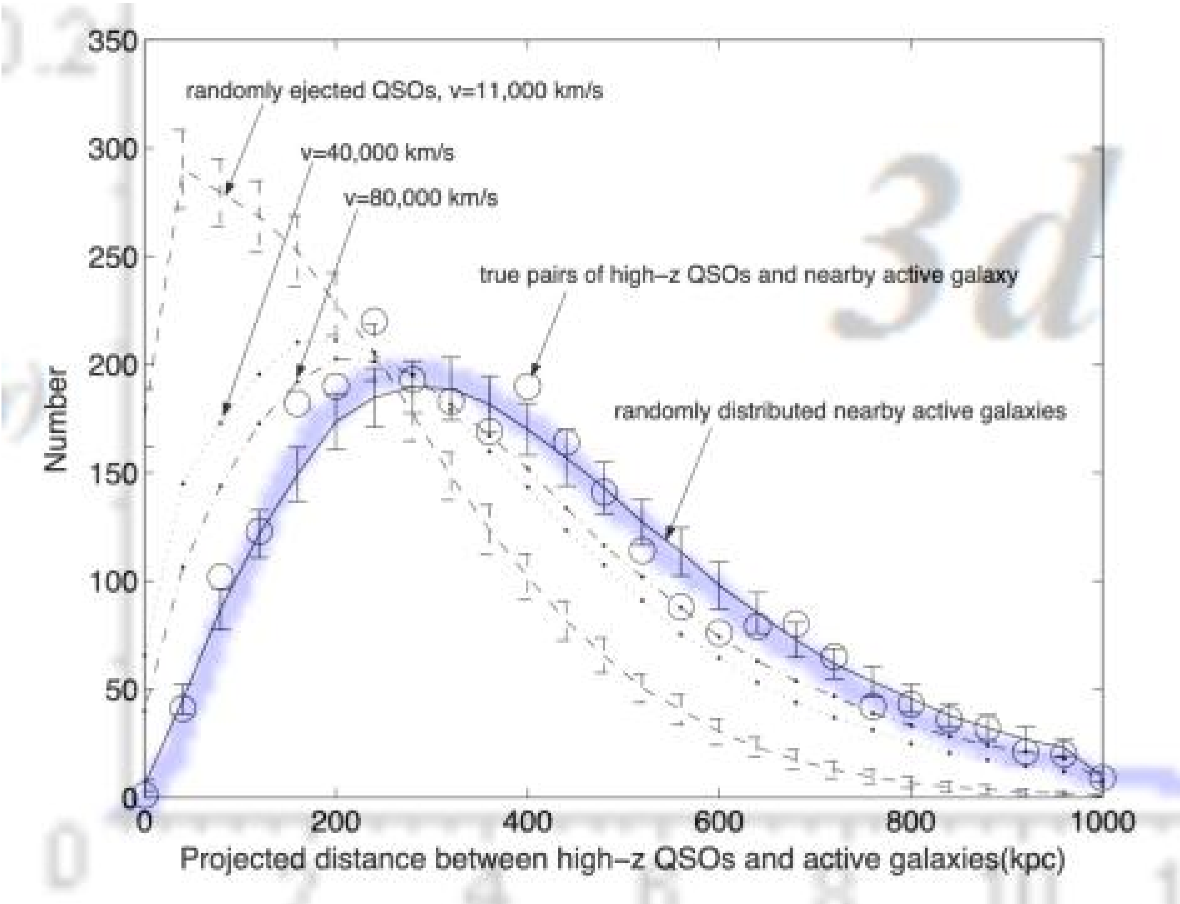

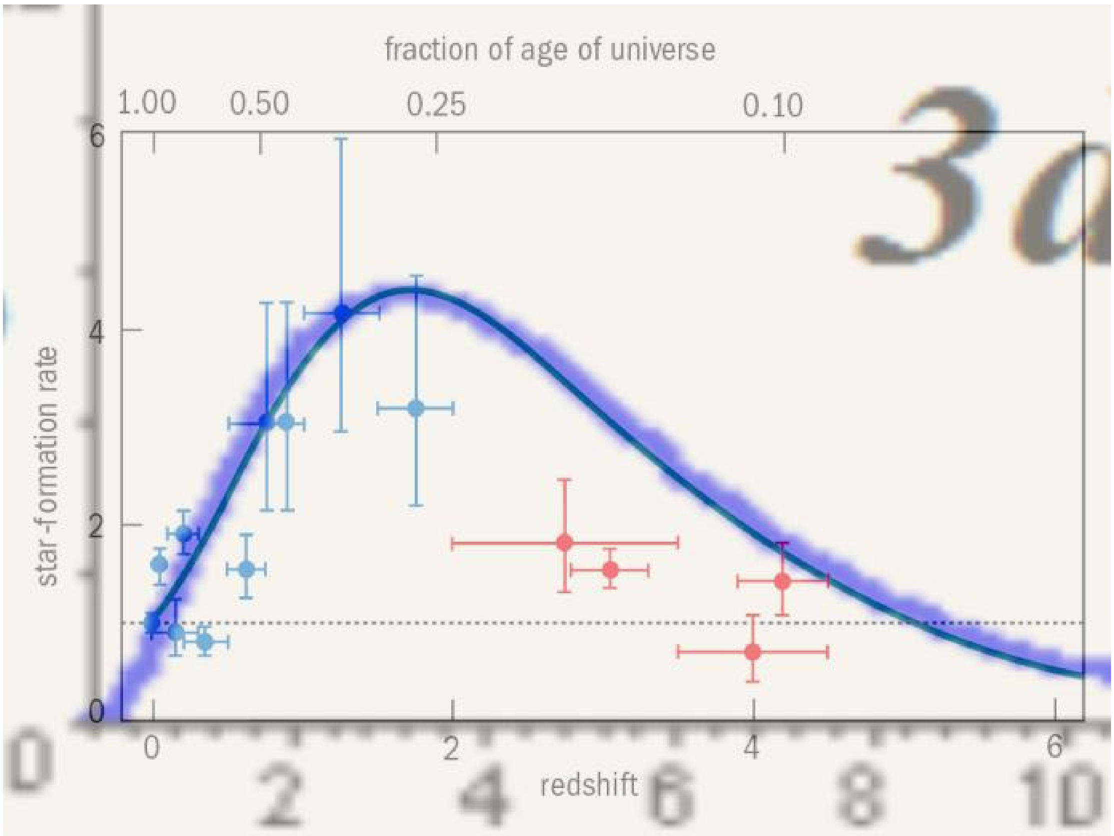
fraction of age of universe
1.00
0.50
0.25
0.10
3d
star-formation rate
redshift
0
2
4
6
8
10

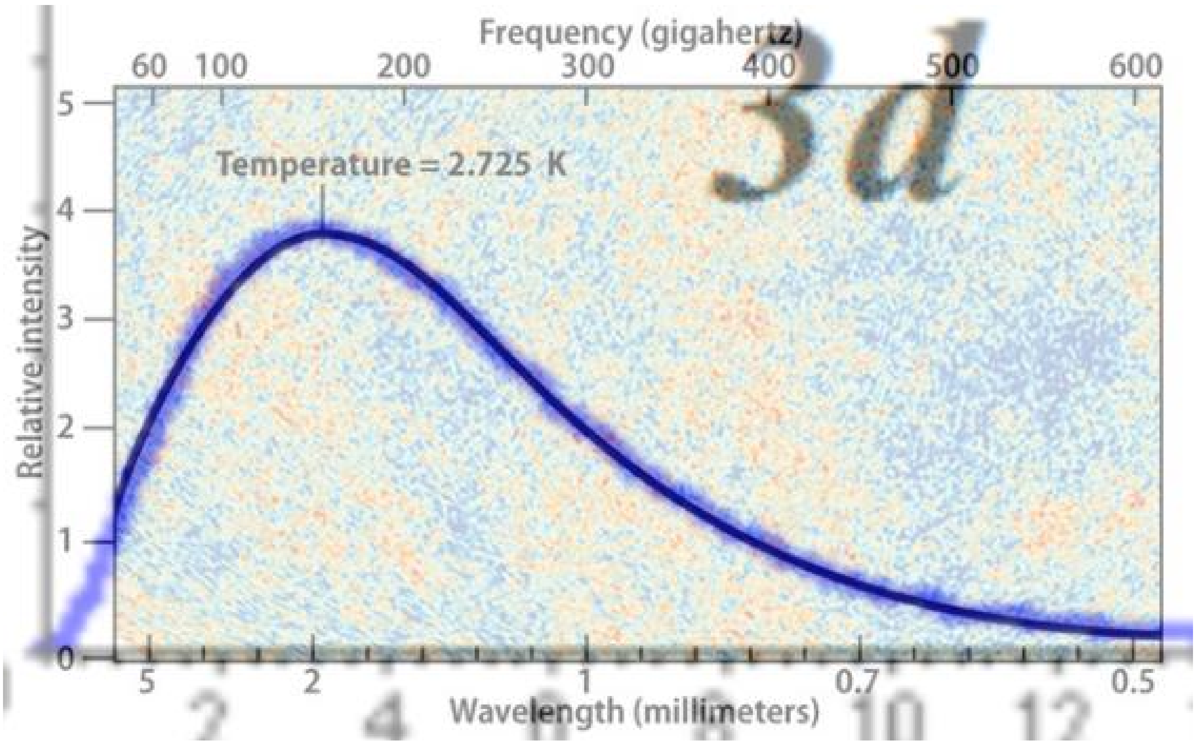
Frequency (gigahertz)
60
100
200
300
400
500
600
3d
Temperature = 2.725 K
Relative intensity
Wavelength (millimeters)
5
2
1
0.7
0.5

Each example will be shown in the following format:
URL link to graph shown
Title of paper and or figure name for the graph

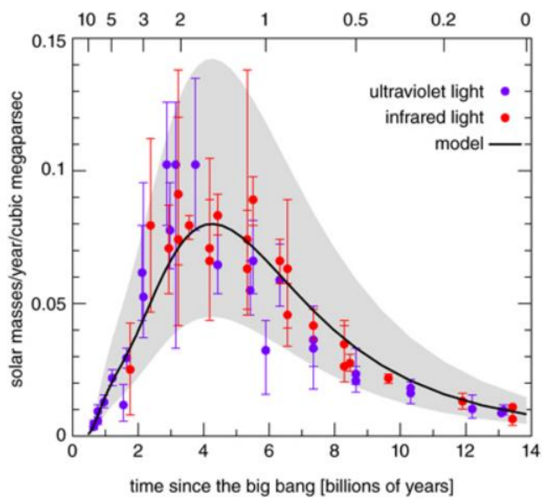

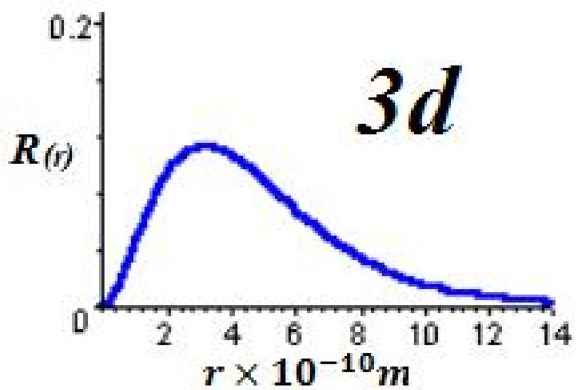

Hydrogen graph name

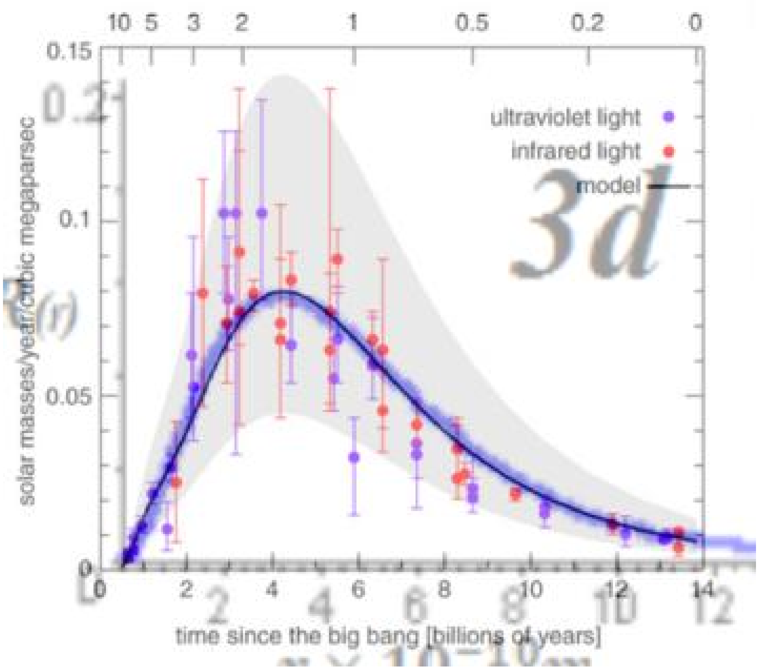

Super imposed graph

Hydrogen graphs used in analysis:

(a) The electronic radial wave function R(r) for a hydrogen atom. (b) The probability density for finding the electrons í µí± 2 í µí± (í µí±) 2 for a hydrogen atom (Adopted from ref. [http://staff.mbi-berlin.de/hertel/physik3/chapter8/8.3html/01.htm).](http://staff.mbi-berlin.de/hertel/physik3/chapter8/8.3html/01.htm)

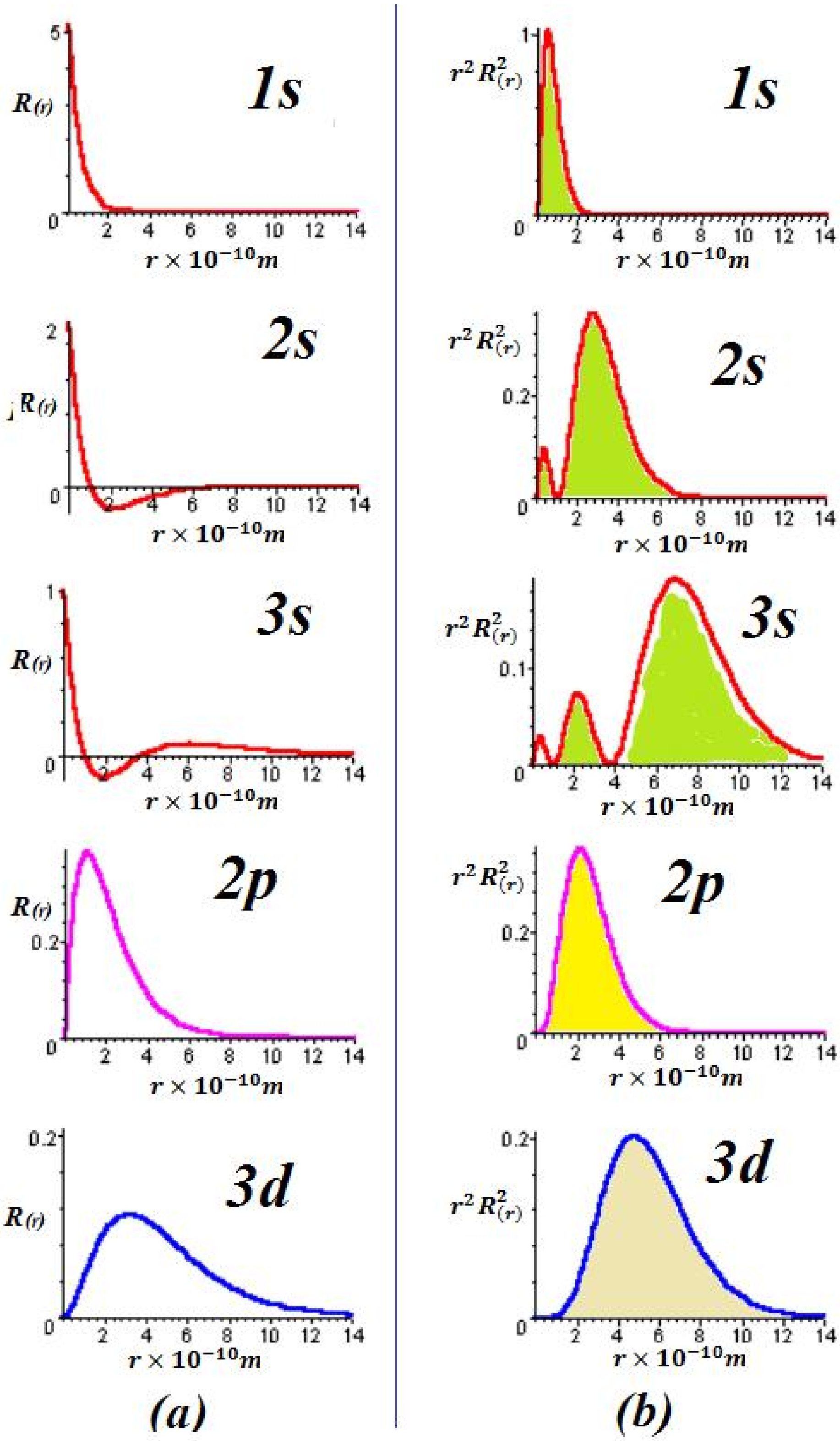

Results:

https://www.scirp.org/html/11-7501495_40053.htm

Gravitational Force between the Black Hole & Light Particle in AGN

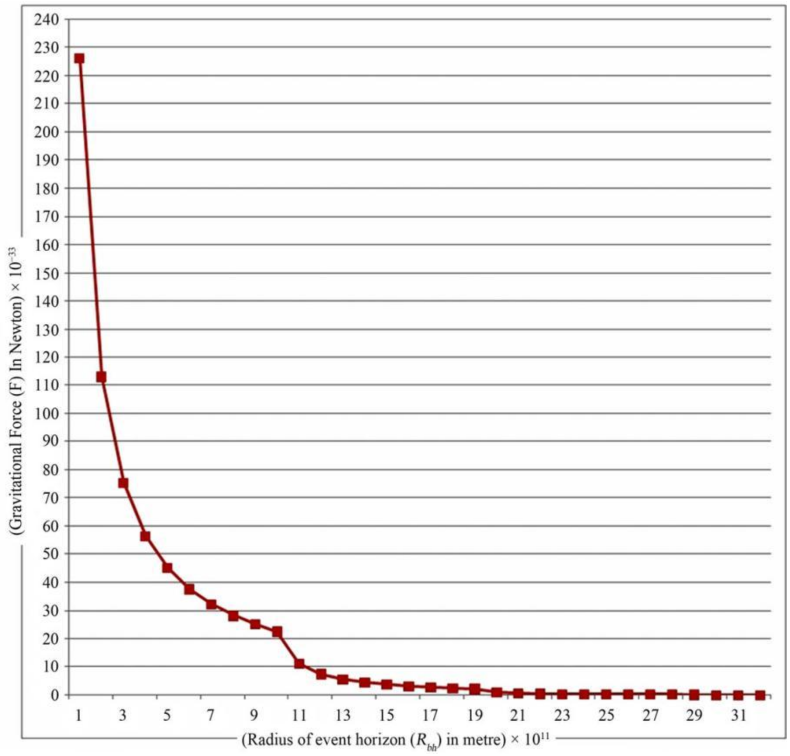

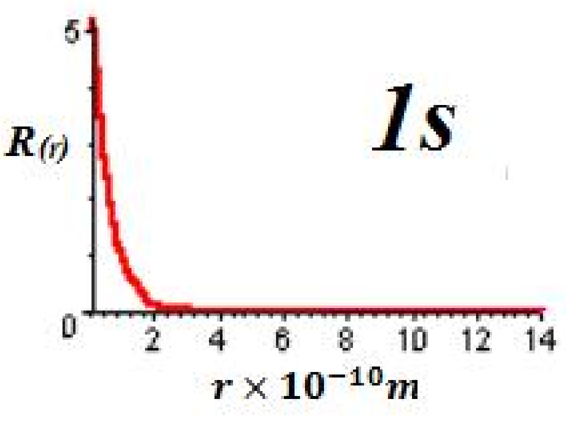

Hydrogen 1s Wave Function

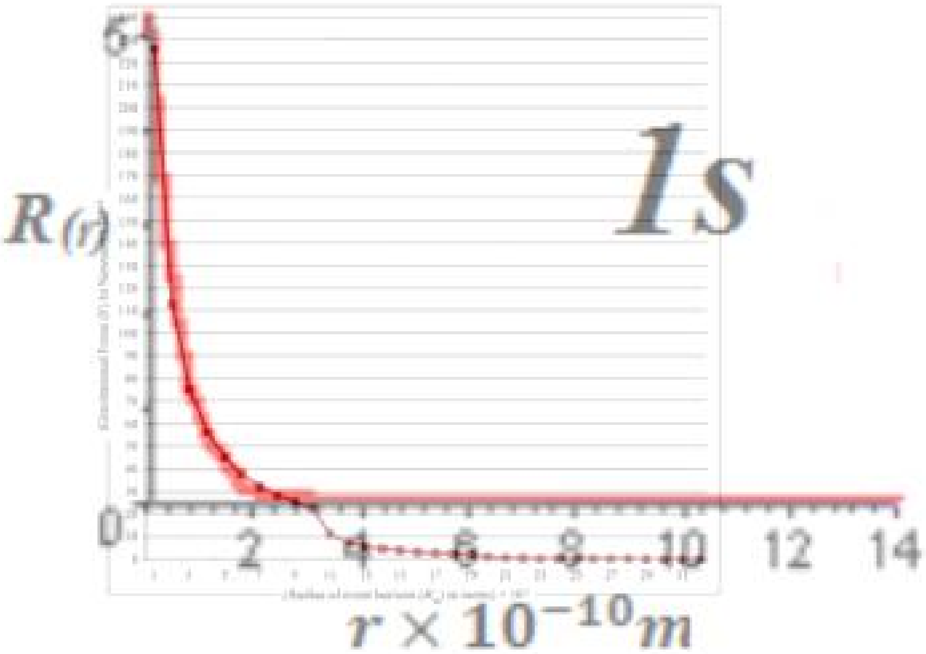

Super imposed graphs

https://sci.esa.int/web/planck/-/51605-planck-s-gravitational-lensing-power-spectrum

Gravitational lensing power spectrum obtained from Planck data

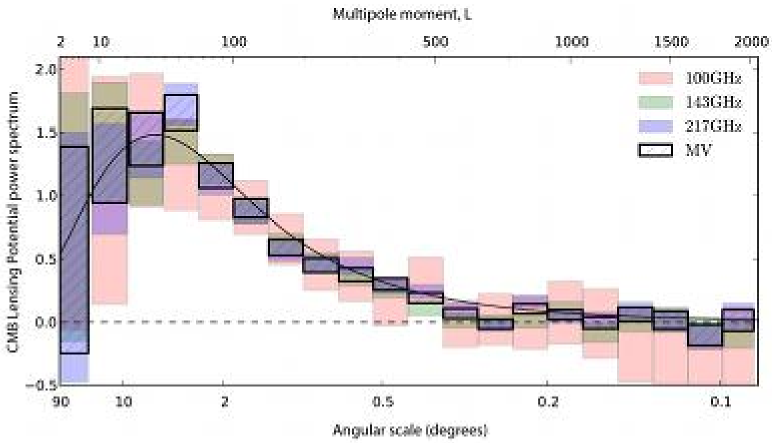

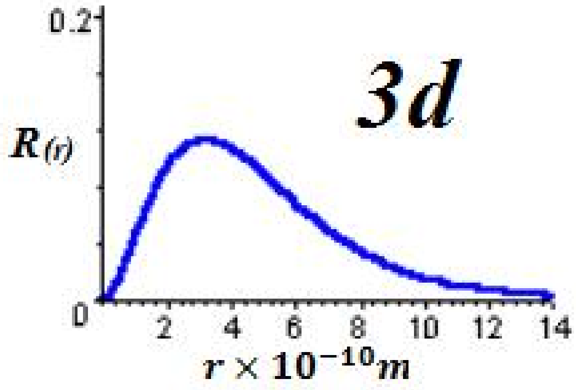

Hydrogen 3d wave function

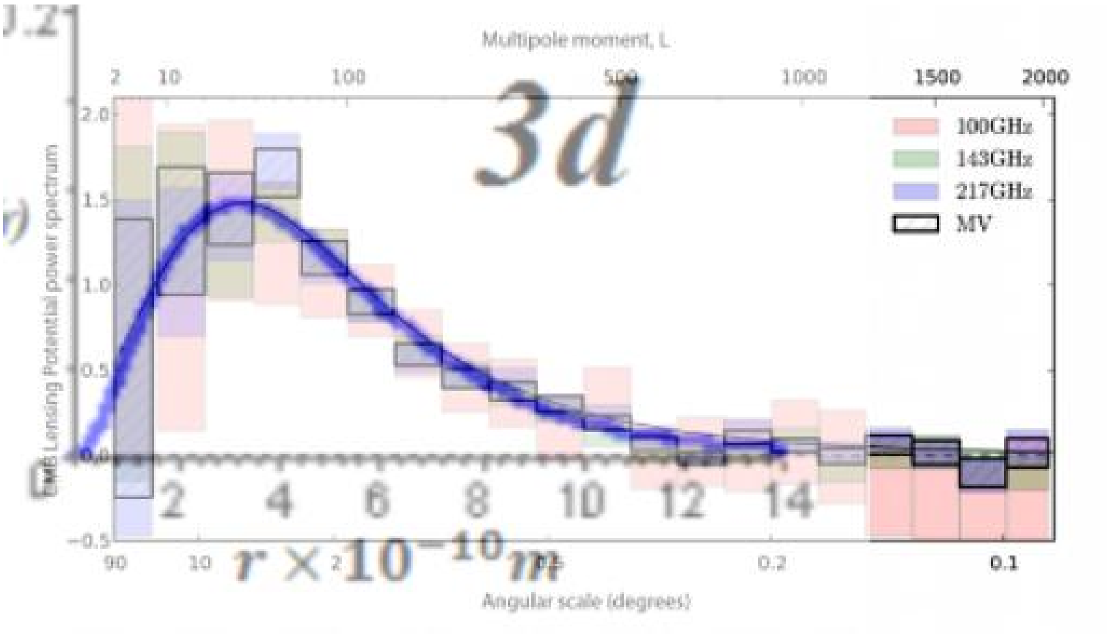

Super imposed graphs

https://iopscience.iop.org/article/10.1088/0004-637X/741/2/103

THE MASS DISTRIBUTION OF STELLAR-MASS BLACK HOLES

Figure 10. Marginalized distributions of the mean mass, ⟨*M*⟩ (solid histogram), and standard deviation of the mass, σ_M (dashed histogram), for the log-normal model in Section 3.3.4. The distributions are similar to the distributions of μ and σ in the Gaussian model of Section 3.3.3.

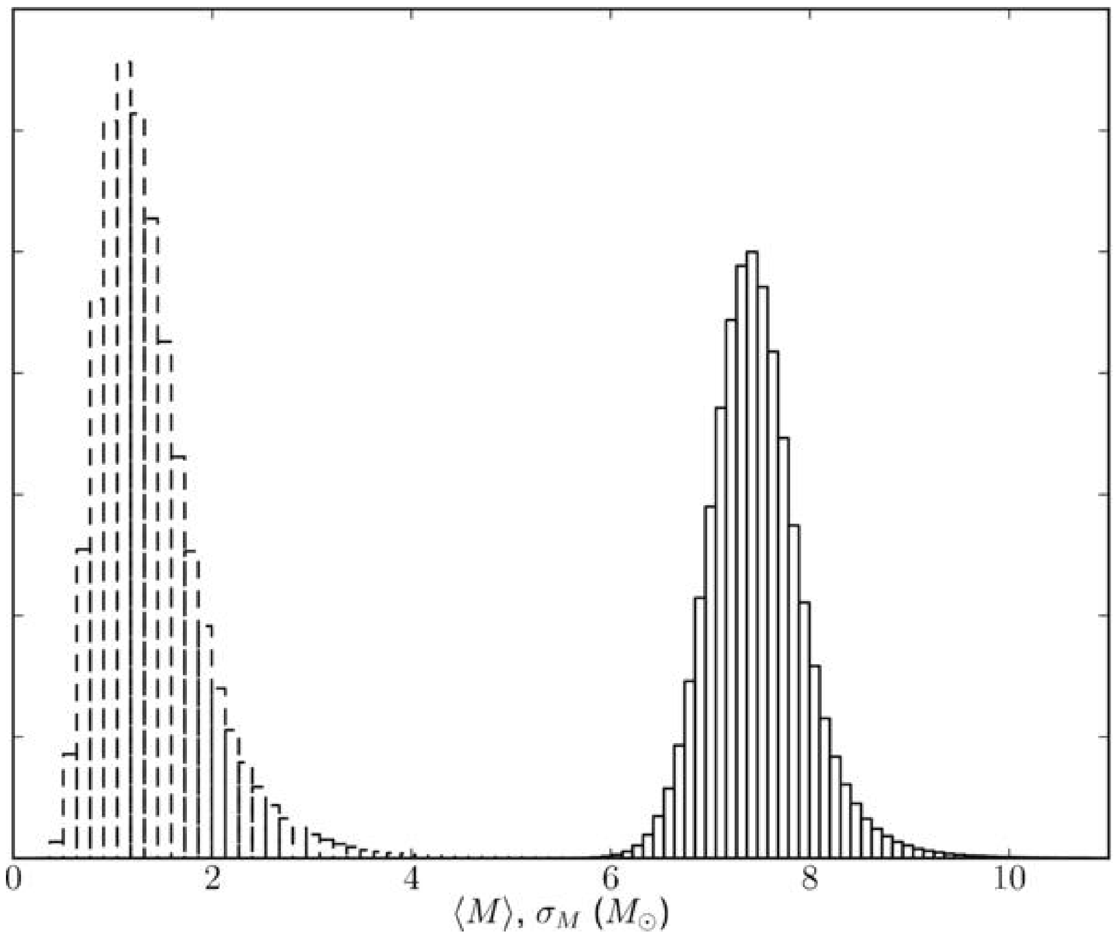

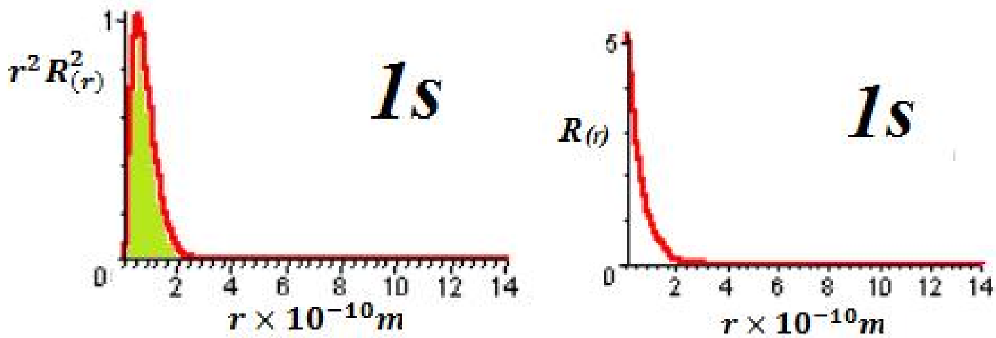

Hydrogen 1s Probability Density and Wave Function

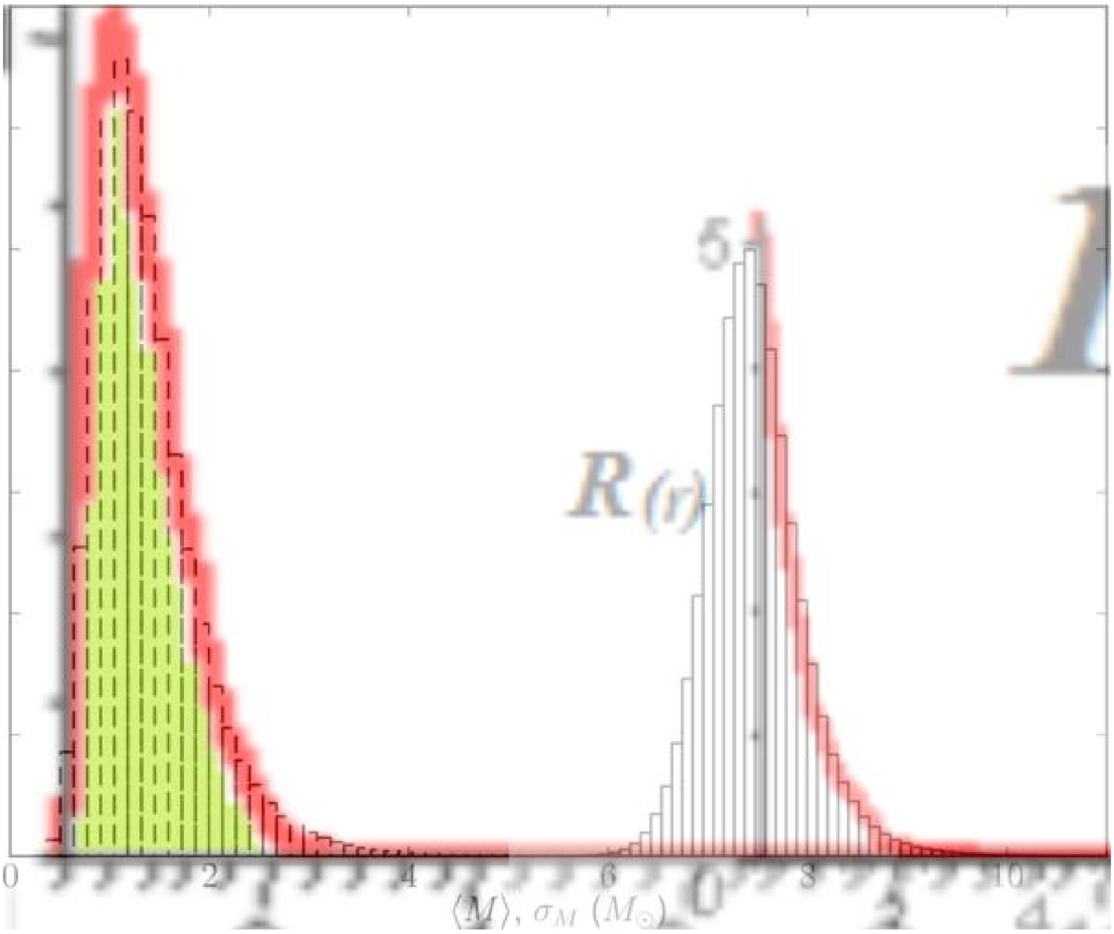

Super imposed graphs

https://iopscience.iop.org/article/10.1088/0004-637X/741/2/103

THE MASS DISTRIBUTION OF STELLAR-MASS BLACK HOLES

Figure 17. Marginalized distributions for the log-normal parameters (Section 3.3.4; $\langle M \rangle$ solid, σ_M dashed) when the high-mass samples are included in the analysis. The changes when the high-mass samples are included (compare to Figure 10) are similar to the changes in the Gaussian distribution: the mean mass moves to higher masses, and the distribution broadens.

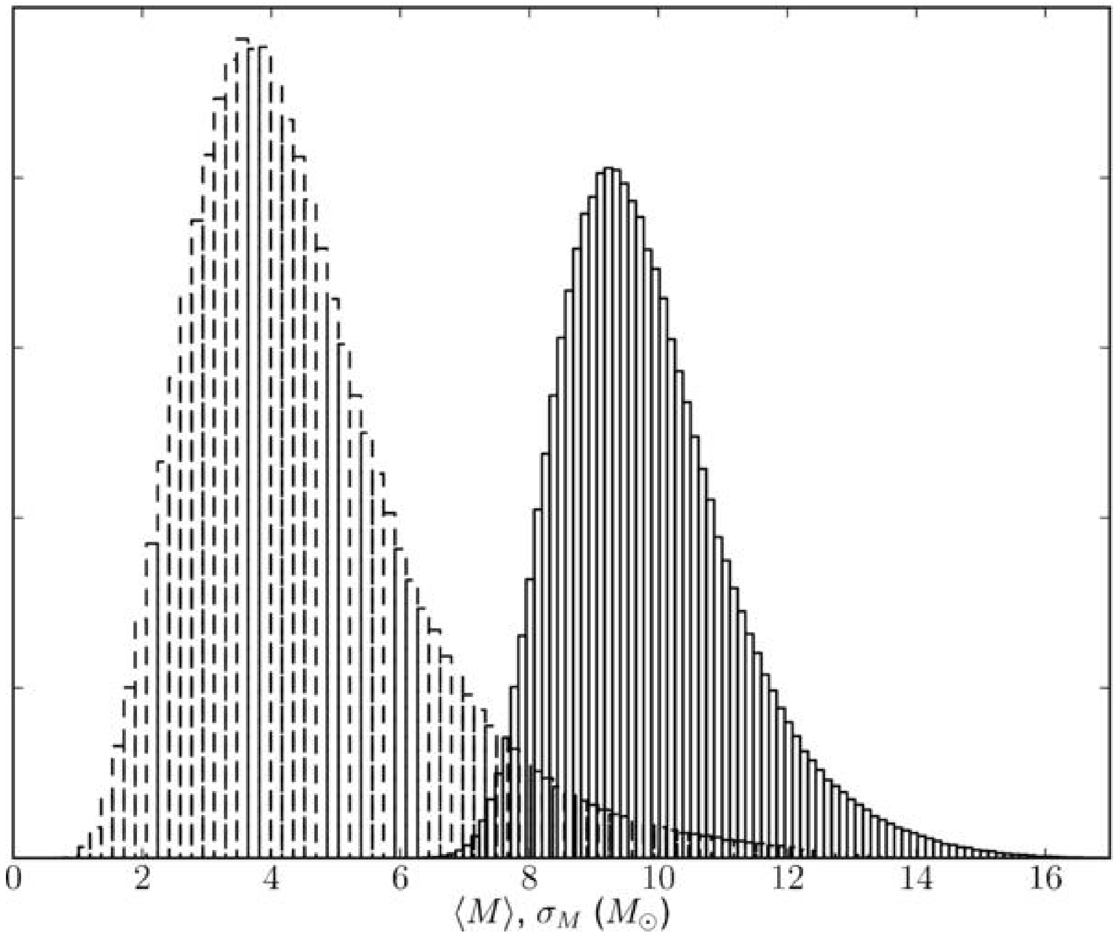

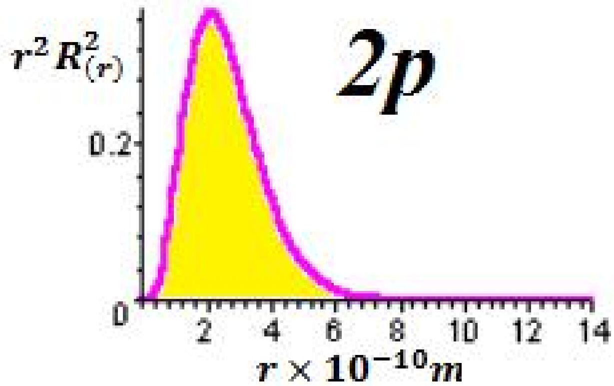

Hydrogen 2p Probability Density

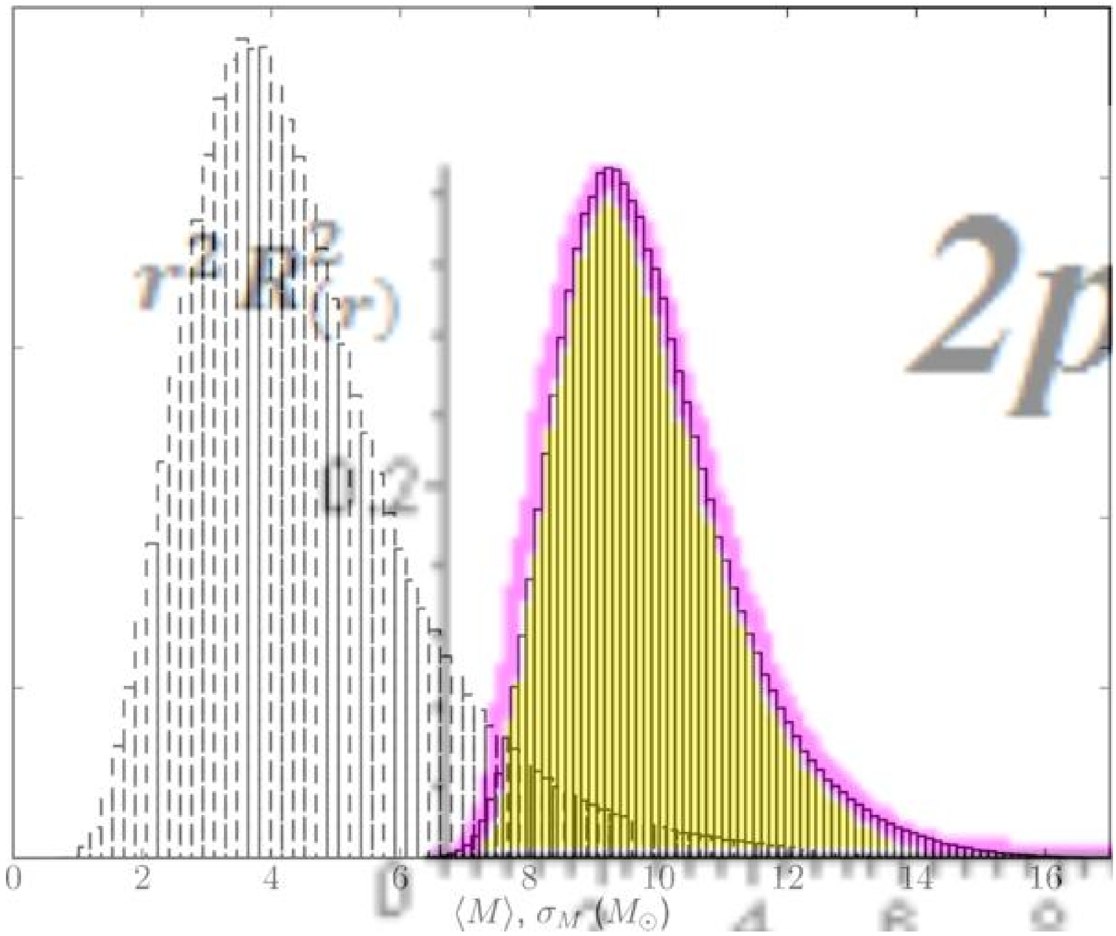

Super imposed graphs

https://iopscience.iop.org/article/10.1088/0004-637X/741/2/103

THE MASS DISTRIBUTION OF STELLAR-MASS BLACK HOLES

Figure 16. Marginalized distributions for the two-Gaussian parameters (Section 3.3.3) when the high-mass samples are included in the analysis. The means (μ_1 and μ_2) are represented by the solid histograms; the standard deviations (σ_1 and σ_2) are represented by the dashed histograms. In stark contrast to Figure 9, there are two well-defined, separated peaks; the low-mass peak reproduces the results from the low-mass samples, while the high-mass peak ($13.5534 \leqslant \mu_2 \leqslant 27.9481$ with 90% confidence; median 20.3839) matches the new high-mass samples. The peak in α near 0.8 is consistent with approximately 15 out of 20 samples belonging to the low-mass peak.

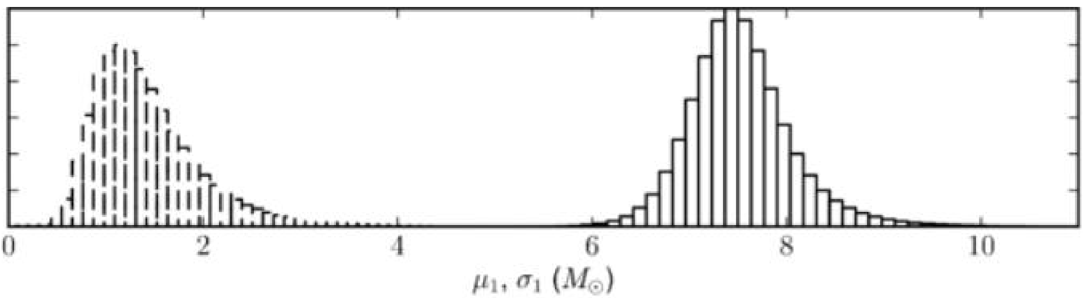

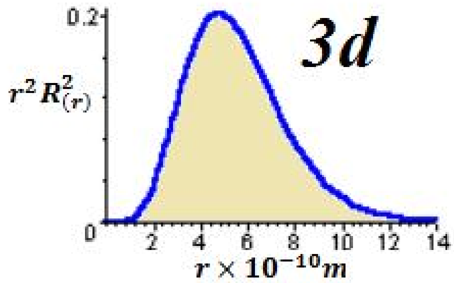

Hydrogen 3d Probability Density

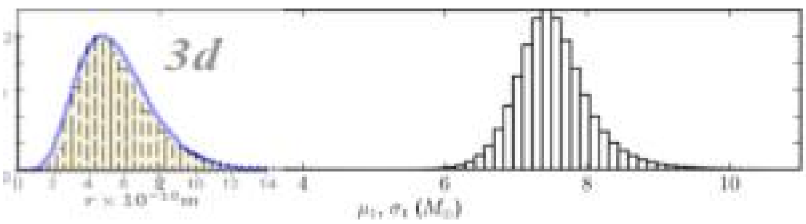

Super imposed graphs

https://iopscience.iop.org/article/10.1088/0004-637X/741/2/103

THE MASS DISTRIBUTION OF STELLAR-MASS BLACK HOLES

Figure 14. Marginalized distributions for the exponential parameters M_{min} (top) and M_0 (bottom) defined in Section 3.3.2 from an analysis including the high-mass systems. The distribution for the scale mass, M_0, has moved to higher masses relative to Figure 6 to fit the tail of the mass distribution; we now have $2.8292 \leqslant M_0 \leqslant 7.9298$ with 90% confidence, with median 4.7003. The distribution for M_{min} is less affected, though it has broadened somewhat toward low masses.

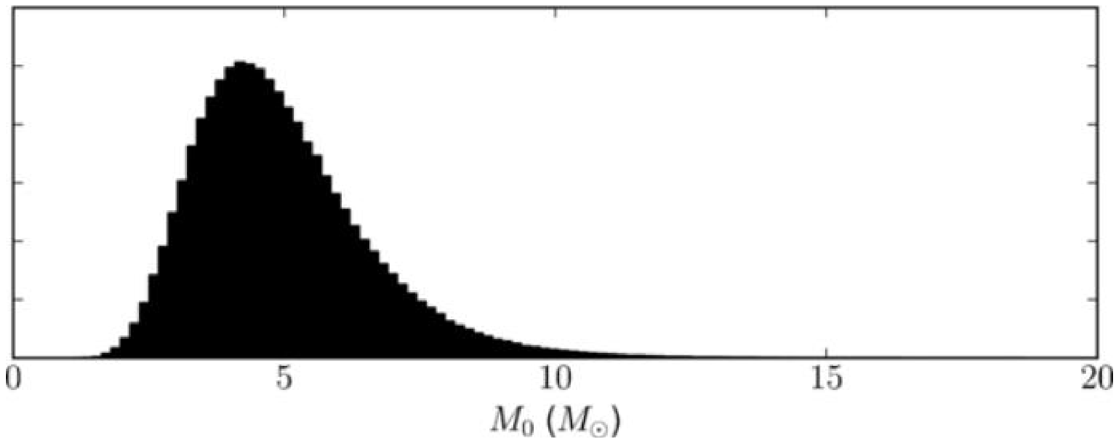

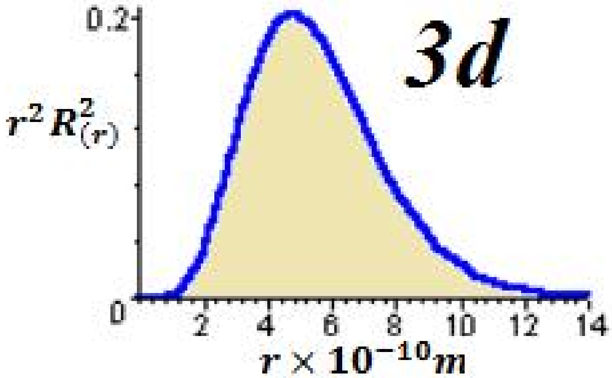

Hydrogen 3d Probability Density

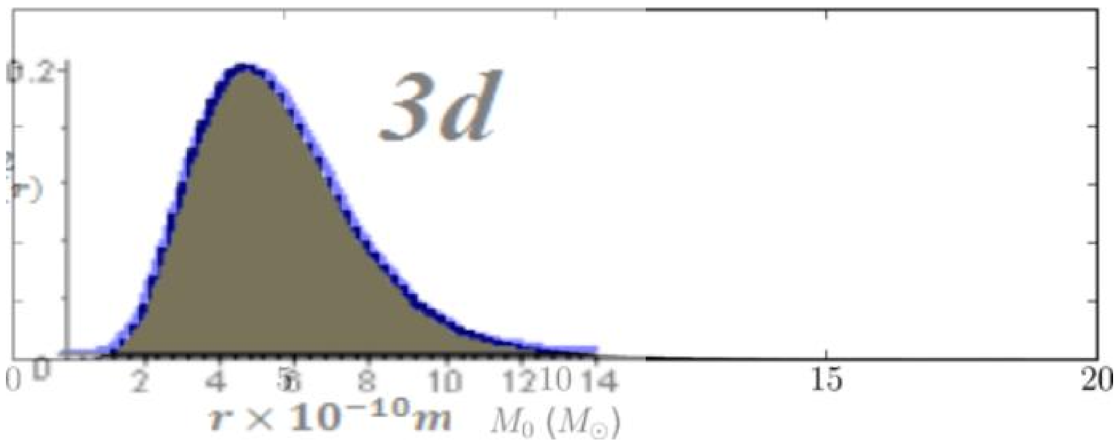

Super imposed graphs

https://physicsworld.com/a/how-are-galaxies-made/

How are galaxies made?

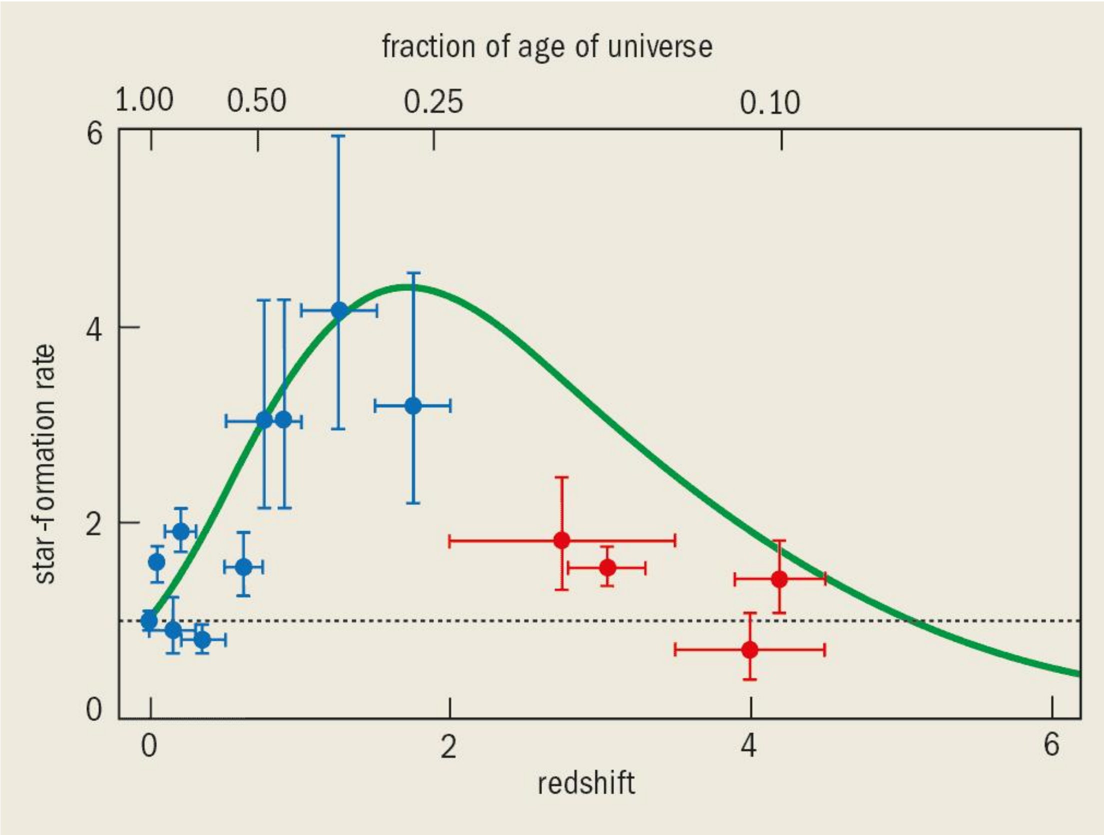

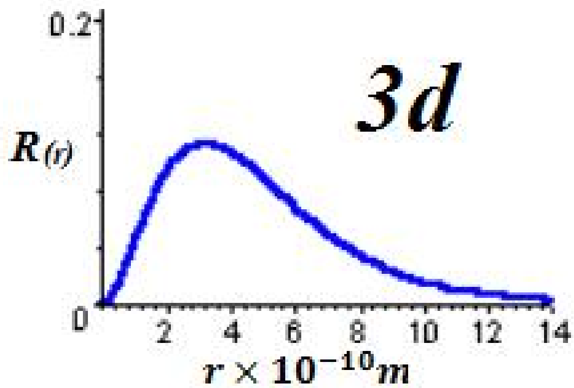

Hydrogen 3d Wave Function

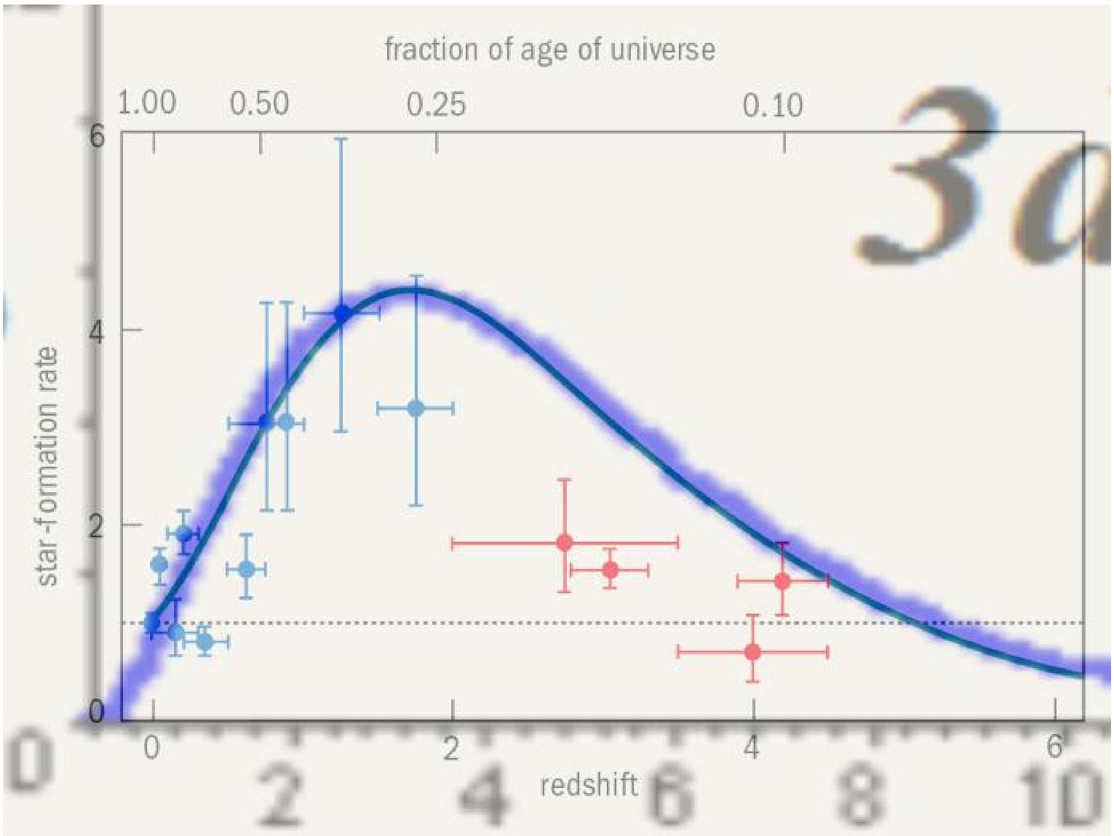

Super imposed graphs

https://ned.ipac.caltech.edu/level5/Sept16/Bertone/Bertone4.html

The rotation curves for the galaxies M31, M101, and M81 (solid lines) obtained by Roberts and Rots in 1973. The rotation curve of the Milky Way Galaxy was included by the authors for comparison. From Ref. [260].

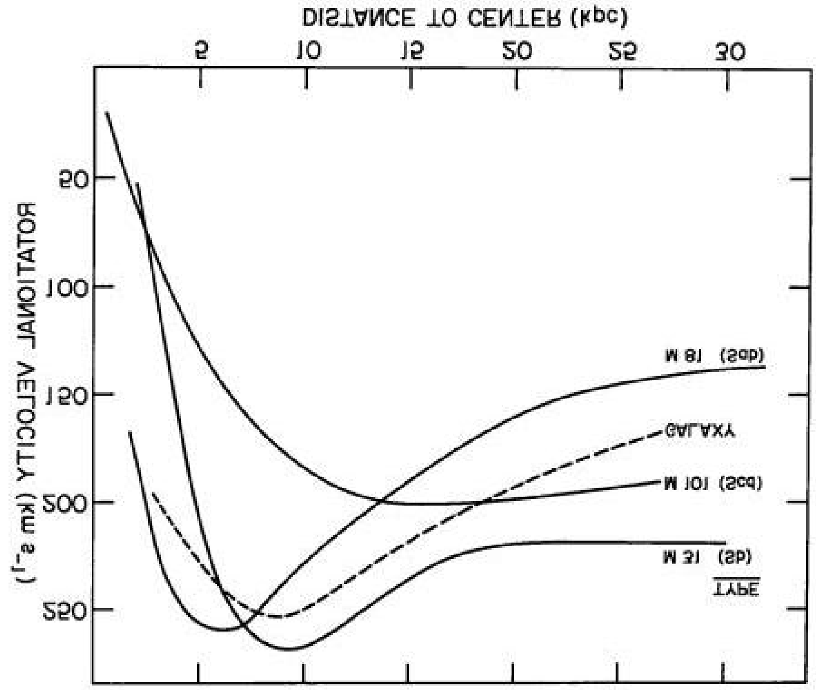

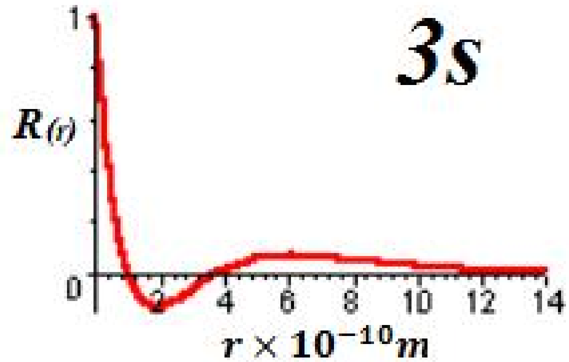

Hydrogen 3s Wave Function

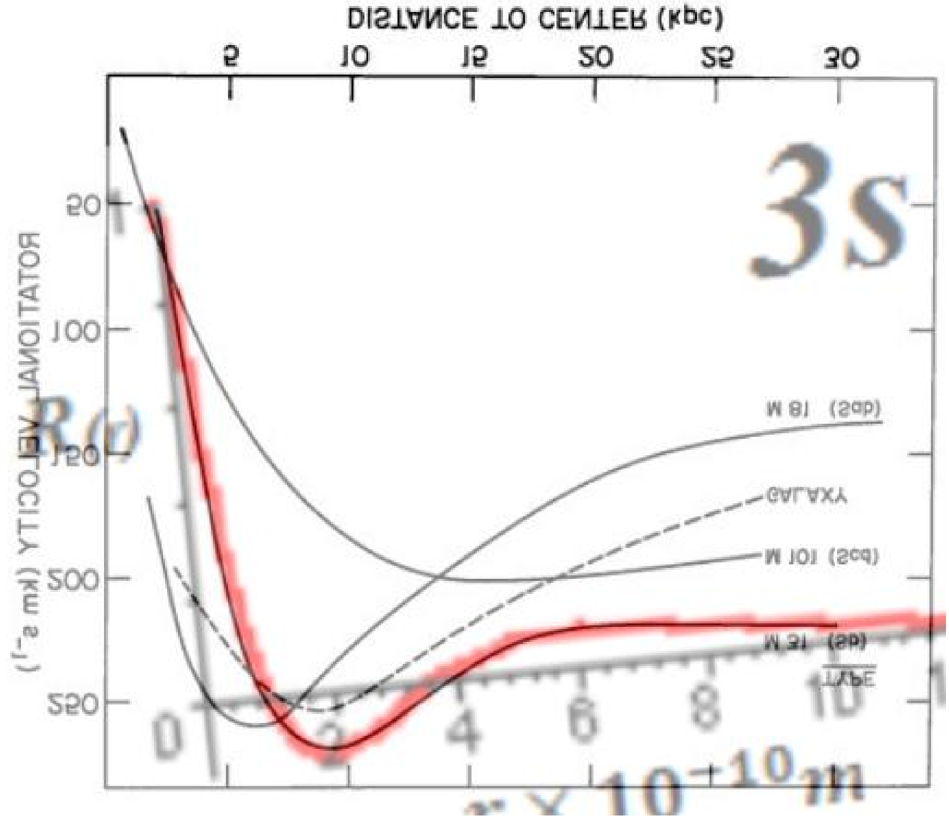

Super imposed graphs

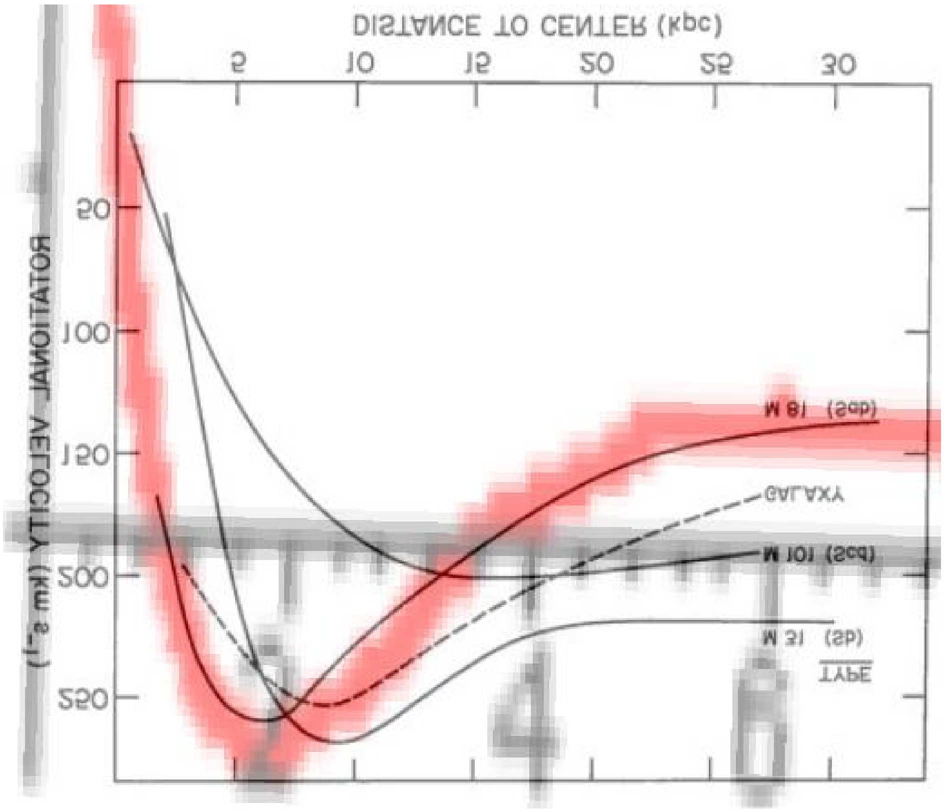

Super imposed graphs

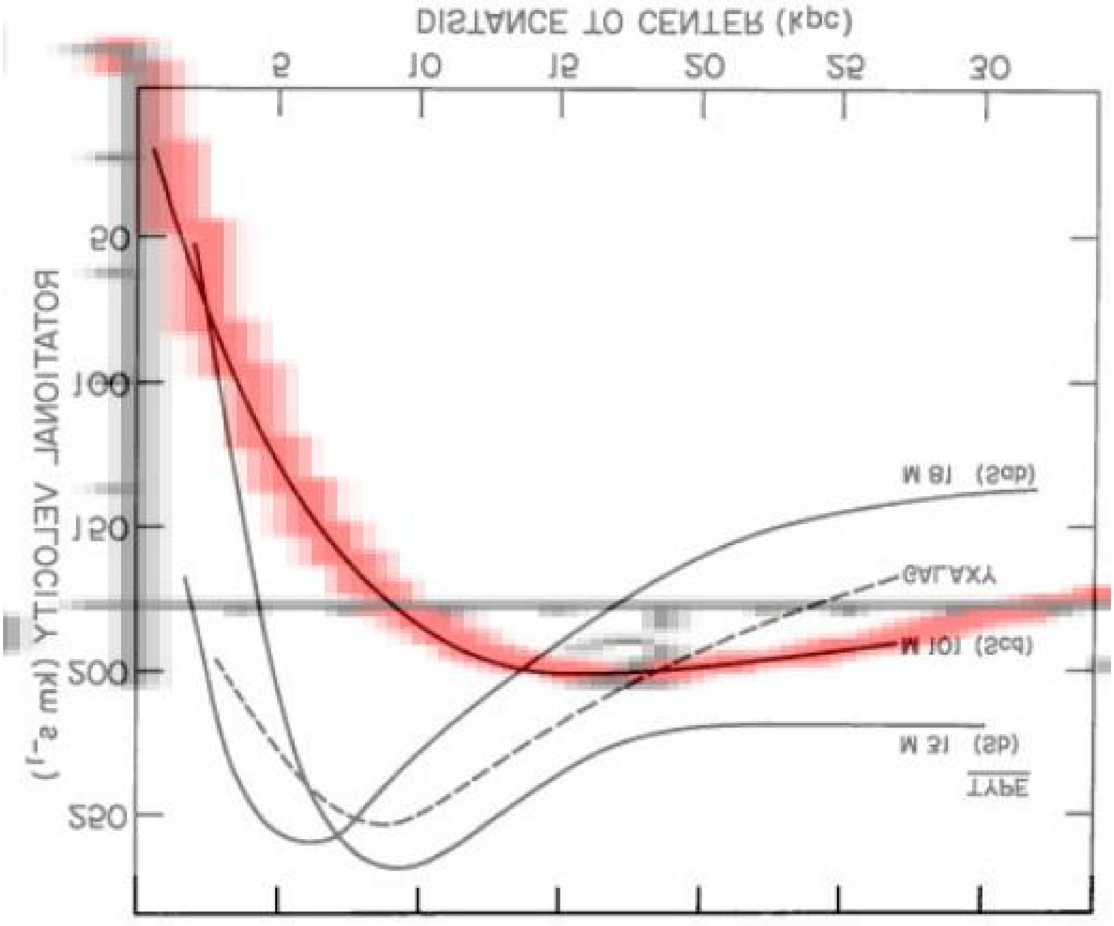

Super imposed graphs

https://www.cosmos.esa.int/web/gaia/iow_20200716
Milky way rotation curve

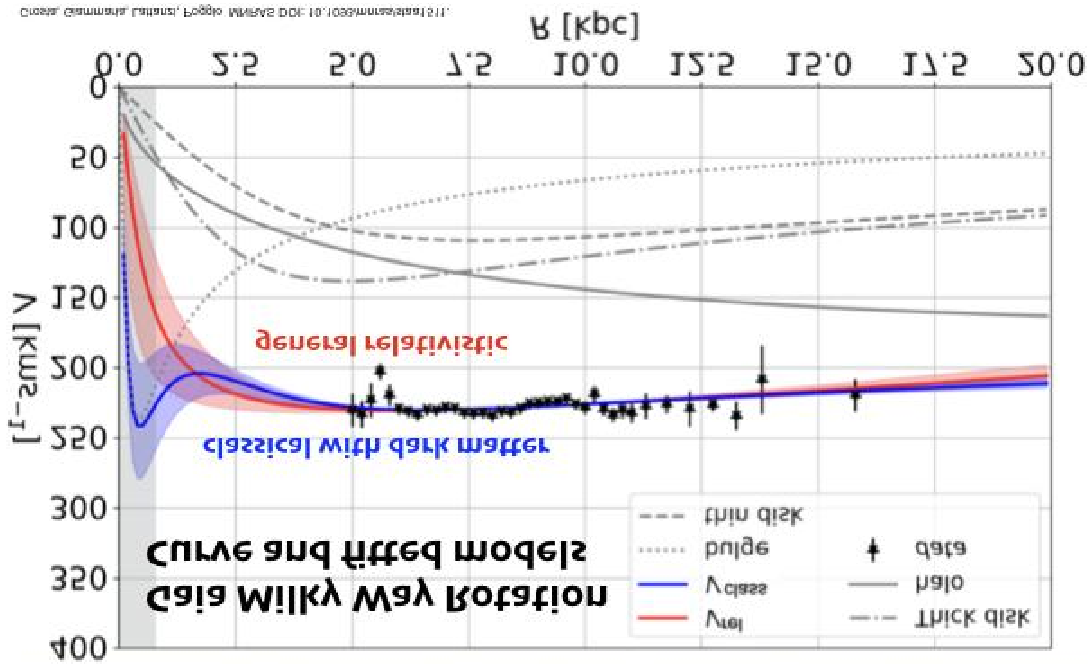

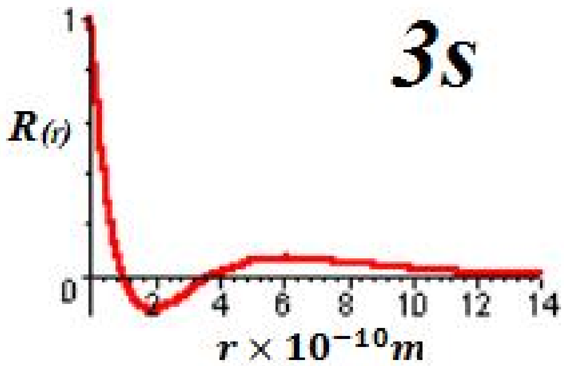

Hydrogen 3s Wave Function

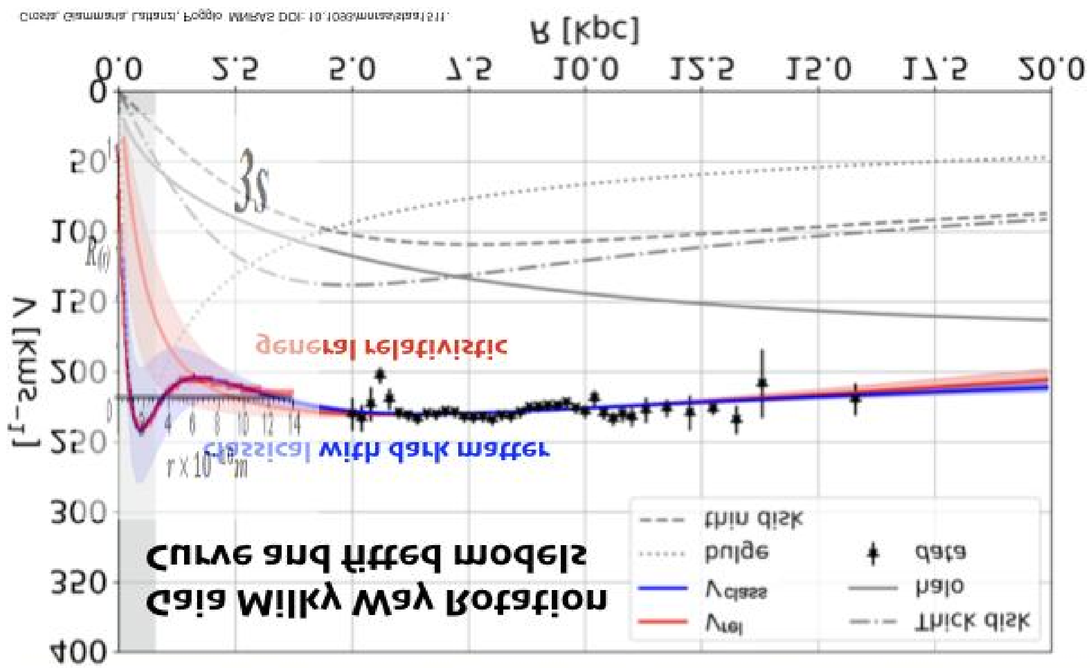

Super imposed graphs

http://roperld.com/science/GeneralRelativityMath.pdf

General Relativity Mathematics

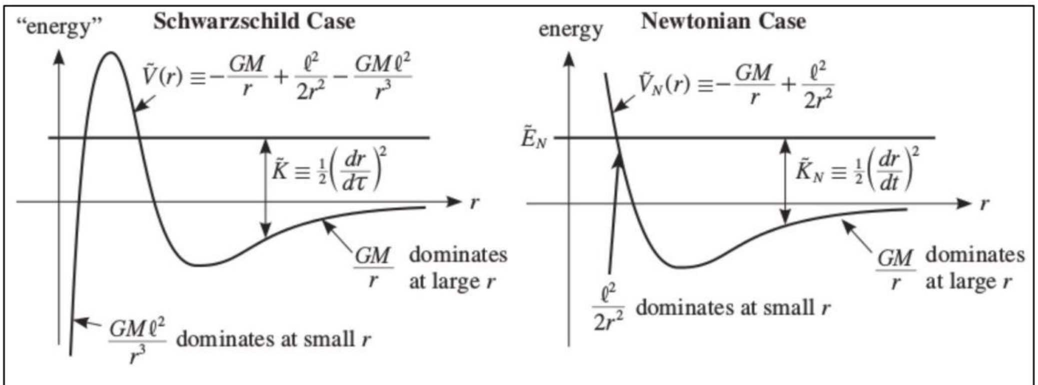

FIG. 10.1 These graphs show the effective potential-energy-per-unit-mass functions governing radial motion in the Schwarzschild case (left) and Newtonian case (right).

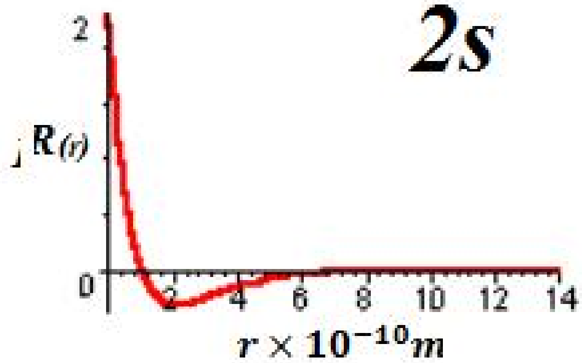

Hydrogen 2s Wave Function

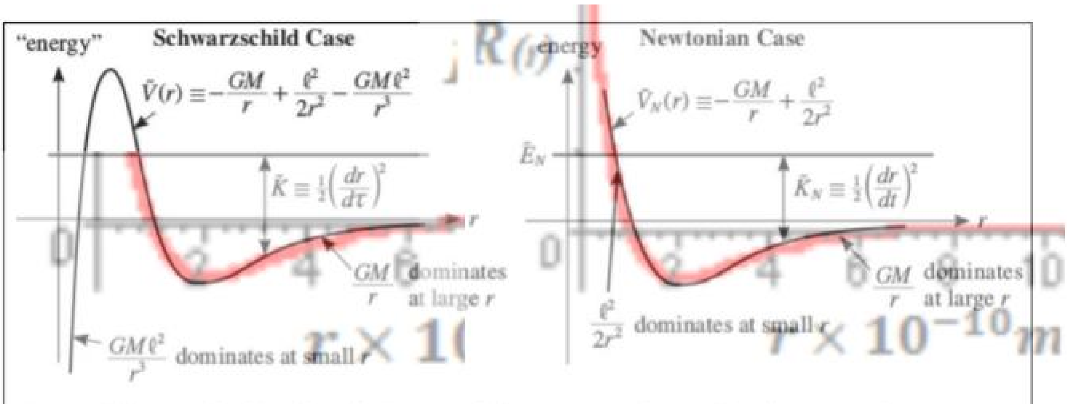

FIG. 10.1 These graphs show the effective potential-energy-per-unit-mass functions governing radial motion in the Schwarzschild case (left) and Newtonian case (right).

Super imposed graphs

https://www.researchgate.net/figure/Probability-distribution-of-galaxy-clusters-in-various-red-shift-ranges_fig3_363402503

Probability distribution of galaxy clusters in various red-shift ranges

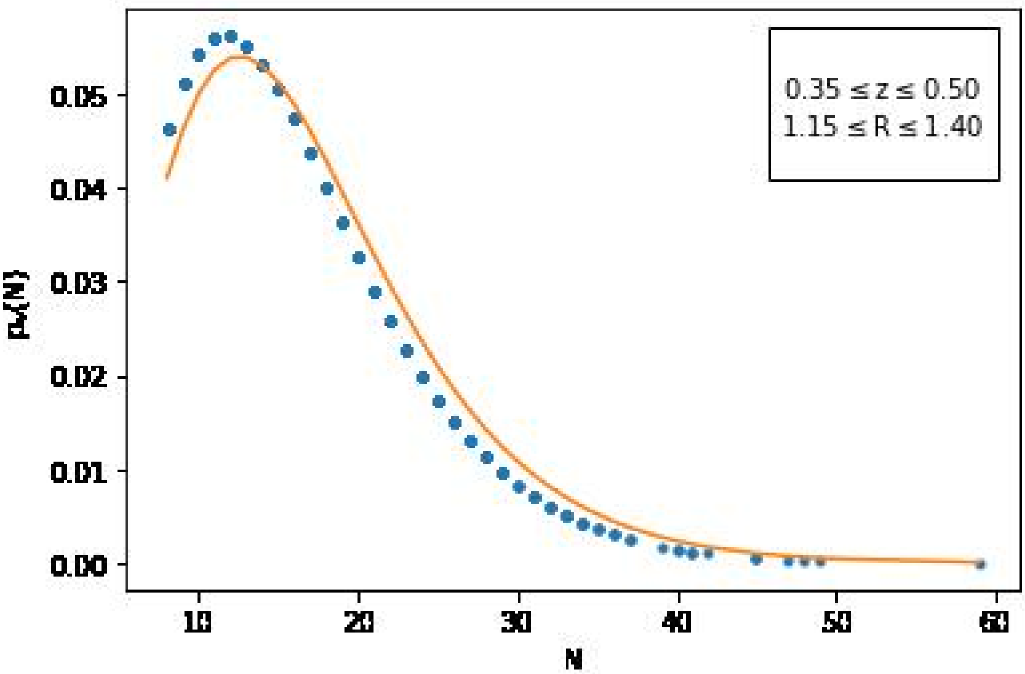

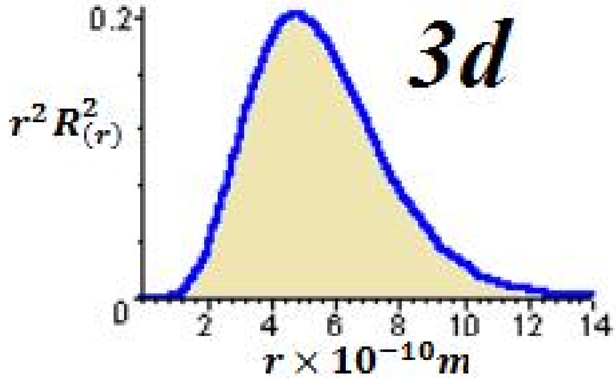

Hydrogen 3d Probability Density

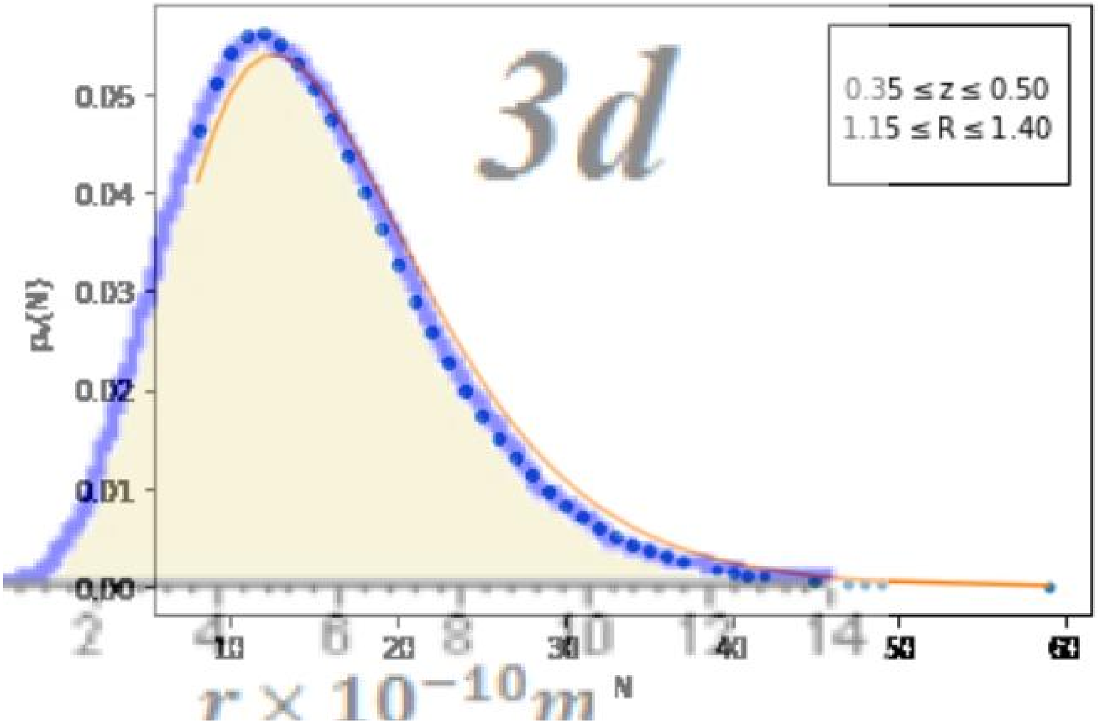

Super imposed graphs

https://en.wikipedia.org/wiki/Gravitational_microlensing
A typical microlensing light curve.

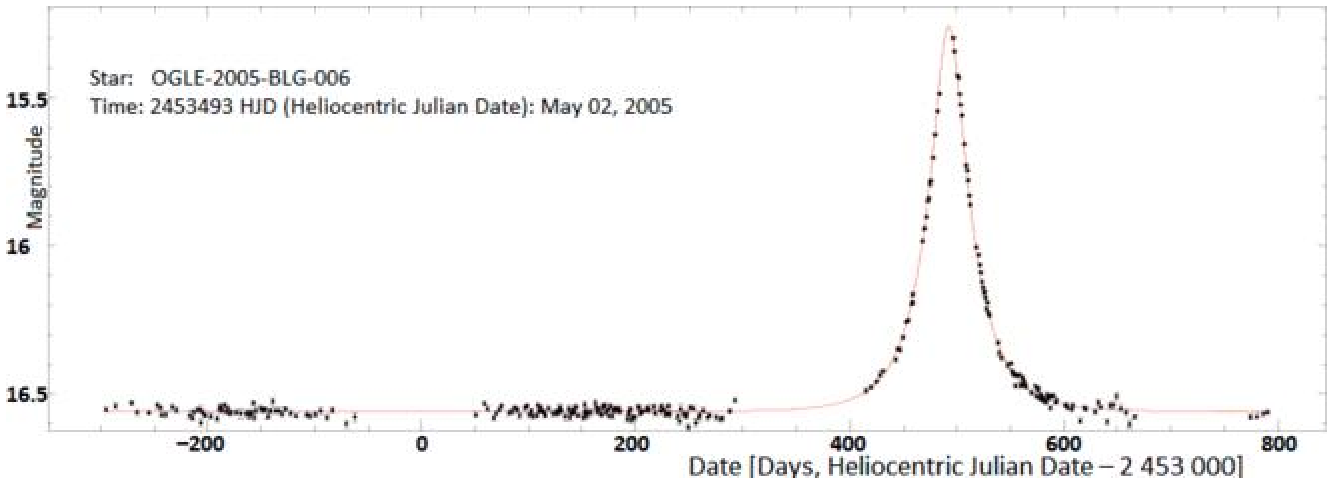

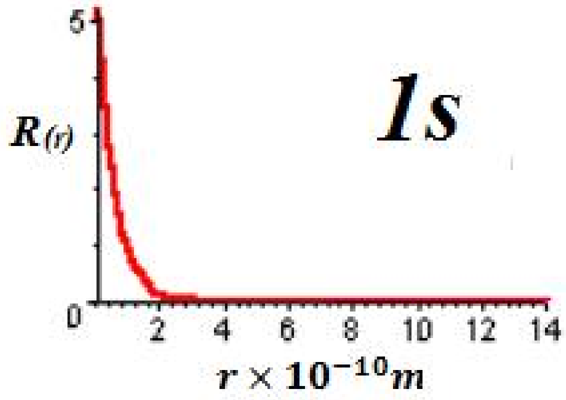

Hydrogen 1s wavefunction

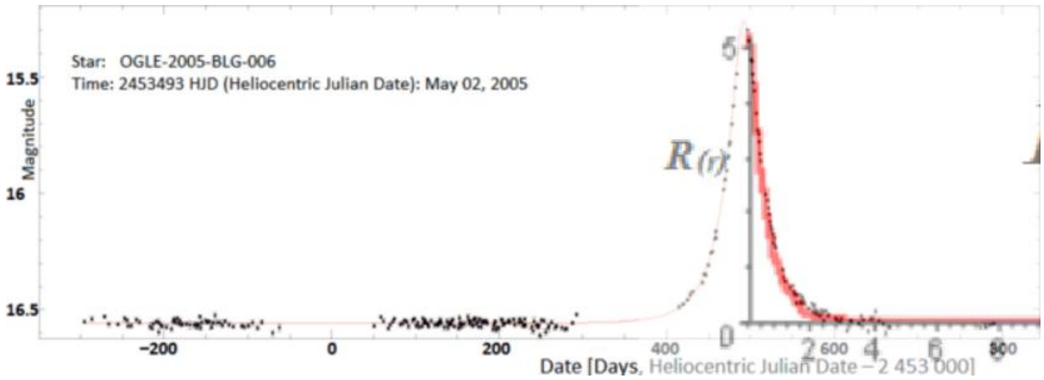

Super imposed graphs

https://www.researchgate.net/figure/COBE-measurements-43-of-the-CMB-spectrum-error-bars-are-multiplied-by-200-in_fig1_51940305

COBE measurements [43] of the CMB spectrum (error bars are multiplied by 200), in agreement with a black-body spectrum of temperature T = 2.725K.

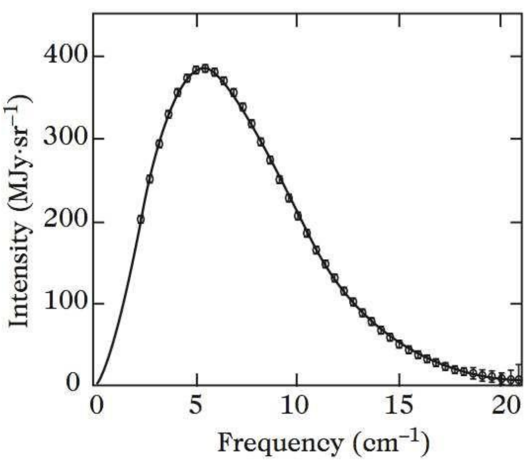

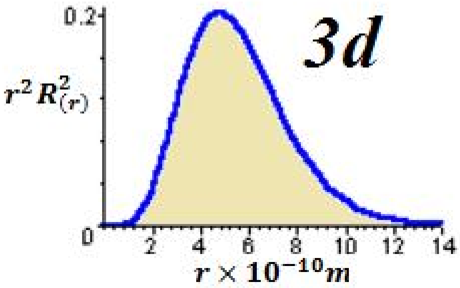

Hydrogen 3d Probability Density

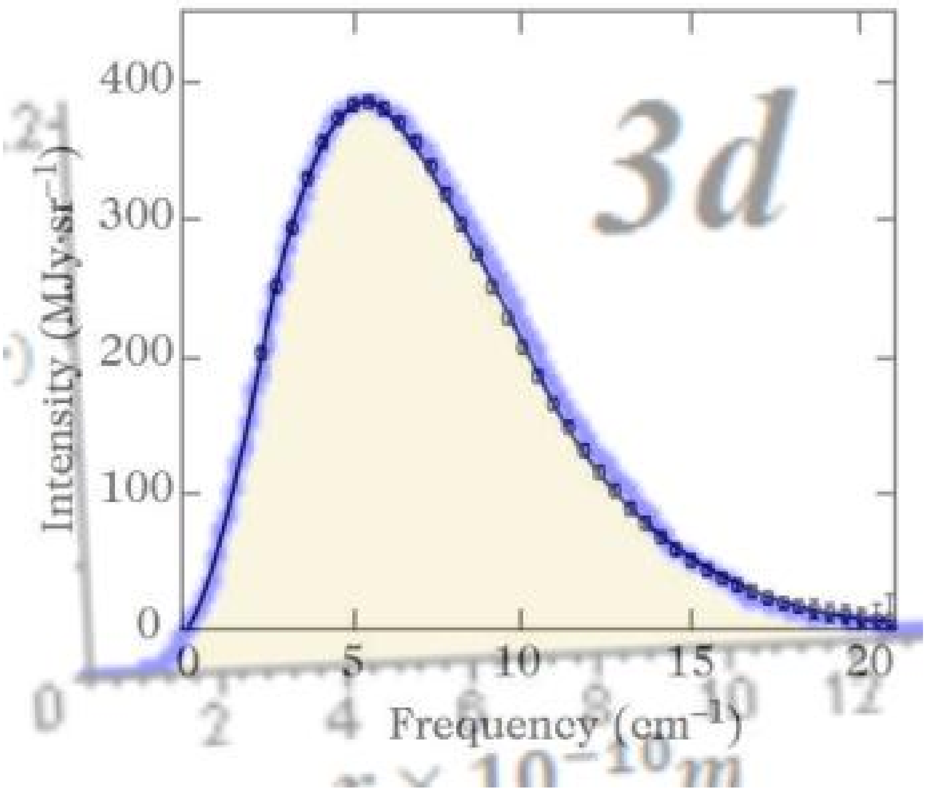

Super imposed graphs

https://www.researchgate.net/figure/The-total-imposed-on-a-photon-during-its-motion-around-the-black-hole-versus-the_fig6_348739685

The total imposed on a photon during its motion around the black hole versus the radius˜rradius˜ radius˜r for different values of angular momentum. The other constants are taken as˜Mas˜ as˜M ≡ M/ɑ = 2.5, ɑ = 0.1, and b = 10.

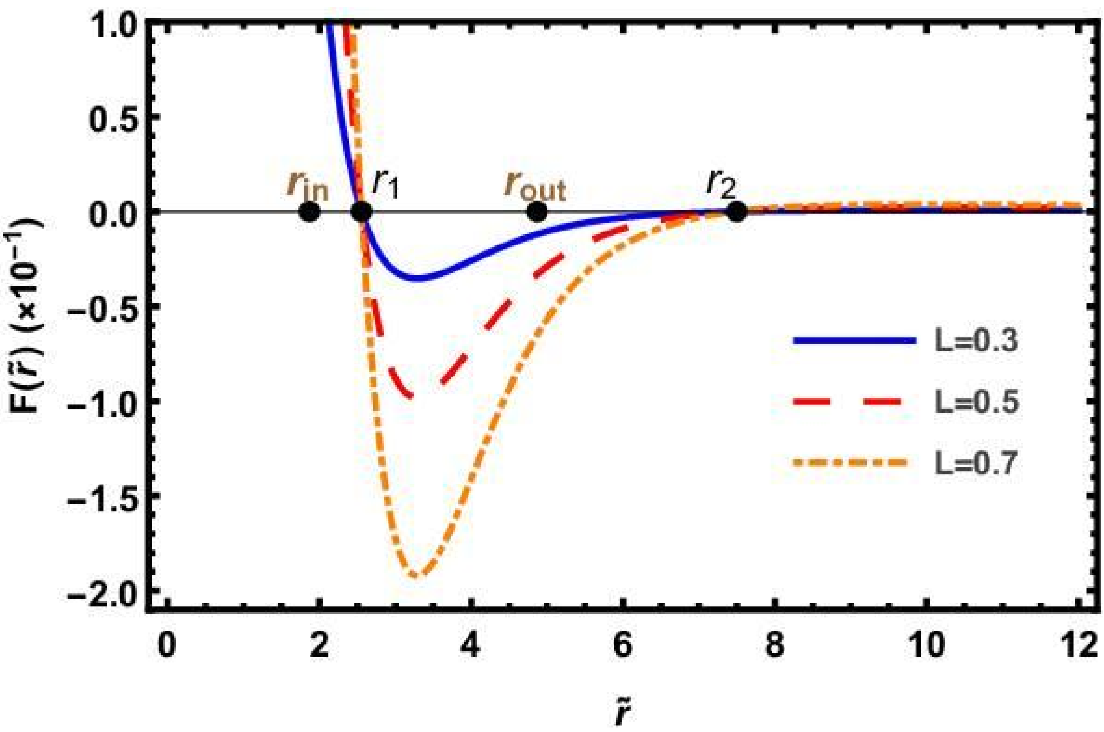

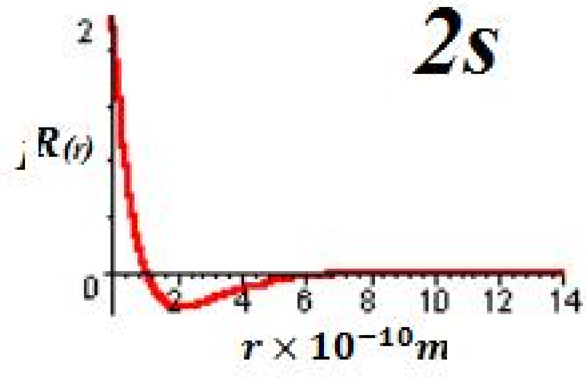

Hydrogen 2s wave function

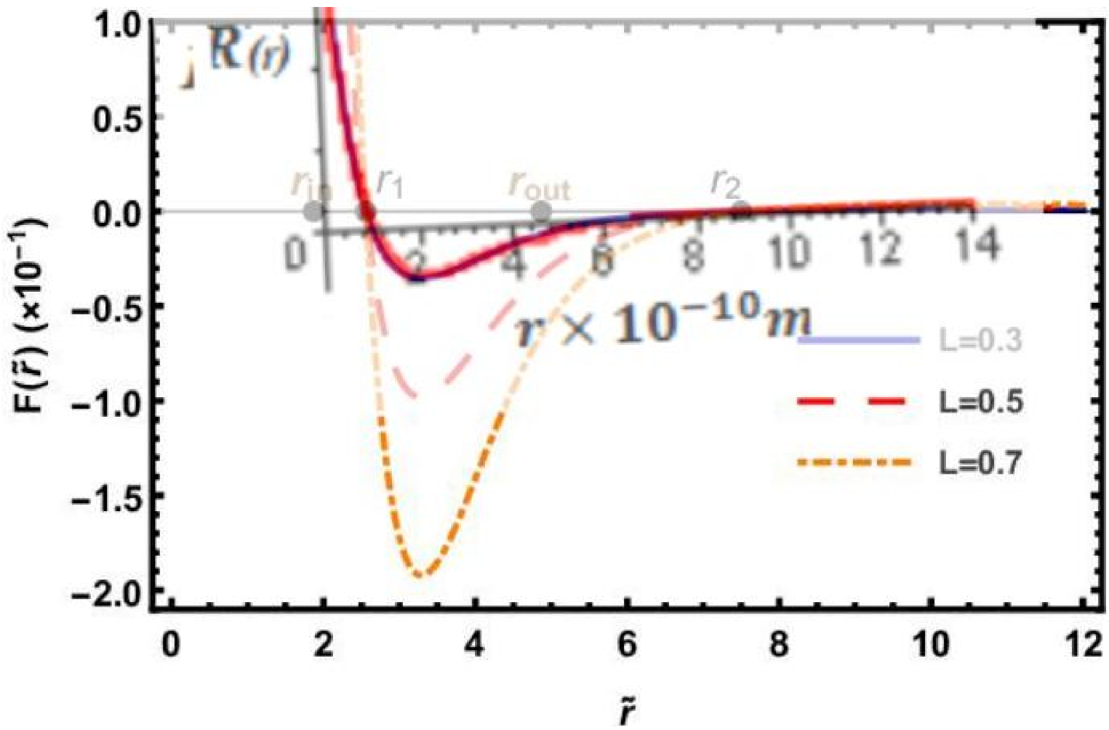

Super imposed graphs

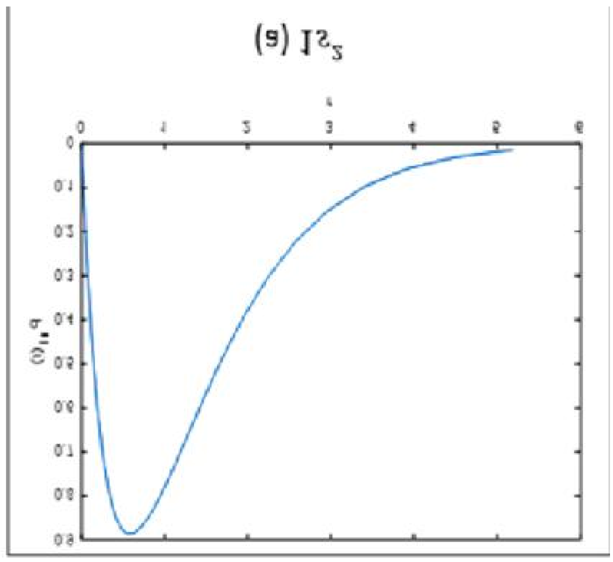

Helium wave function also matches the other line.

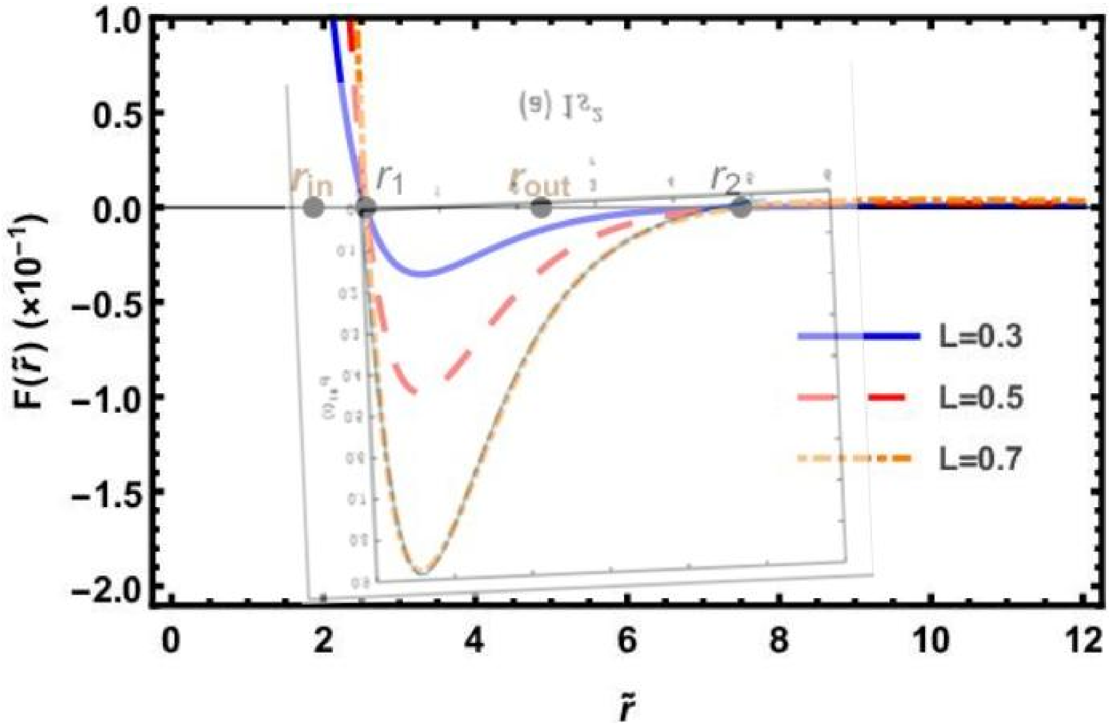

Super imposed graphs

https://link.springer.com/article/10.1140/epjc/s10052-019-6871-8/figures/1

Analysis of black hole thermodynamics with a new higher order generalized uncertainty principle

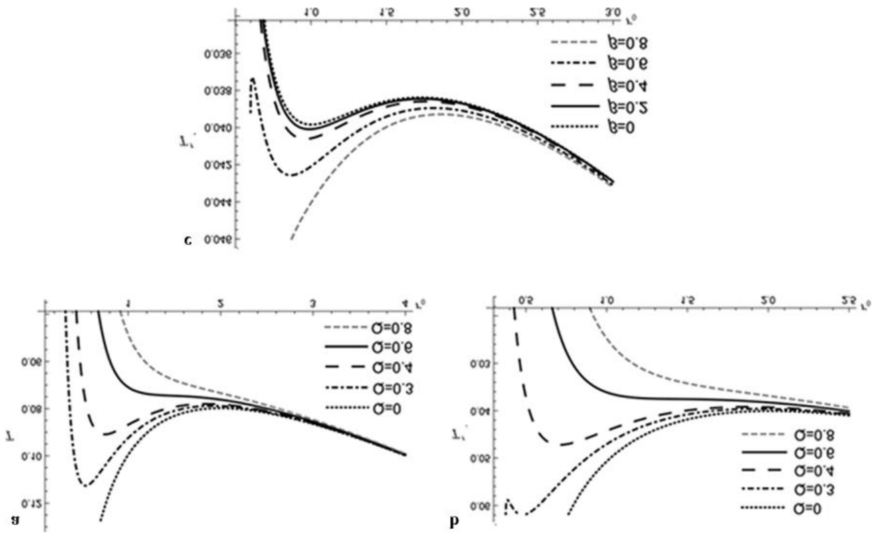

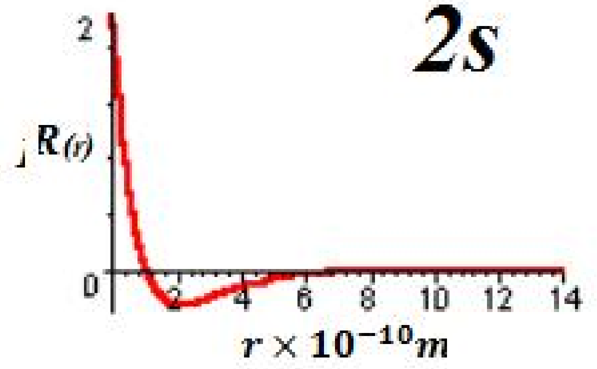

Hydrogen 2s Wave Function

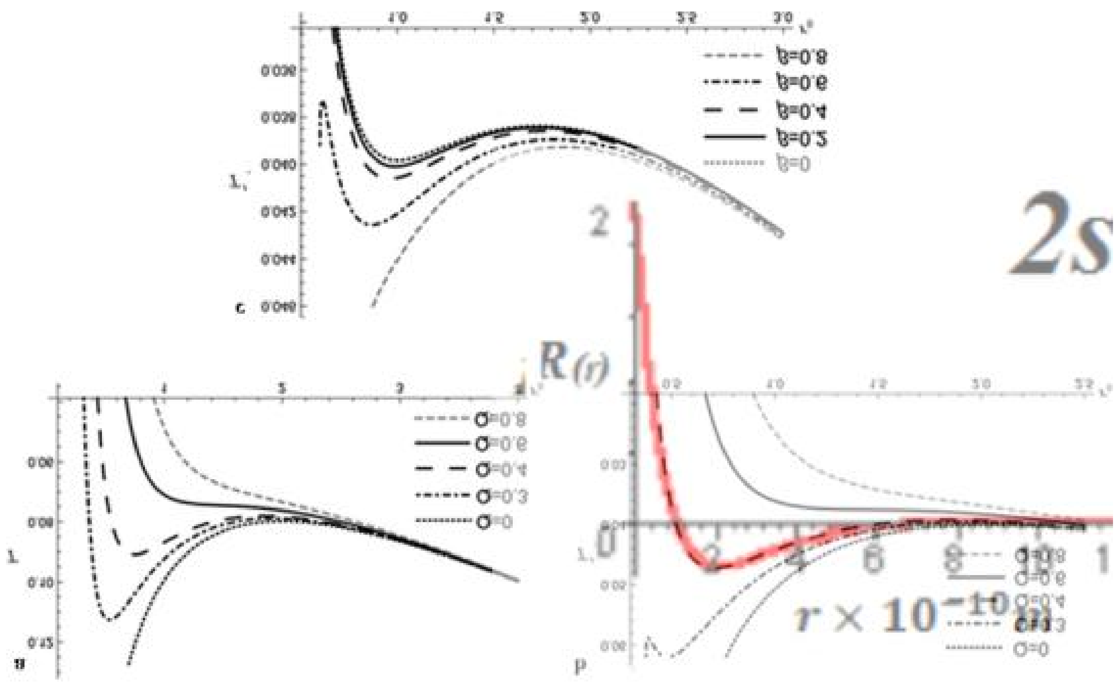

Super imposed graphs

https://www.ligo.org/science/Publication-S5S6RD/index.php

RINGING OF THE COSMIC BELLS: A SEARCH FOR BLACK HOLE VIBRATIONS

We analyzed data from LIGO's fifth and sixth science runs (S5 and S6) and Virgo's science runs 2 and 3 (VSR2/3). In order to gauge the sensitivity of our search to GWs from perturbed IMBHs, we can plot the ringdown horizon distance as a function of black hole mass, for example for the LIGO detectors (H1, H2, and L1) during S5 as shown above. Horizon distances are comparable for data from S6-VSR2/3. The horizon distance shown here is the maximum distance to which we could see a perturbed black hole with a signal-to-noise ratio of 8.

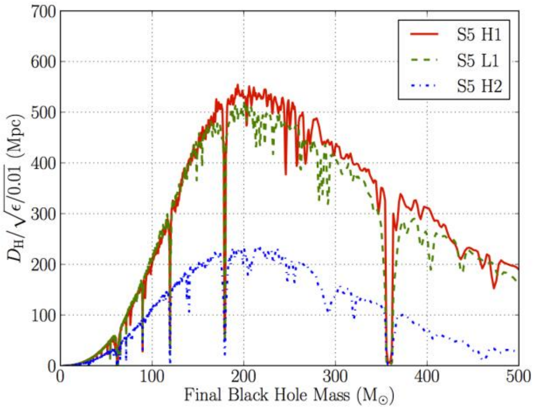

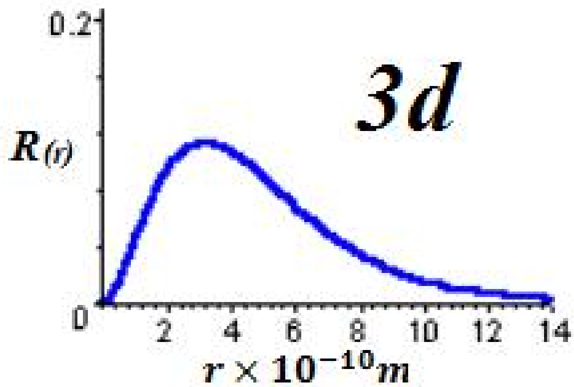

Hydrogen 3d wave function

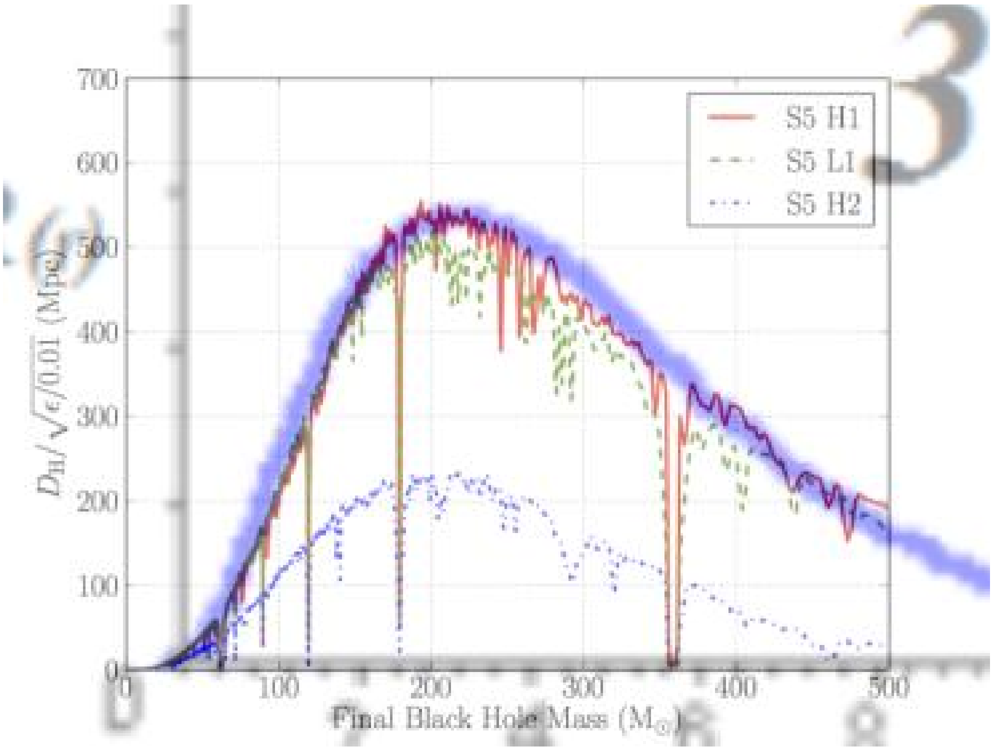

Super imposed graphs

https://iopscience.iop.org/article/10.3847/1538-4357/aab719

Distributions of nearest neighbor distances for gas-rich TF (orange) and NTF (blue) galaxies. Panel (a) shows the two distributions, whose difference is not statistically significant. These populations are further divided into galaxies whose nearest neighbors are within the same groups (b) and galaxies with neighbors outside of their groups (c).

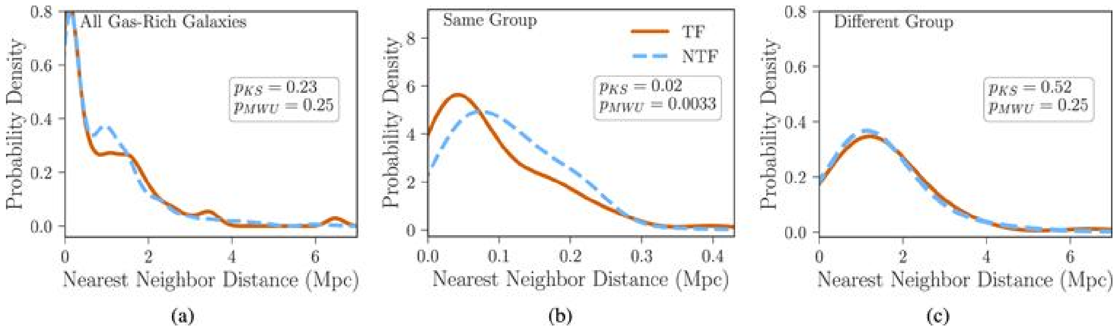

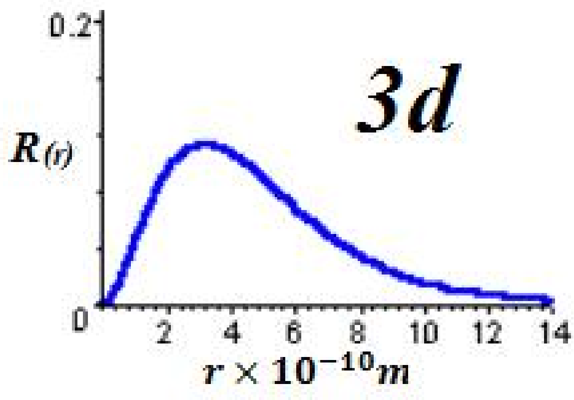

Hydrogen 3d Wave Function

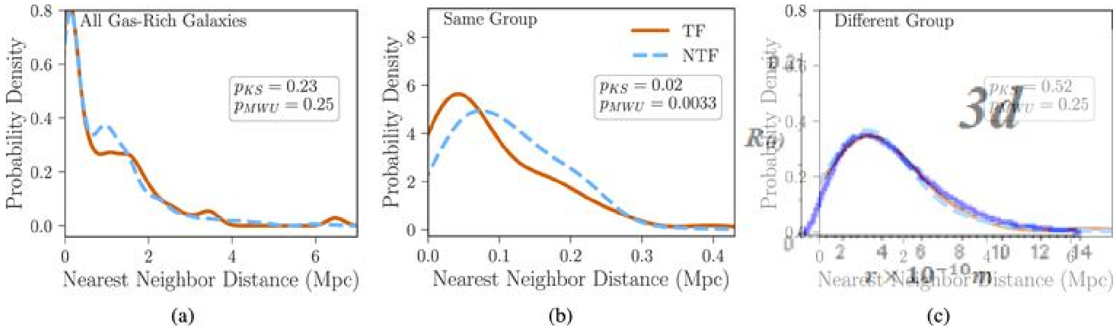

https://astronomy.com/magazine/ask-astro/2014/04/remnant-radiation

The cosmic microwave background's "black body" curve

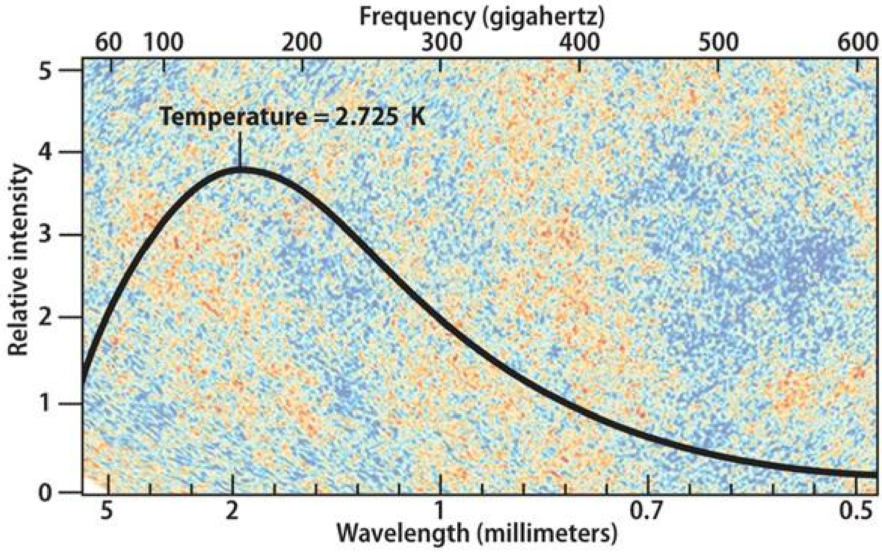

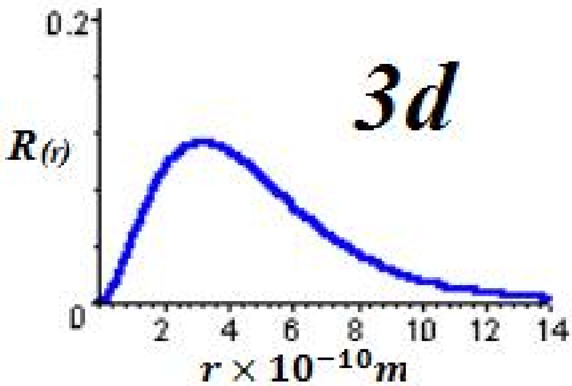

Hydrogen 3d wave function

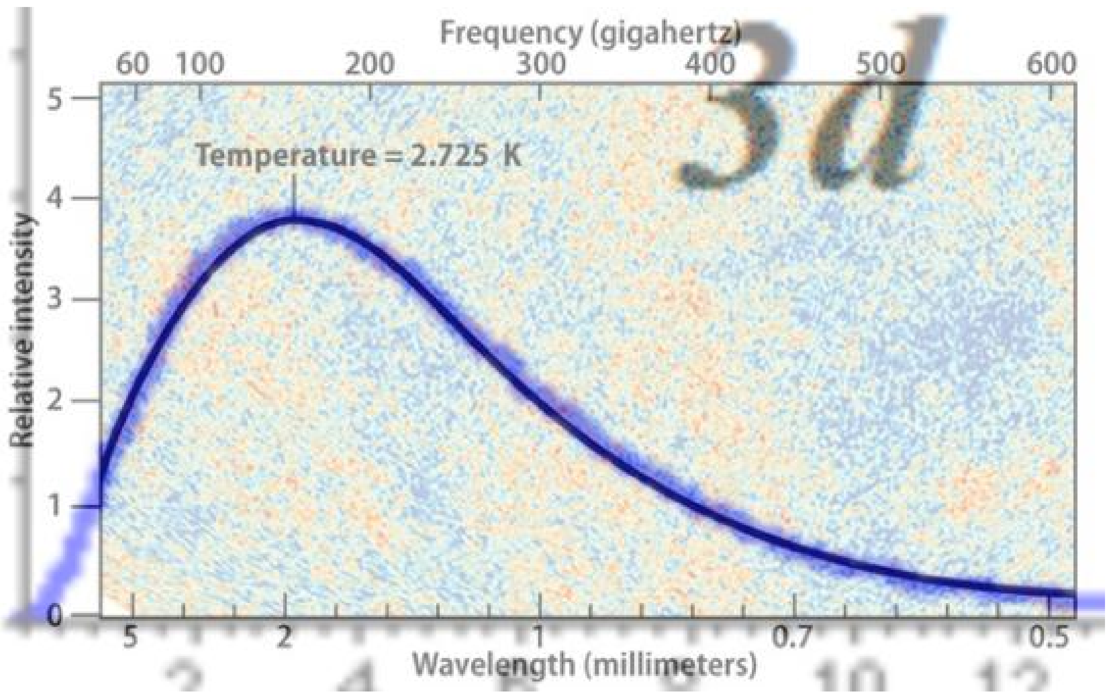

Super imposed graphs

https://www.gw-openscience.org/s/events/GW150914/GW150914.html

Data release for event GW150914

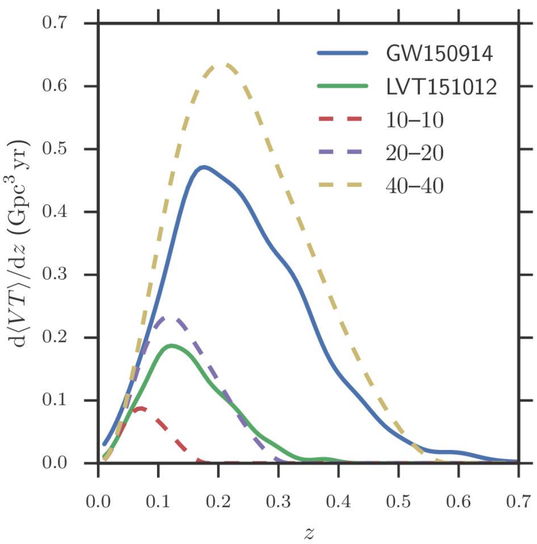

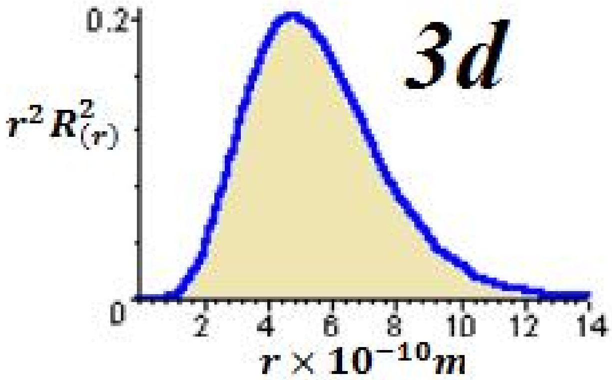

Hydrogen 3d Probability Density

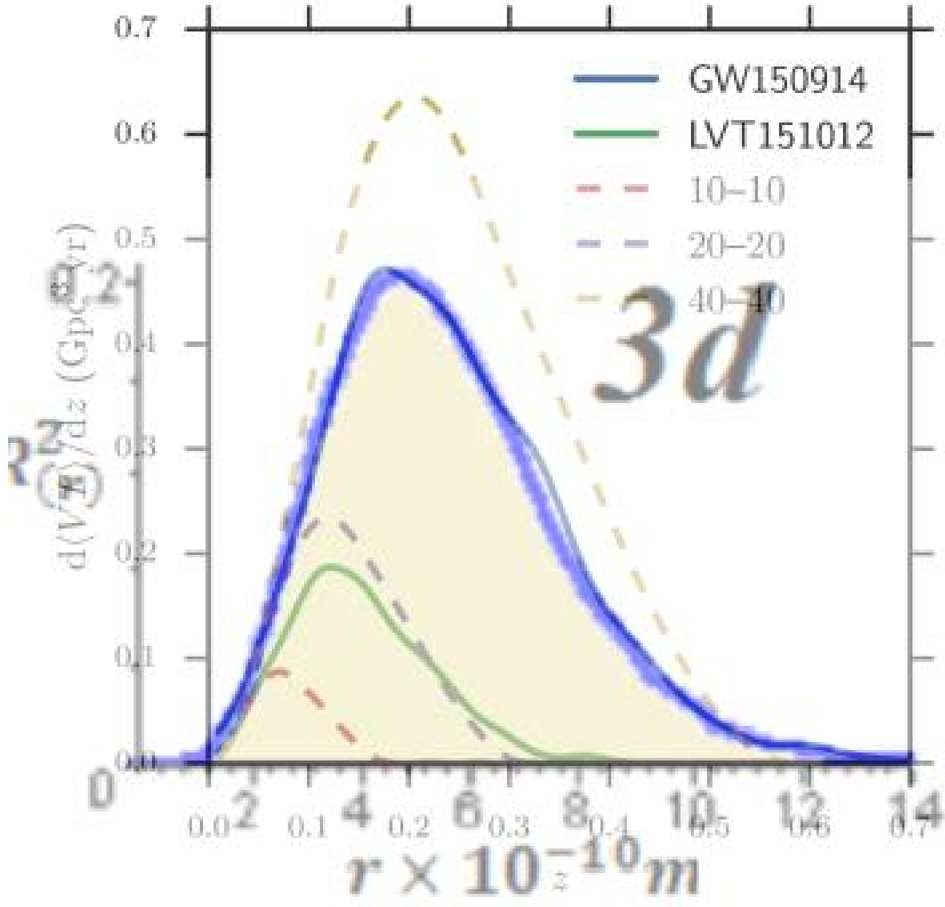

Super imposed graphs

https://phy.princeton.edu/sites/g/files/toruqf2261/files/resource-links/jacobson_jp1.pdf

Empirical velocity distributions for metal-poor stars in the RAVE-TGAS halo

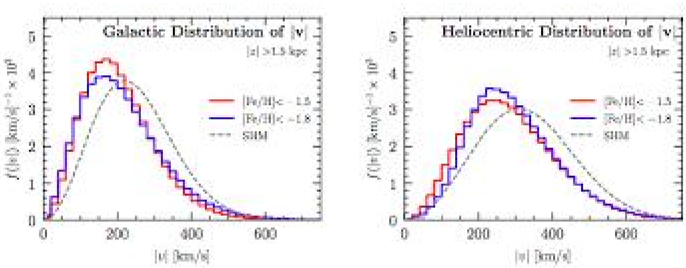

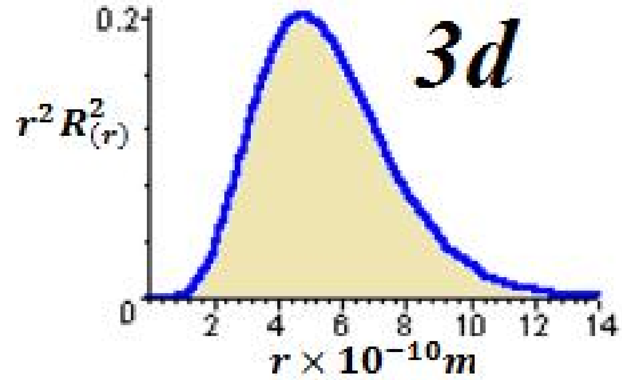

Hydrogen 3d Probability Density

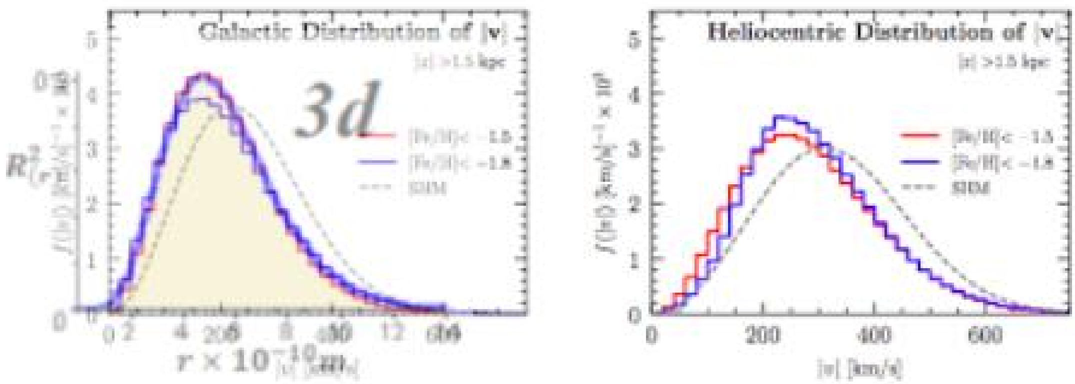

Super imposed graphs

https://www.researchgate.net/figure/The-probability-distribution-of-the-number-of-star-nearest-neighbors-for-a-r-s-s-3-s_fig2_255765312

The probability distribution of the number of (star) nearest-neighbors for (a) r s s 3 s 1/4 0.1 and (b) r s s 3 s 1/4 0.2 as the number of chain

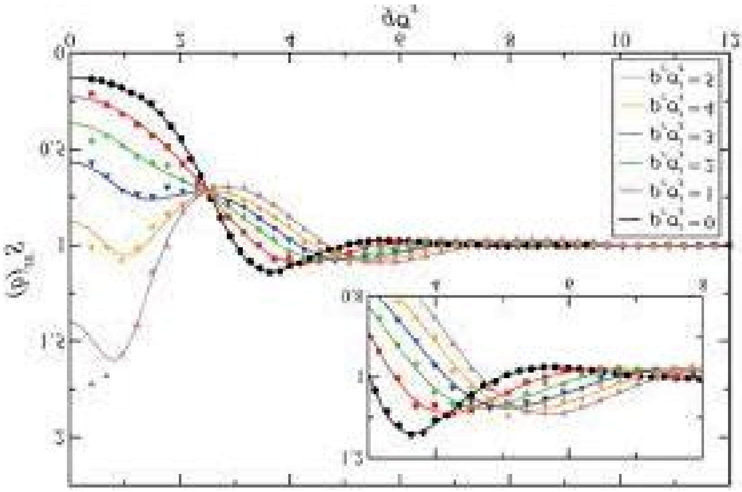

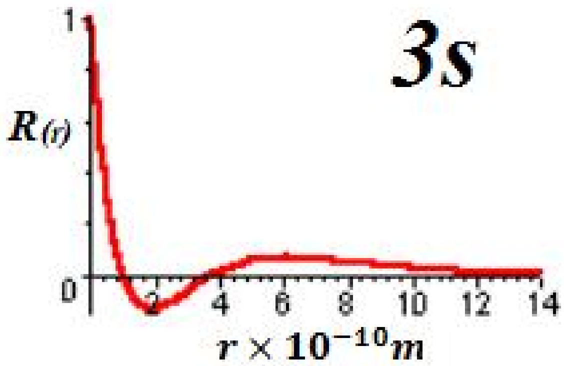

Hydrogen 3s Wave Function

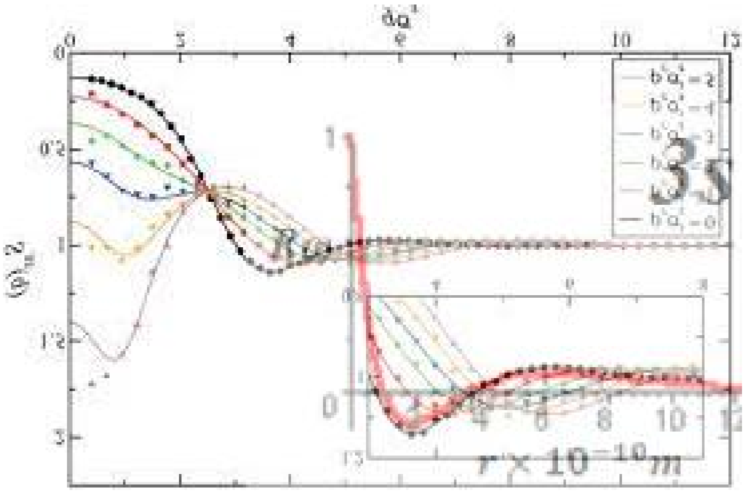

Super imposed graphs

https://www.researchgate.net/figure/Chain-mediated-effective-star-star-potential-as-obtained-by-inversion-of-the-OZ-equation_fig4_255765312

Chain-mediated effective star–star potential as obtained by inversion of the OZ equation in the limit r s s 3 s / 0 (see Ref. 27).

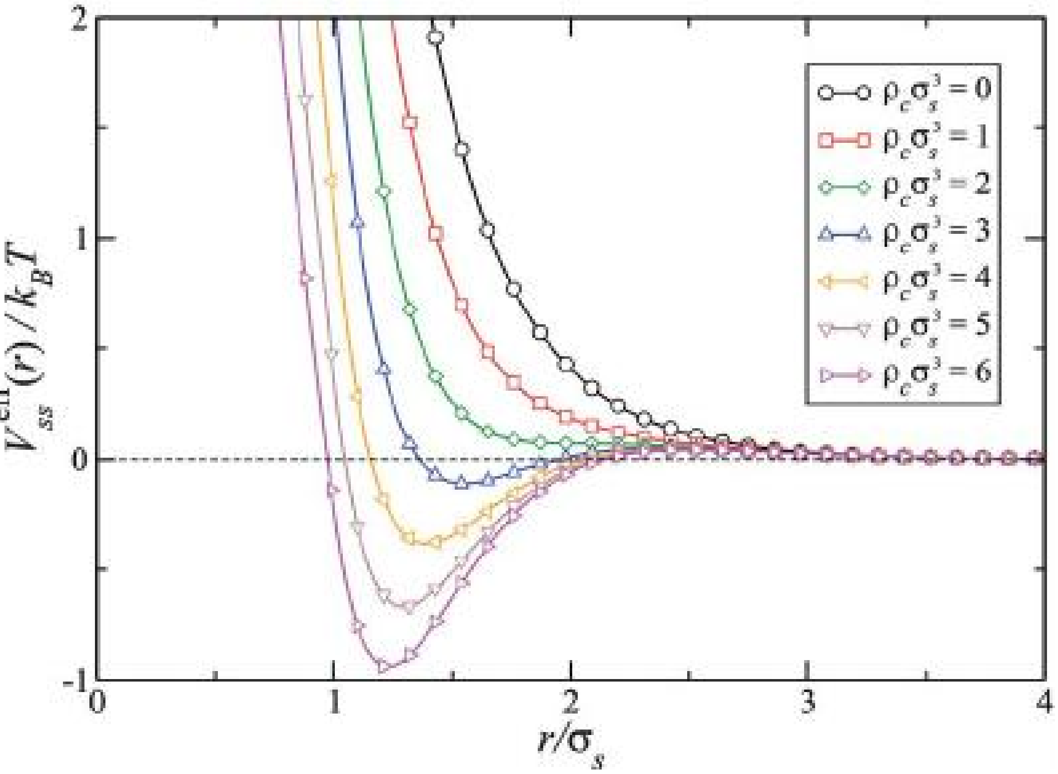

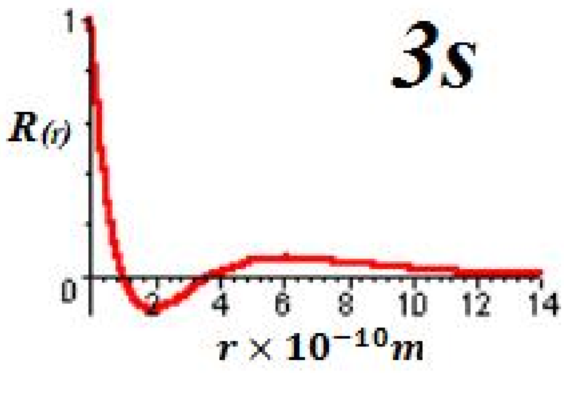

Hydrogen 3s Wave Function

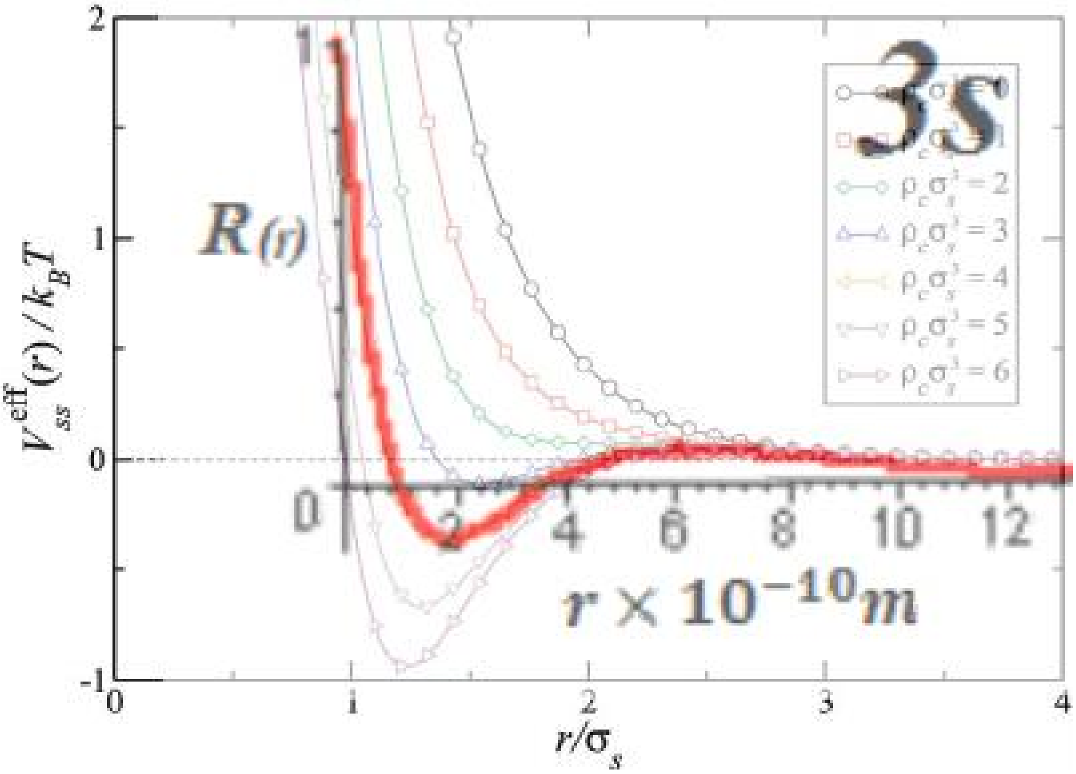

Super imposed graphs

https://www.researchgate.net/figure/Various-cosmic-ray-source-supernova-remnants-distributions-are-available-in-the_fig10_258539610

Various cosmic ray source (supernova remnants) distributions are available in the literature. They are plotted here as a function of the Galactocentric distance r.

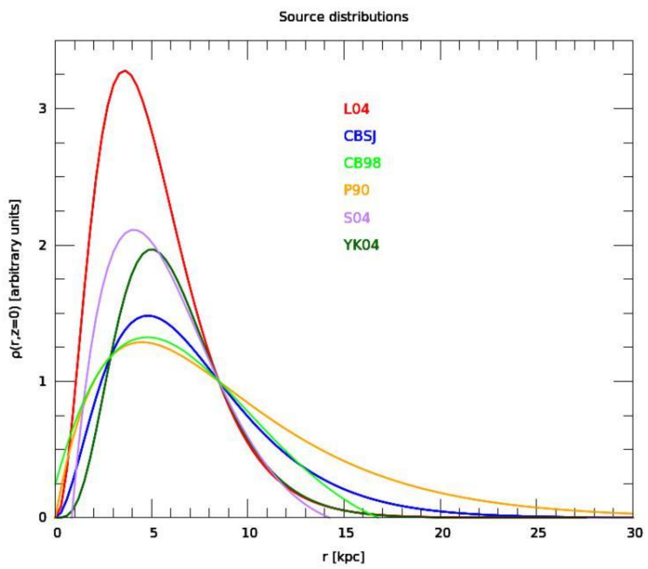

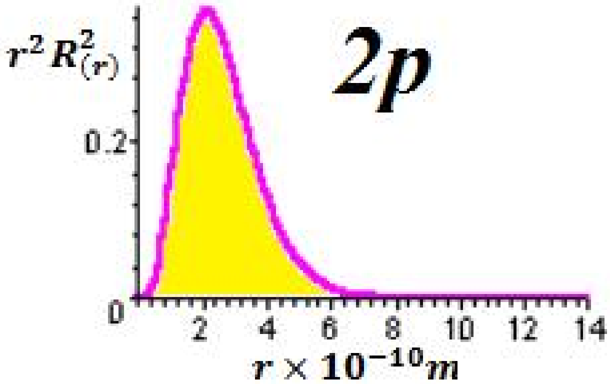

Hydrogen 2p Probability Density

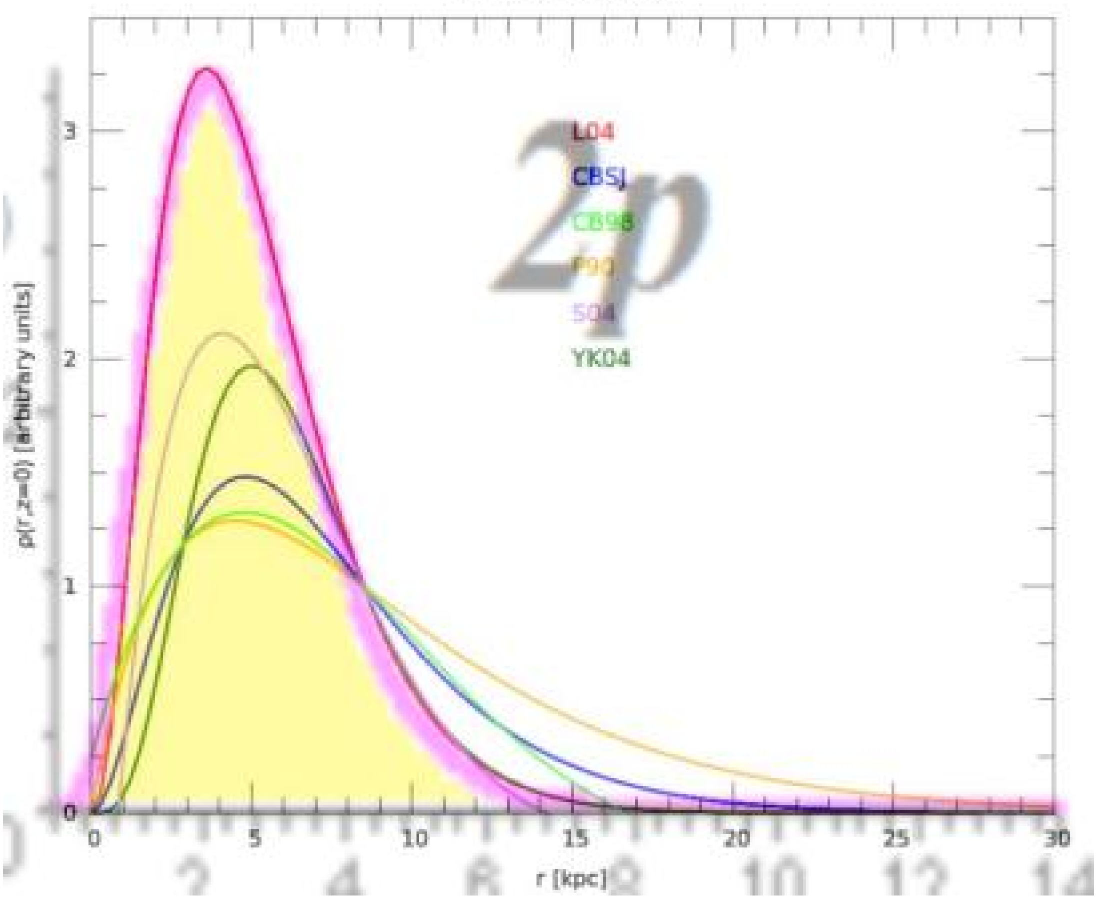

Super imposed graphs

https://briankoberlein.com/blog/seeing-red/

Distribution of galaxies. The solid line of random distribution matches observation. The dotted lines of ejected quasars does not.

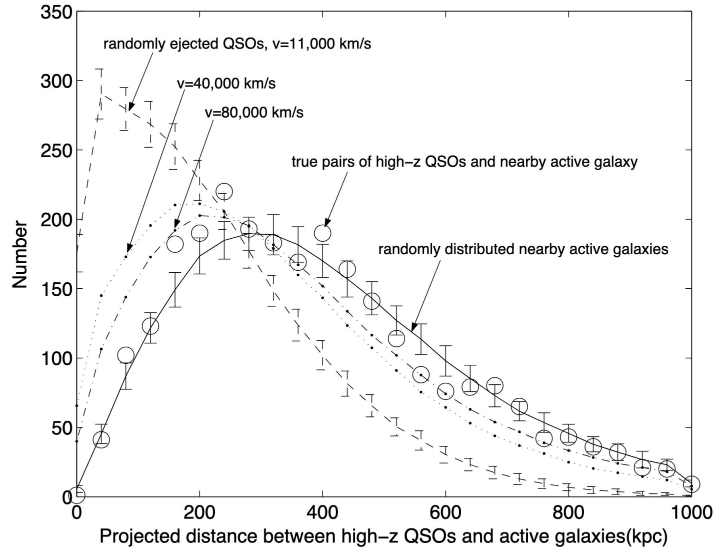

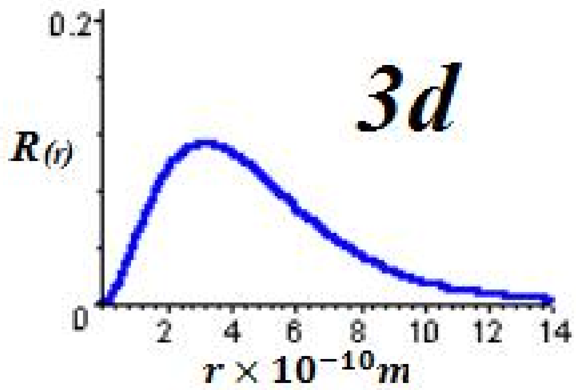

Hydrogen 3d Wave Function

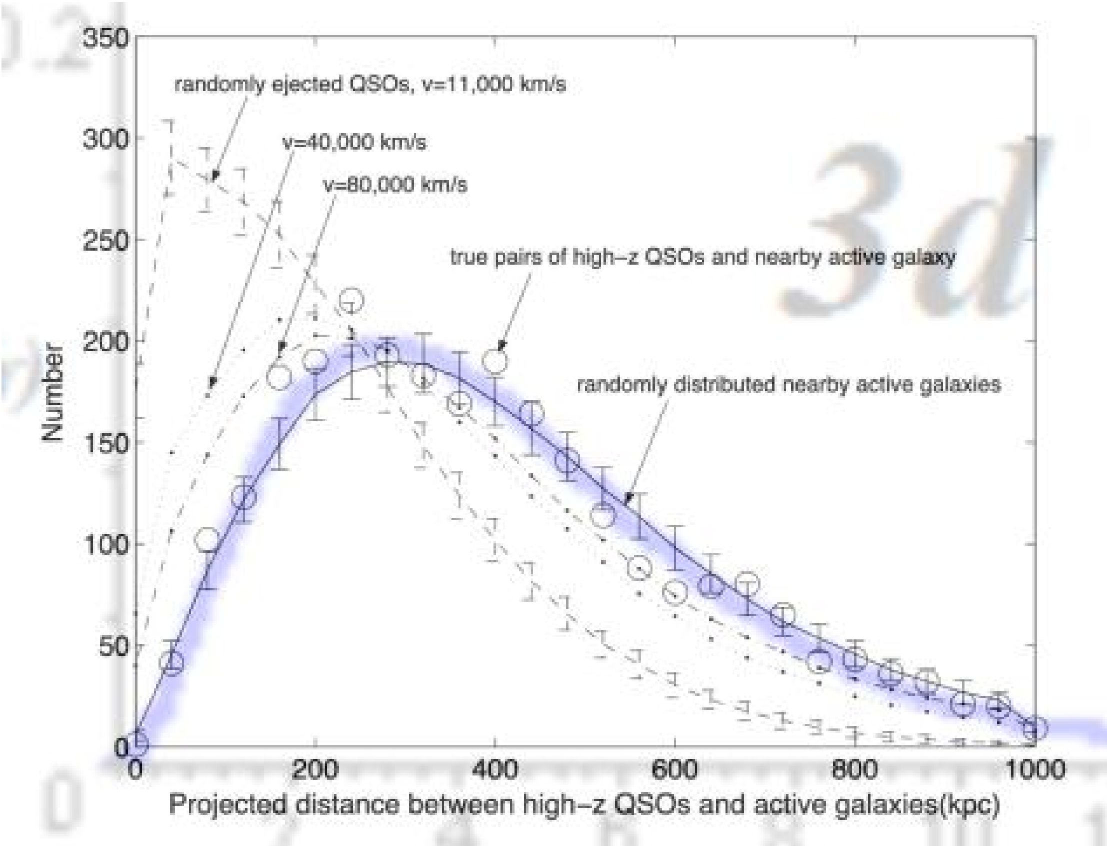

Super imposed graphs

https://ned.ipac.caltech.edu/level5/Sept02/Saslaw/Saslaw1_4.html

The unnormalized frequency distribution of Hubble's galaxy counts compared to a random Gaussian distribution, after Bok (1934). The inset shows a recent fit of Bok's points to the distribution of Equation 27.24.

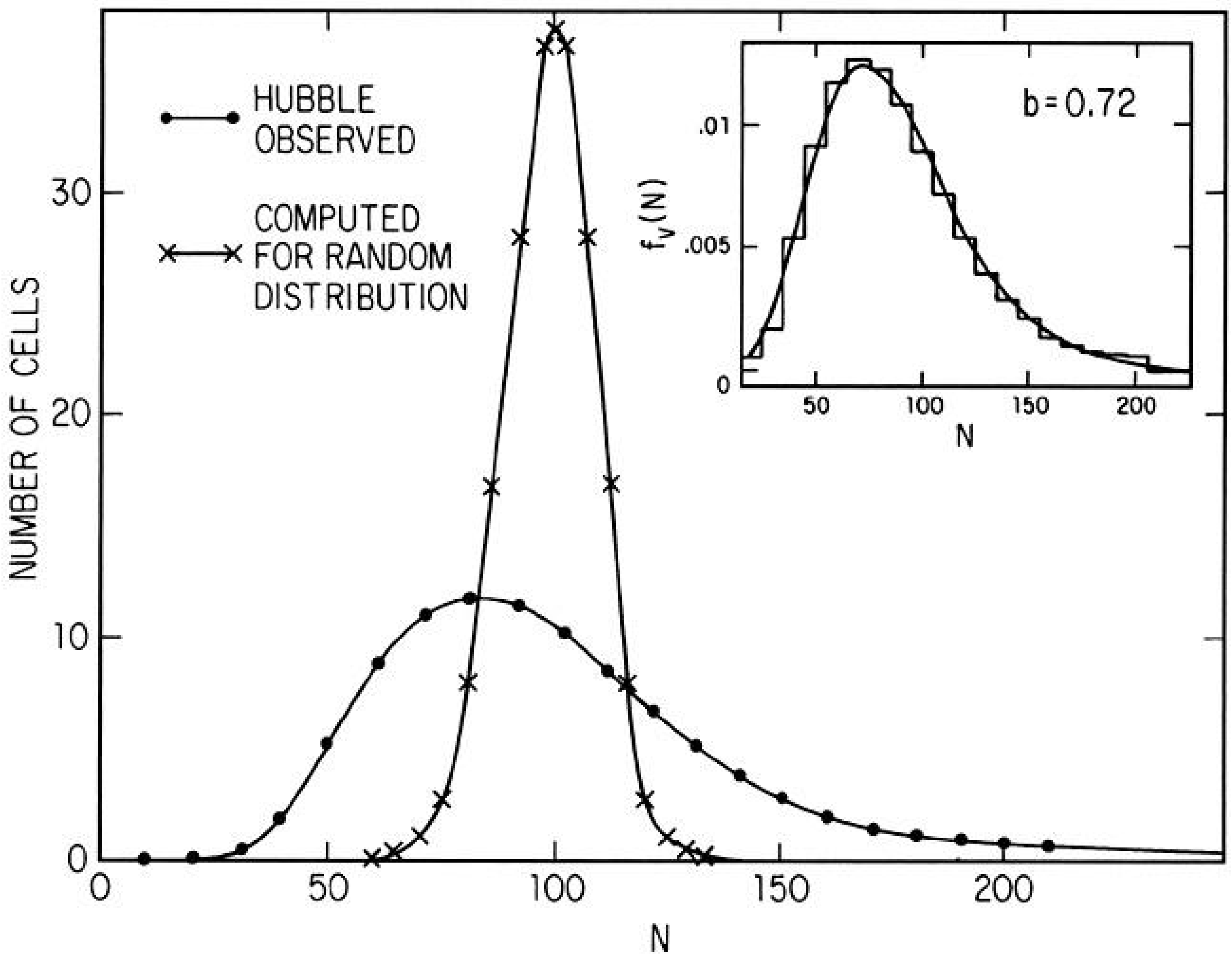

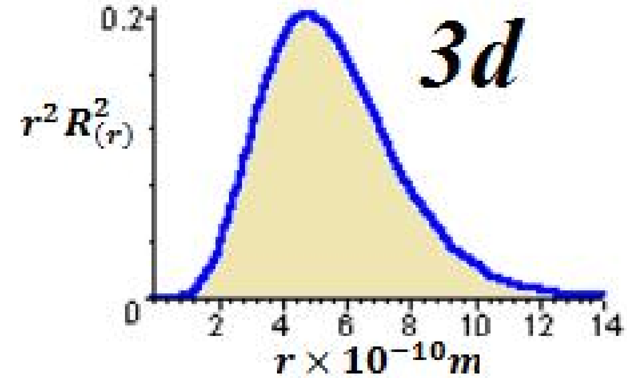

Hydrogen 3d Wave Probability Density

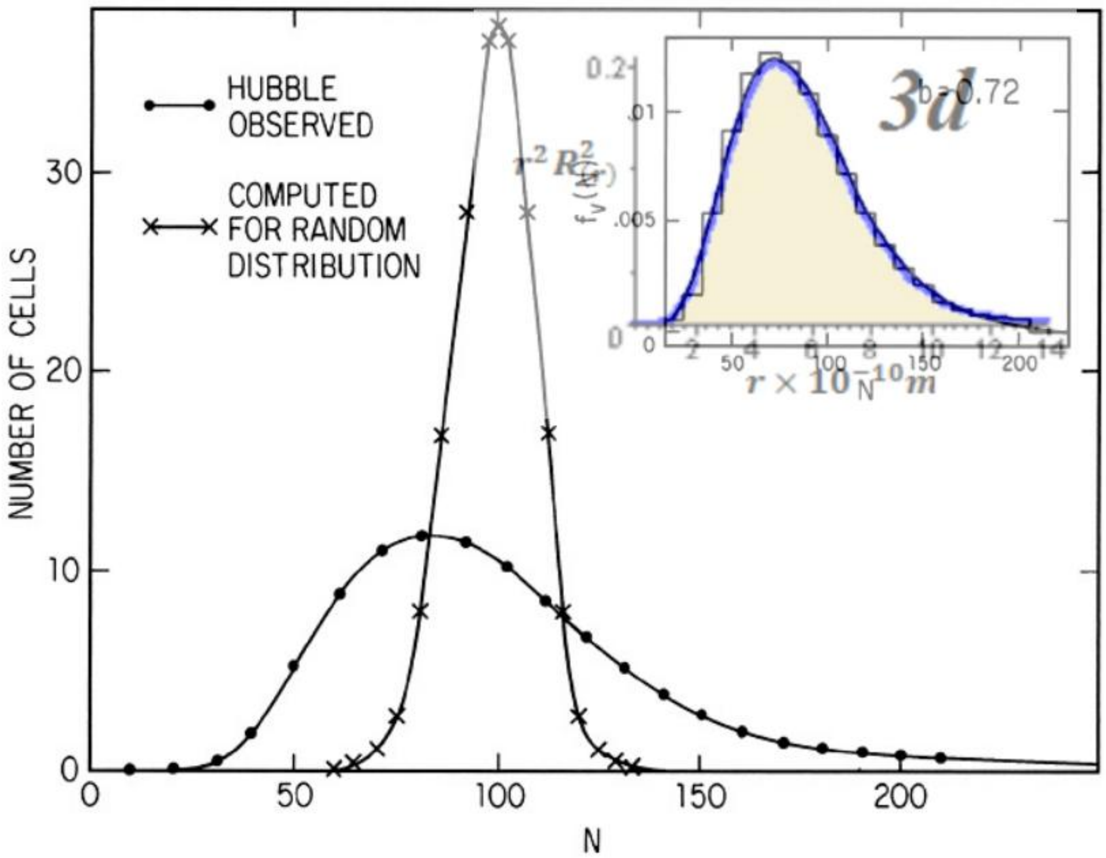

Super imposed graphs

https://link.springer.com/article/10.1140/epjc/s10052-020-08623-2

Charged particle motion around non-singular black holes in conformal gravity in the presence of external magnetic field

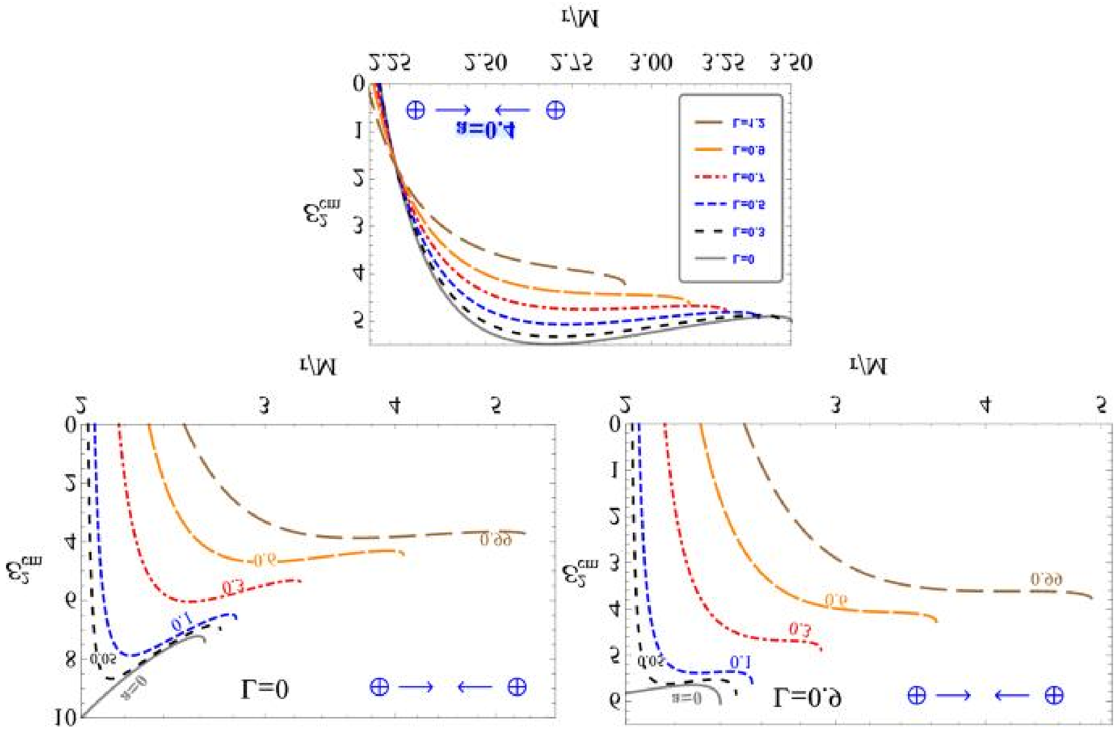

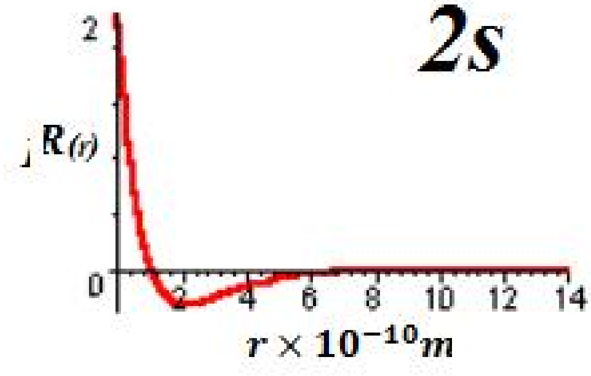

Hydrogen 2s Wave Function

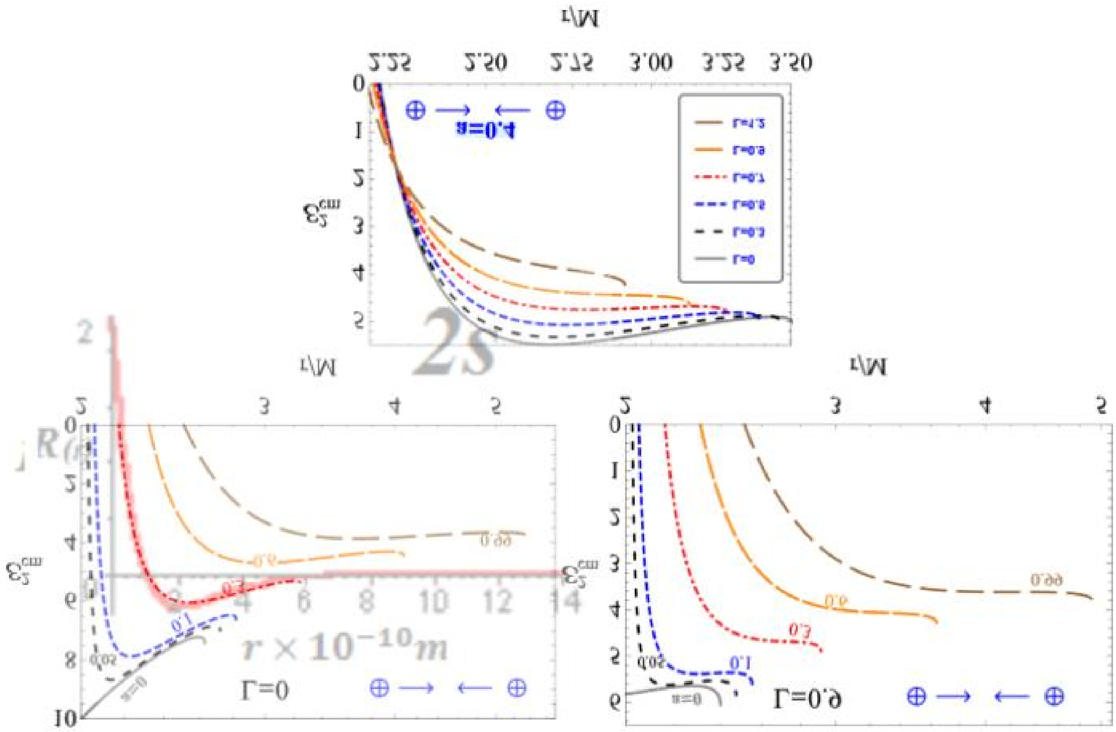

Super imposed graphs

https://www.zora.uzh.ch/id/eprint/163632/1/20070192.pdf

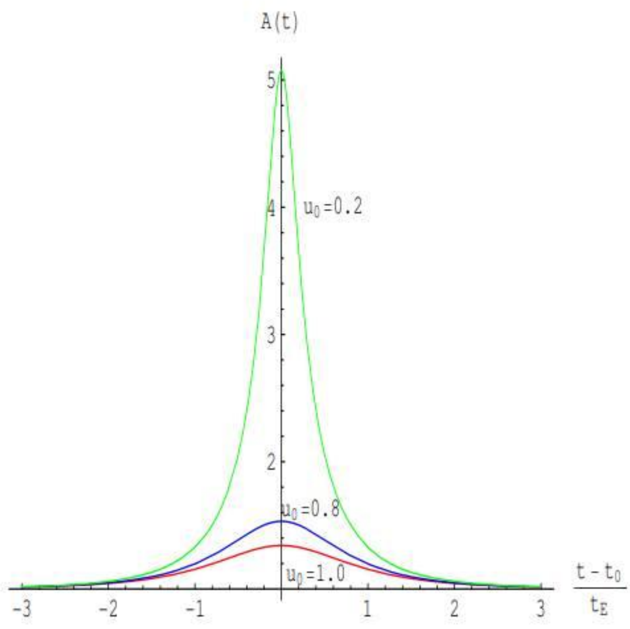

Figure 2.5: Paczyński curves: amplification factor as a function of the distance of the source from the lens, for different values of the minimum impact parameter u_0.

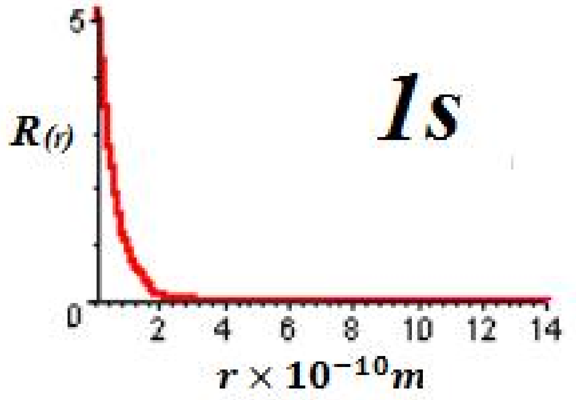

Hydrogen 1s wave function

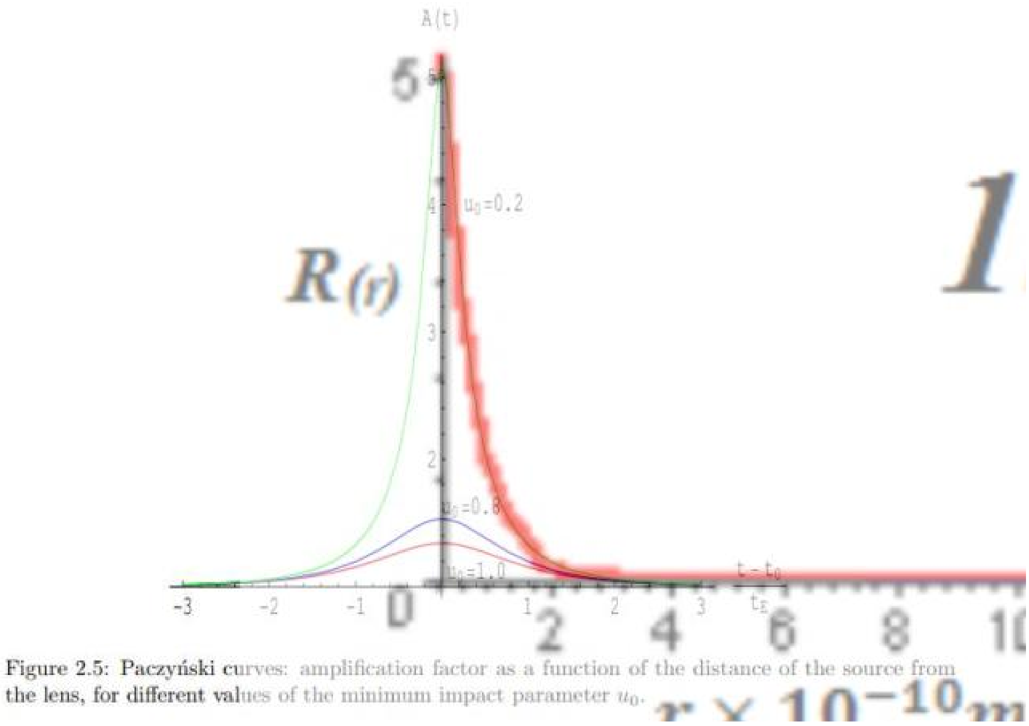

Super imposed graphs

https://www.researchgate.net/figure/The-effective-potential-V-m-of-an-extreme-Kerr-black-hole-for-a-test-particle-with-a_fig30_51933647

The effective potential V/μ of an extreme Kerr black hole for a test particle with a fixed orbital angular momentum as function of r/M.

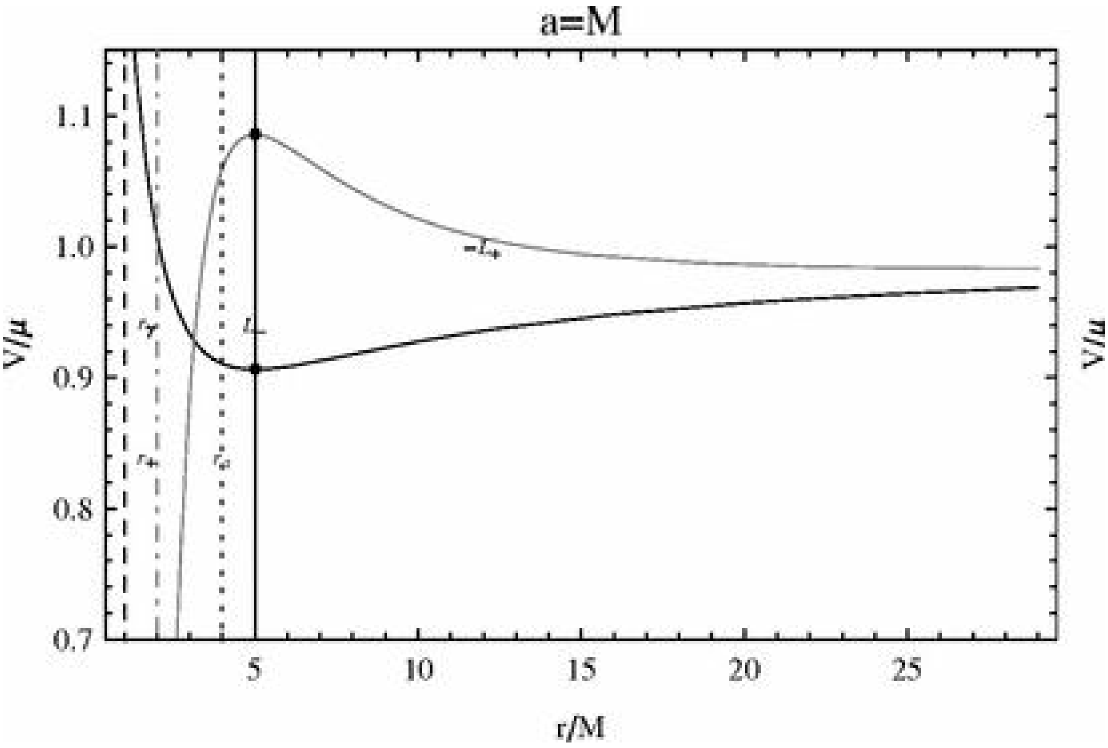

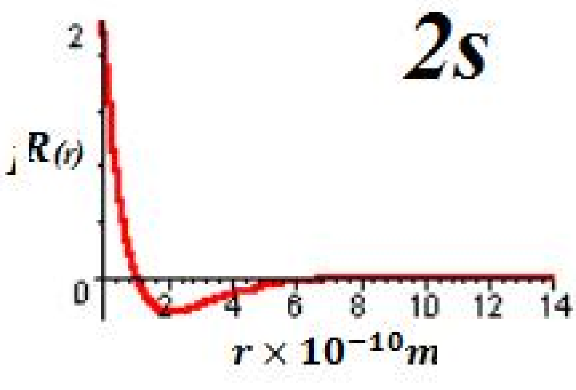

Hydrogen 2s Wave Function

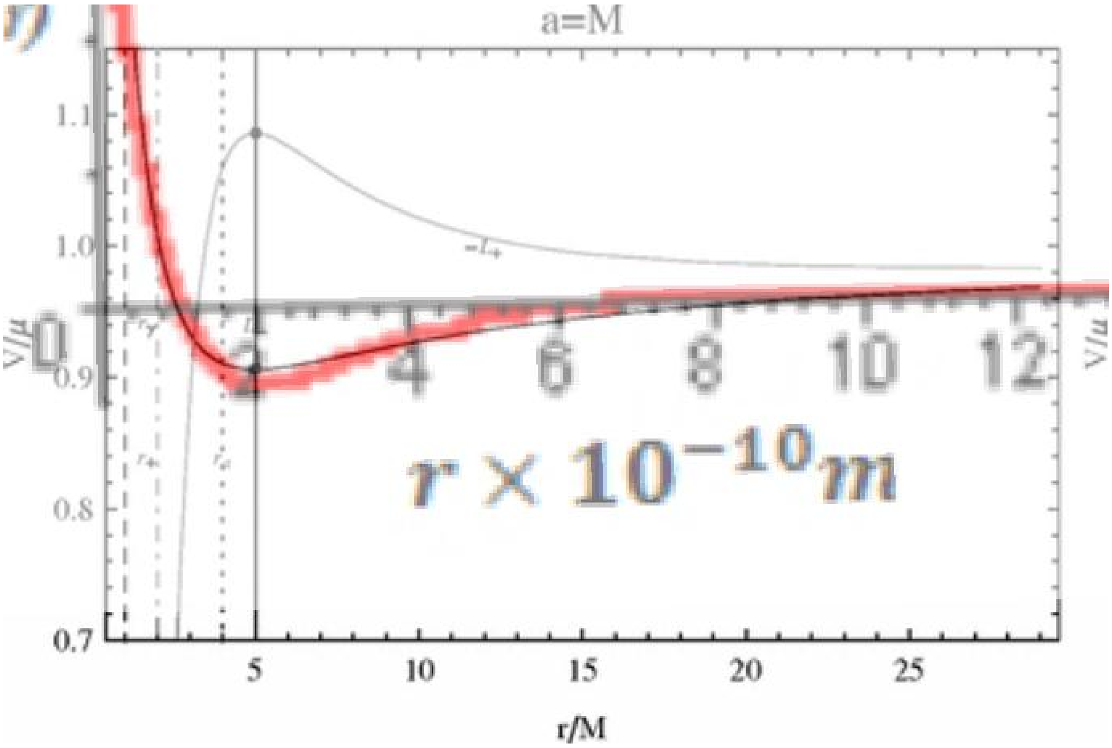

Super imposed graphs

https://www.semanticscholar.org/paper/Accelerated-expansion-of-the-Universe-in-the-of-Rezaei/e3ca26244fbf1deeaa0261761f0d91cf799307f8

Accelerated expansion of the Universe in the presence of dark matter pressure

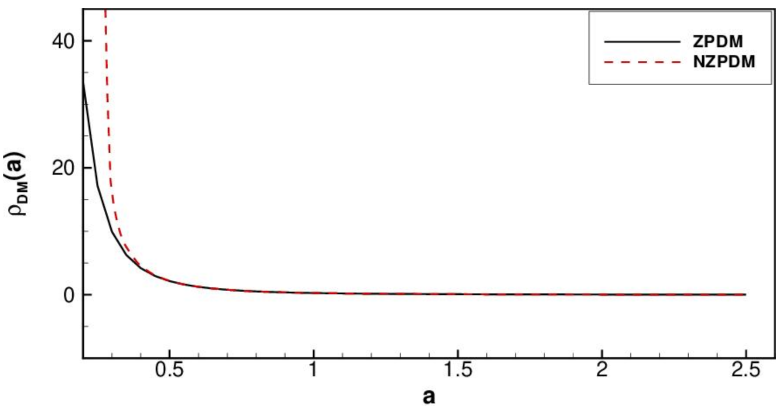

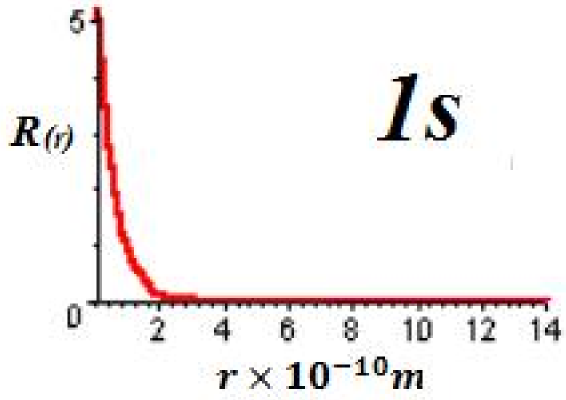

Hydrogen 1s Wave Function

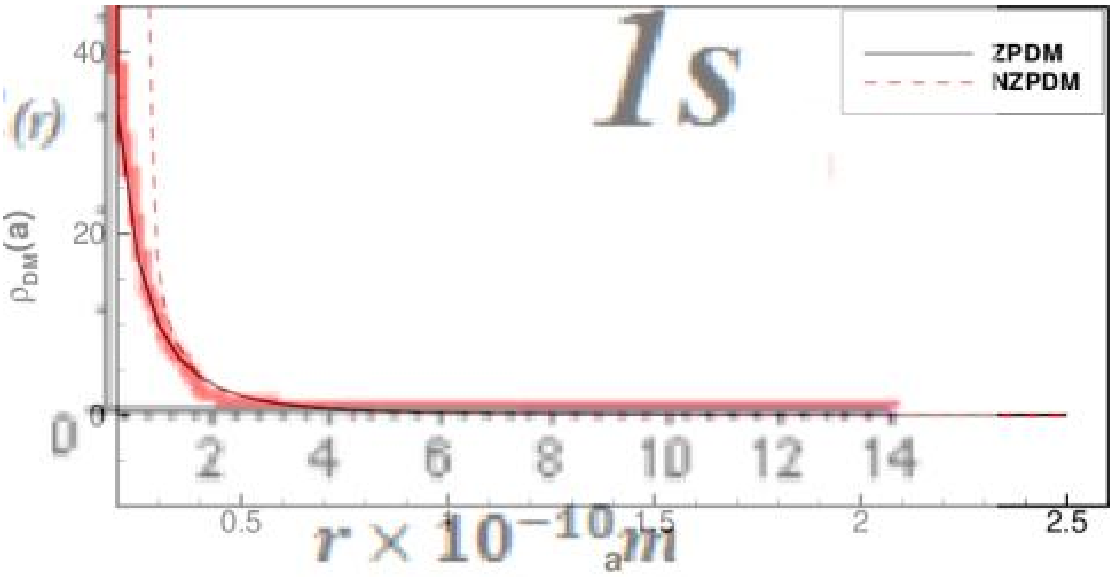

Super imposed graphs

https://www.gw-openscience.org/s/events/GW150914/GW150914.html

Data release for event GW150914

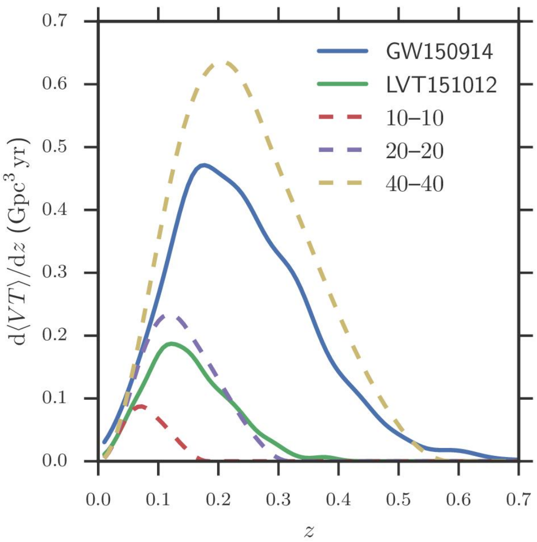

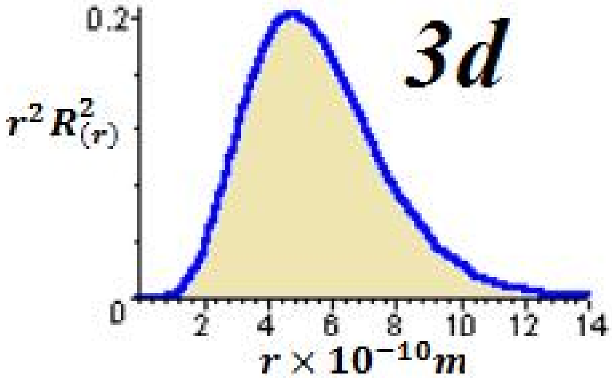

Hydrogen 3d Probability Density

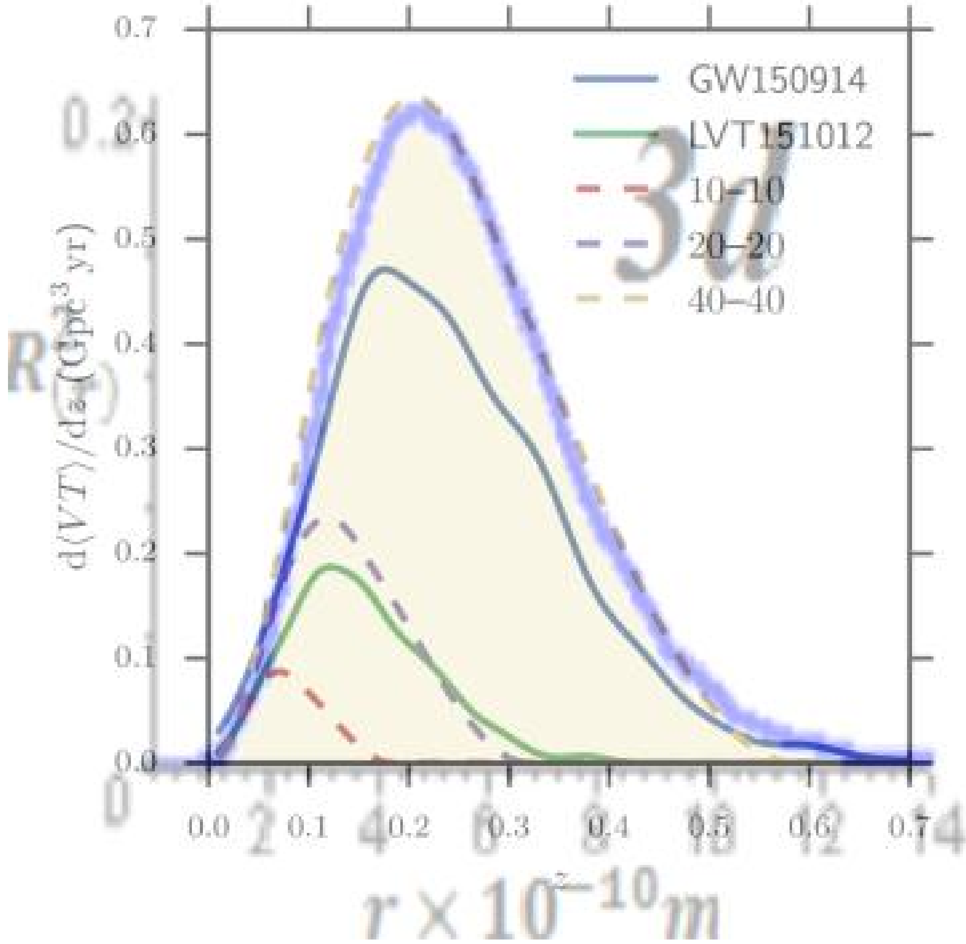

Super imposed graphs

https://cds.cern.ch/record/2729754/plots
Supernova Neutrino Burst Detection with the Deep Underground Neutrino Experiment

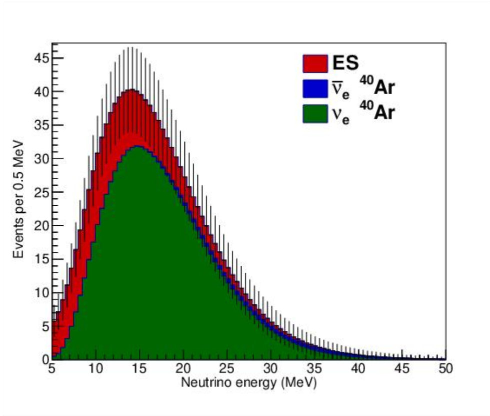

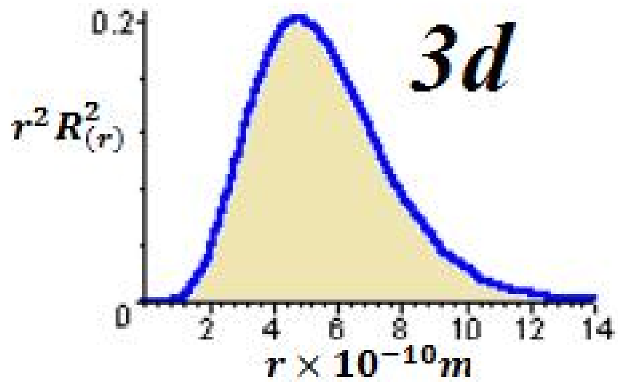

Hydrogen 3d Probability Density

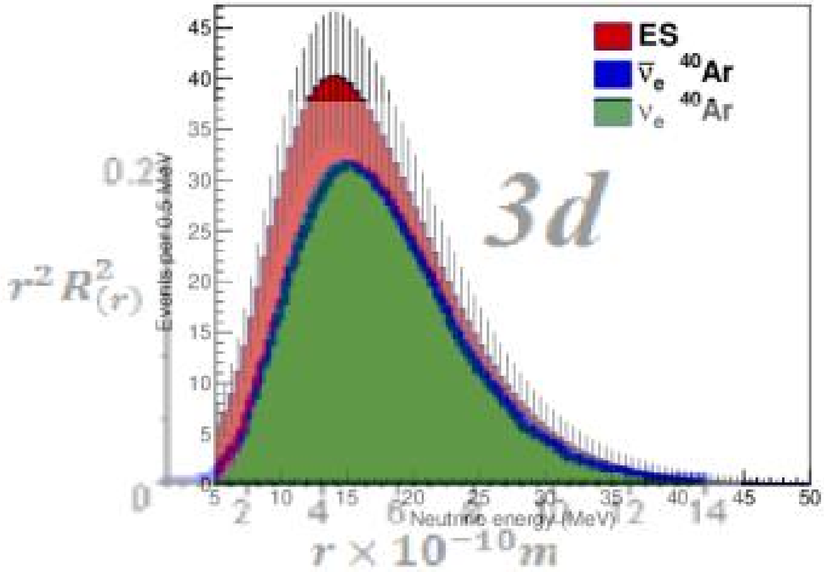

Superimposed graphs

https://iopscience.iop.org/article/10.1086/498208/pdf
Rotation curve of ngc 4448

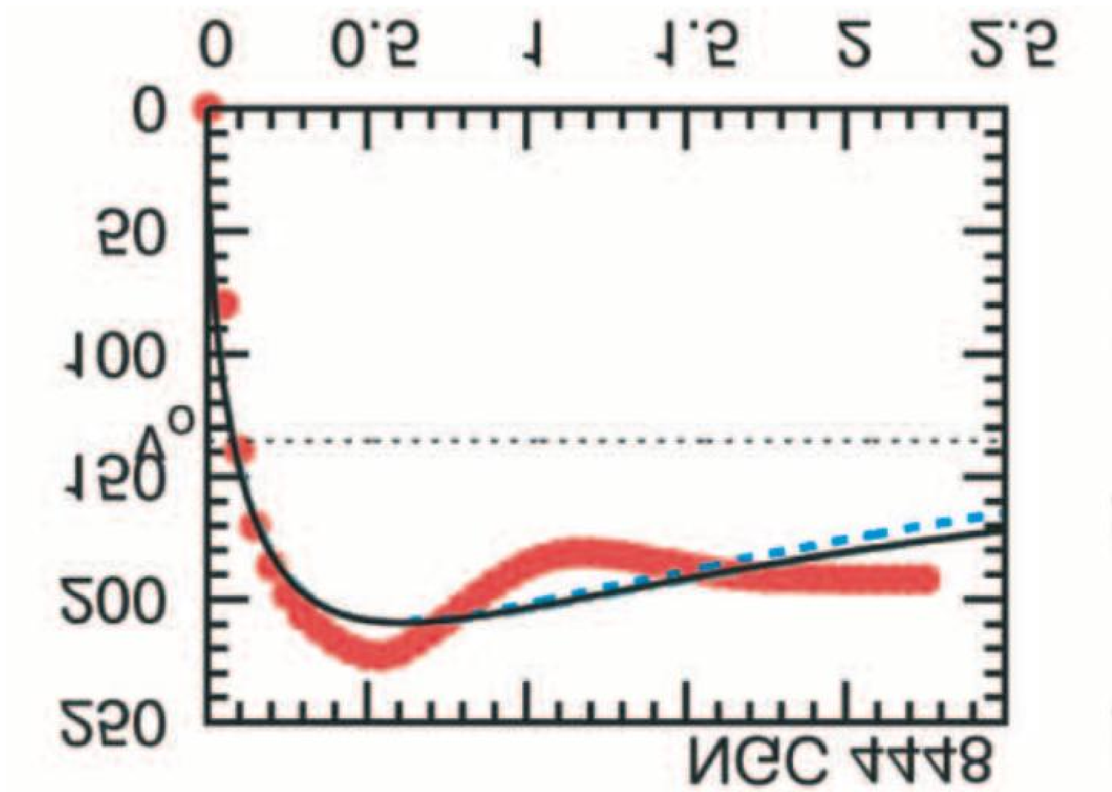

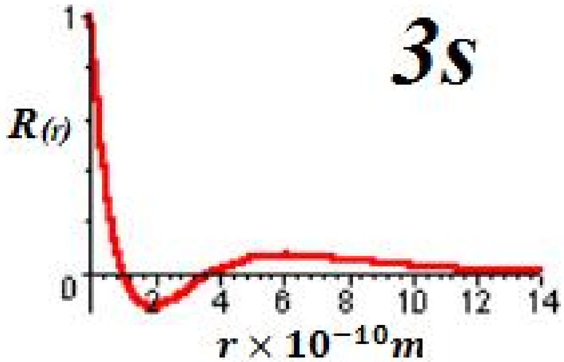

Hydrogen 3s Wave Function

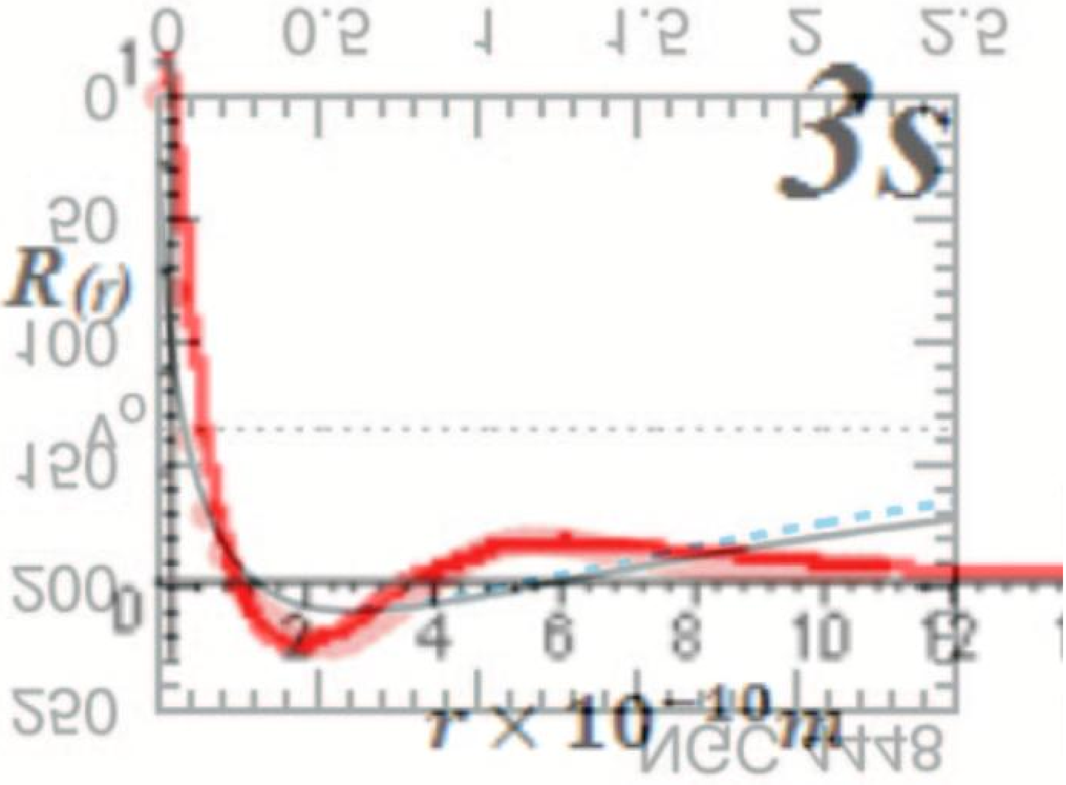

Super imposed graphs

https://www.researchgate.net/figure/Redshift-distribution-of-2MRS-galaxies-Blue-histogram-same-dN-ds-as-in-Fig-1-Curves_fig3_221666162

Redshift distribution of 2MRS galaxies. Blue histogram: same dN/ds as in Fig. 1. Curves: dN/ds predicted from different LF estimators. Black, continuous : Φ Sch. Red, continuos: Φ Spl. Black, dashed Φ V .

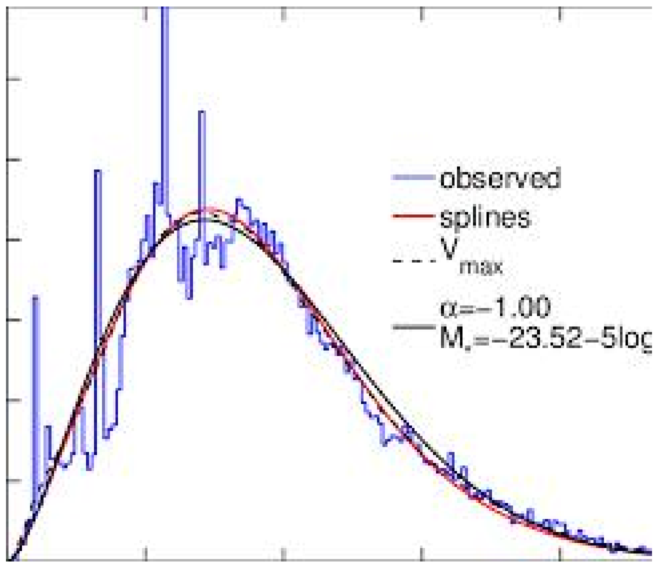

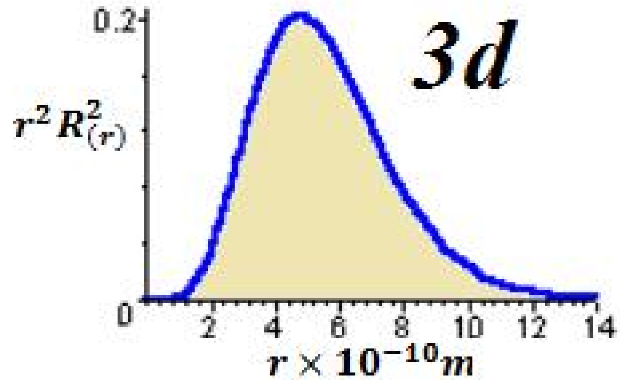

Hydrogen 3d Probability Density

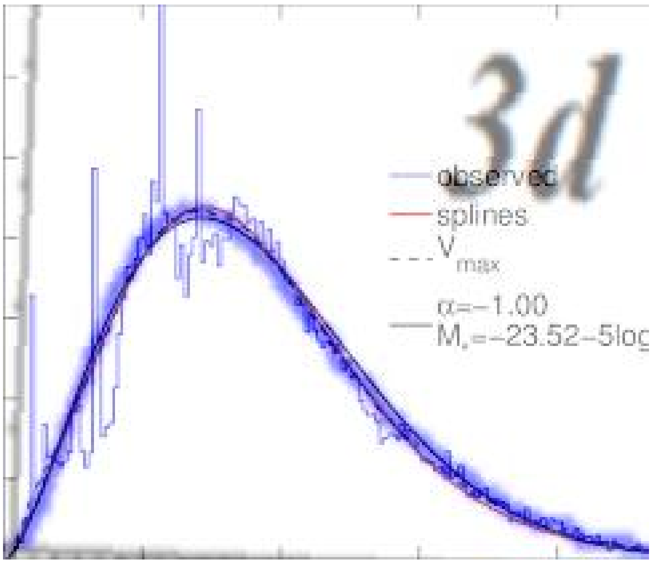

Super imposed graphs

https://www.researchgate.net/figure/Normalized-redshift-distribution-of-GRBs-detectable-with-Swift-ie-with-observed_fig1_51962876

Normalized redshift distribution of GRBs detectable with Swift , i.e. with observed photon flux in excess to P lim = 0 . 4 ph s − 1 cm − 2 . The data show the observed redshift distribution

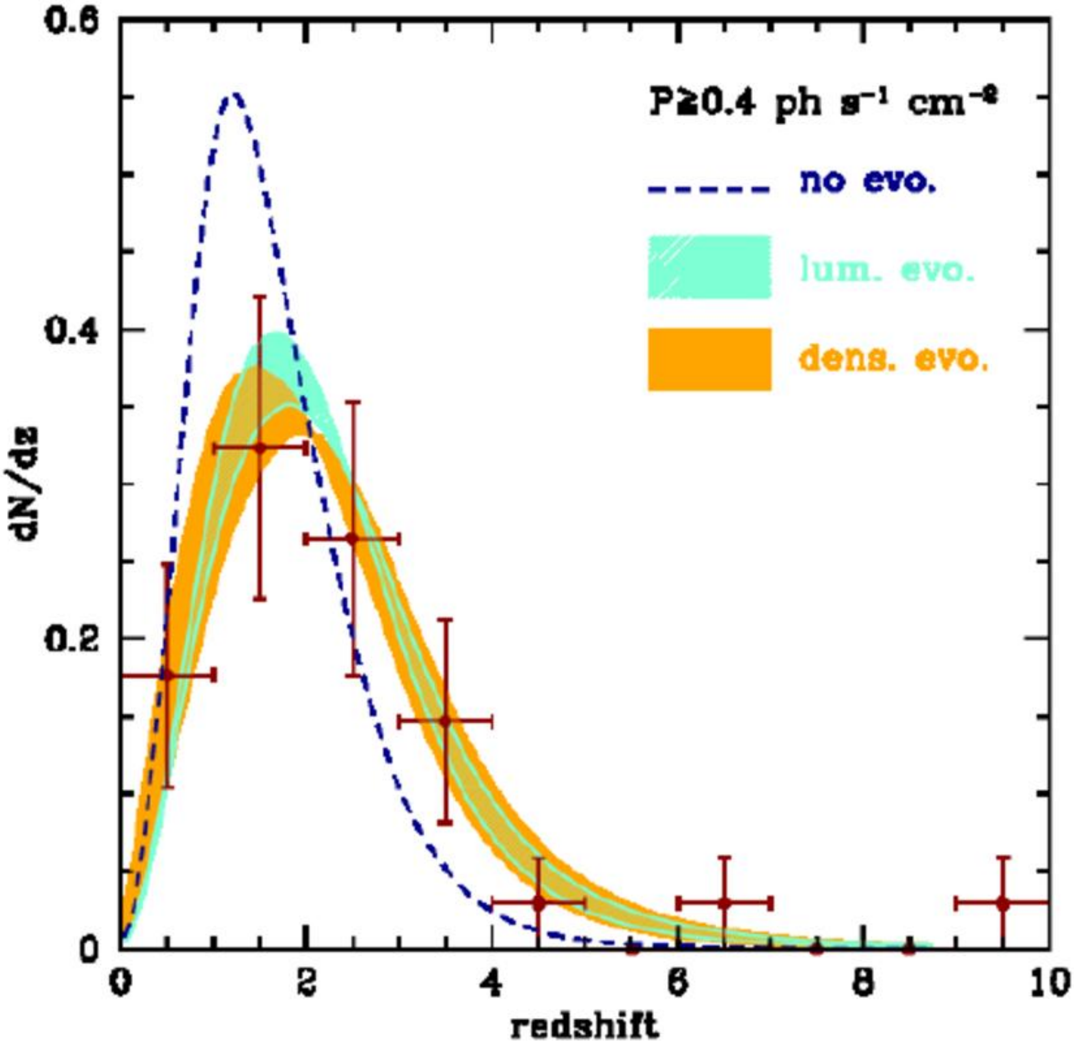

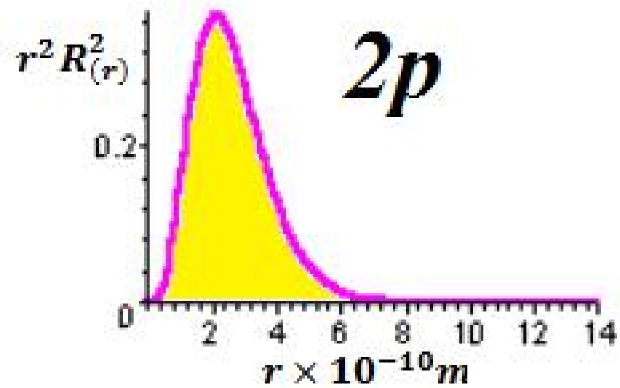

Hydrogen 2p Probability Density

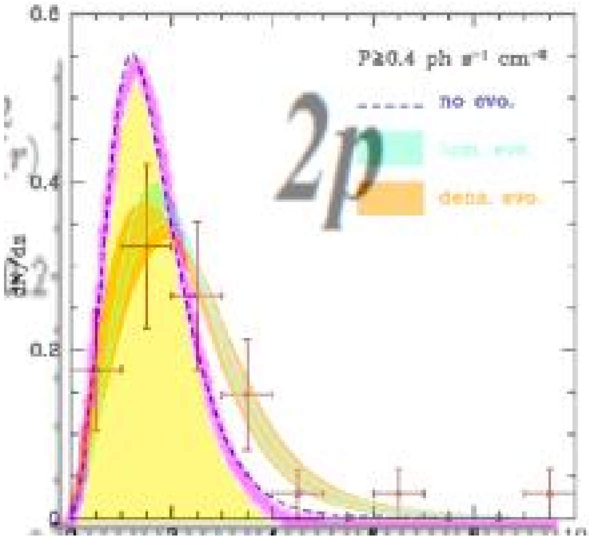

Super imposed graphs

https://link.springer.com/article/10.1140/epjc/s10052-019-6630-x

Constraints on the matter density parameter in the flat DGP model, which are obtained from the lens redshift distribution of current SGL systems with and without the redshift evolution of lensing galaxies. Fitting results from recent observational Hubble parameter data (OHD) are also added for comparison

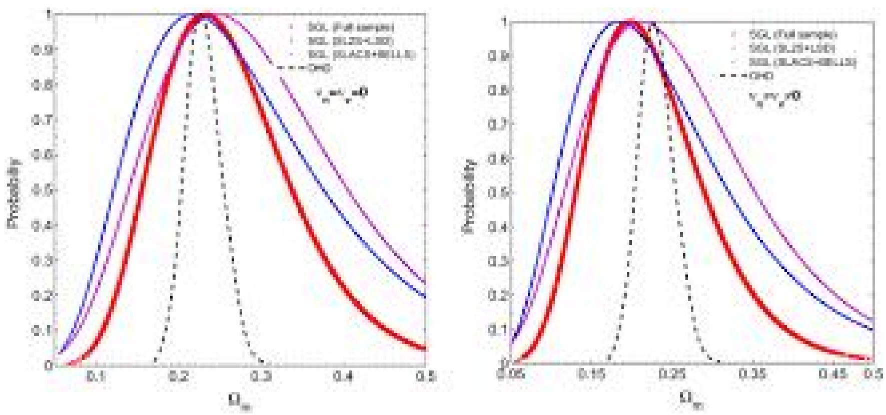

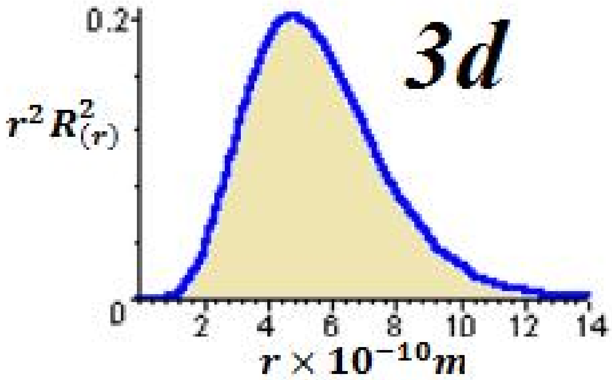

Hydrogen 3d Probability Density

Hydrogen graph expanded with ratio locked and shrunken on x axis

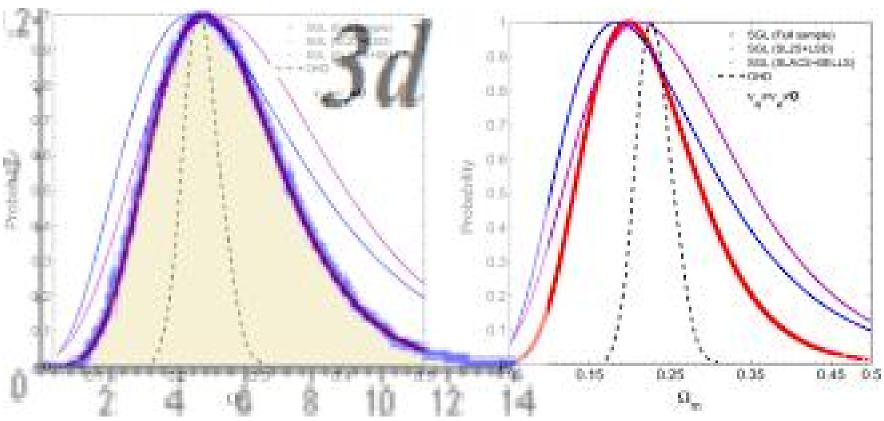

Super imposed graphs

https://www.researchgate.net/figure/Observed-redshift-distribution-of-335-galaxy-clusters-in-the-ISCS-The-curve-a-fit-to_fig1_1922486

Observed redshift distribution of 335 galaxy clusters in the ISCS. The curve, a fit to the distribution, is used in the clustering analysis in §4.

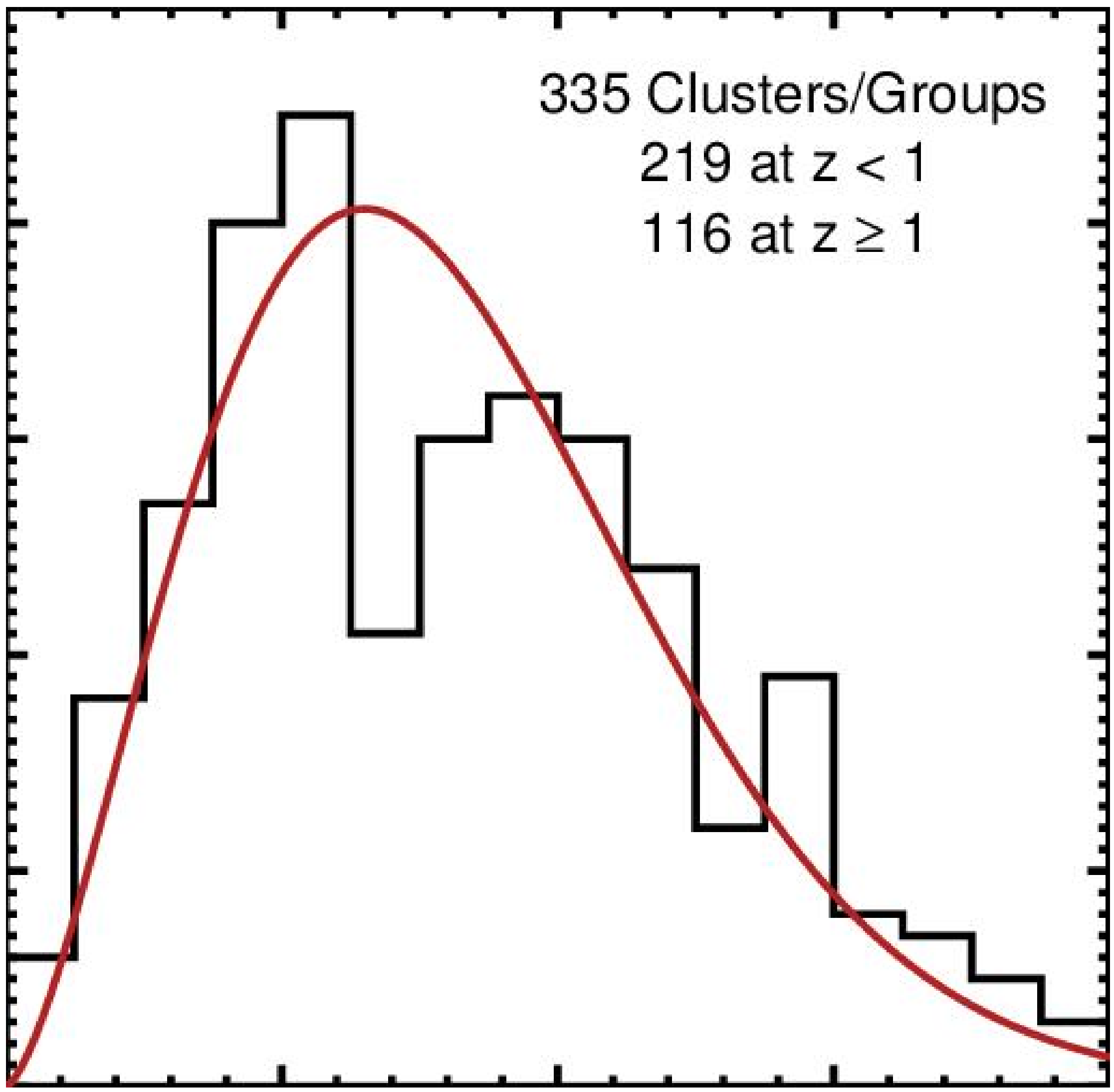

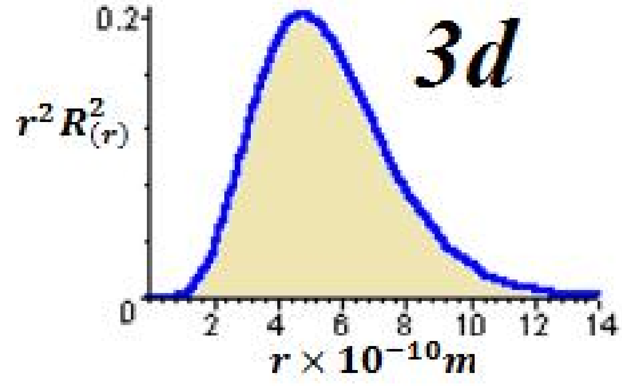

Hydrogen 3d Probability Density

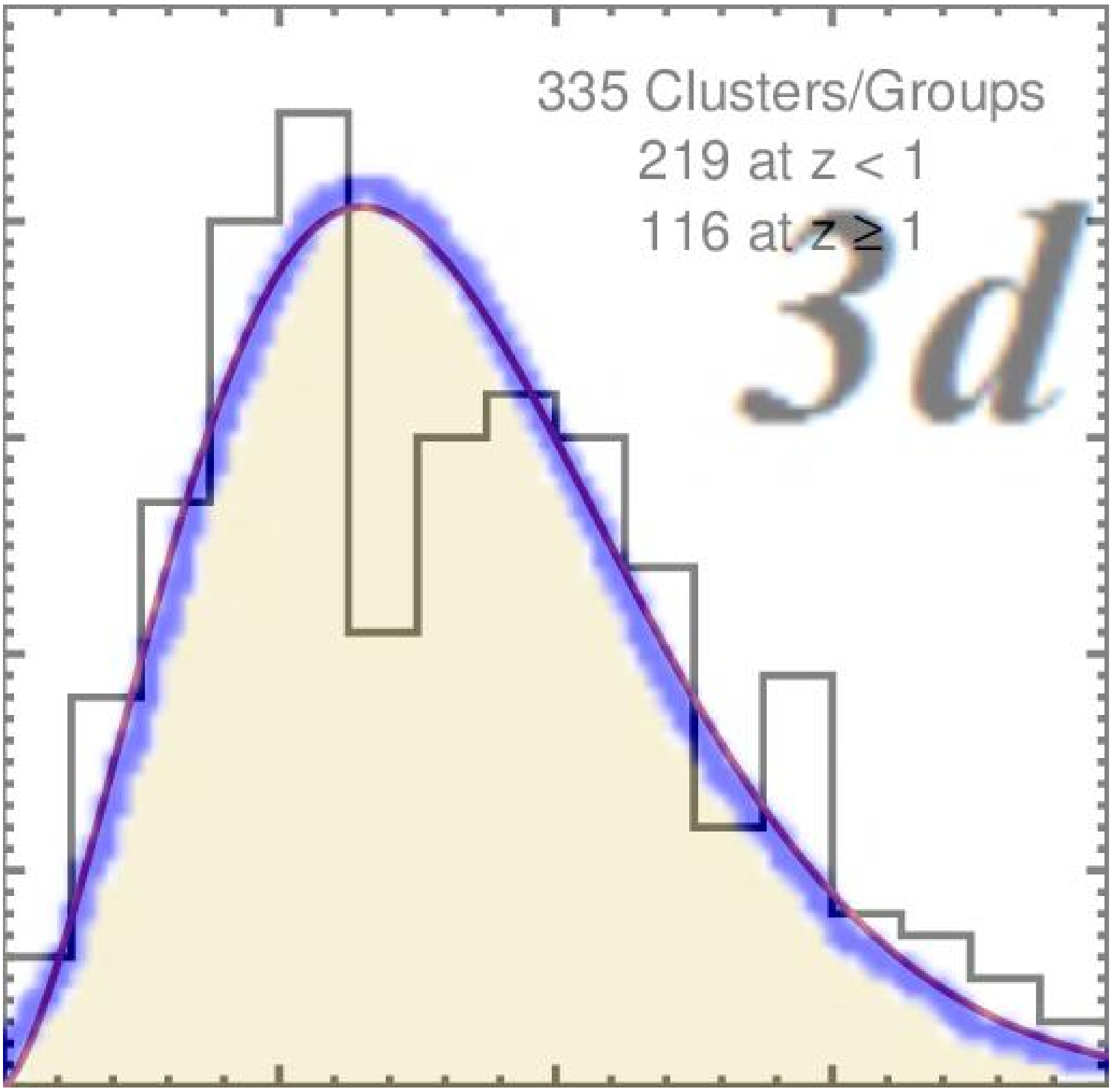

Super imposed graphs

https://www.americanscientist.org/article/why-do-galaxies-start-out-as-cosmic-pickles

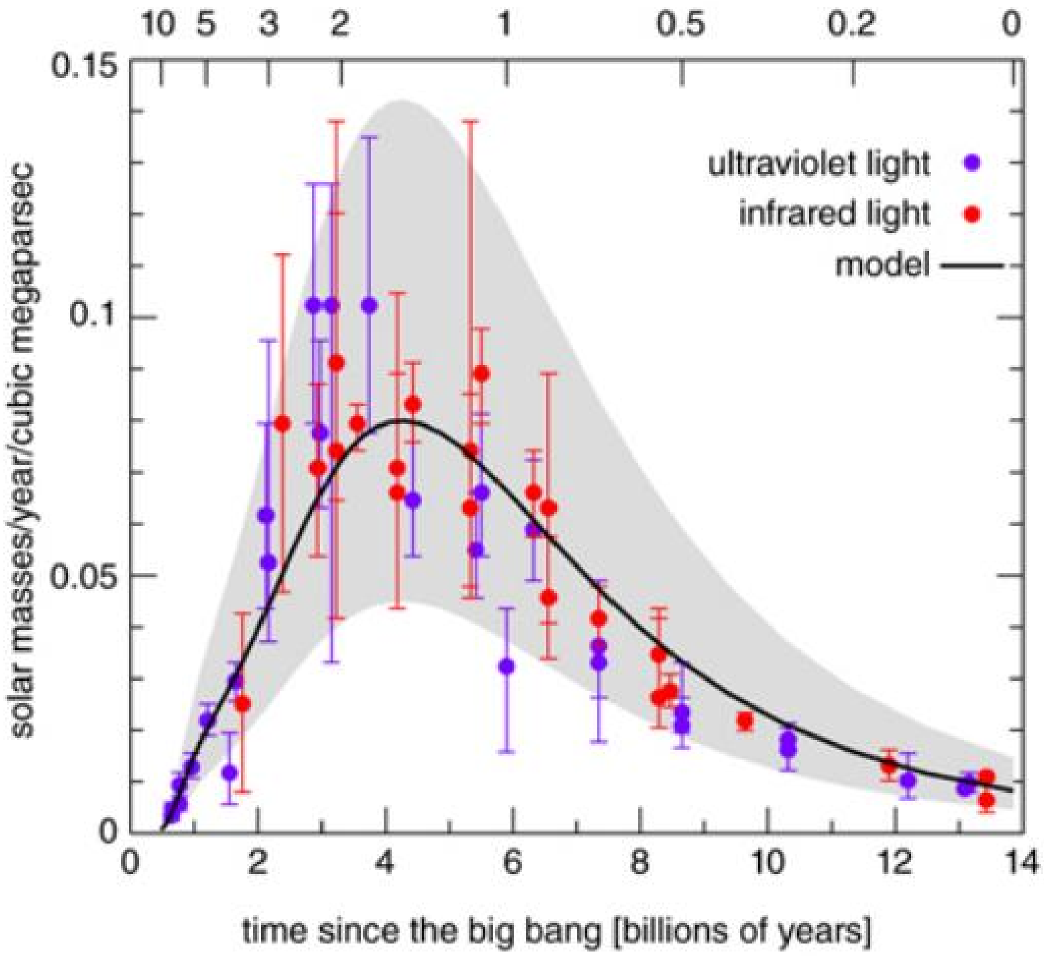

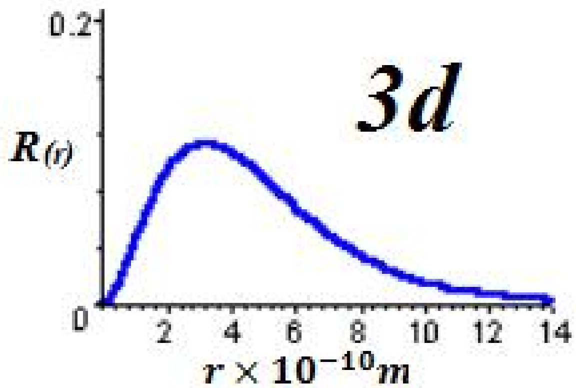

Hydrogen 3d Wave Function

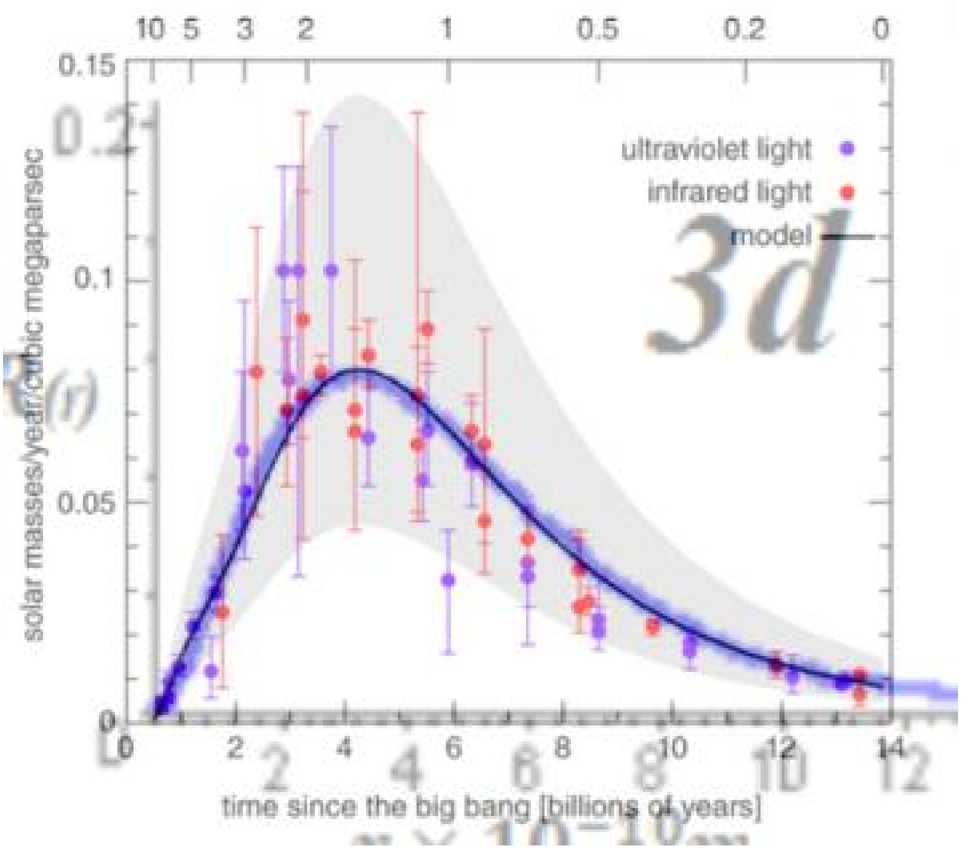

Super imposed graphs

https://indico.ictp.it/event/a04193/session/15/contribution/10/material/0/0.pdf

The power in individual modes is Rayleigh distributed around the mean DISTRIBUTION OF MODE AMPLITUDES RELATIVE TO THE MEAN

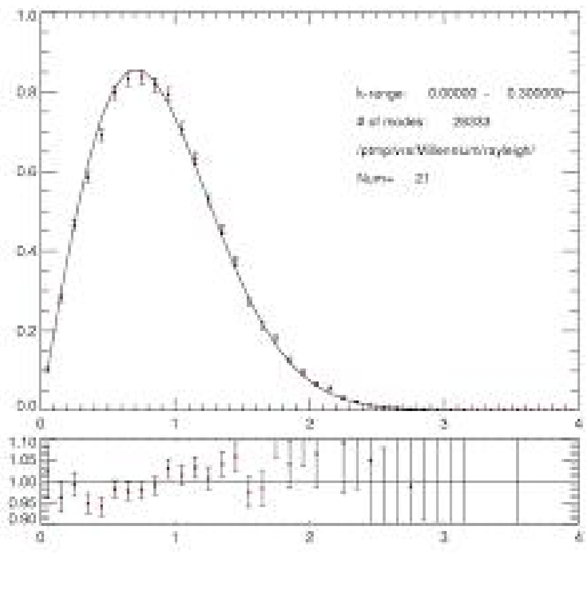

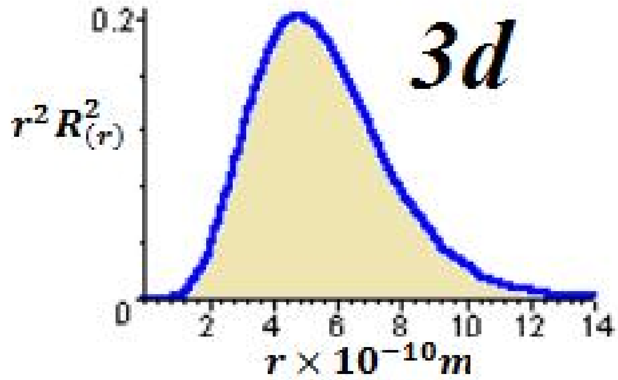

Hydrogen 3d Probability Density

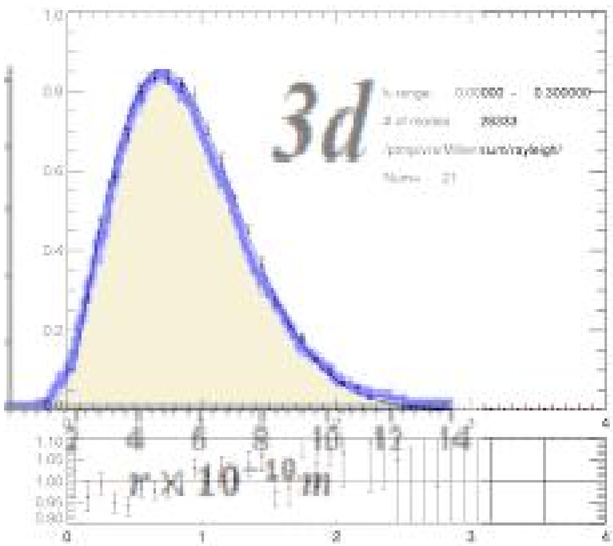

https://www.physics.mcgill.ca/~soudal/docs/SNEWS_CASCA_poster.pdf

Neutrino energy MEV vs Event rate per 0.5 MEV

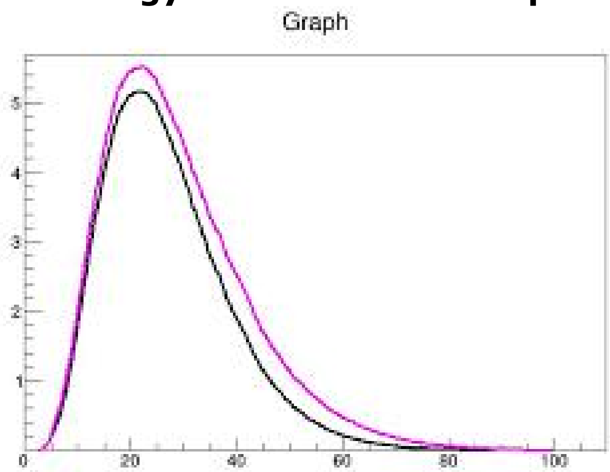

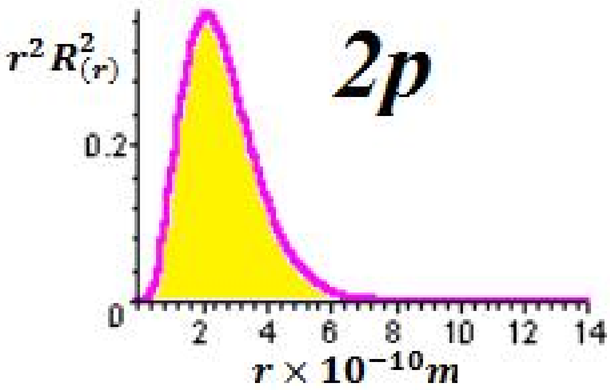

Hydrogen 2p Probability Density

Graph

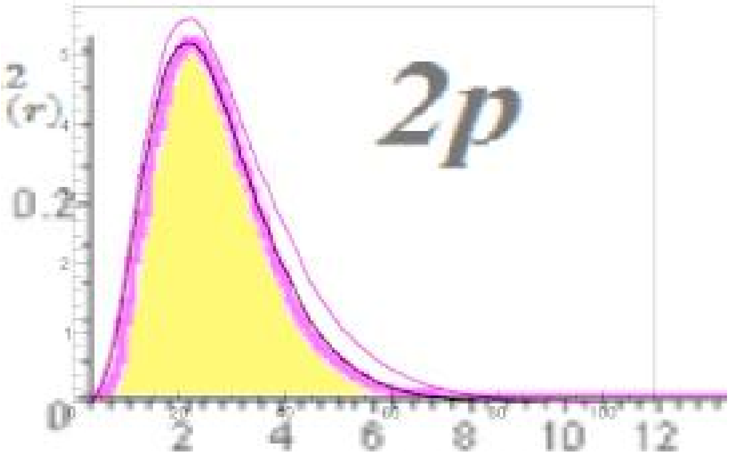

Super imposed graphs

https://iopscience.iop.org/article/10.3847/1538-4357/abb9a6

Probing the Nature of High-redshift Weak Emission Line Quasars: A Young Quasar with a Starburst Host Galaxy

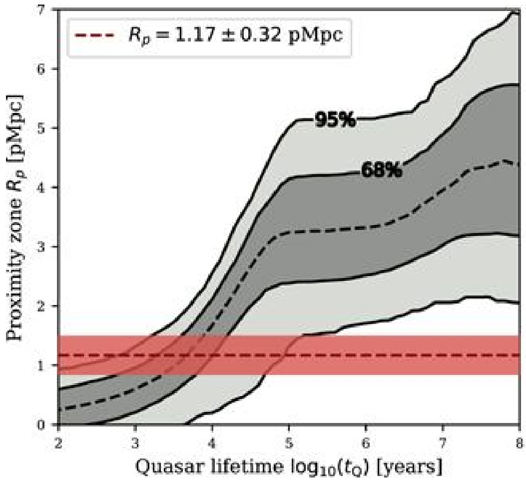

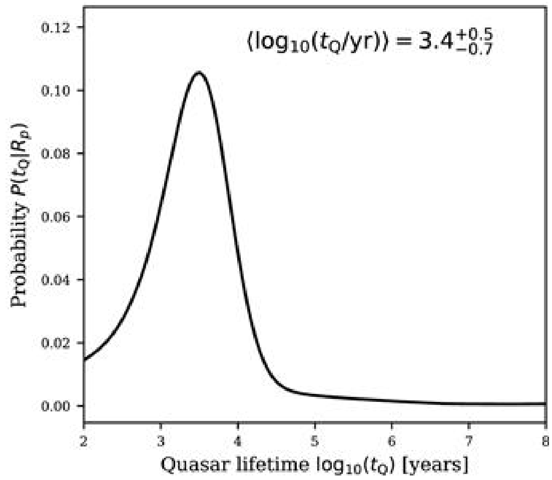

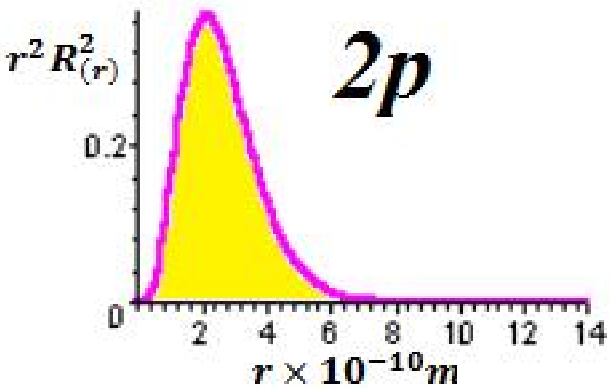

Hydrogen 2p Probability Density

Squished x axis

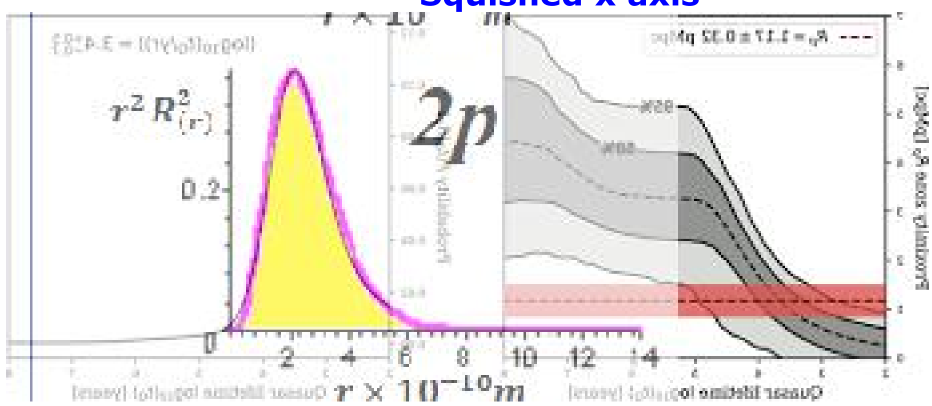

Super imposed graphs

https://iopscience.iop.org/article/10.3847/1538-3881/ab665d/pdf

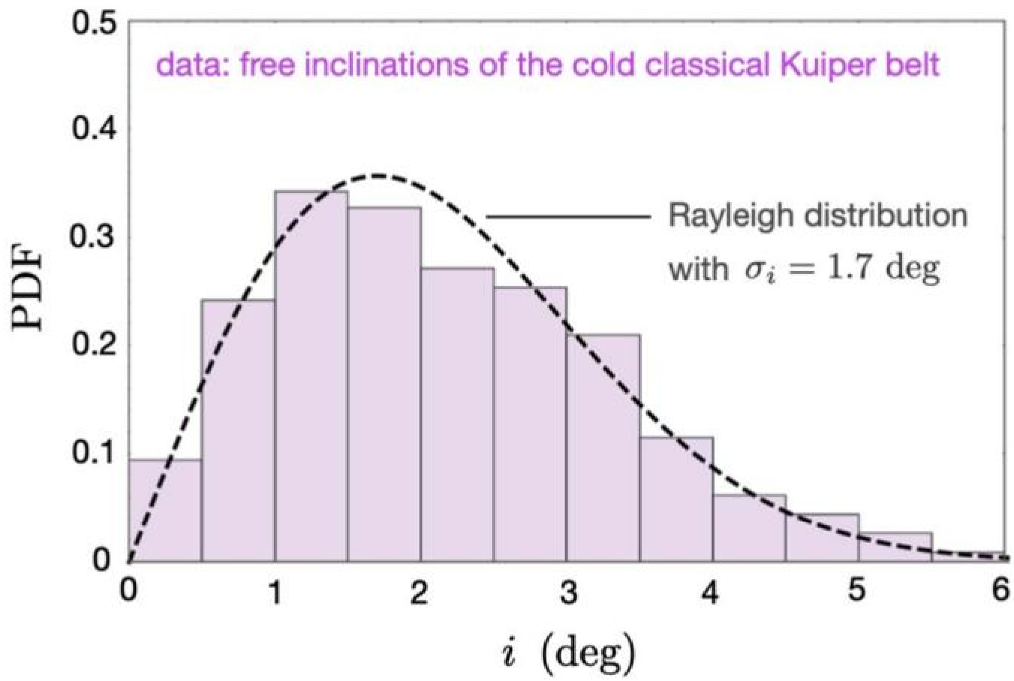

Figure 11. Distribution of free inclinations of the cold classical Kuiper Belt. The observational data—shown here as a purple histogram—are well described by a Rayleigh distribution with a scale parameter of $\sigma_i = 1^\circ.7$.

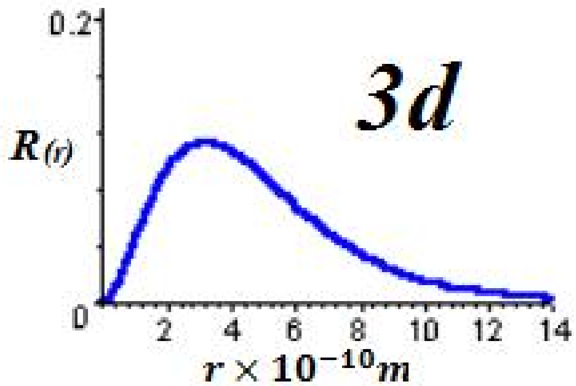

Hydrogen 3d Wave Function

Dynamics of Planetary Systems within Star Clusters

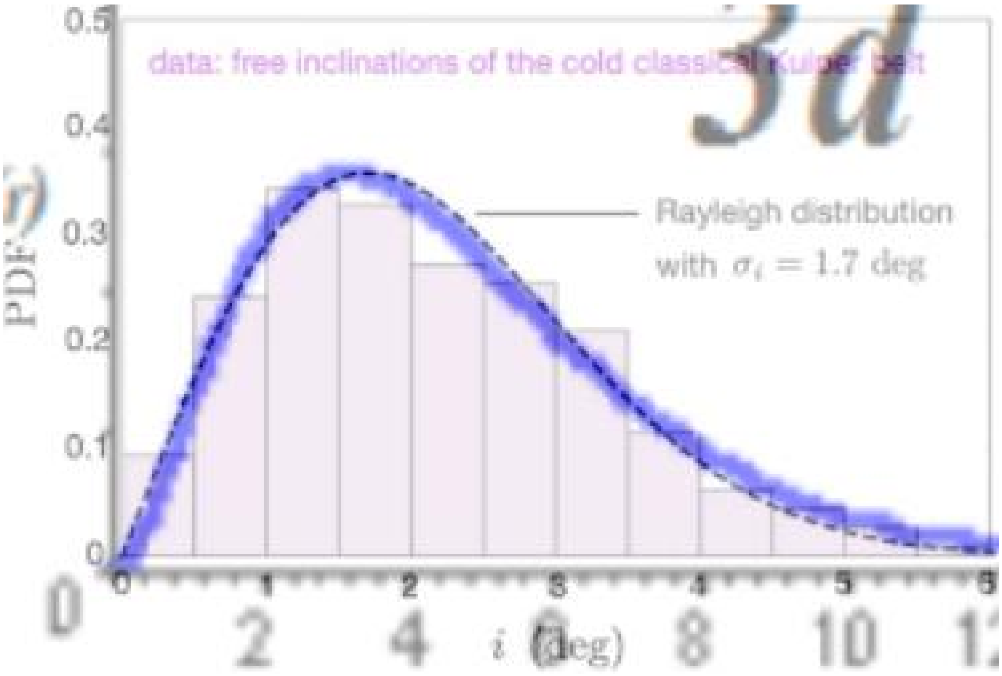

Super imposed graphs

https://www.science.org/doi/10.1126/science.1075631

Age Estimates of Globular Clusters in the Milky Way: Constraints on Cosmology

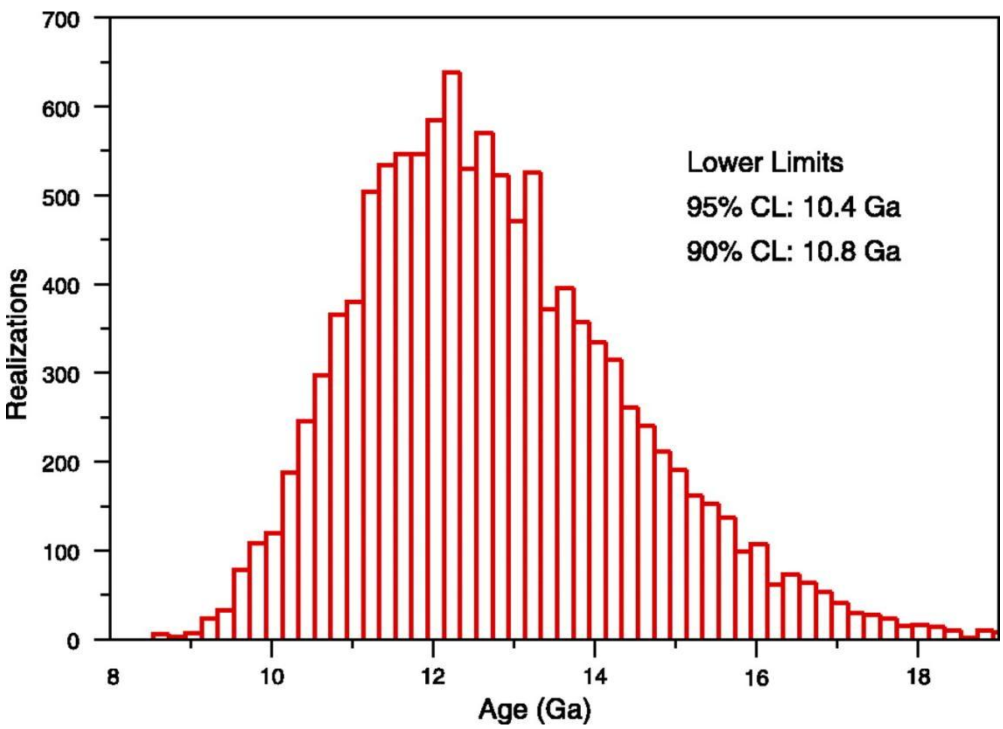

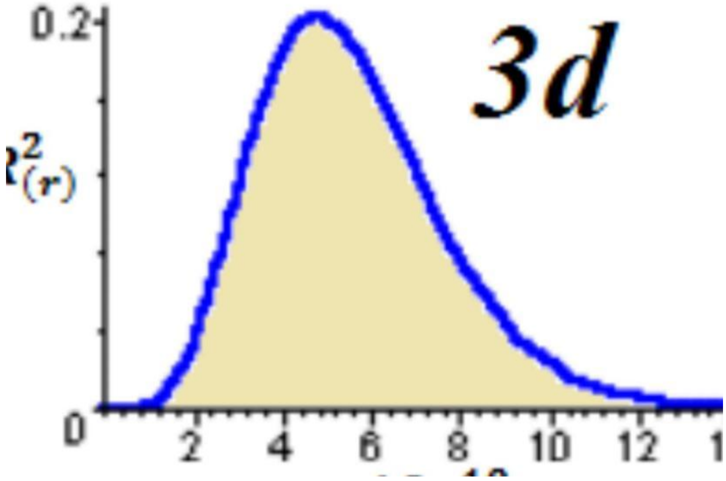

Hydrogen 3d Probability Density

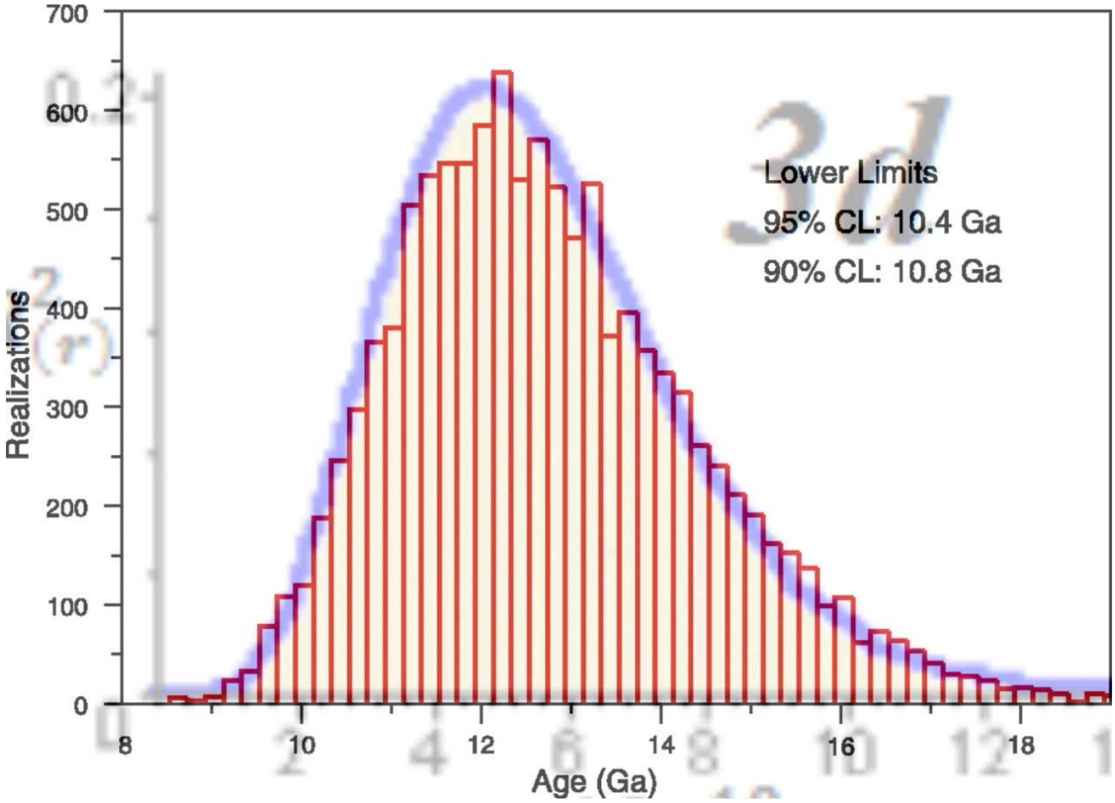

Super imposed graphs

https://arxiv.org/pdf/2110.13070.pdf

Spherical timelike orbits around Kerr black holes

Two physically viable solutions, k1 and k2, at which the discriminant of the polynomial (18) vanishes are plotted as a function of the rotation parameter, u.

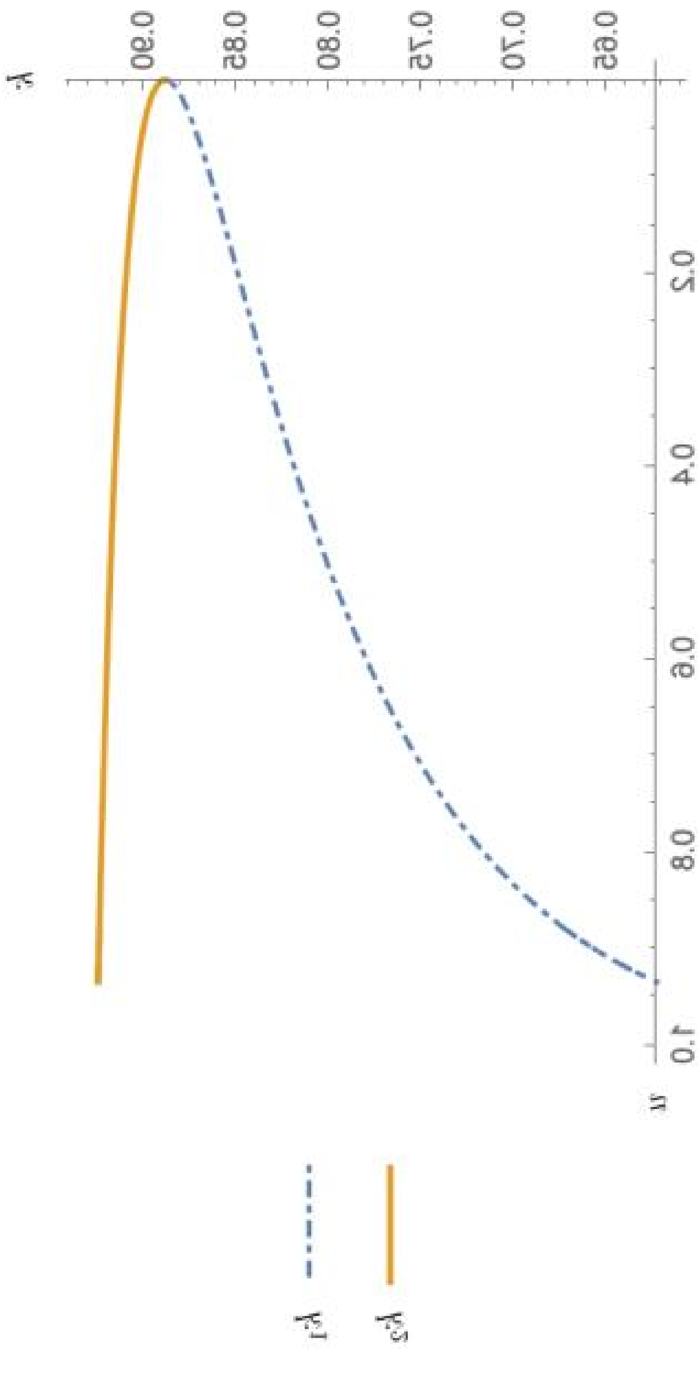

Figure 4: Two physically viable solutions, k_1 and k_2, at which the discriminant of the polynomial (18) vanishes are plotted as a function of the rotation parameter, u.

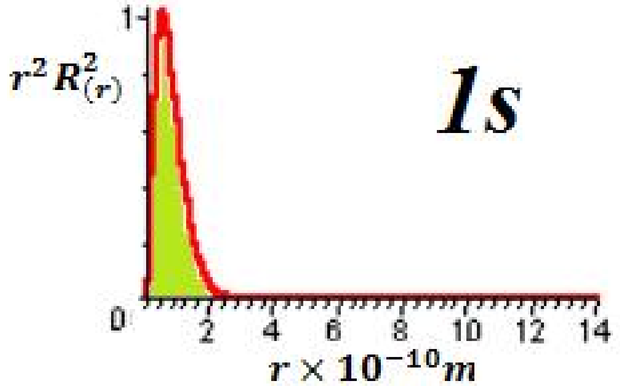

Hydrogen 1s Probability Density

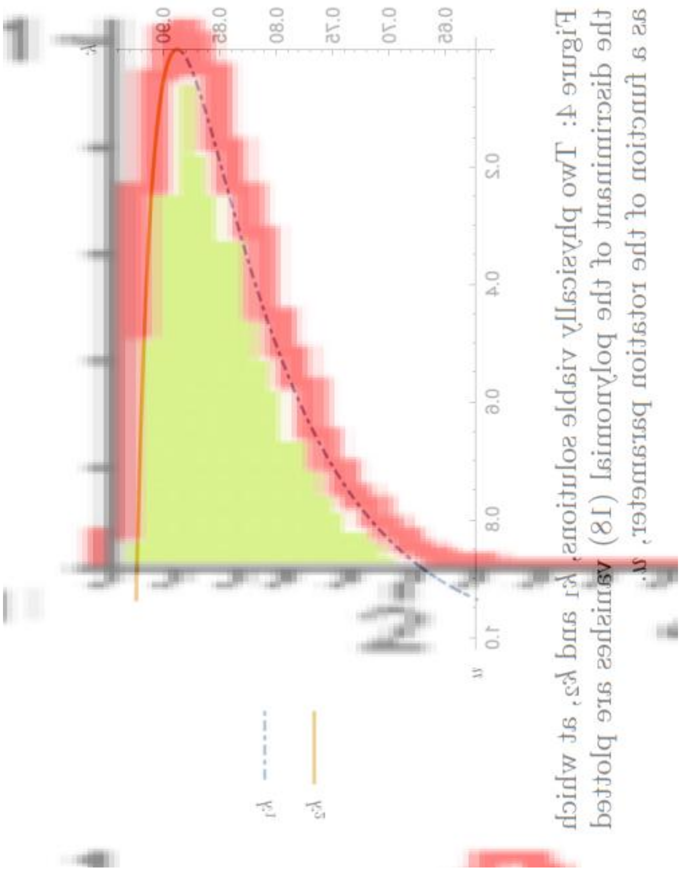

Super imposed graphs

https://www.semanticscholar.org/paper/Hawking-radiation-of-five-dimensional-charged-black-Miao-Xu/ee3d5dad12102723eecea76ff22ffb71828ce3eb

Hawking radiation of five-dimensional charged black holes with scalar fields

Figure 2: (Top) Plots of the power spectrum dE(ω)/(dtdω) with respect to frequency ω at l = 1, e = 1, and rh = 2 for q = −10,−5, and 8, respectively, from left to right. (Down) Plots of the power spectrum dE(ω)/(dtdω) with respect to frequency ω at l = 1, q = 1, and rh = 2 for e = 0, 2.8, and 3.5, respectively, from left to right.

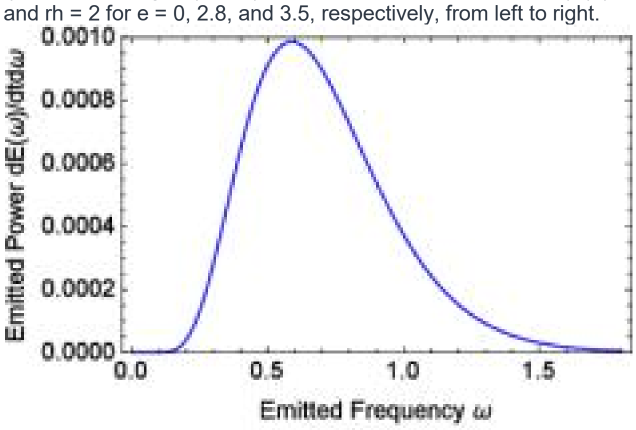

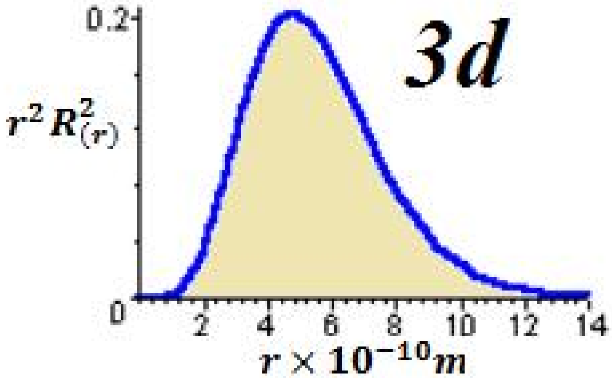

Hydrogen 3d Probability Density

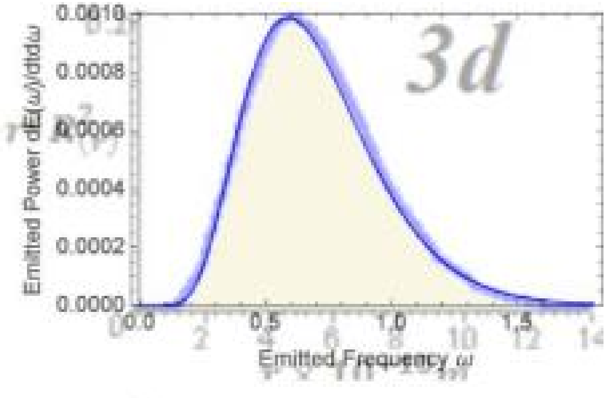

https://www.semanticscholar.org/paper/Photon-ring-and-observational-appearance-of-a-hairy-Gan-Wang/ac4380e6c9e2fa7328dc097bc766ebb27efc4114

Photon ring and observational appearance of a hairy black hole

FIG. 2. Behavior of photons in a HBH with α = 0.9 and Q = 1.03, which is in the single-peak I family, and the observational appearance of an optically and geometrically thin accretion disk around the HBH, viewed from a face-on orientation. Upper Left: The profile of the effective potential, which possesses a single maximum.

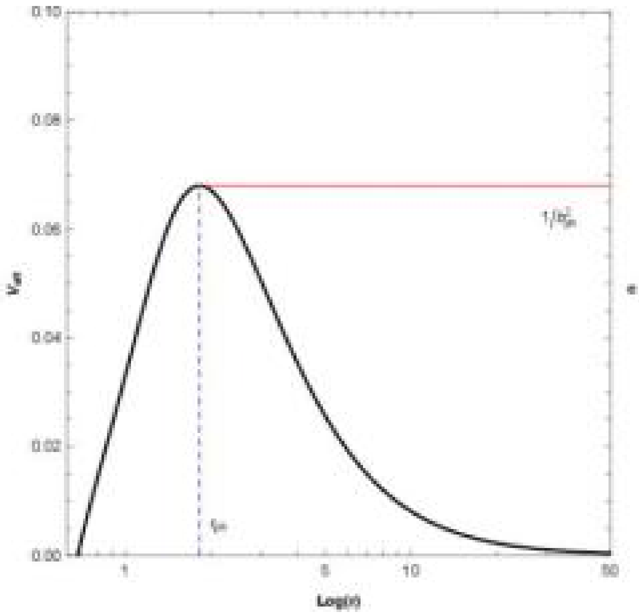

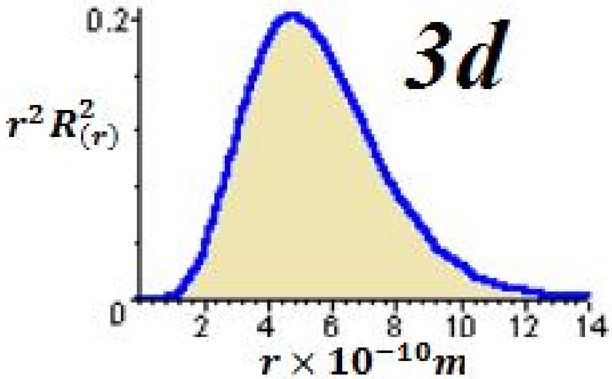

Hydrogen 3d Probability Density

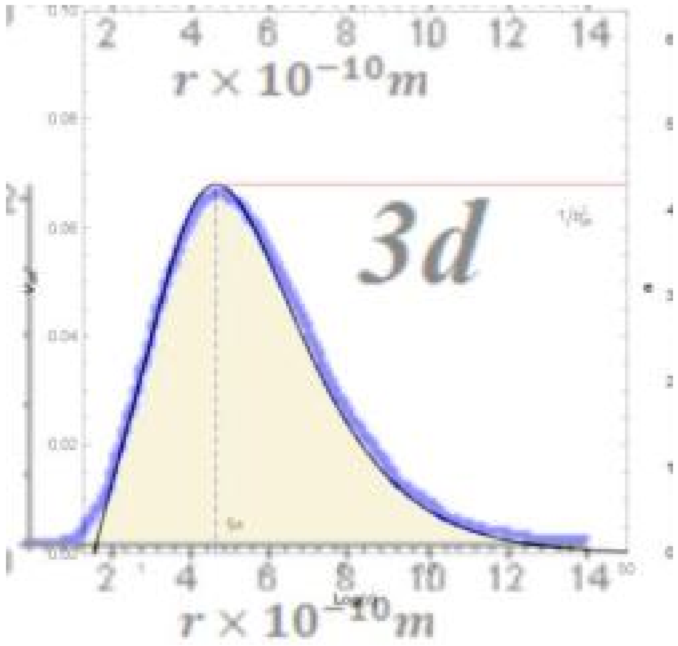

Super imposed graphs

FIG. 1. Left: Regions of four different HBH families in the Q-α plane: single-peak I (green), single-peak II (blue), double-peak I (orange) and double peak II (red). The domain of the HBH solutions is bounded by the existence line (blue) and the critical line (red). The black dashed line and the vertical dashed line denote Qr ≡ (Q − Qexi)/(Qcr − Qexi) = 0.98 and α = 0.9, respectively. Middle: The profiles of the effective potentials at fixed Qr = 0.98 for different α. Right: The profiles of the effective potentials at fixed α = 0.9 for different Qr.

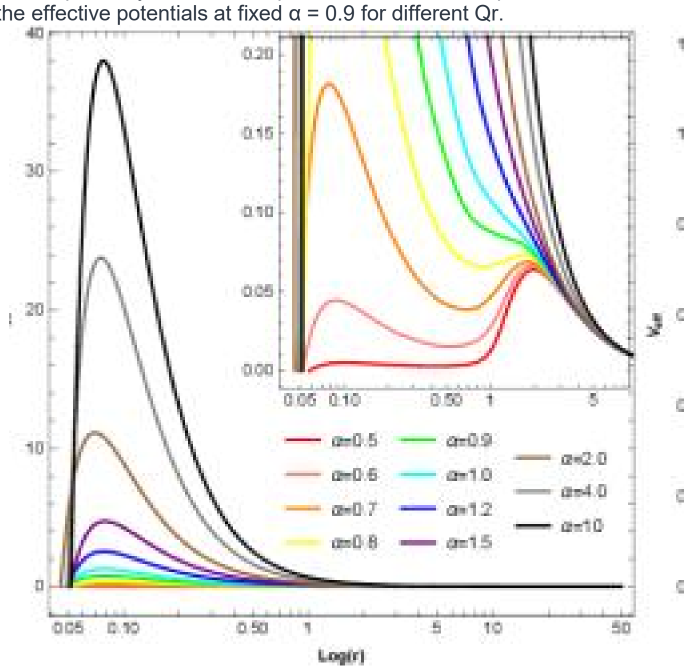

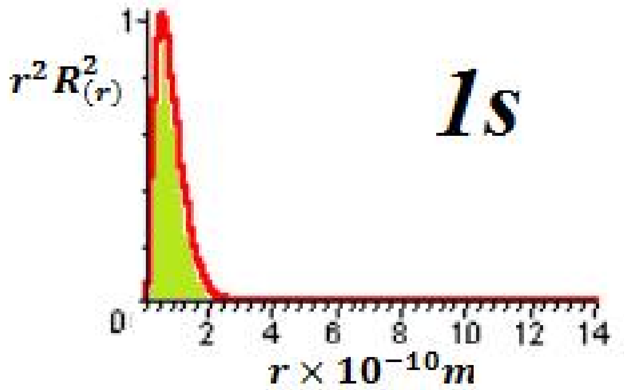

Hydrogen 1s Probability Density

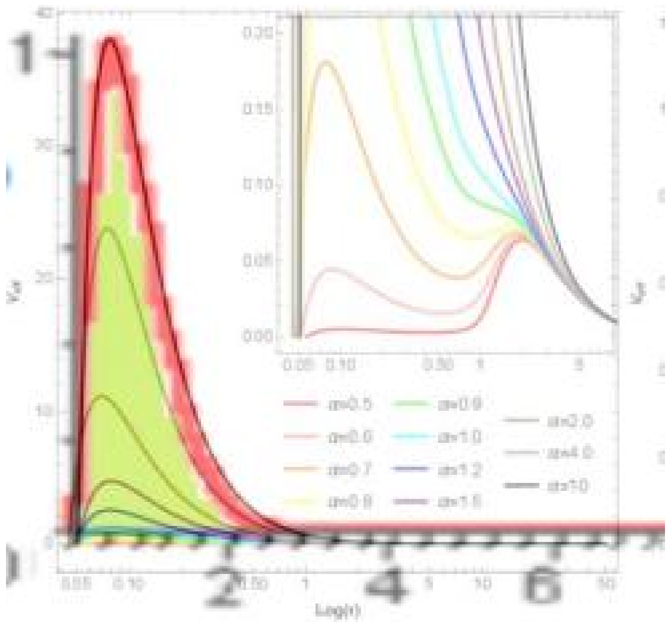

Super imposed graphs

https://www.researchgate.net/figure/Radial-distribution-in-the-Galactic-plane-of-the-CR-source-models-employed-in-this-work_fig1_316728846

Radial distribution in the Galactic plane of the CR source models employed in this work. In black, distributions from Ackermann et al. (2012): the pulsars (PSRs) distribution by Lorimer et al. (2006) used in the Sample Model, the alternative PSRs distribution by Yusifov & Küçük (2004), the OB stars distribution from Bronfman et al. (2000), and the SNRs distribution from Case & Bhattacharya (1998). In red the source models in the inner Galaxy introduced in our work: sources in the bulge (azimuthal average) following the distribution of the old stellar population as in model B from Robin et al. (2012), and sources in the central molecular zone (CMZ) following the distribution of molecular gas fromFerrì ere et al. (2007). The source distributions are independently

normalized for display.

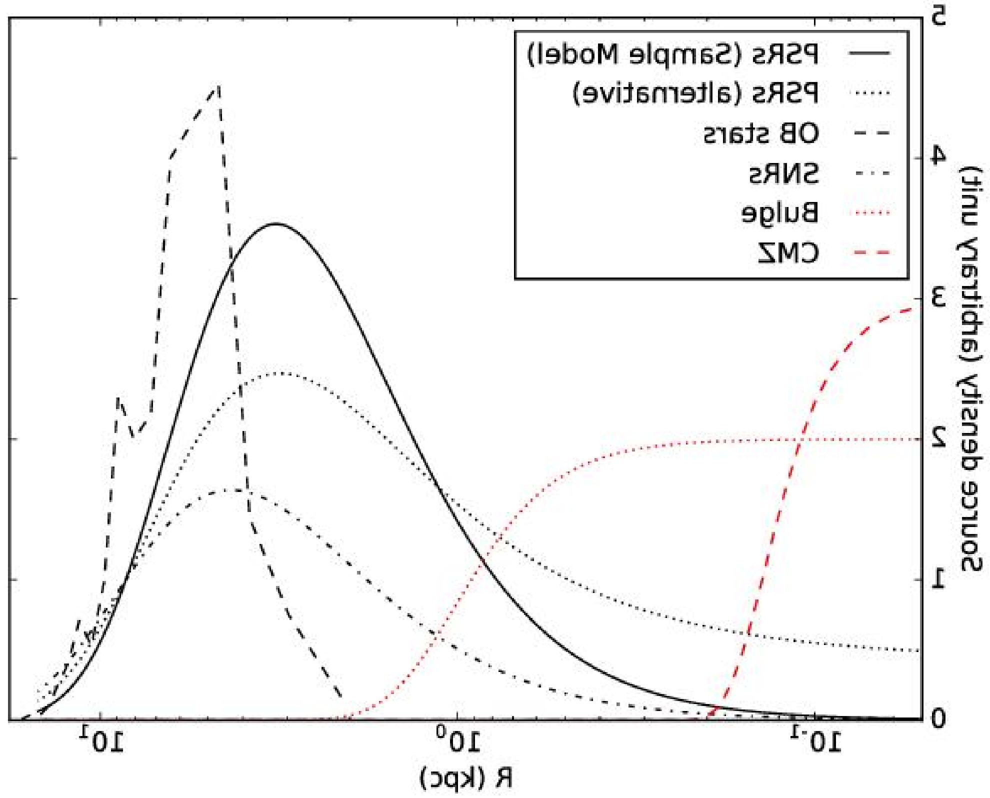

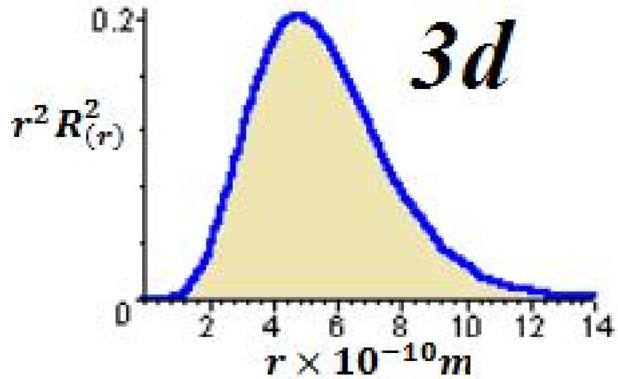

Hydrogen 3d Probability Density

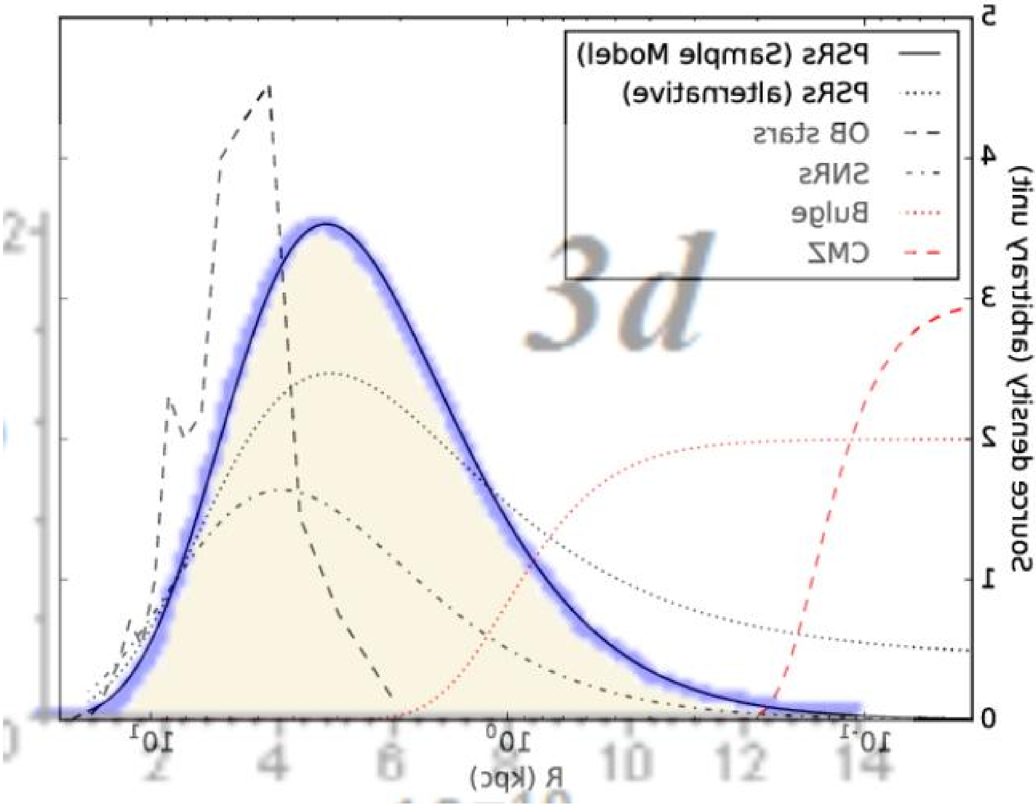

Super imposed graphs

https://arxiv.org/pdf/1808.05114.pdf

A quantitative analysis of systematic differences in positions and proper motions of Gaia DR2 with respect to VLBI

Figure 5. The distribution of normalized VLBI/Gaia arc-lengths over 2313 matched sources. The sample includes all the sources with known jet directions and excludes the sources with $\psi \in [-0.5, -0.5]$ and $\psi \in [\pi-0.5, \pi+0.5]$ rad. Scaling factors 1.05 and 1.30p $\chi 2$/ndf were applied to Gaia and VLBI. The blue smooth curve shows Rayleigh distribution with $\sigma = 1$.

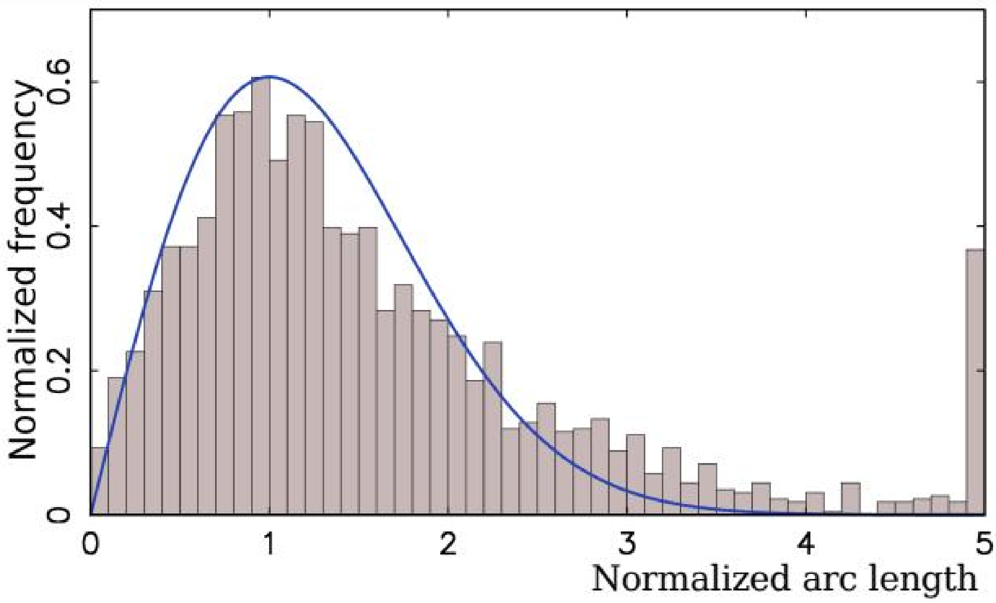

Figure 5. The distribution of normalized VLBI/Gaia arc-lengths over 2313 matched sources. The sample includes all the sources with known jet directions and excludes the sources with $\psi \in [-0.5, -0.5]$ and $\psi \in [\pi - 0.5, \pi + 0.5]$ rad. Scaling factors 1.05 and $1.30\sqrt{\chi^2/\text{ndf}}$ were applied to Gaia and VLBI. The blue smooth curve shows Rayleigh distribution with $\sigma = 1$.

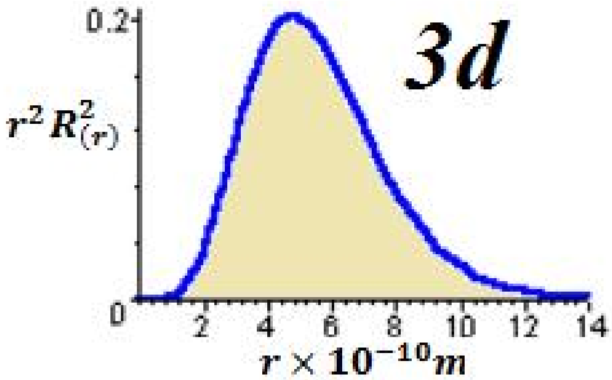

Hydrogen 3d Probability Density

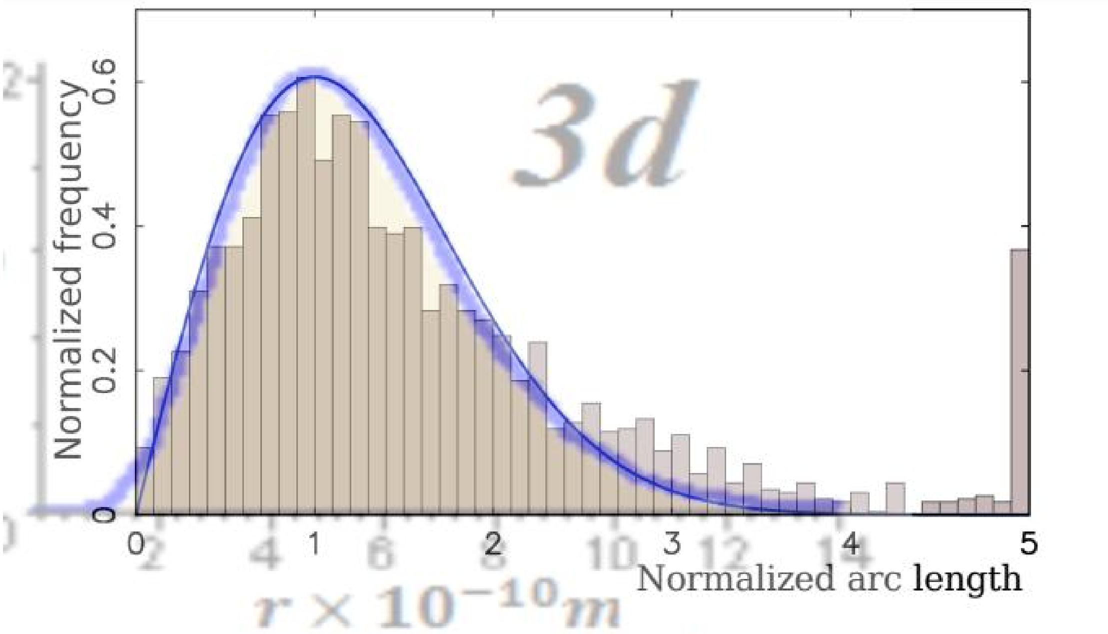

Figure 5. The distribution of normalized VLBI/Gaia arc-lengths over 2313 matched sources. The sample includes all the sources with known jet directions and excludes the sources with $\psi \in [-0.5, -0.5]$ and $\psi \in [\pi - 0.5, \pi + 0.5]$ rad. Scaling factors 1.05 and $1.30\sqrt{\chi^2/\text{ndf}}$ were applied to Gaia and VLBI. The blue smooth curve shows Rayleigh distribution with $\sigma = 1$.

Super imposed graphs

https://royalsocietypublishing.org/doi/10.1098/rsta.2016.0271

The mechanism(s) of core-collapse supernovae

Figure 2. Average shock radii from the 1D and 2D CCSN simulations of O' Connor & Couch [49] for four progenitors from [68], along with the 15 M model from Woosley & Weaver [51]. Models s15, s20 and s25 all explode within about one second post-

bounce.

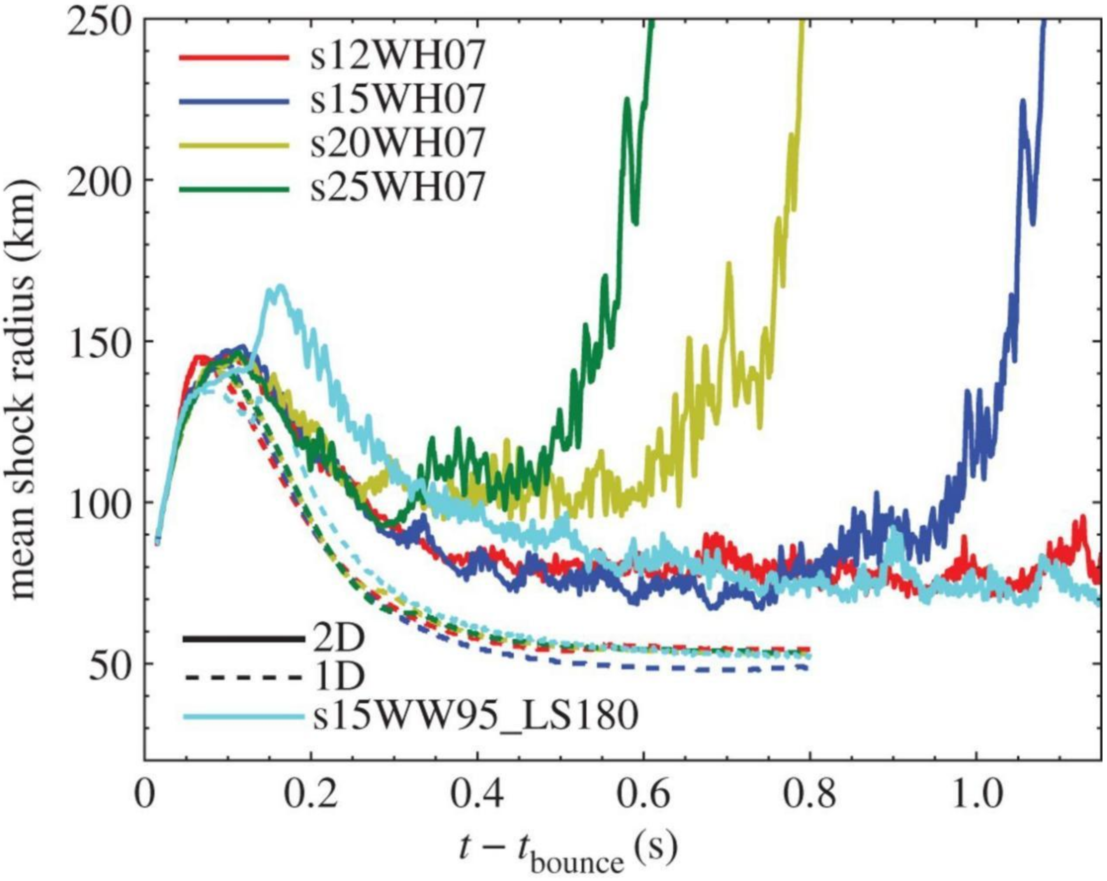

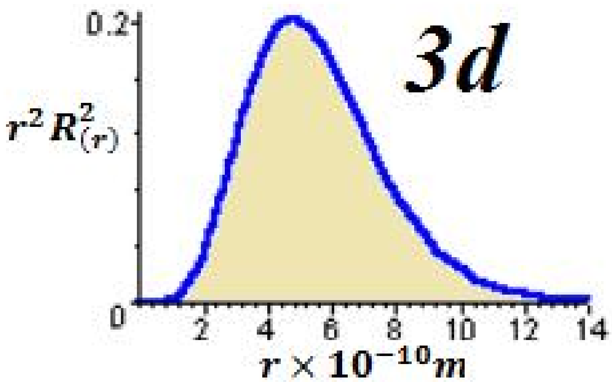

Hydrogen 3d Probability Density

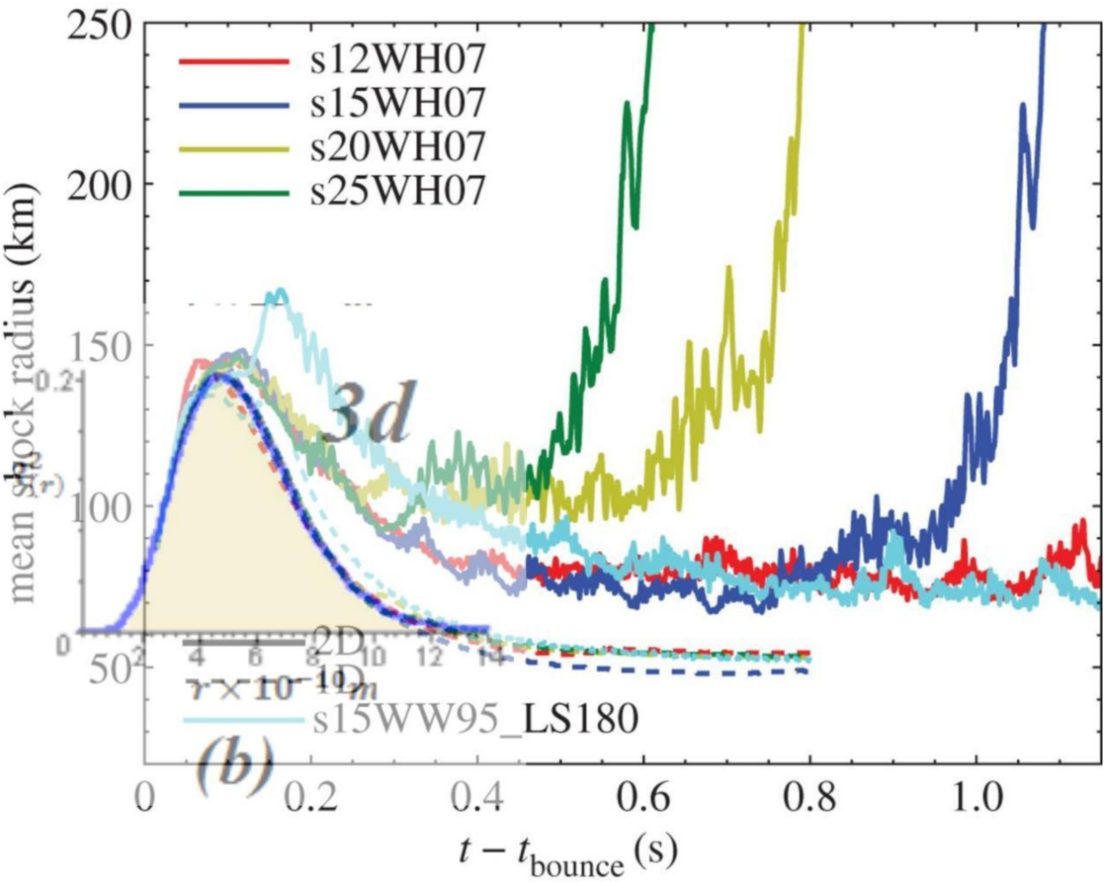

Super imposed graphs

The Mach's Principle and large-scale modification of Newtonian gravitation as alternative approach to Cold Dark matter and Dark Energy

Figure 1. *The Yukawa-like potential, complementary contribution to the inverse-square law, in comoving scale, at several astronomical ranges (Own source).*

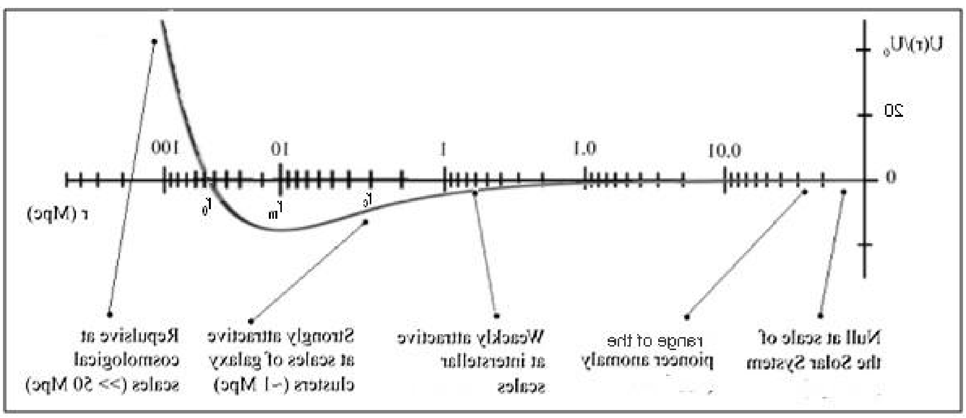

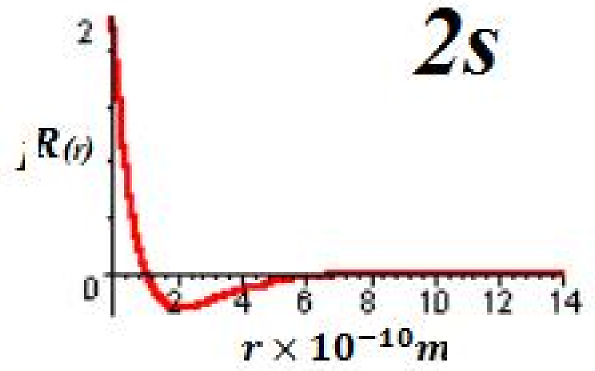

Hydrogen 2s Wave Function

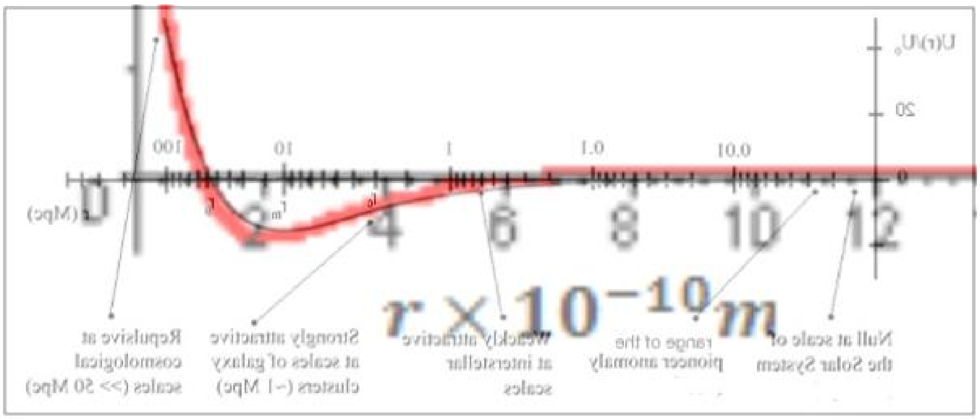

Super imposed graphs

https://digital.csic.es/bitstream/10261/269350/1/earthmatter.pdf

EARTH-STOPPING OF MILLICHARGED DARK MATTER

Figure 1.1. Optically studied rotation curve of ionized hydrogen in the Andromeda galaxy (M31), Rubin and Ford

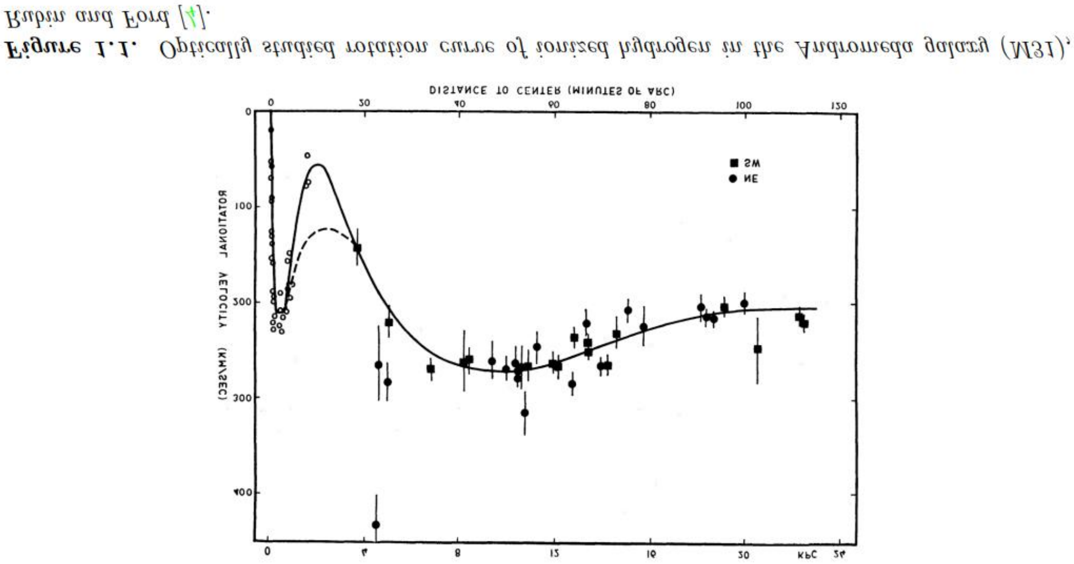

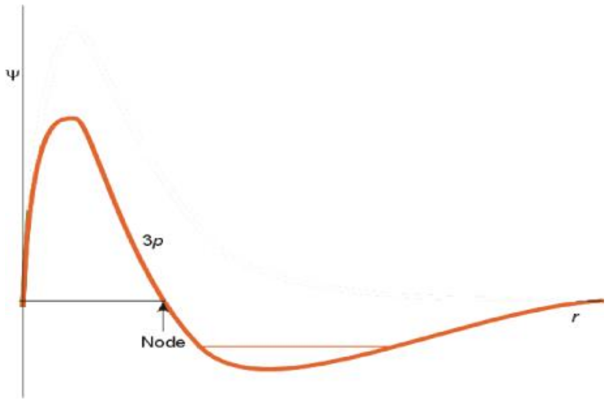

Hydrogen 3p Wave Function

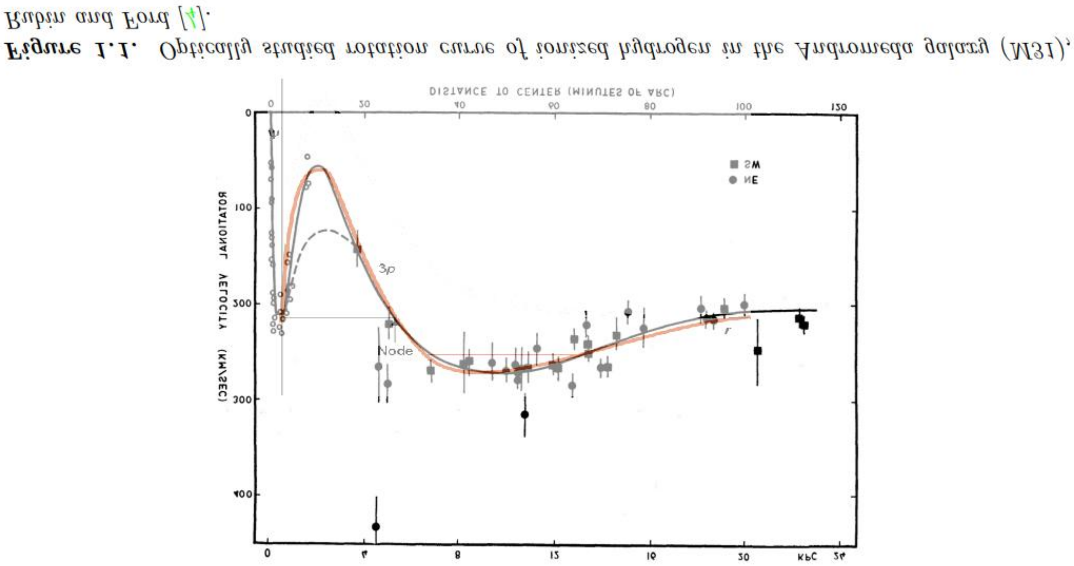

Super imposed graphs

https://www.mdpi.com/1099-4300/24/3/385/htm

Information Dark Energy can resolve Hubble tension and is falsifiable by experiment.

Difference in
Hubble parameter, $H(a)$ to be expected for an information energy source of dark energy relative to
that due to a cosmological constant. Both plots assume the power law fits to Fig. 1 data.

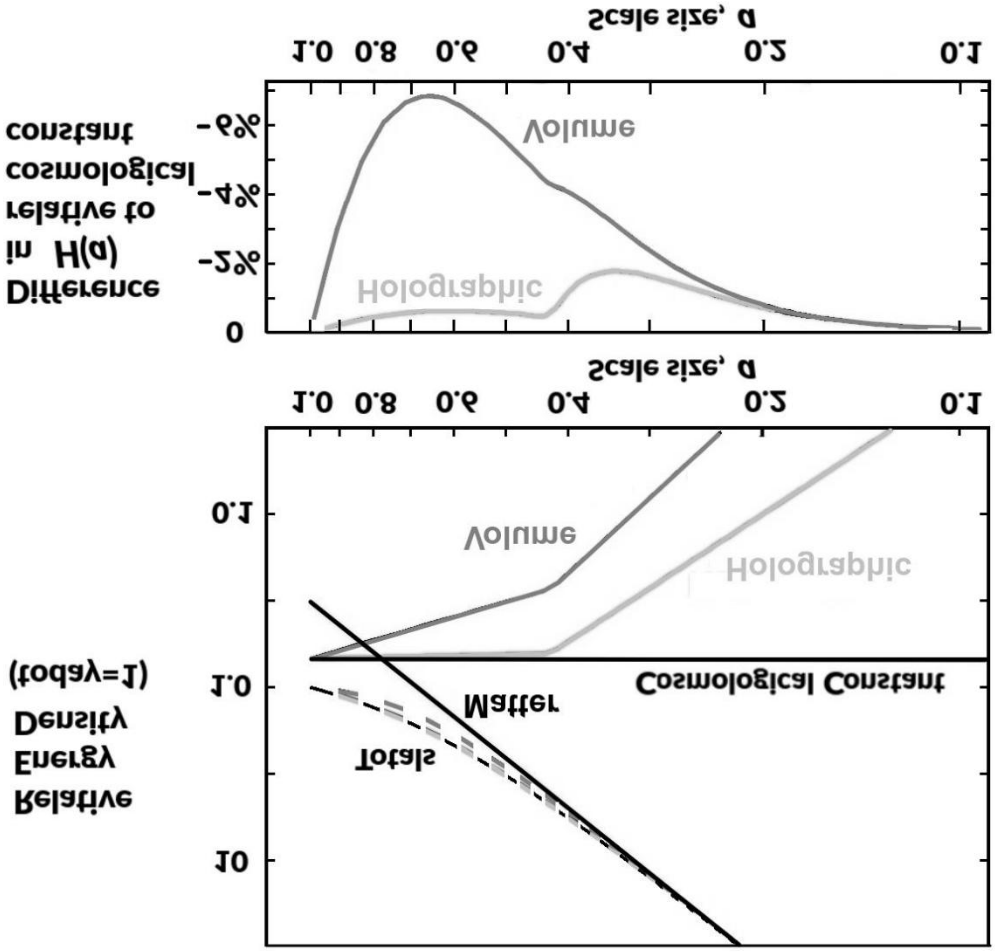

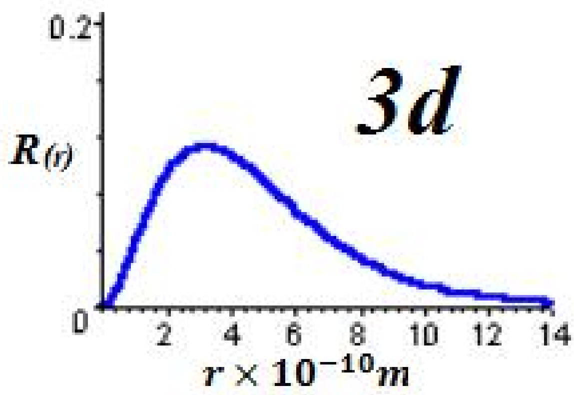

Hydrogen 3d Probability Density

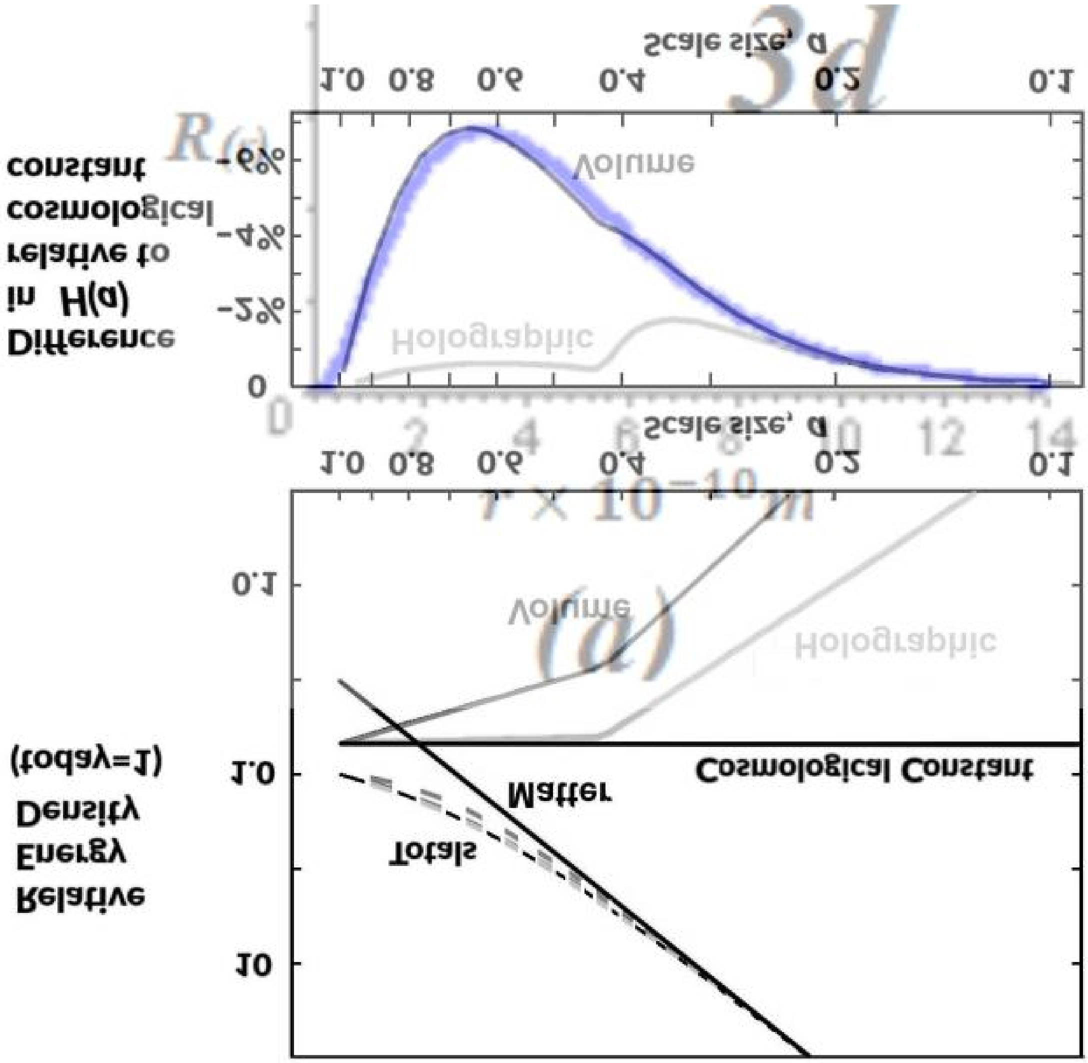

Super imposed graphs

https://physicstoday.scitation.org/doi/10.1063/1.3120896

Introducing the black hole

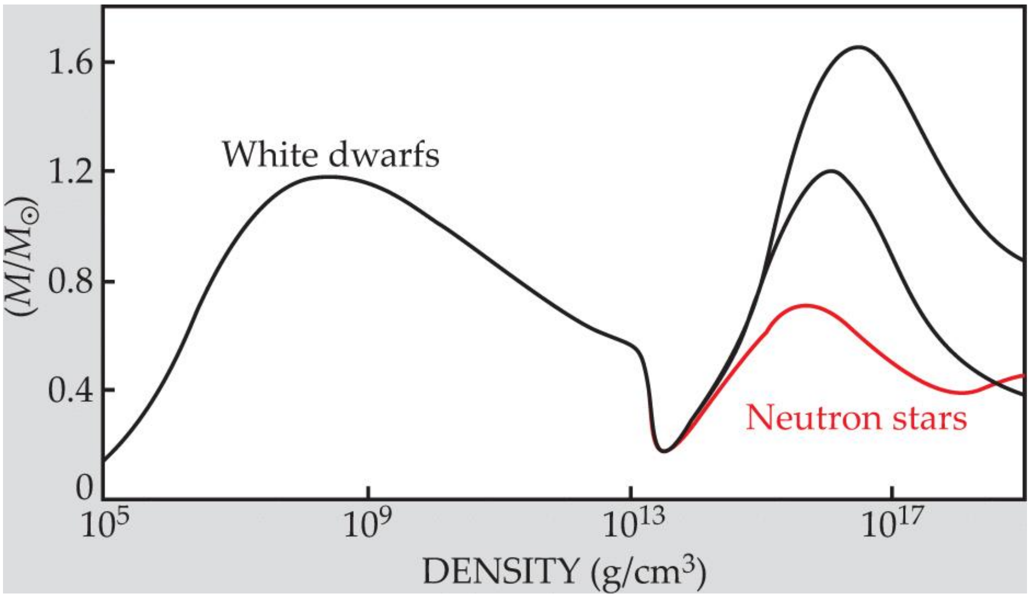

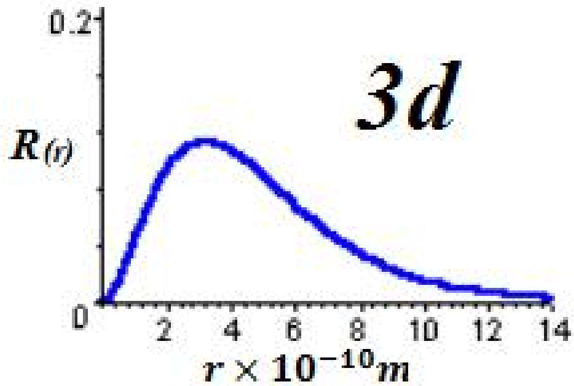

Hydrogen 3d Wave Function

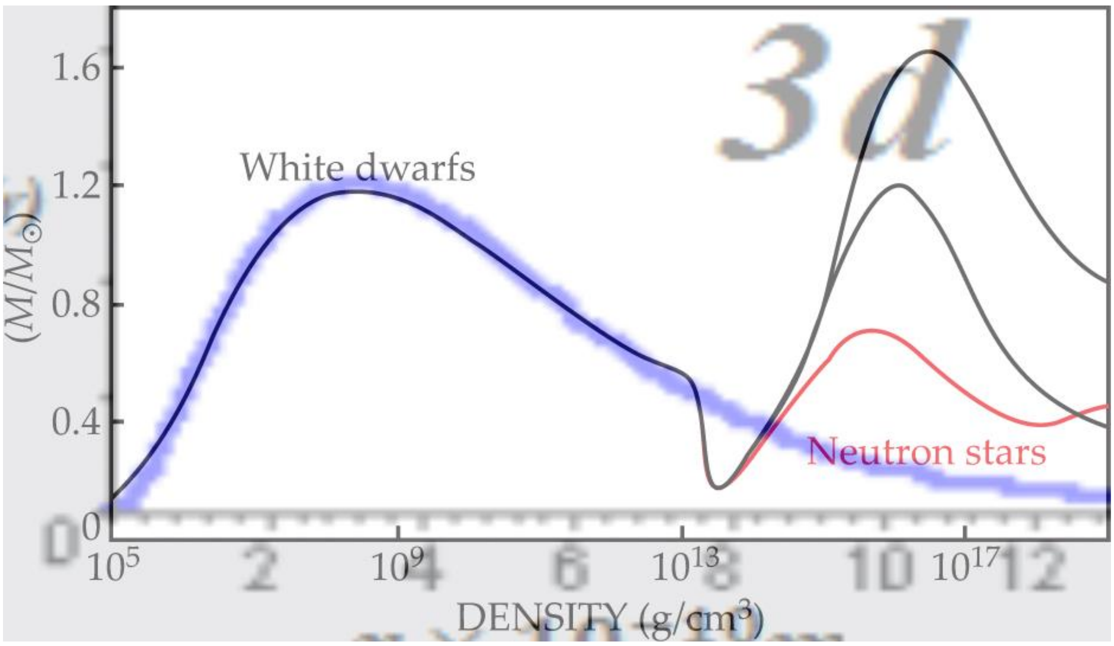

Super imposed graphs

https://www.researchgate.net/figure/Maxwellian-velocity-distribution-fg-of-the-collisions-velocities-of-the-aggregates_fig12_252340625

Maxwellian velocity distribution f(g) of the collisions velocities of the aggregates. Note, impact speeds of the range of mm s À1 up to cm s À1 are expected in Saturn's rings.

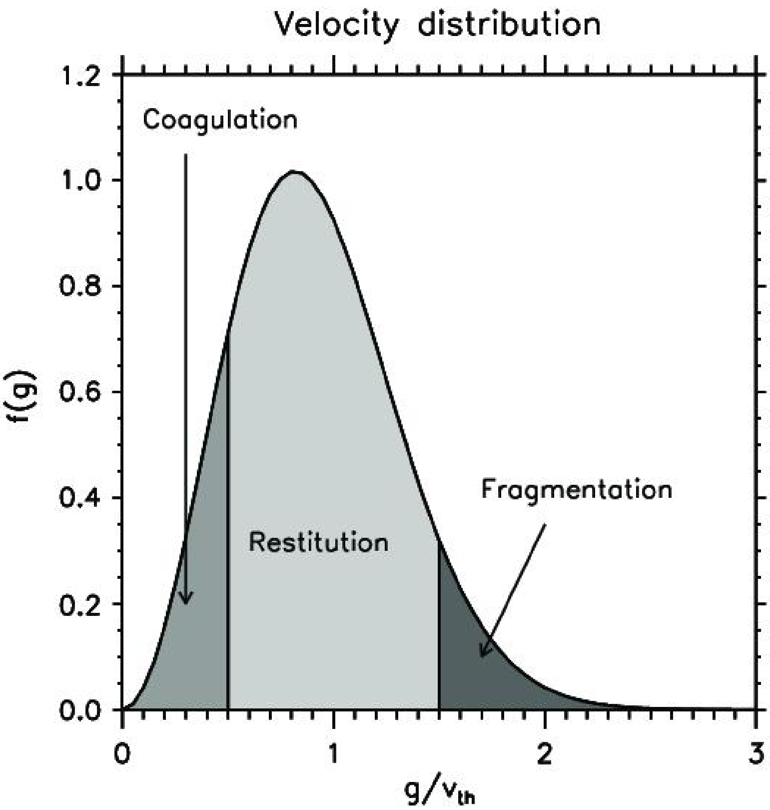

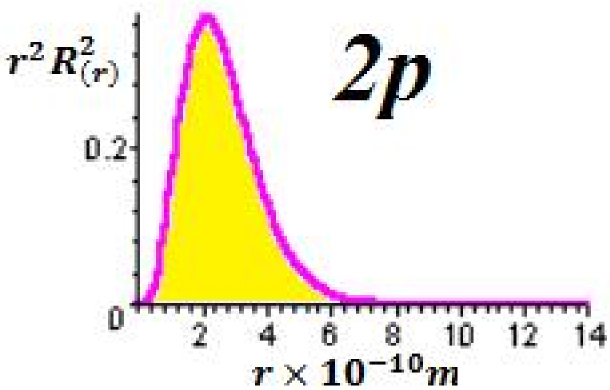

Hydrogen 2p Probability Density

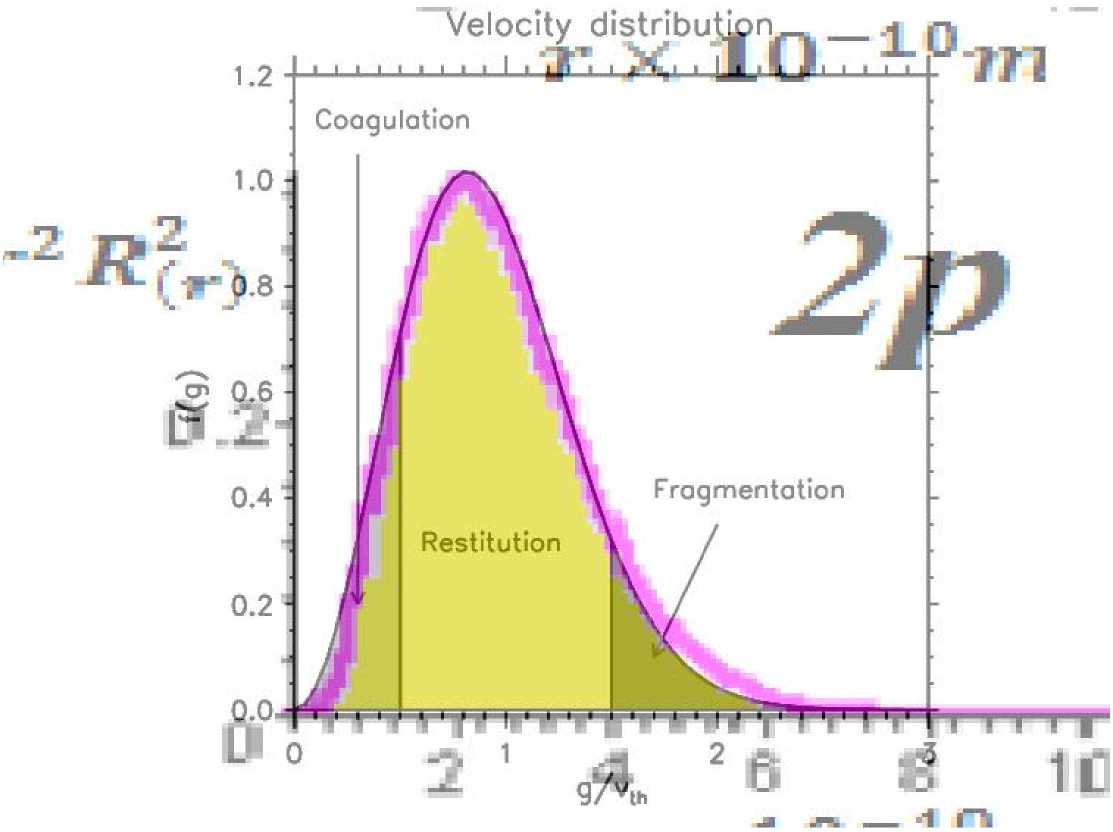

Super imposed graphs

https://arxiv.org/pdf/1801.00133.pdf

A Model of the Collapse and Evaporation of Charged Black Holes

Figure 3: The plot of Hawking temperature against a0 − e0. All the units are Planck units.

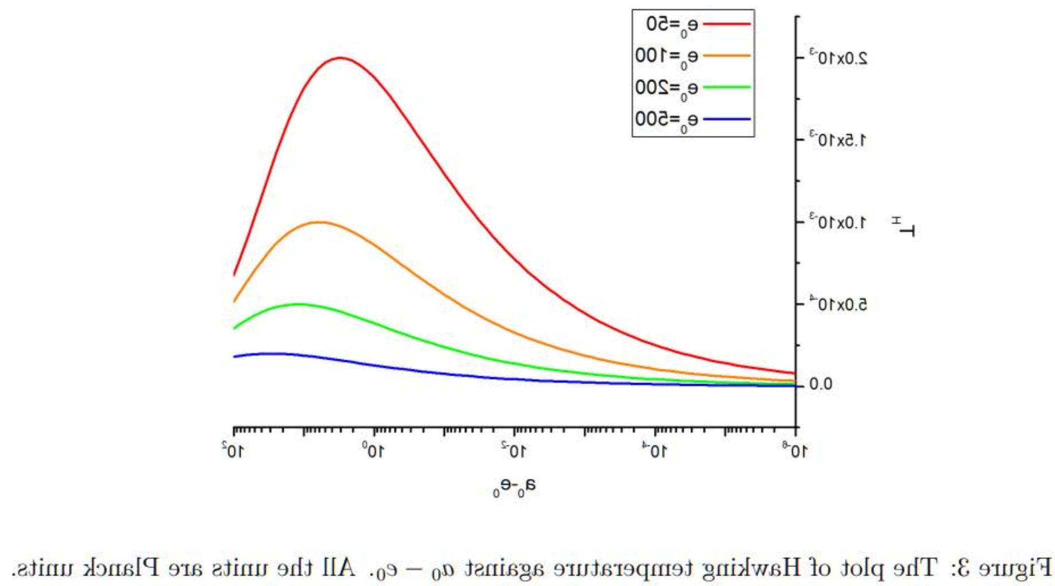

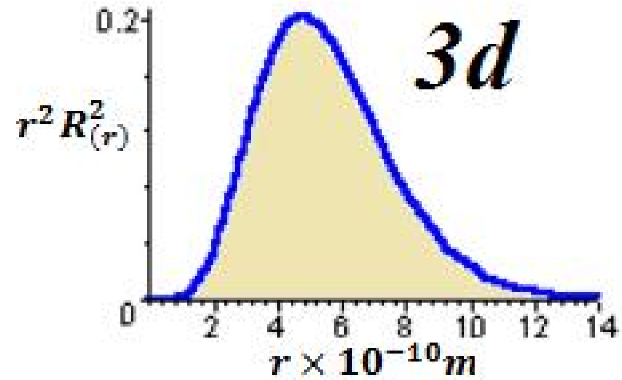

Hydrogen 3d Probability Density

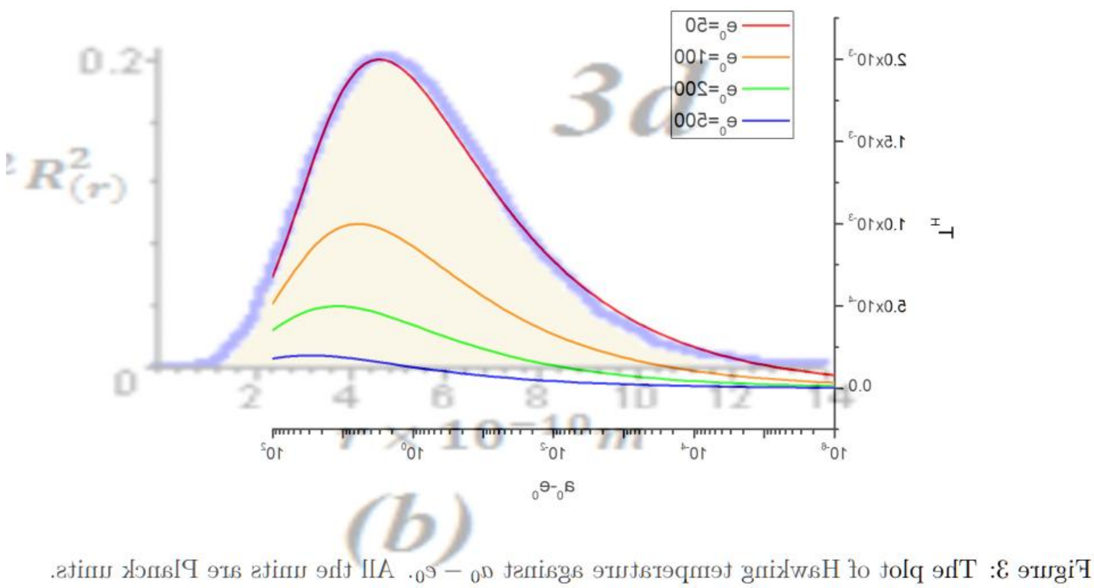

Super imposed graphs

https://digitalcommons.lsu.edu/cgi/viewcontent.cgi?article=3761&context=physics_astronomy_pubs
Anomalies In The Cosmic Micr Anomalies In The Cosmic Microwave Background And Their Non- ound And Their NonGaussian Origin In Loop Quantum
Cosmology

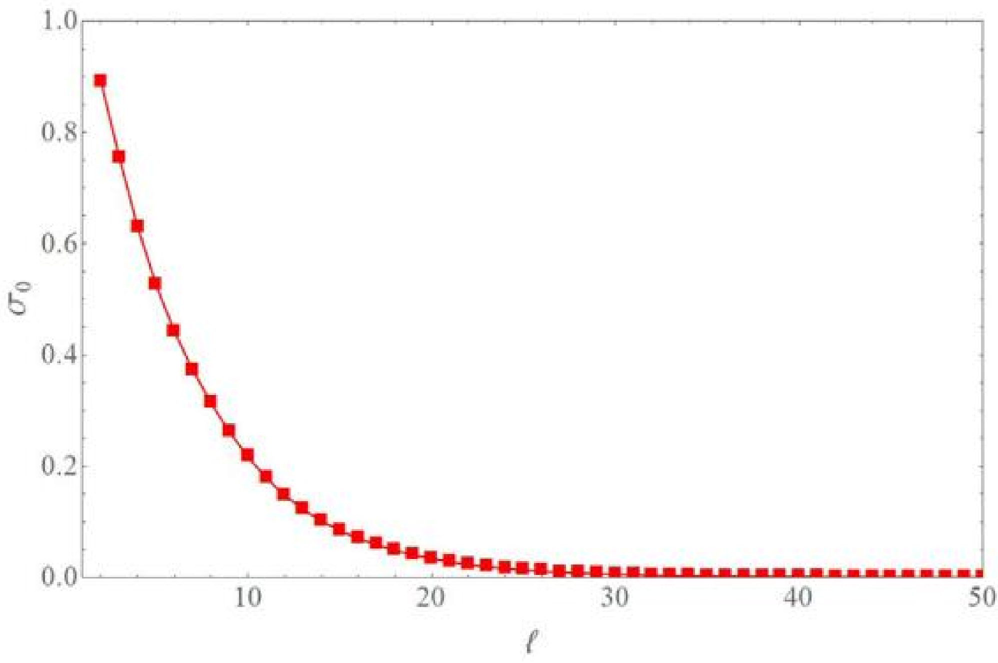

FIGURE 5 | Root-mean-square of the monopolar modulation $\sigma_0(\ell)$ generated in LQC. Note the dependence of σ_0 on ℓ. The scale dependence introduced by the bounce in LQC makes the effects of the modulation significant only for $\ell \lesssim 30$.

1s orbital

$n := 1 \quad l := 0$

$$R(\rho) := 2 \cdot e^{-\rho}$$

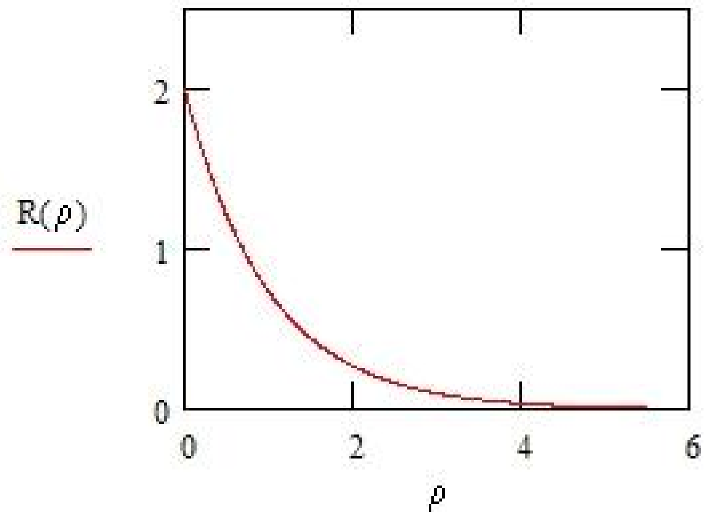

Hydrogen 1s Wave Function

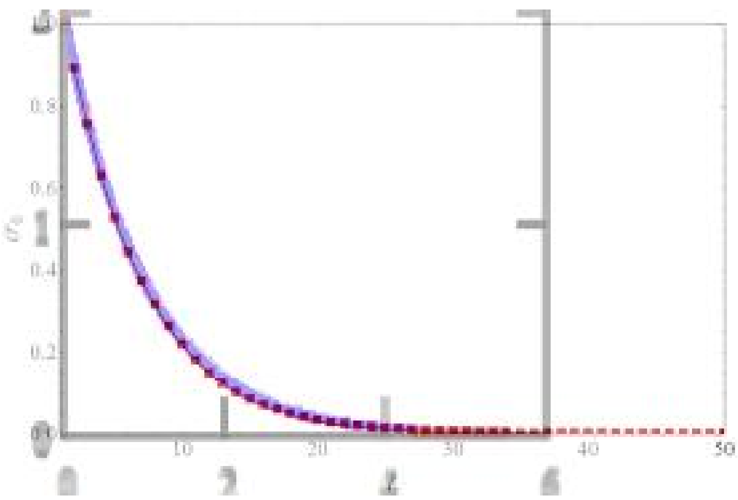

Super imposed graphs

https://phy.princeton.edu/sites/g/files/toruqf2261/files/resource-links/jacobson_jp1.pdf

Velocity Dependence of Dark Matter Electron Scattering
Dark matter velocity distributions f(|v|) in the heliocentric frame: [Fe/H] < −1.8 distribution (blue) and Standard Halo Model (yellow). (right) The function g(vmin) is plotted on a logarithmic scale with respect to minimum scattering velocity, using both velocity distributions

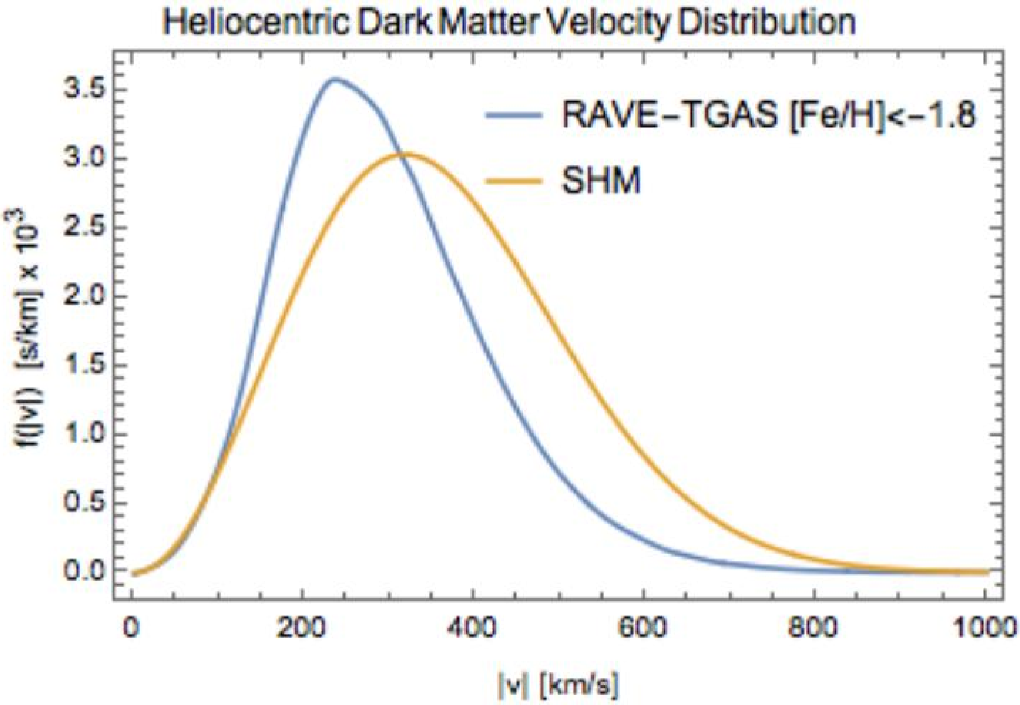

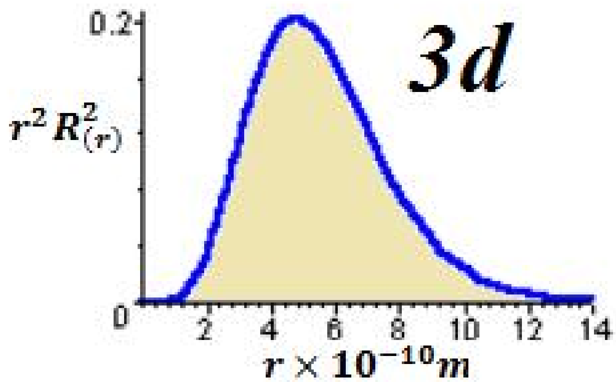

Hydrogen 3d Probability Density

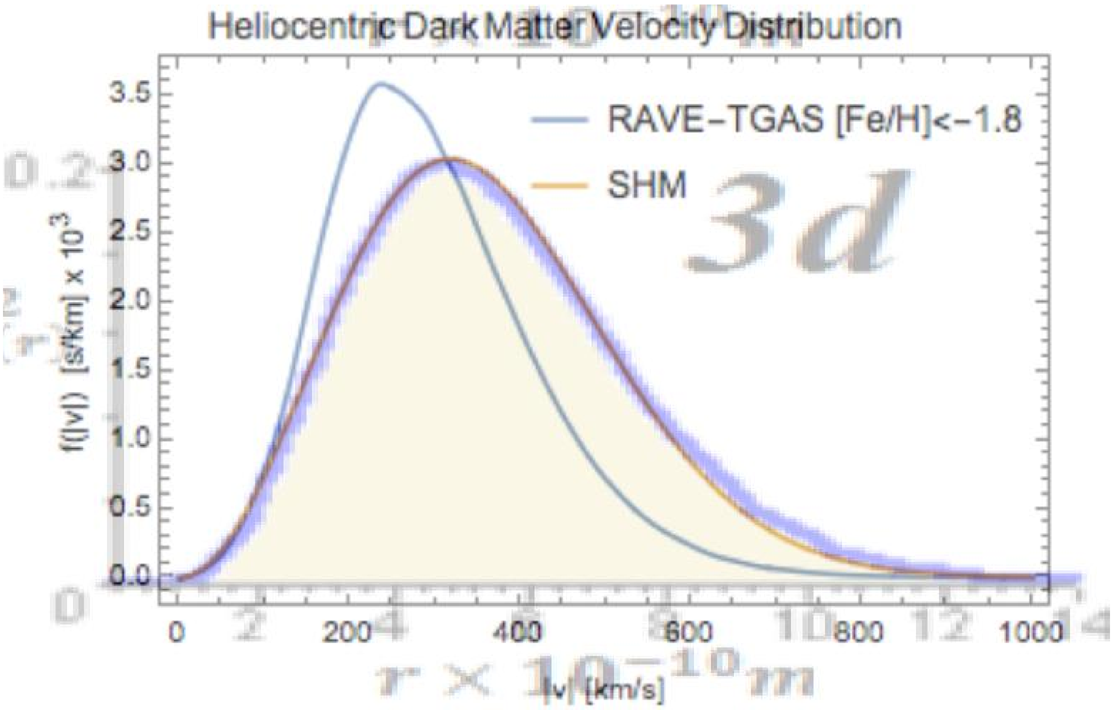

Super imposed graphs

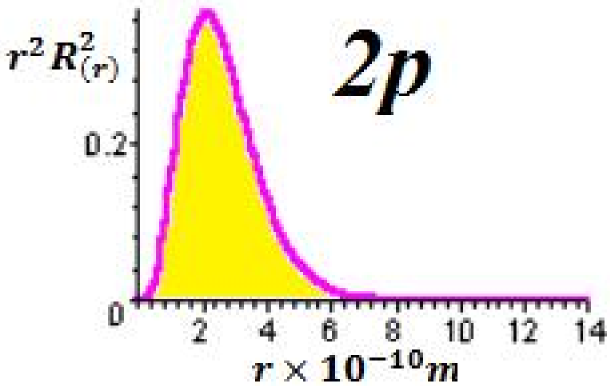

Hydrogen 2p Probability Density

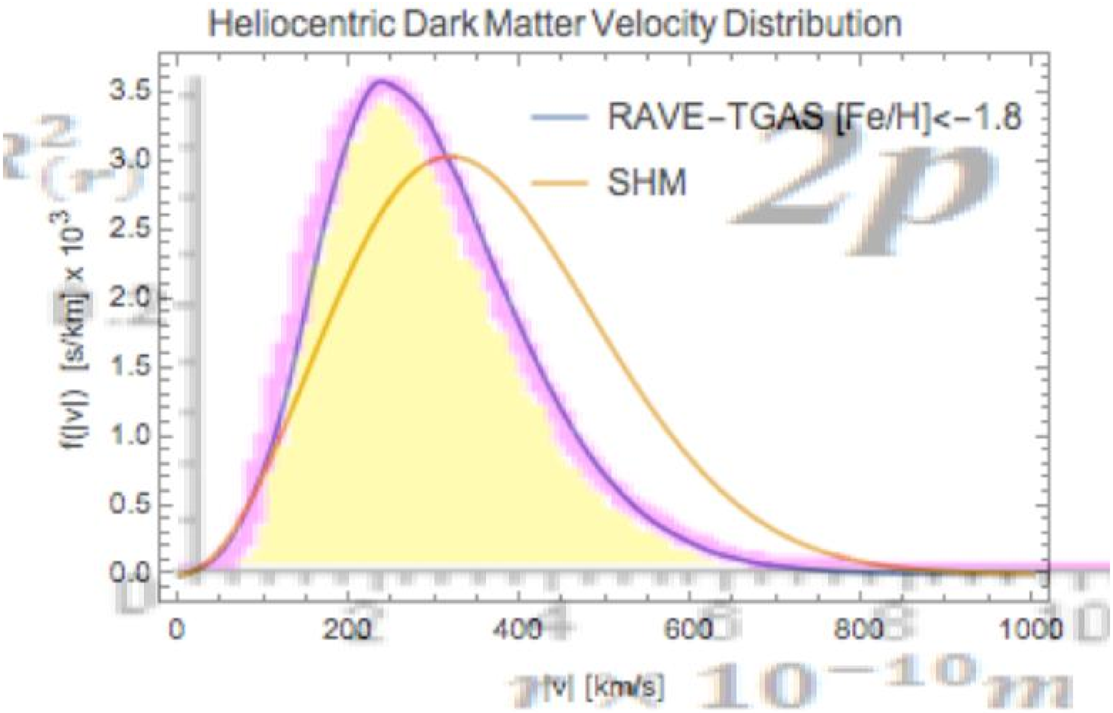

Super imposed graphs

https://www.researchgate.net/figure/A-5800-K-Planck-distribution-function-divided-into-equal-100-nm-wavelength-intervals_fig2_236003842

A 5800 K Planck distribution function divided into equal 100 nm wavelength intervals.

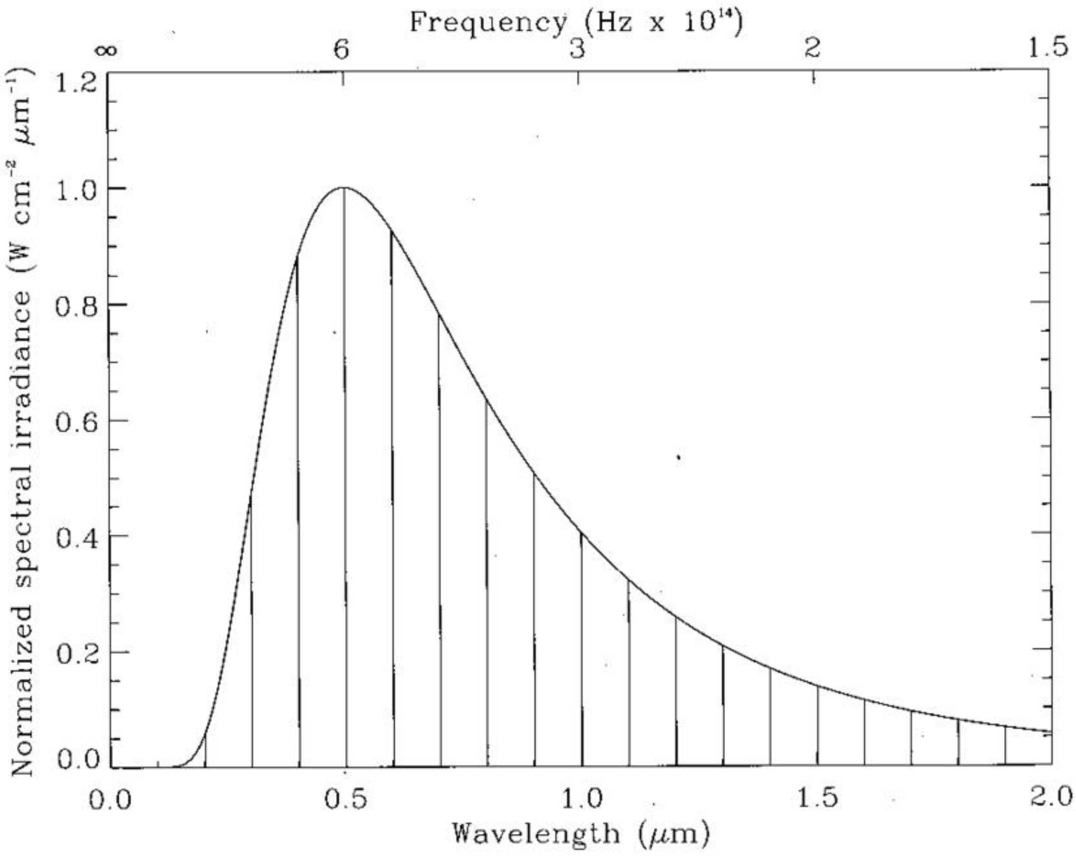

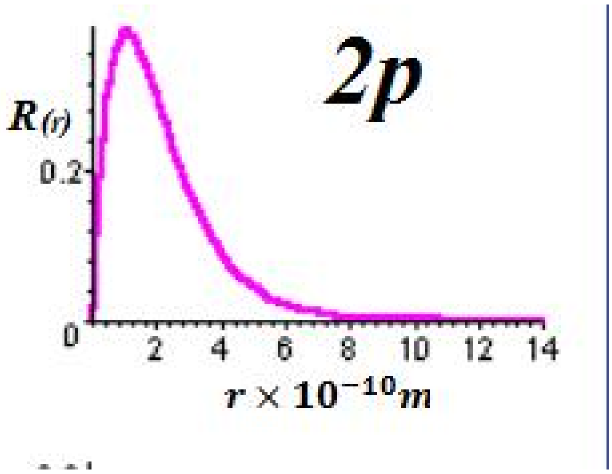

Hydrogen 2p Wave Function

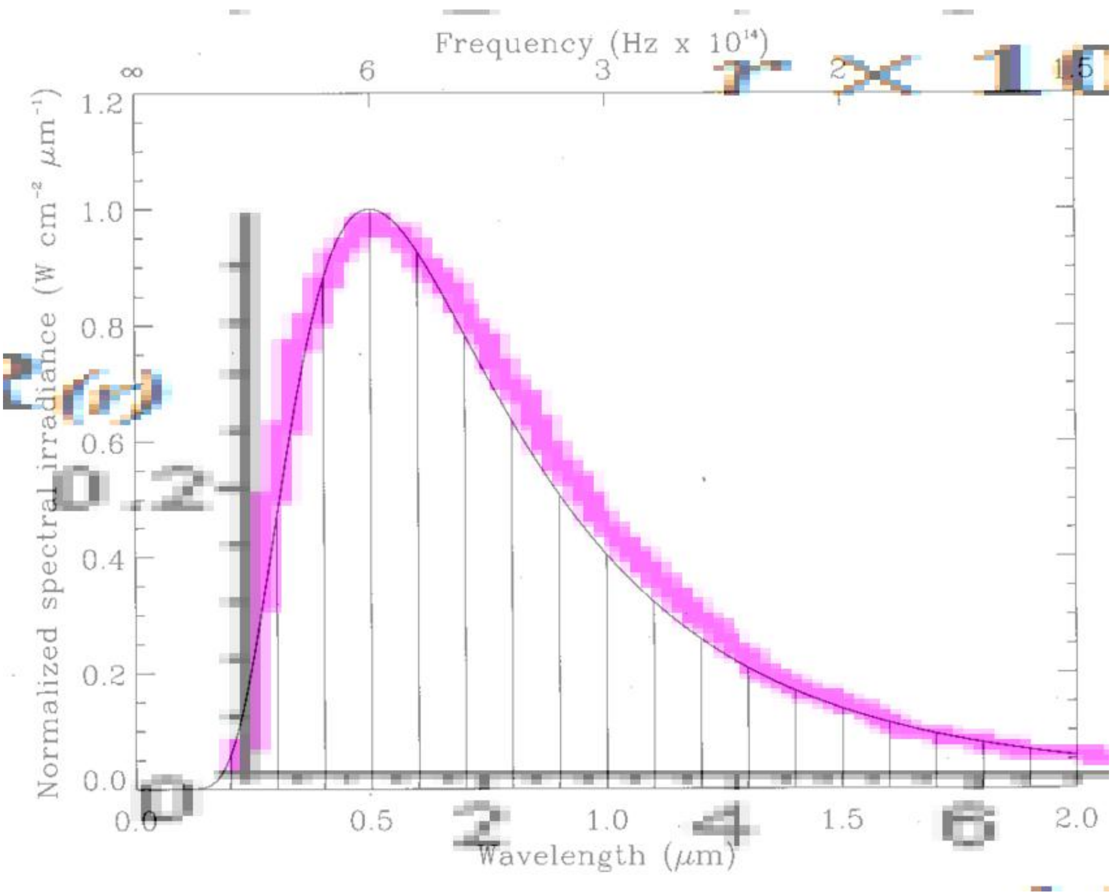

Super imposed graphs

https://en.wikibooks.org/wiki/A-level_Physics_(Advancing_Physics)/Gravitational_Fields/Worked_Solutions

gravitational field strength against distance

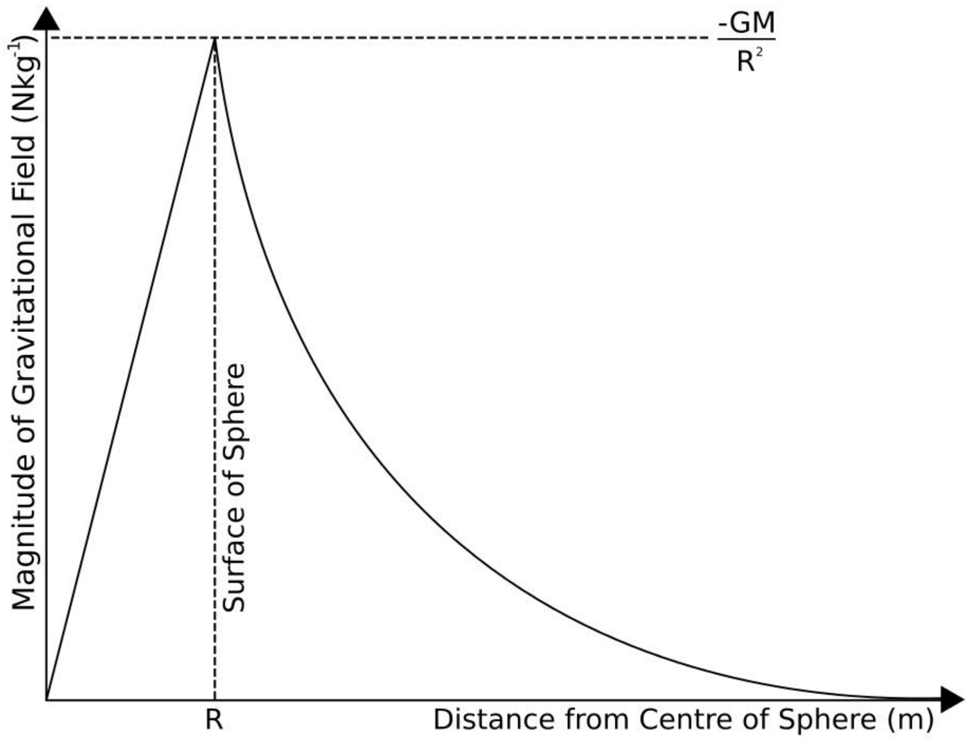

1s orbital

$n := 1 \quad l := 0$

$R(\rho) := 2 \cdot e^{-\rho}$

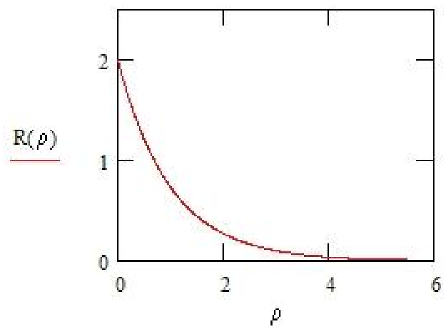

Hydrogen 1s Wave Function

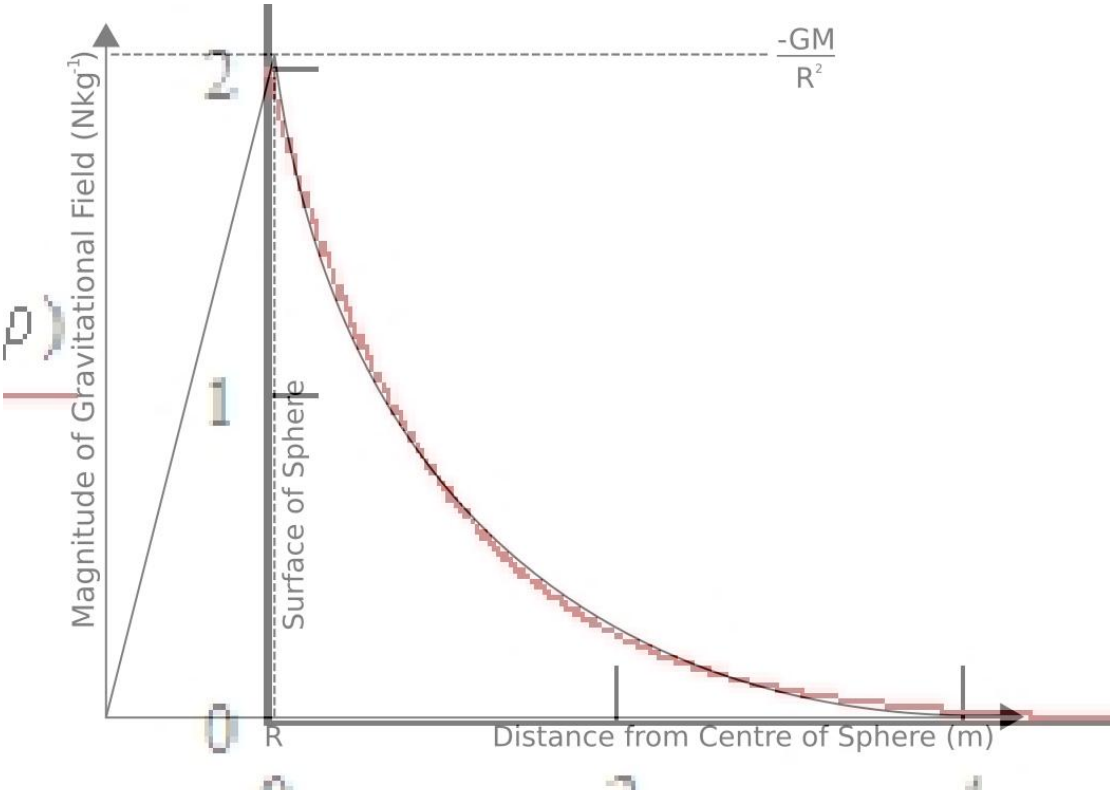

Super imposed graphs

https://chem.libretexts.org/Bookshelves/Physical_and_Theoretical_Chemistry_Textbook_Maps/Physical_Chemistry_(LibreTexts)/01%3A_The_Dawn_of_the_Quantum_Theory/1.01%3A_Blackbody_Radiation_Cannot_Be_Explained_Classically

Graphic representation of spectral distribution of blackbody radiation at different temperatures. The Stefan-Boltzmann's Law is observed as the increase in the emission amplitude with increasing temperature and the Wien's Displacement Law is observed as the shift to smaller wavelength with increasing temperature. (CC-BY 4.0; OpenStax)

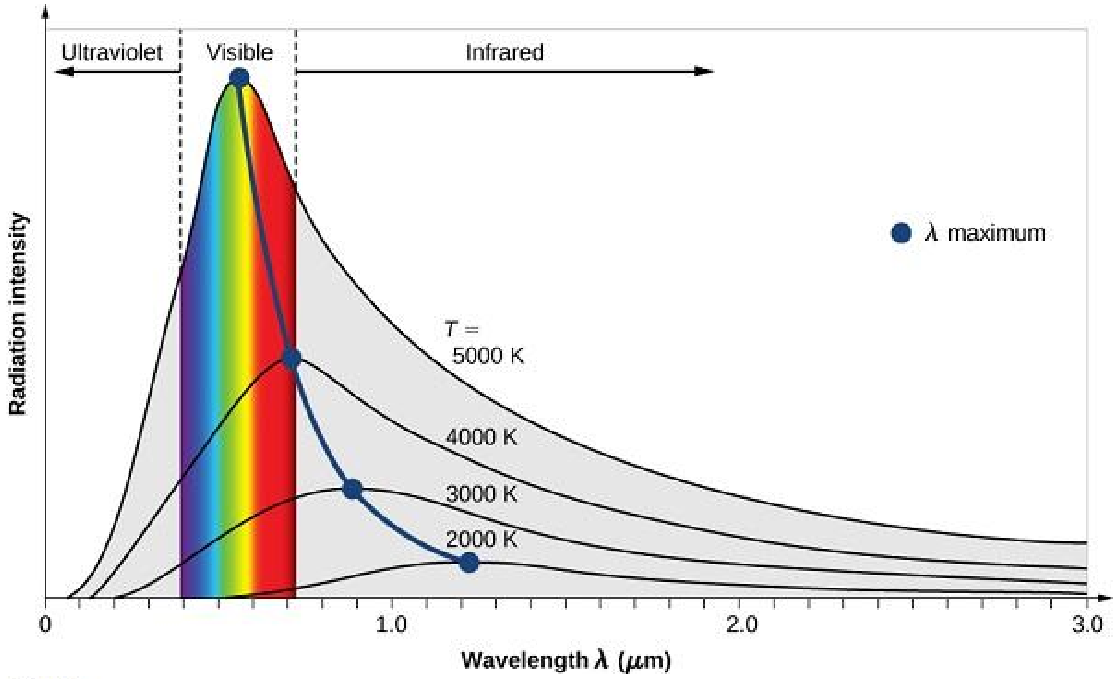

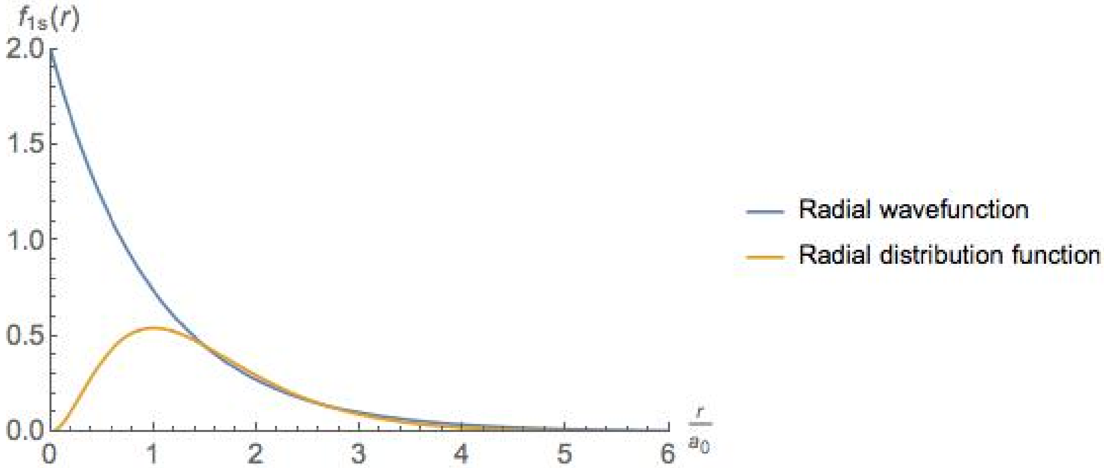

Hydrogen 1s Wave Function

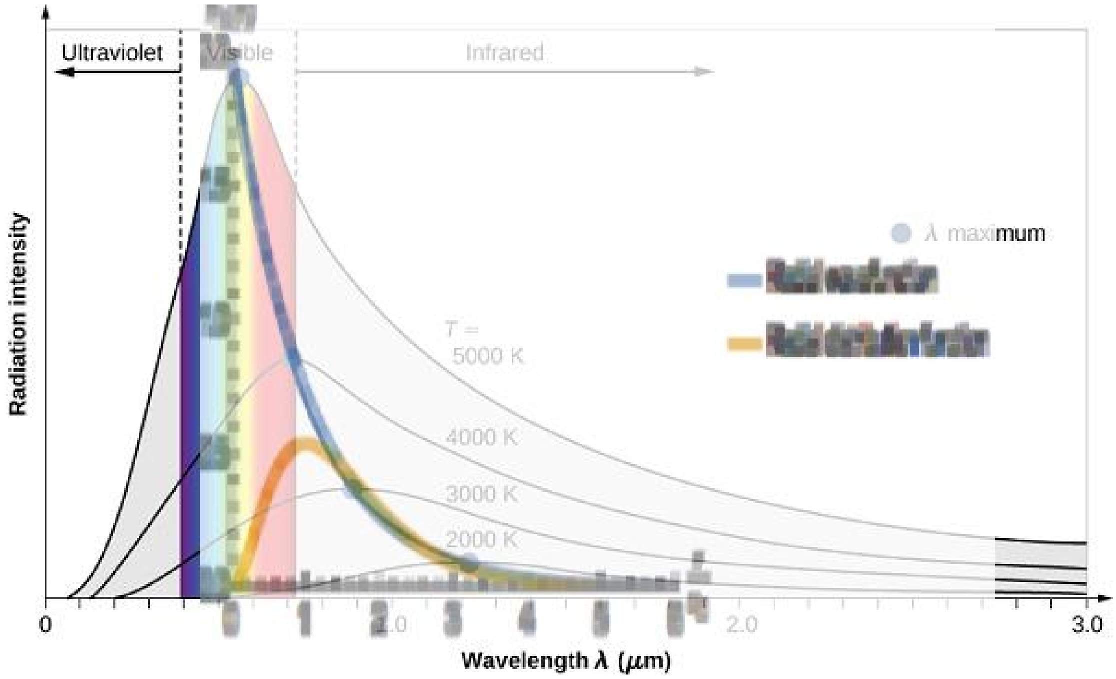

Super imposed graphs

https://www.semanticscholar.org/paper/Study-of-variation-of-temperature-of-black-holes-to-Mehta-Prasad/32908f5d6c7495fc2cabe7a4ce078c0b4d9671a9

Graph plotted between mass of different test of black holes and variation of temp. w. r. t. mass in XRBs.

6. Graph

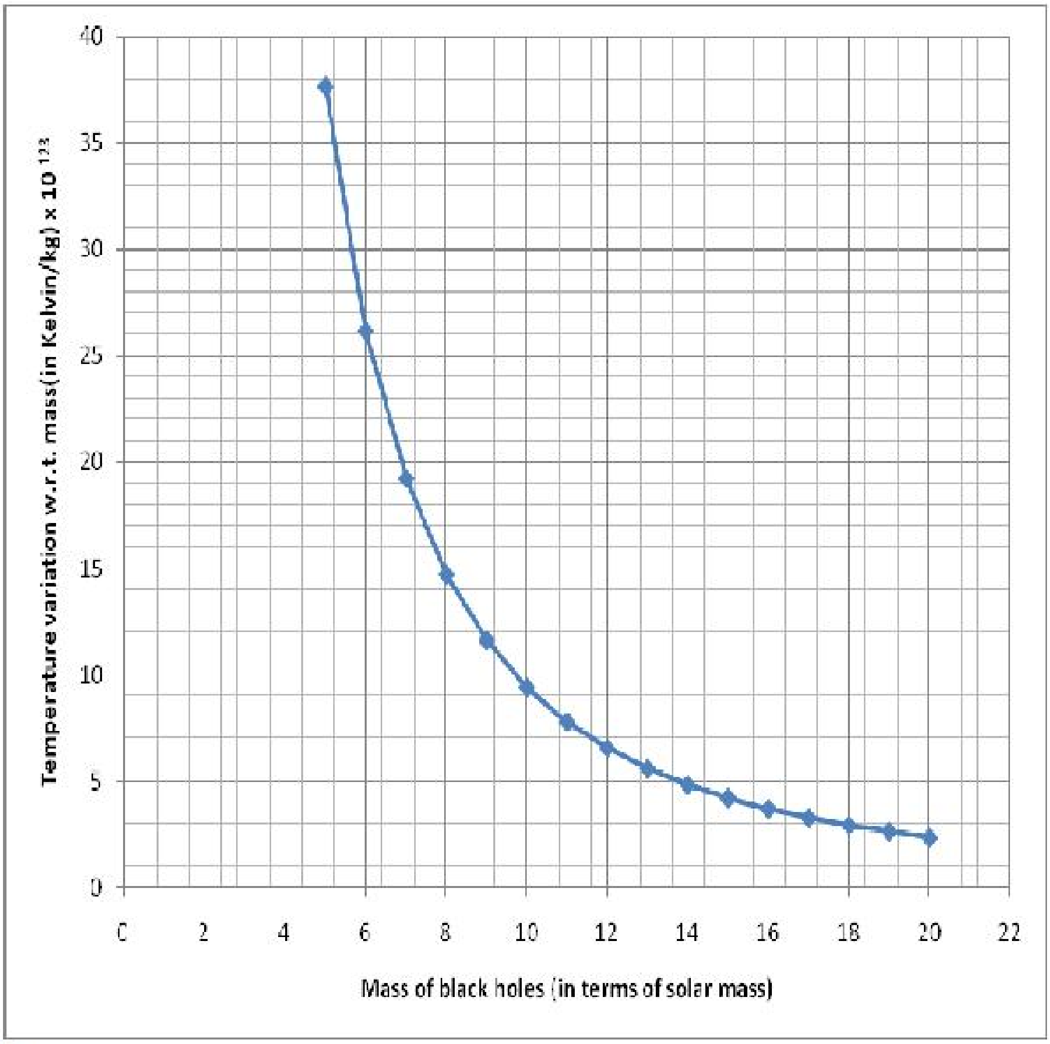

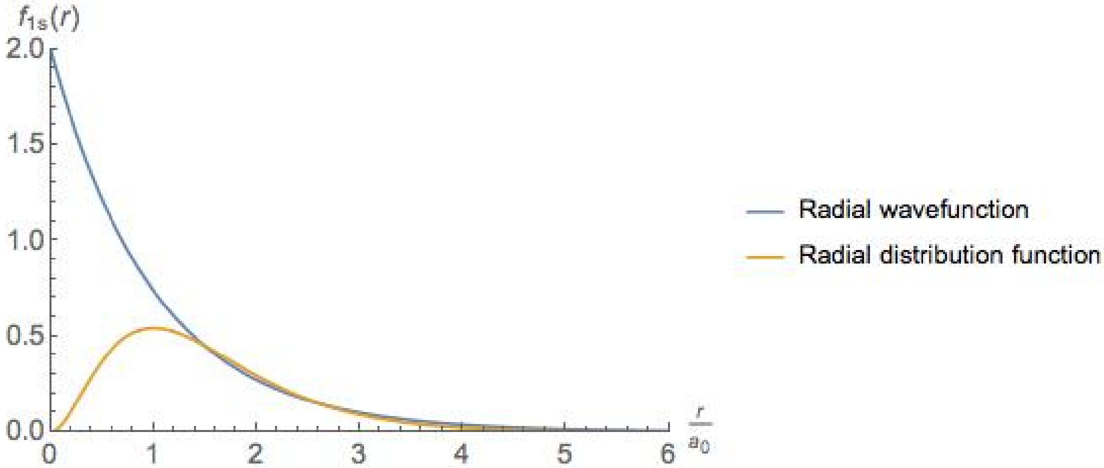

Hydrogen 1s Wave Function

6. Graph

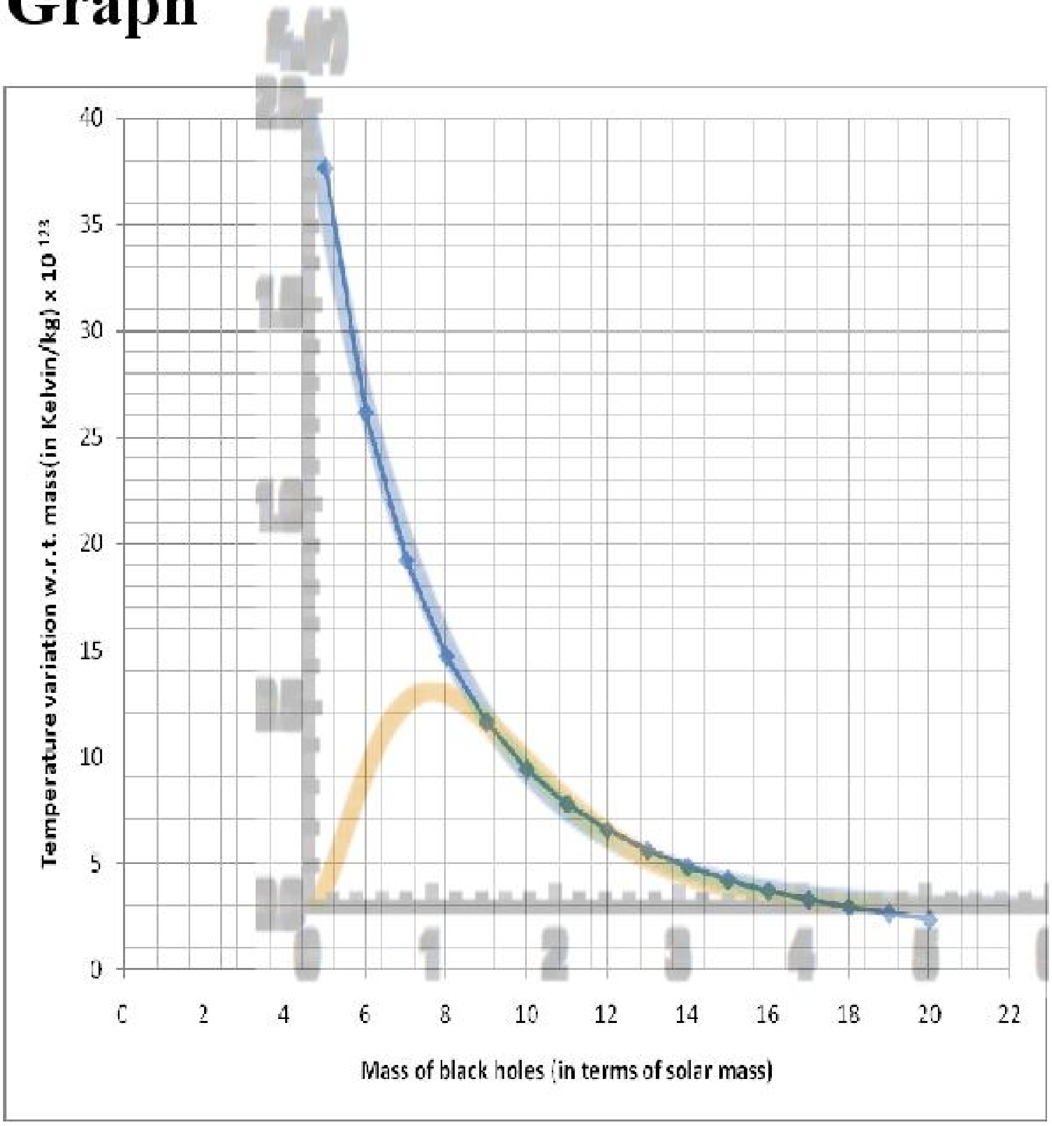

Super imposed graphs

https://link.springer.com/article/10.1140/epjc/s10052-015-3428-3

Electromagnetic fluxes from accretion disks gravitating around compact general relativistic objects, having different equations of state, with mass $M=1.8M_\odot$M=1.8M⊙, and rotating at an angular velocity of $\Omega=5\times10^{3}s^{-1}$

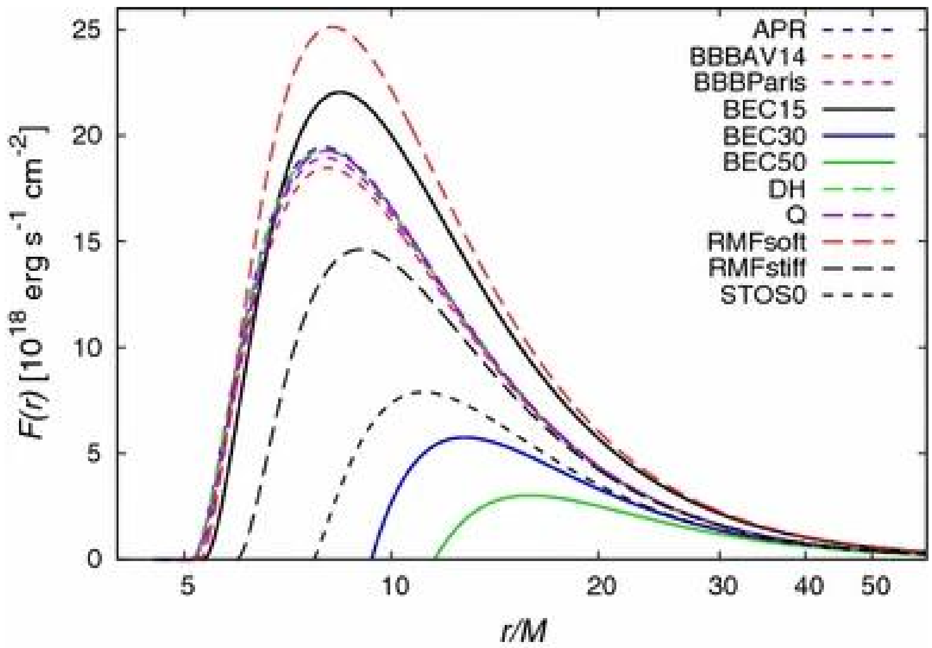

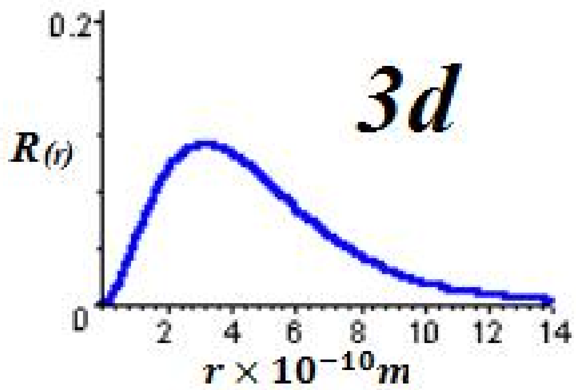

Hydrogen 3d Wave Function

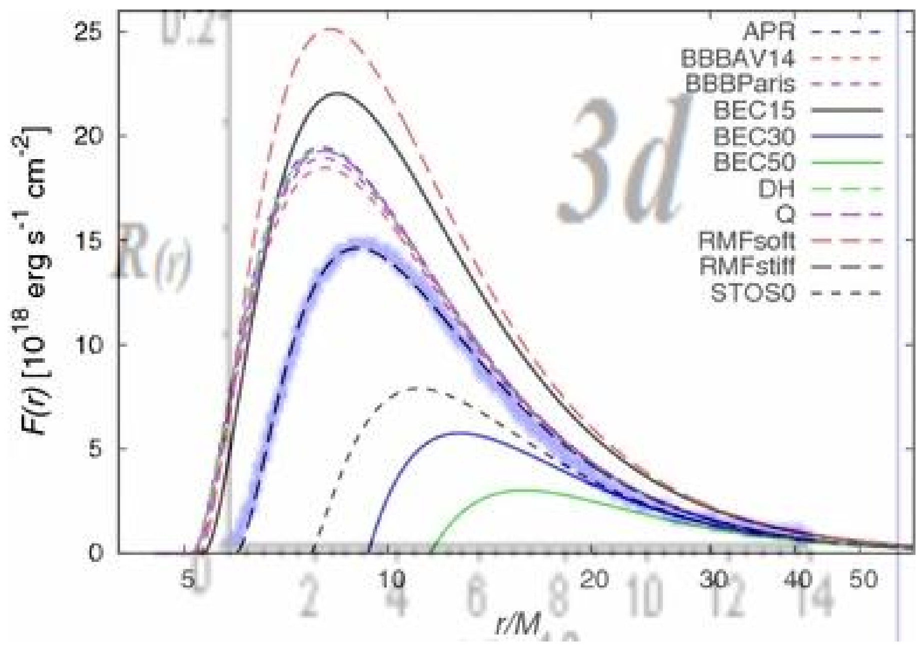

Super imposed graphs

https://link.springer.com/article/10.1140/epjc/s10052-015-3636-x

Unfolded normalised distribution of the mass of C/A $R=1.2$ jets with $300<p_T<400$ GeV **a** before and **b** after splitting and filtering in an inclusive jet sample without pile-up (number of primary vertices $N_{PV}=1$). From [53], used under CC BY 4.0 and unchanged from original

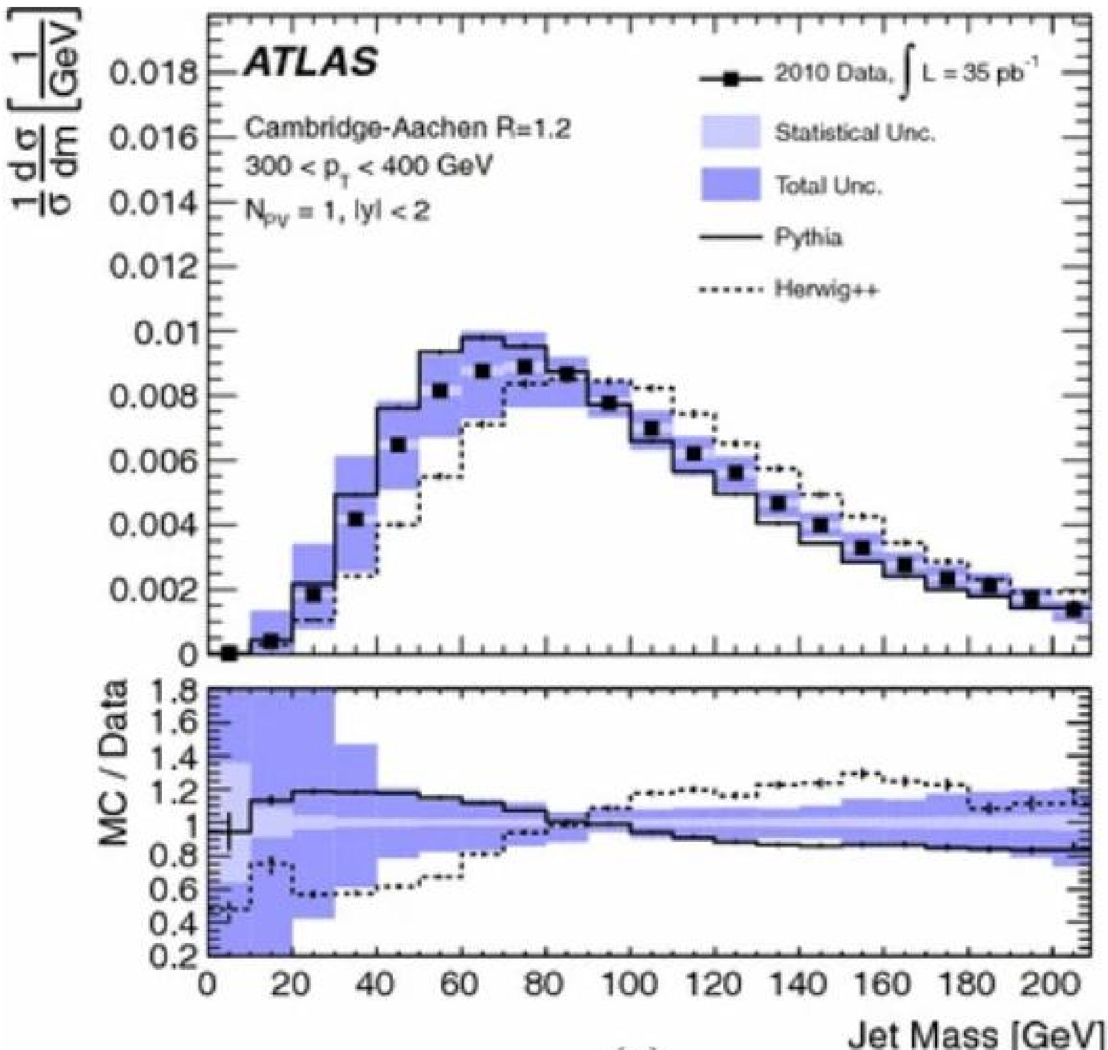

(a)

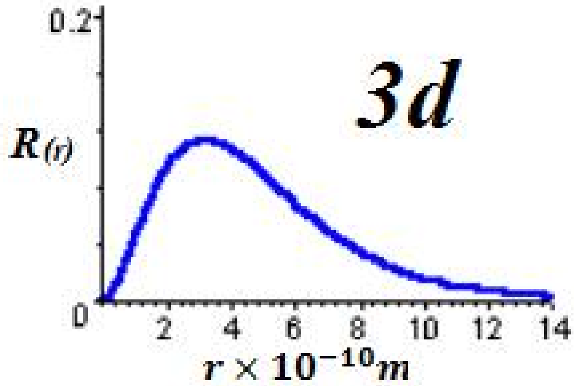

Hydrogen 3d Wave Function

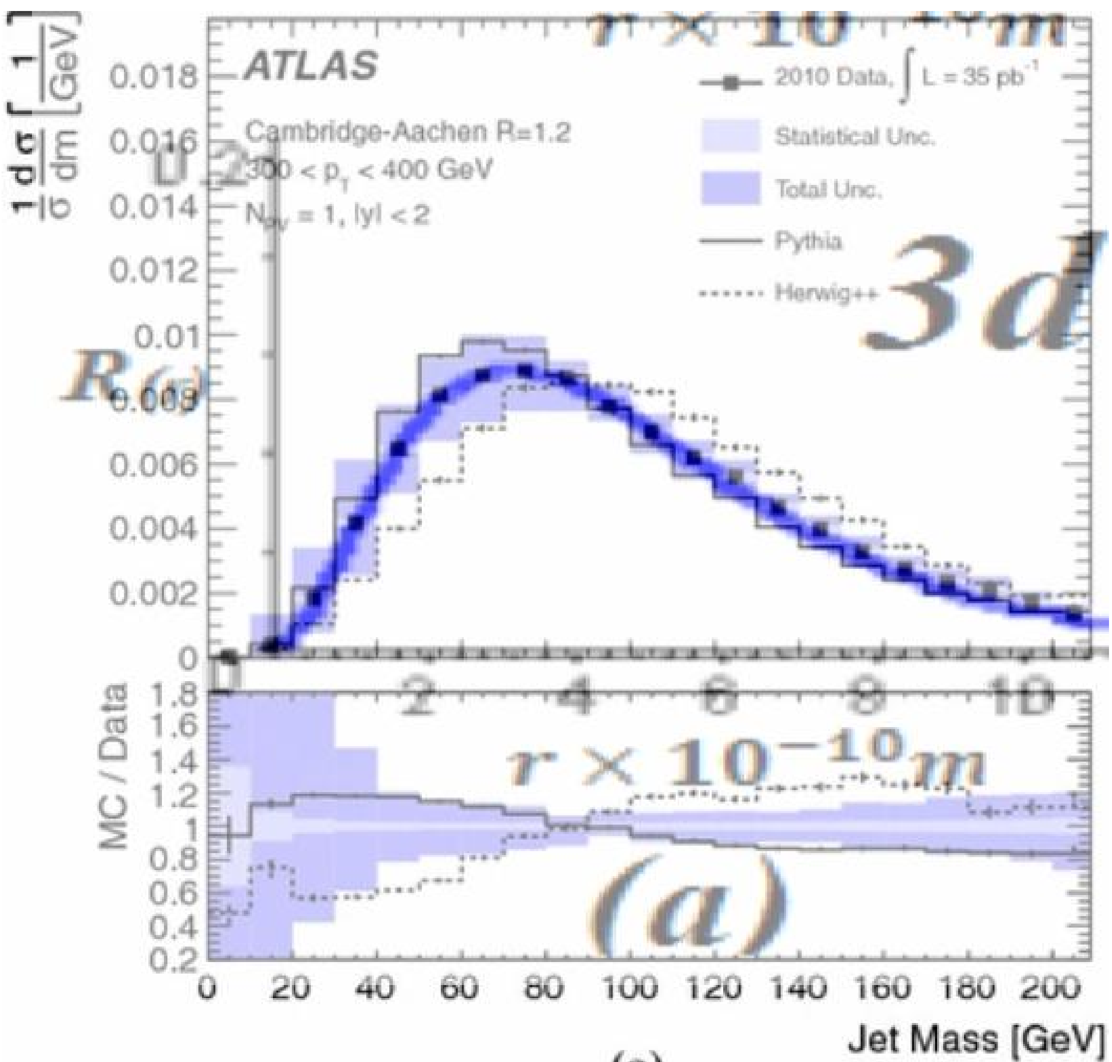

(a)

Super imposed graphs

https://www.researchgate.net/figure/Relative-velocity-distribution-eq-49-for-an-NFW-dark-matter-halo-only-The-dotted_fig8_242331467

Relative velocity distribution, eq. (4.9), for an NFW dark matter halo only. The dotted lines show a Maxwell-Boltzmann distribution with the same velocity dispersion: σ = 51.8km/s, 110.1km/s, 163.2km/s for r = 0.1kpc, 1kpc, 10kpc.

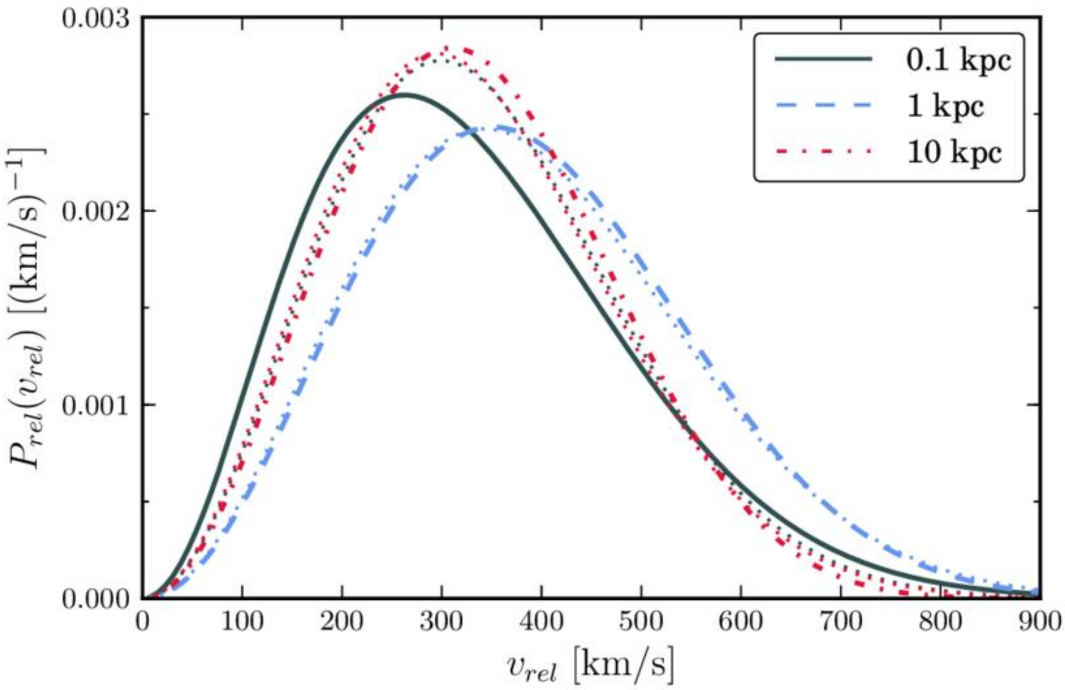

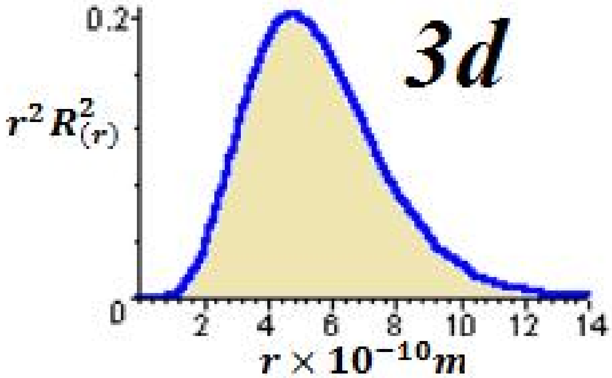

Hydrogen 3d Probability Density

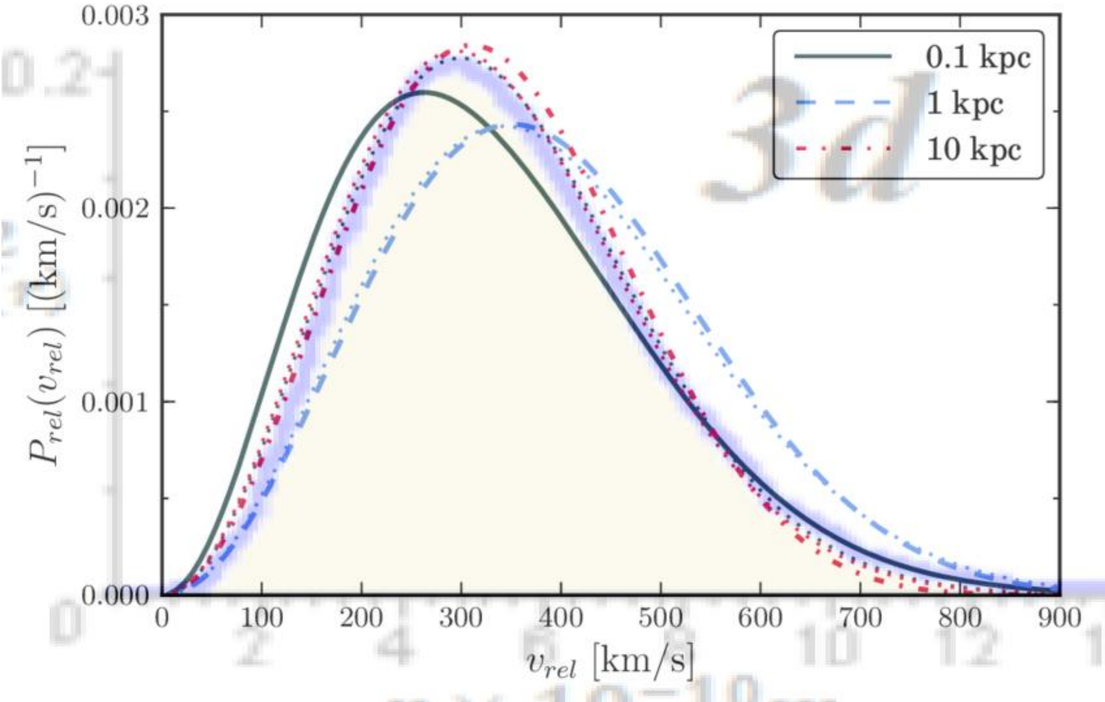

Super imposed graphs

https://www.researchgate.net/figure/Radial-probability-density-distribution-of-interplanetary-matter-Upper-panel-a-is-the_fig1_253003364

Radial probability density distribution of interplanetary matter. Upper panel a) is the distribution of H with 3/4 of the nebular mass. Giant planets and the center of Kuiper Belt are all at the wave crests. Terrestrial planets are all at the first wave. Bottom panel b) is the distribution of He with 1/4 of the nebular mass and the first wave of H. Each terrestrial planet lies at a separate wave of He. It is interesting that the Kuiper Belt and Asteroid Belt lie in the sixth wave of H and He, and the widths of belts are consistent with wavelengths, respectively.

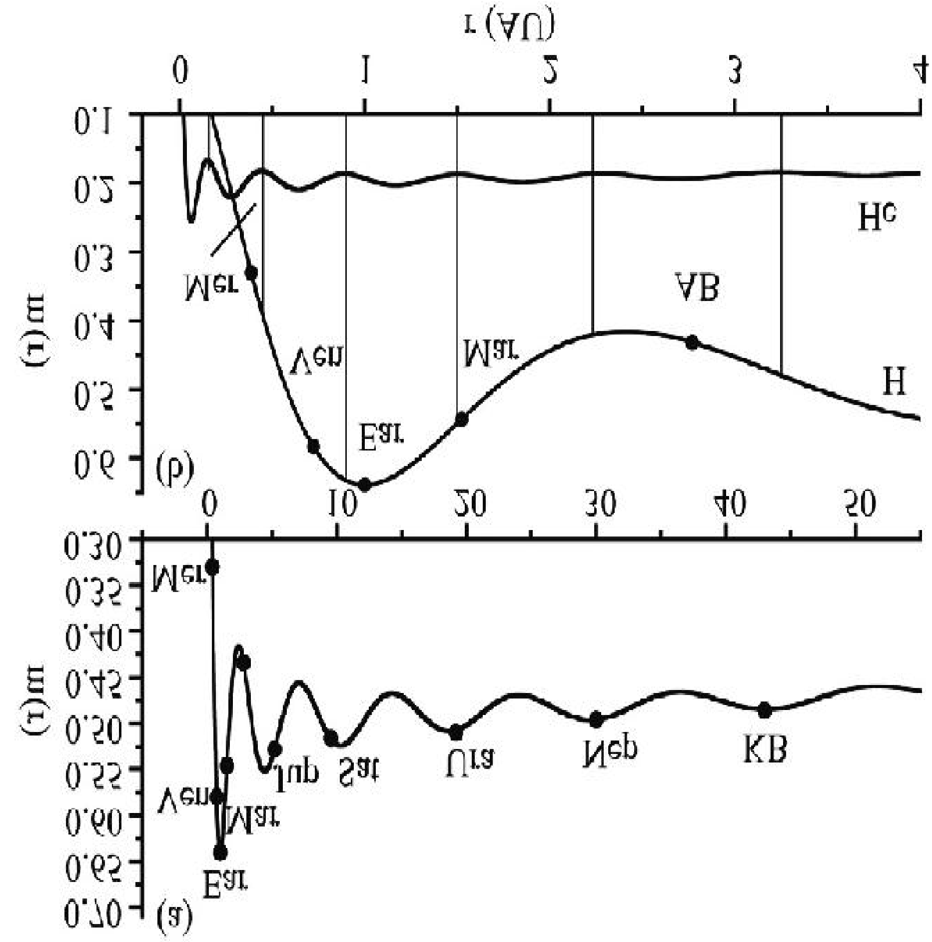

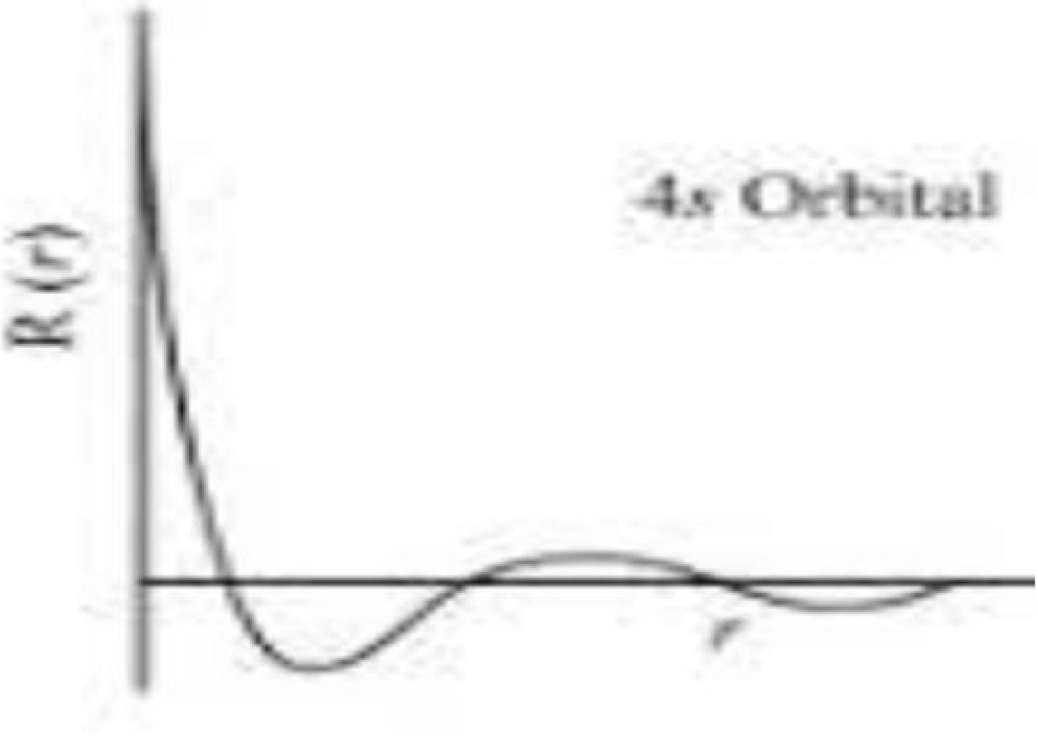

Hydrogen 4s Wave Function

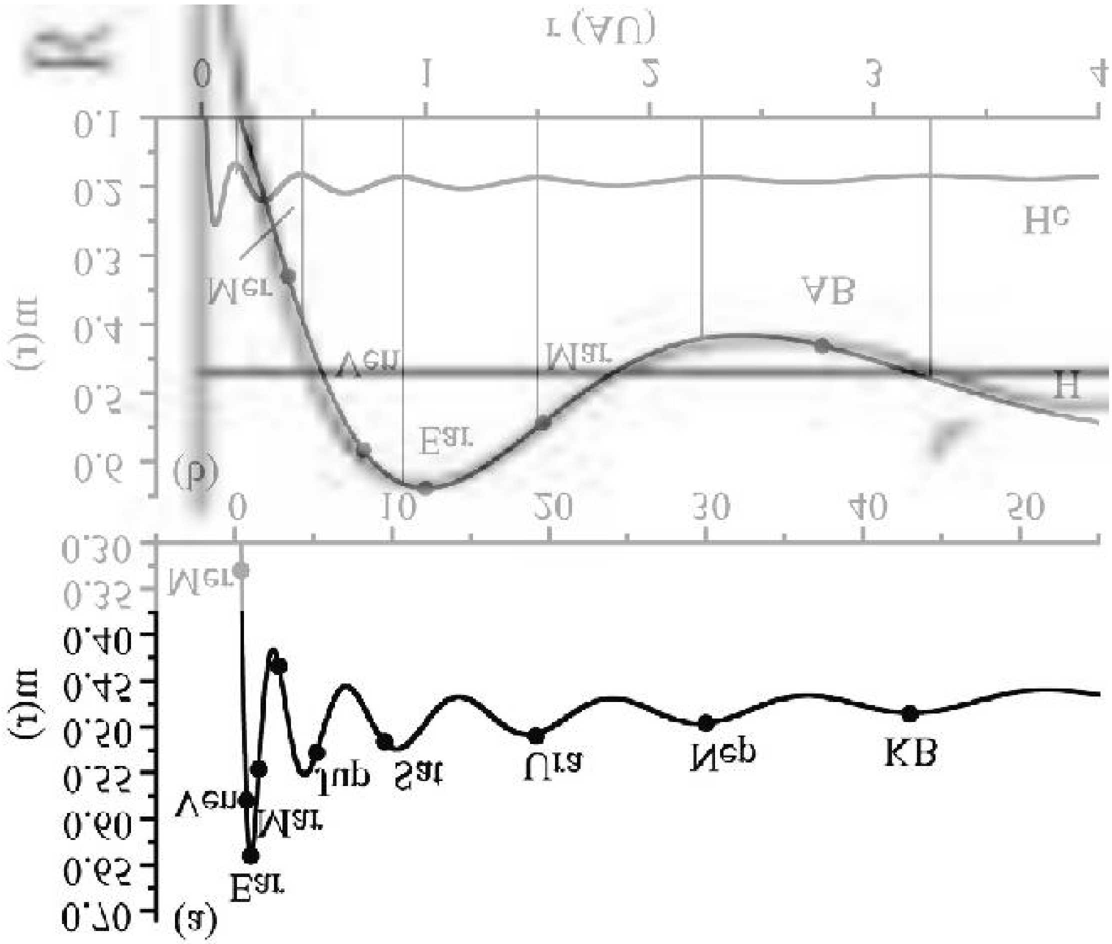

Super imposed graphs

https://link.springer.com/article/10.1140/epjc/s10052-018-6273-3

Cascade analysis: best-fit energy distribution for the signal hypothesis (components stacked to illustrate the dark matter component), with the best fit parameters listed in Table 2. The fit is performed on un-binned data, but for visualization purposes a binning is applied in the figure

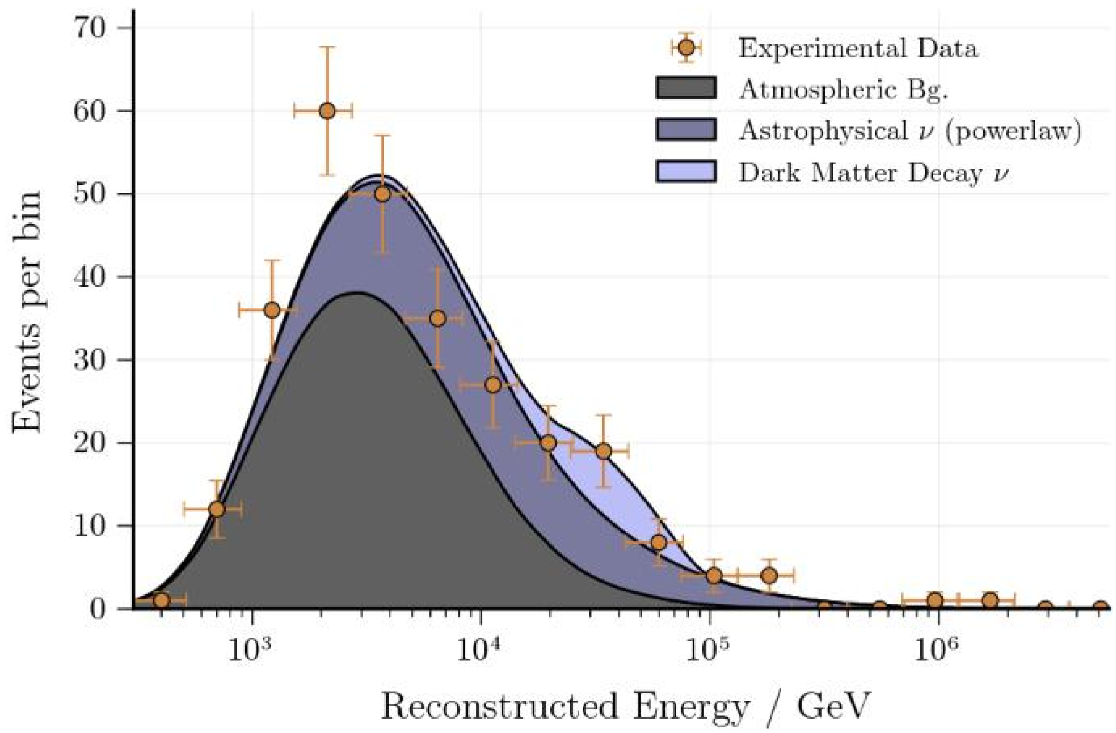

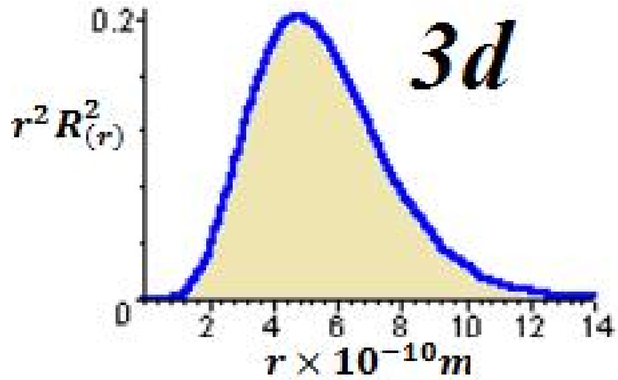

Hydrogen 3d Probability Density

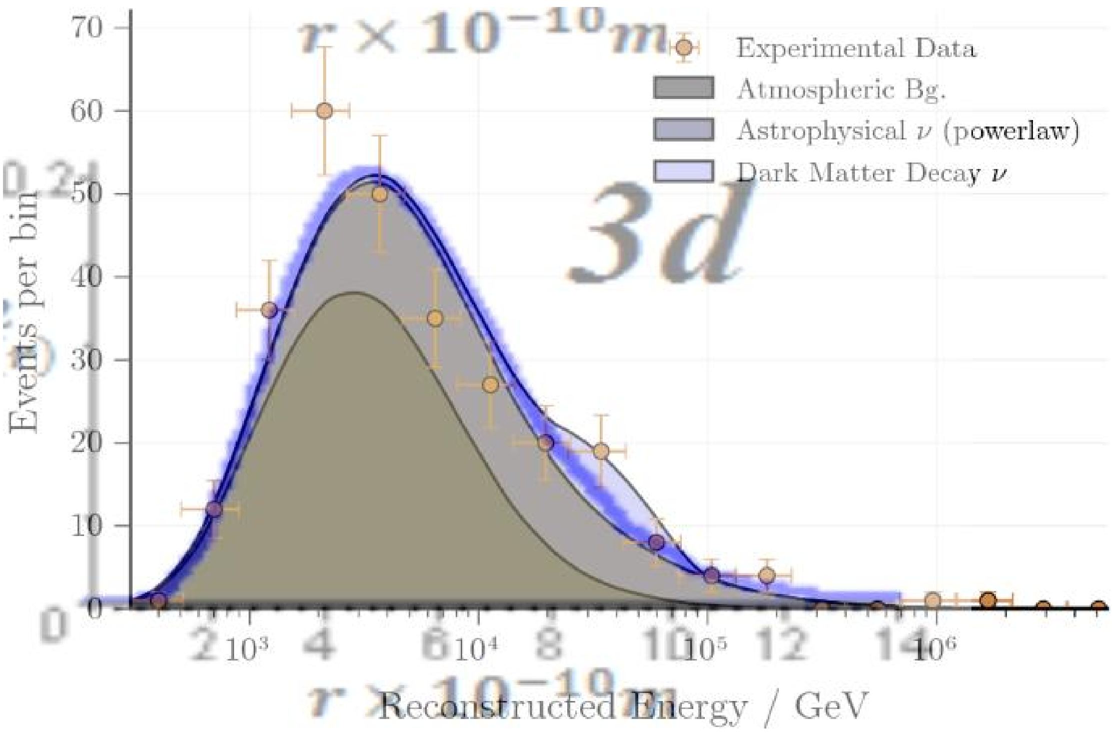

Super imposed graphs

https://www.mdpi.com/2218-1997/7/8/264/htm

Figure 1. The distribution function $f_0(y)=n(y;\infty)$.

It is remarkable that for $y \ll 1$

$$f_0(y) \propto \frac{1}{y^{1/2}}, \tag{76}$$

in striking contrast to the thermal Fermi–Dirac distribution function. The enhancement for small *y* indicates that this is a cold dark matter species.

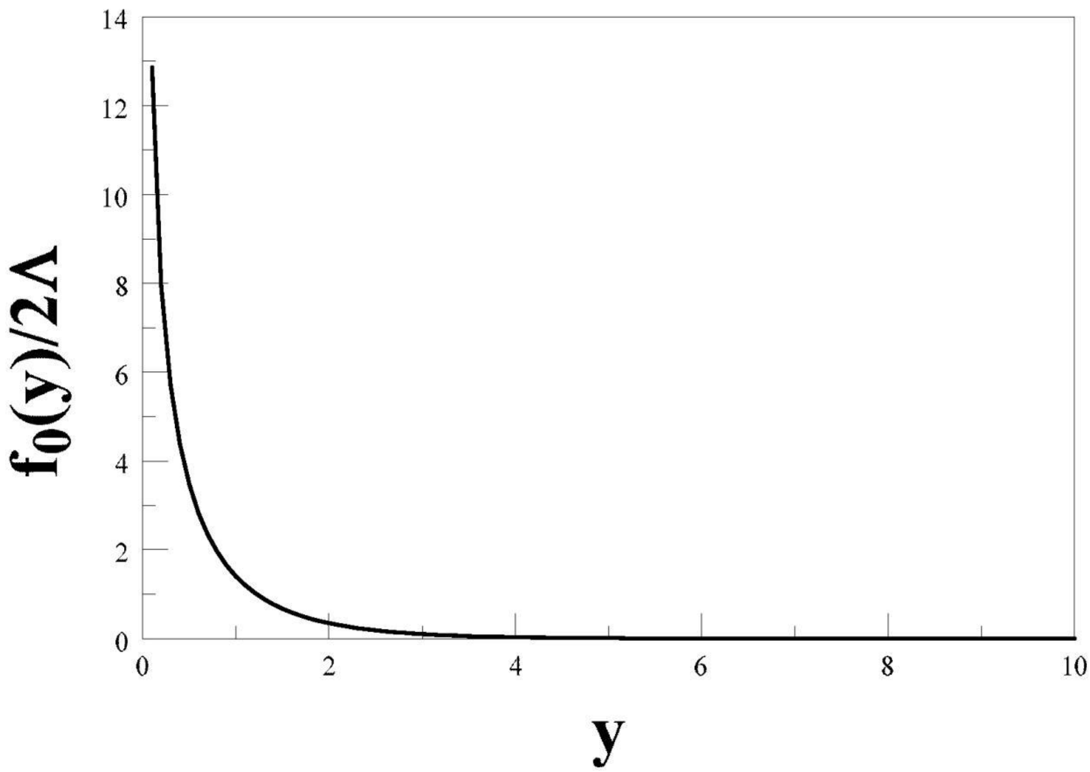

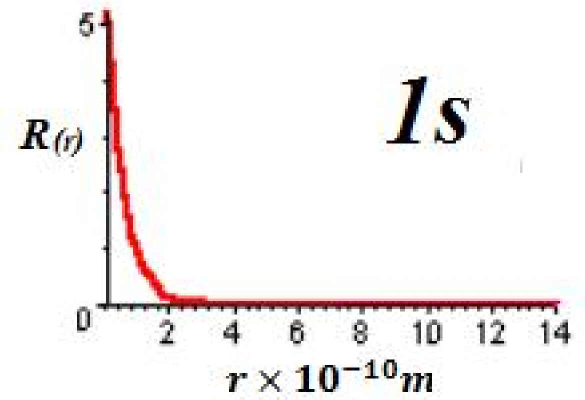

Hydrogen 1s Wave Function

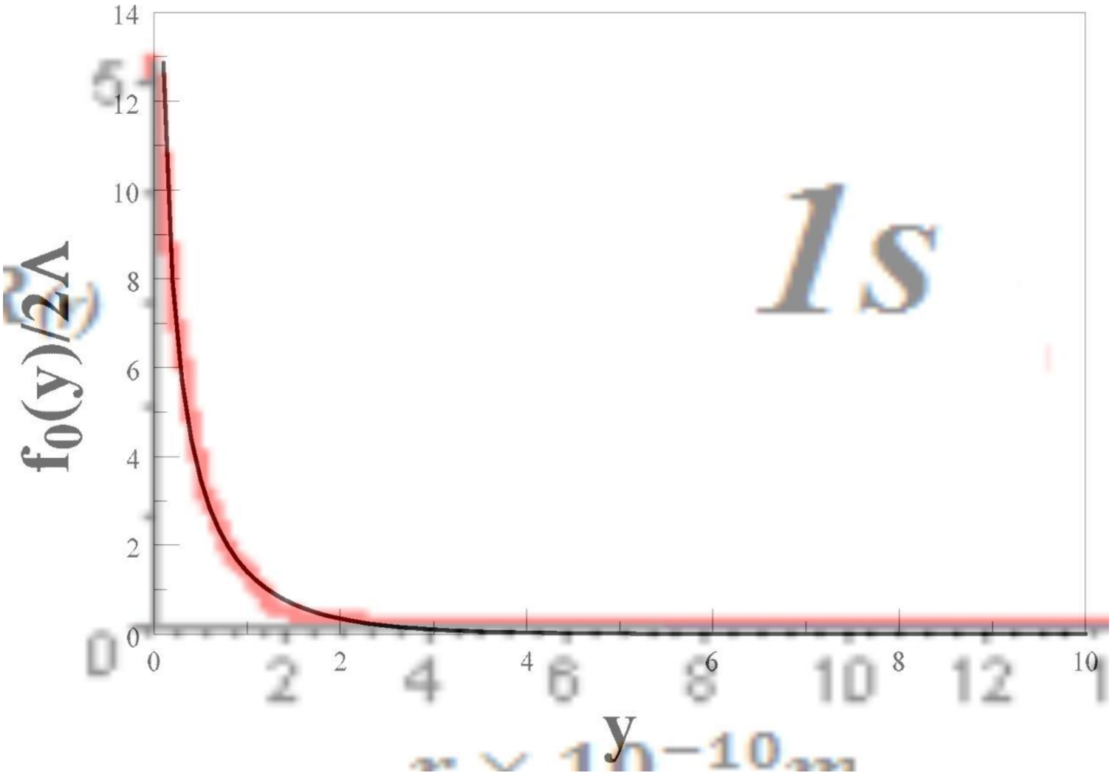

Super imposed graphs

The Hydrogen Wave Function or Probability Density may also describe other Quantum Systems:

https://link.springer.com/article/10.1007/s12043-019-1820-5
Radius of the proton

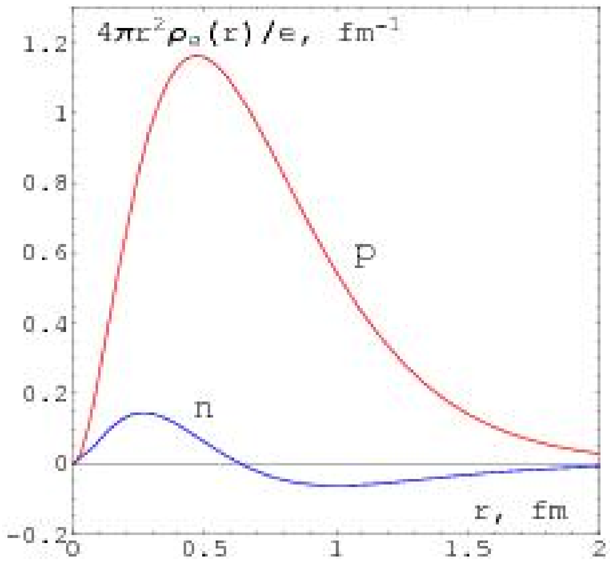

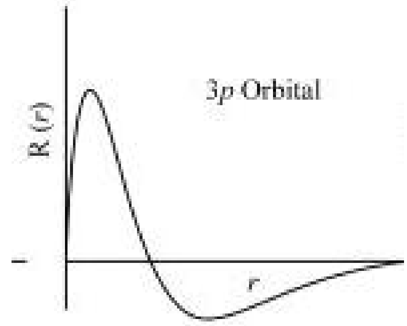

Hydrogen 3p Wave Function

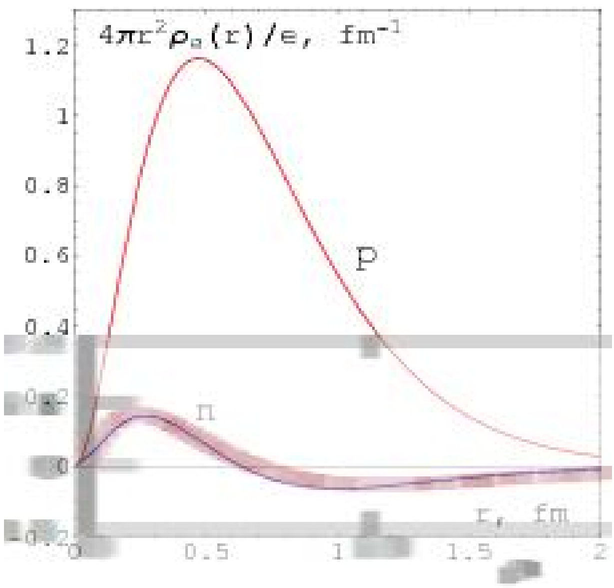

Super imposed graphs

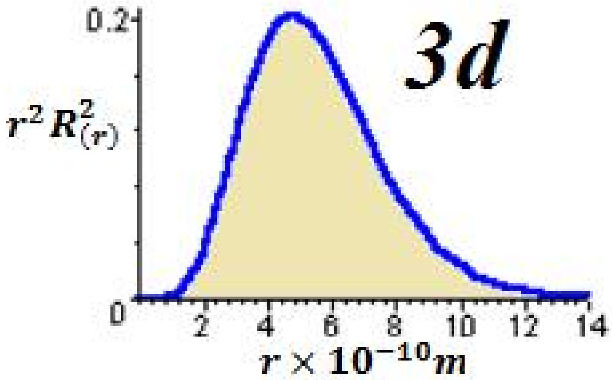

Hydrogen 3d Probability Density

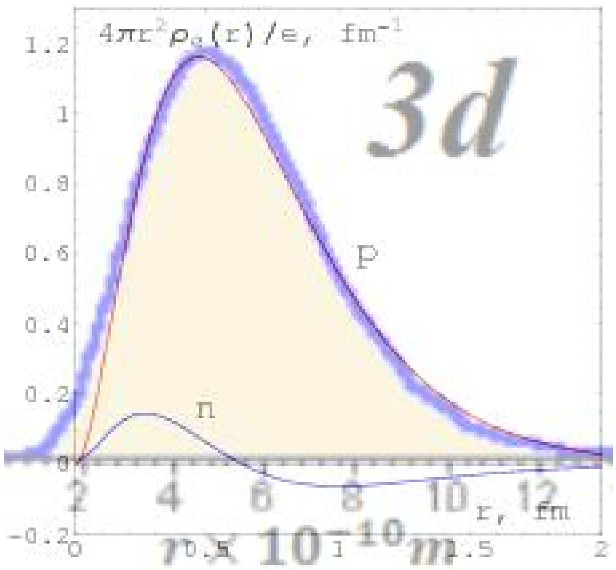

Super imposed graphs

https://iopscience.iop.org/article/10.1088/1402-4896/ab34c2

Nonlinear oscillations of ultra-cold atomic clouds in a magneto-optical trap - IOPscience

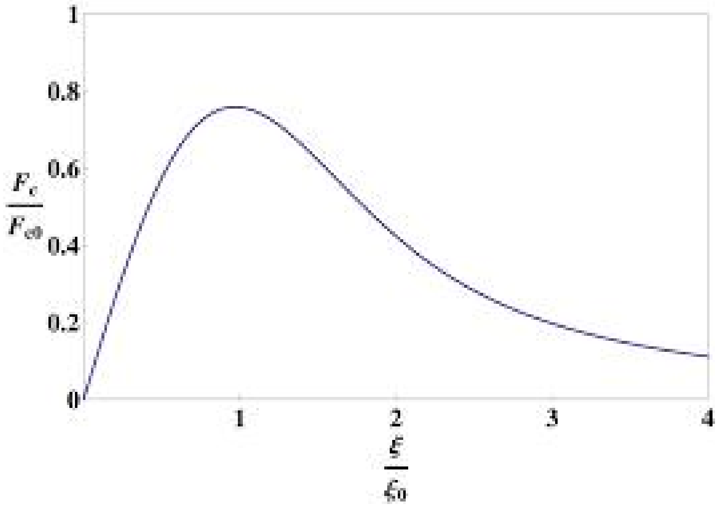

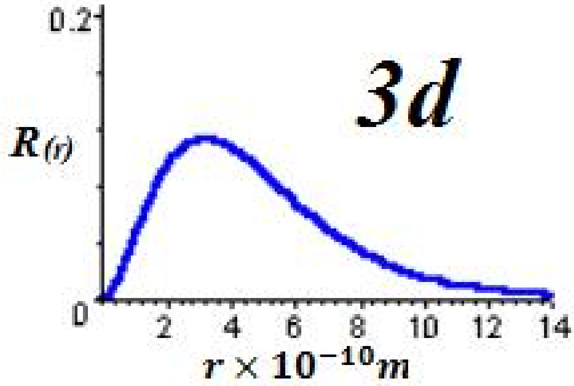

Hydrogen 3d Wave Function

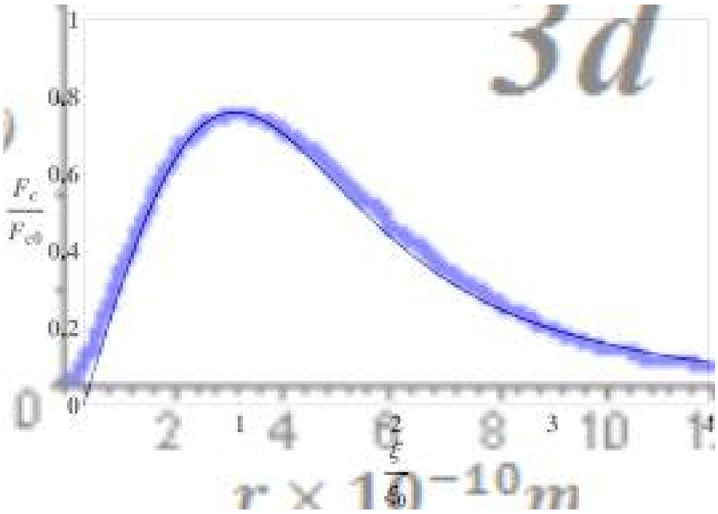

Super imposed graphs

https://iopscience.iop.org/article/10.1088/1402-4896/ab34c2

Nonlinear oscillations of ultra-cold atomic clouds in a magneto-optical trap

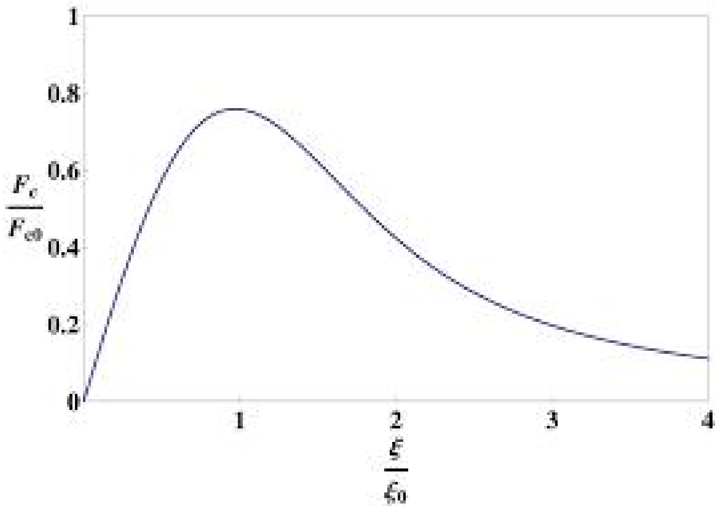

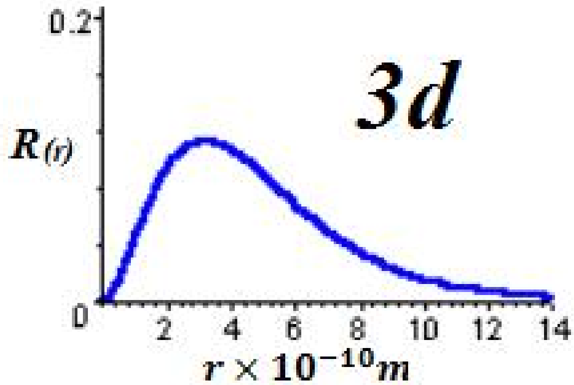

Hydrogen 3d Wave Function

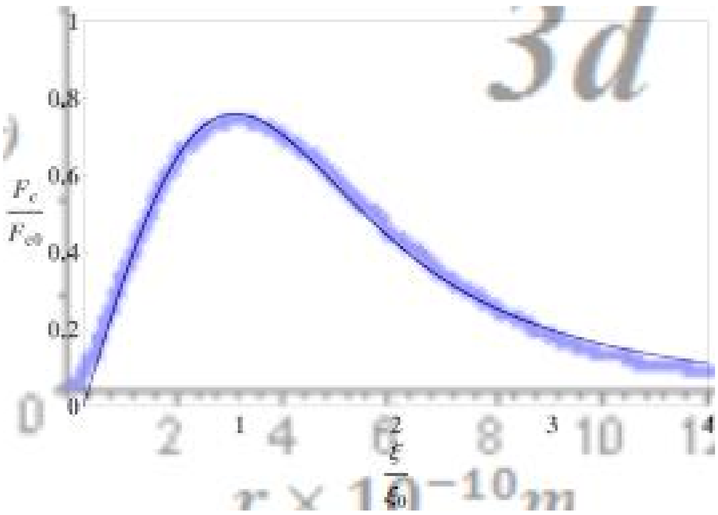

Super imposed graphs

https://iopscience.iop.org/article/10.1088/1361-6455/abd2d1

Absorption spectroscopy of the atomic beam under a 30° angle at the exit of the Zeeman slower. The resulting spectrum shows the longitudinal velocity distribution and the effect of the slowing laser beam. Atoms exiting the oven with a velocity below $v_c \approx 390$ m s^{-1} are slowed down to below 50 m s^{-1}. The frequency axis is calibrated using a simultaneous spectroscopy measurement under an axis perpendicular to the atomic beam. The dashed curve is a fit to the thermal velocity distribution by a Maxwell–Boltzmann function at T_{oven} = 450 °C.

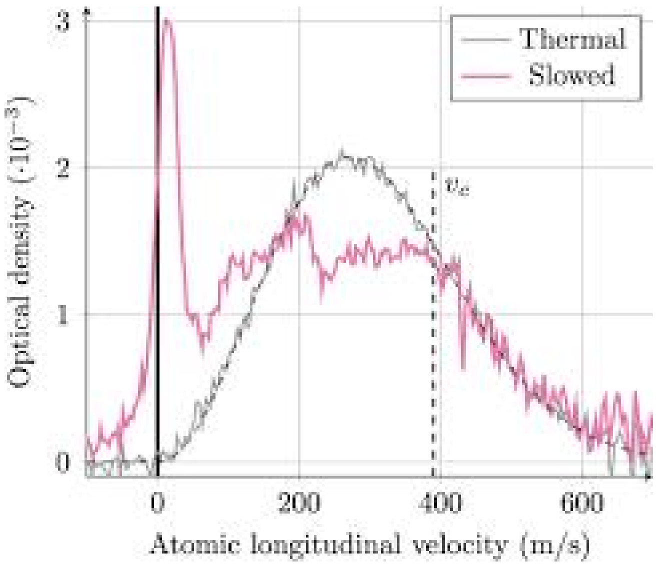

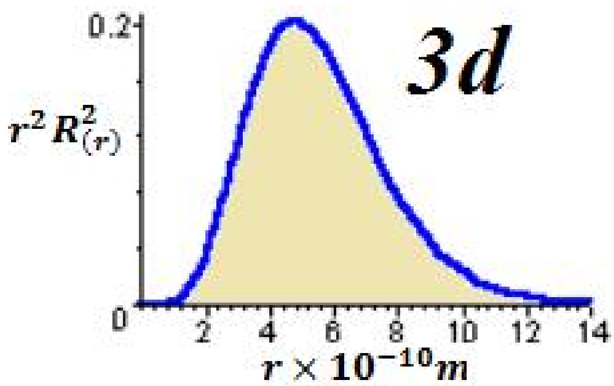

Hydrogen 3d Probability Density

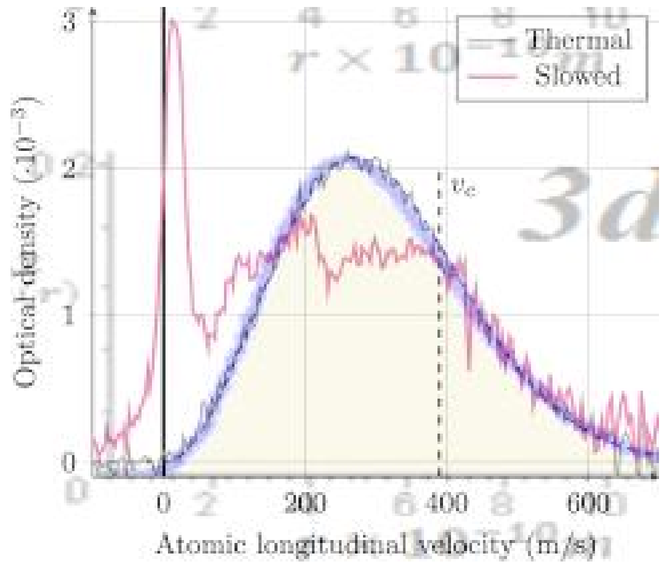

Super imposed graphs

https://www.pnas.org/doi/10.1073/pnas.2017646117

The pressure as a function of specific volume at temperatures of 0.1 (crosses), 0.2 (squares), 0.32 (circles), 0.4 (stars), 0.5 (diamonds). This serves as a tool for detecting coexistence between two phases of different densities, as explained in the text. This particular result is for LJ boson 4He. (Inset) Same as the main graph but with a smaller PP *scale and only* T=0.32T=0.32*. Different symbols distinguish the superfluid phase (open), the normal phase (solid black), and the gas phase (gray).*

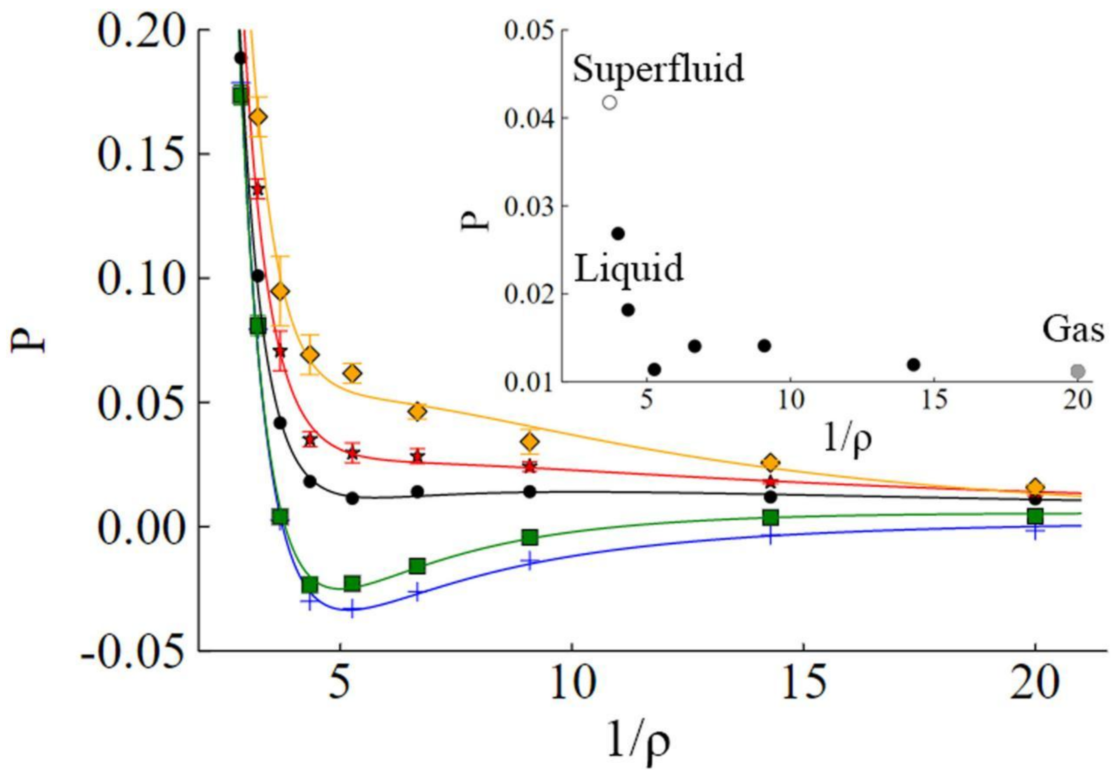

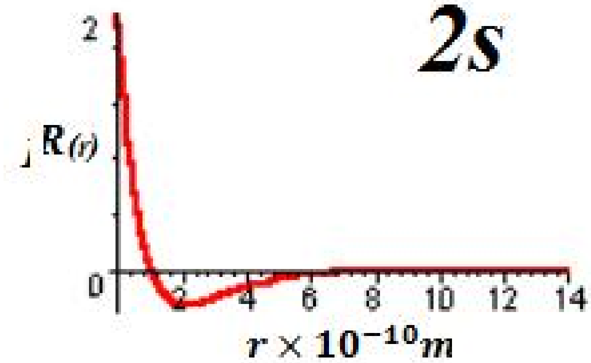

Hydrogen 2s Wave Function

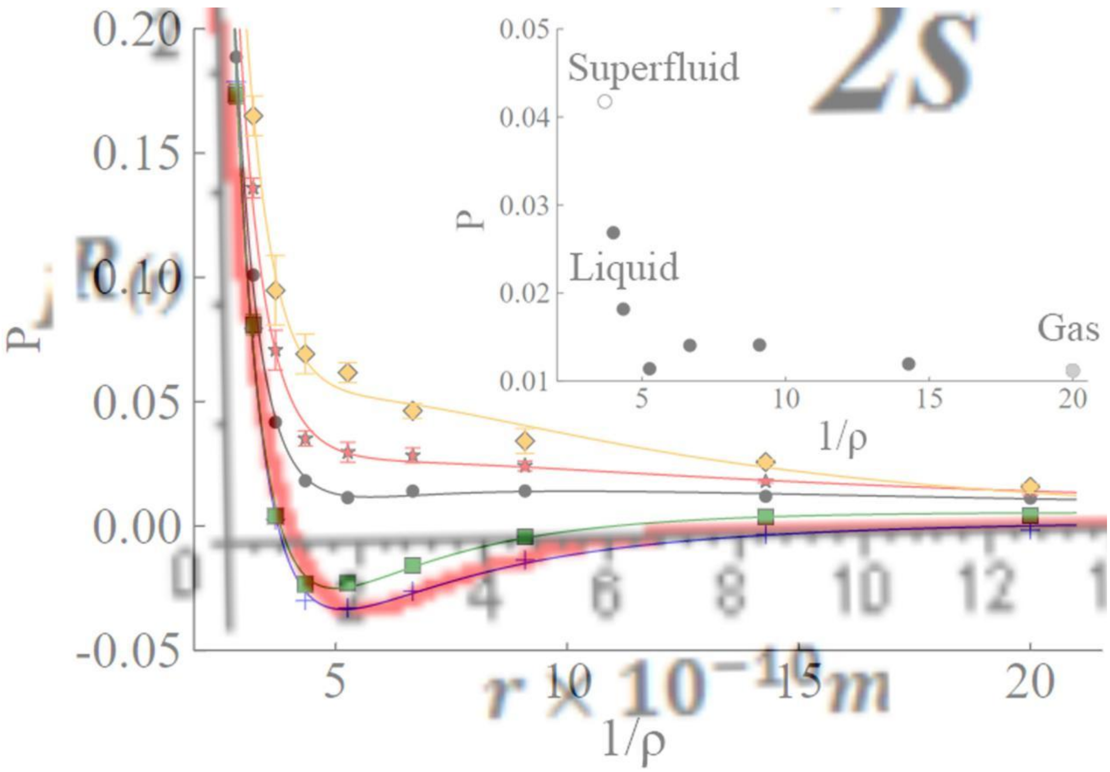

Super imposed graphs

https://www.mdpi.com/2571-712X/2/2/19

The dependence of a quantity β−1(ω¯) on the dimensionless frequency. As calculations show, in the frequency range under consideration (see table) there are only eight values of β−1 (red points), for which the quantization conditions (45) and (46) are satisfied. The blue dots denote such states for which the quantization conditions are not satisfied.

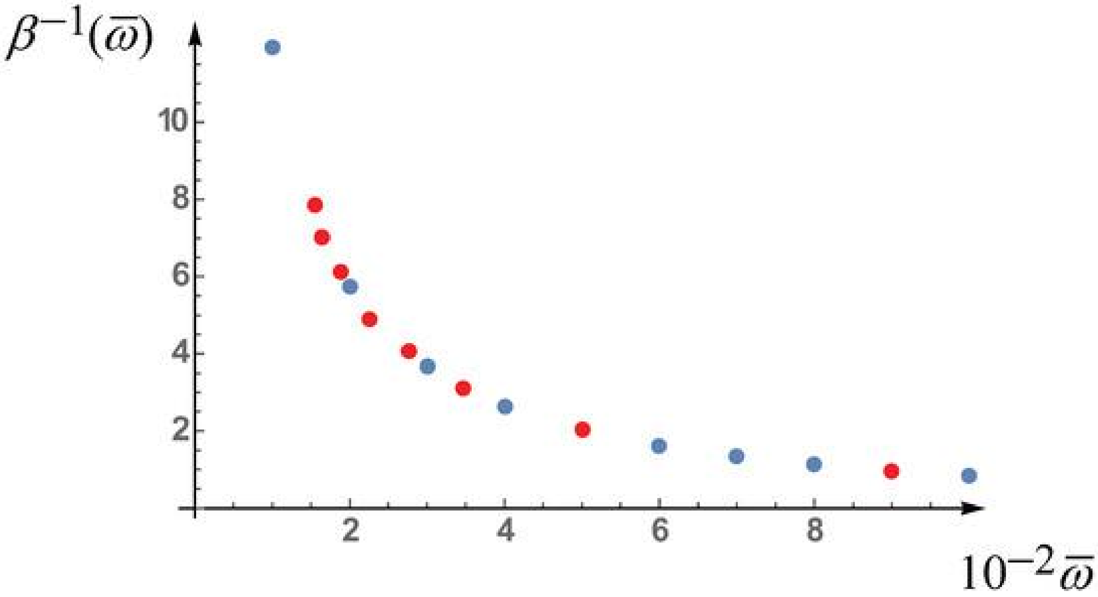

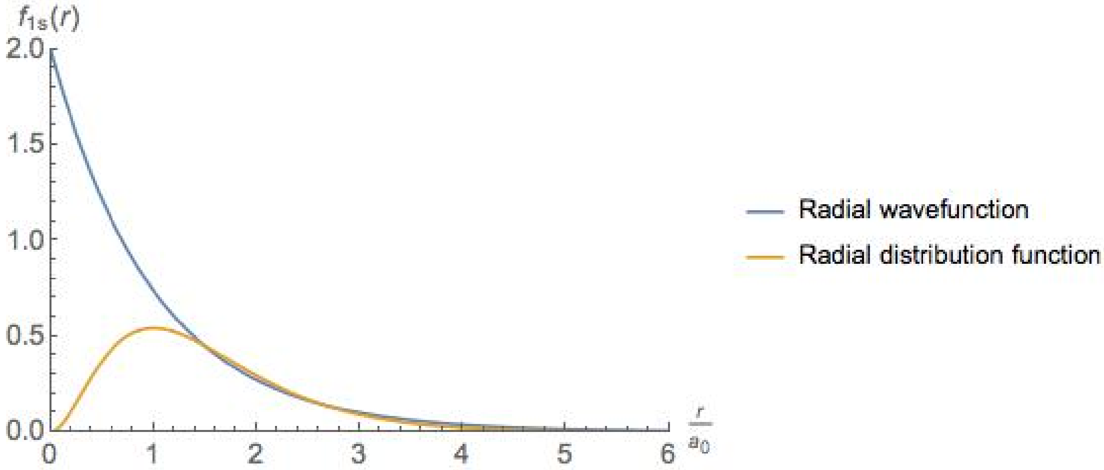

Hydrogen 1s Wave Function

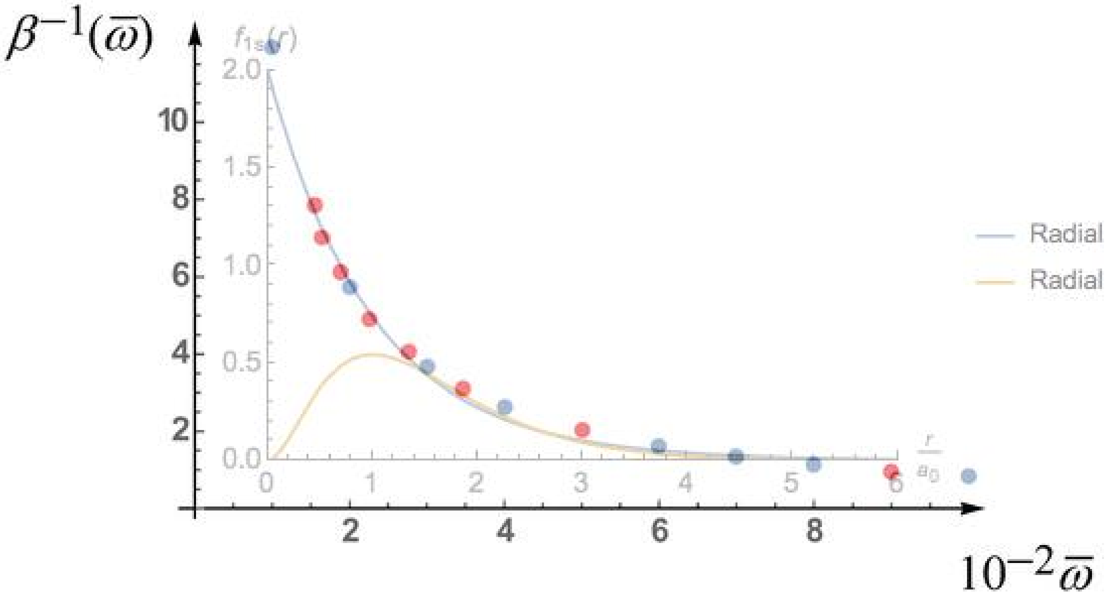

Super imposed graphs

https://study.com/academy/lesson/newton-s-law-of-cooling.html

The plot of the temperature difference between the body and the surroundings with time gives the law of cooling graph.

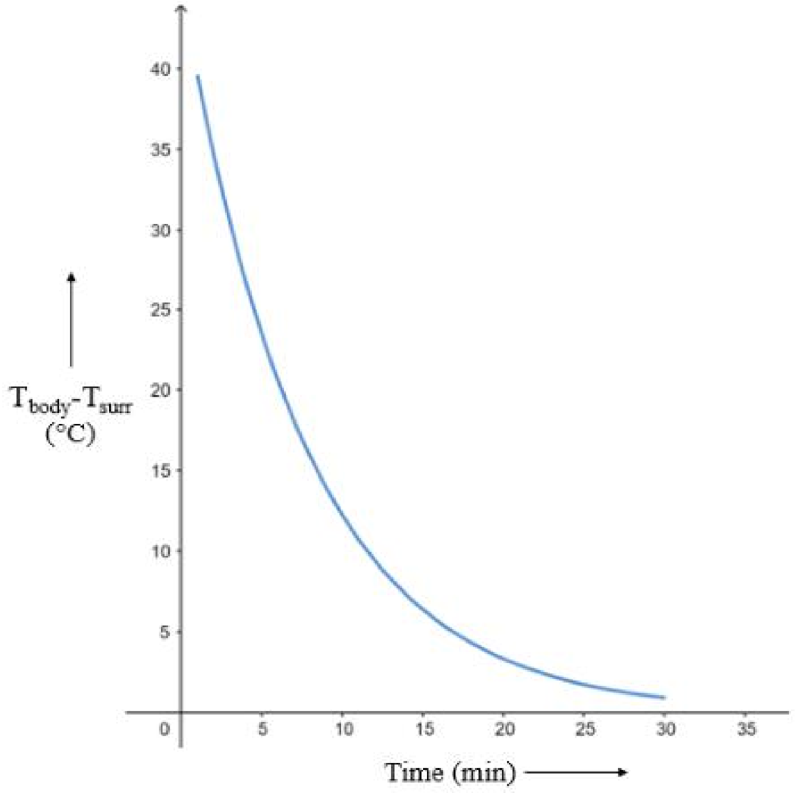

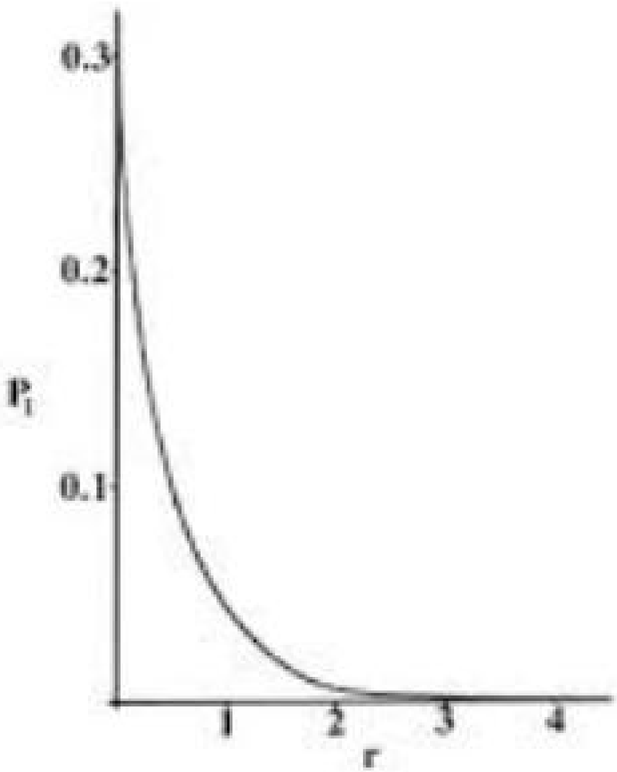

Hydrogen 1s Wave Function

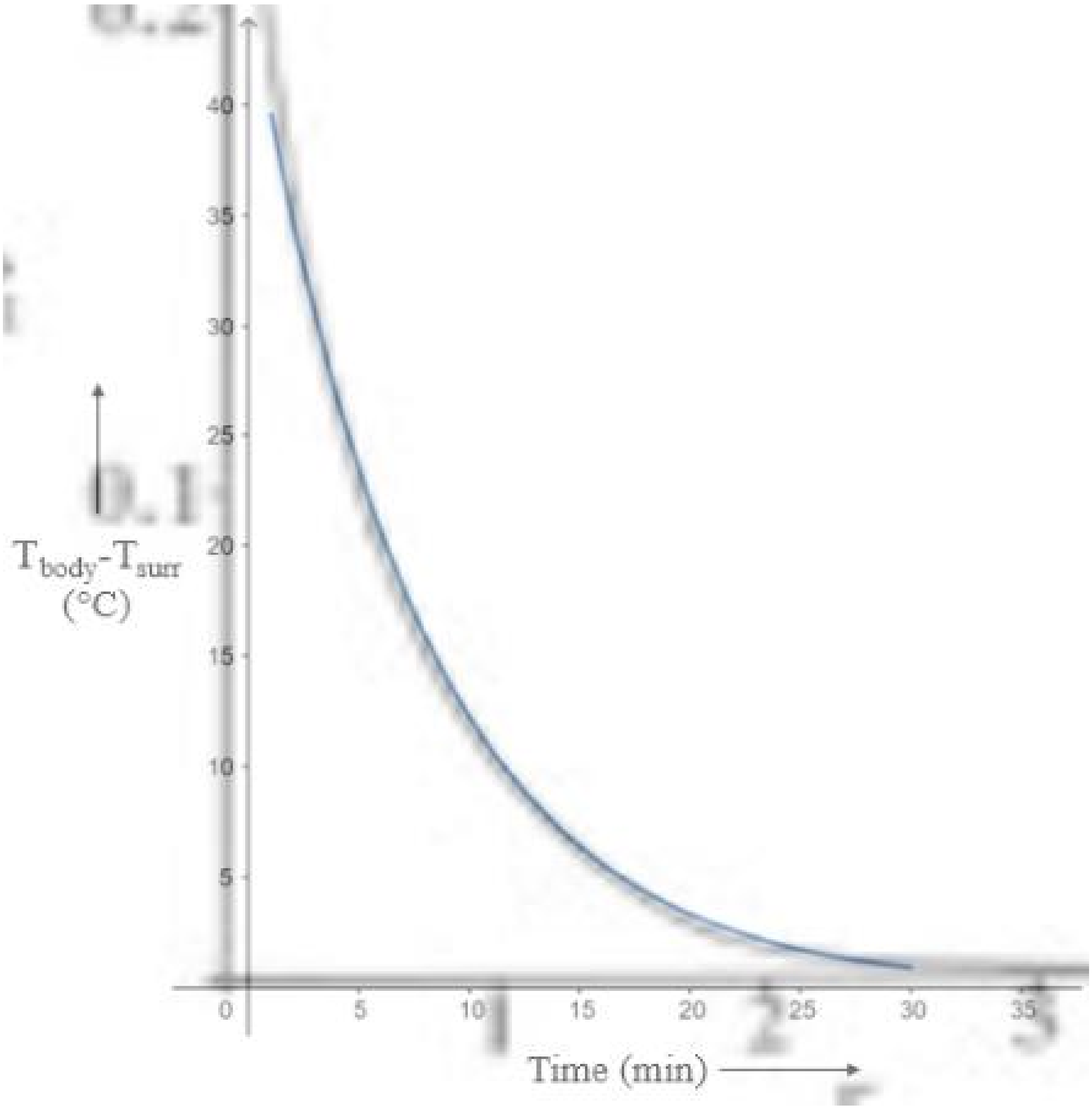

Super imposed graphs

https://www.scielo.br/j/bjp/a/t3fFWtyg4MHpmQTpxCbW6sD/?lang=en

Bose-Einstein condensation in a constant magnetic field

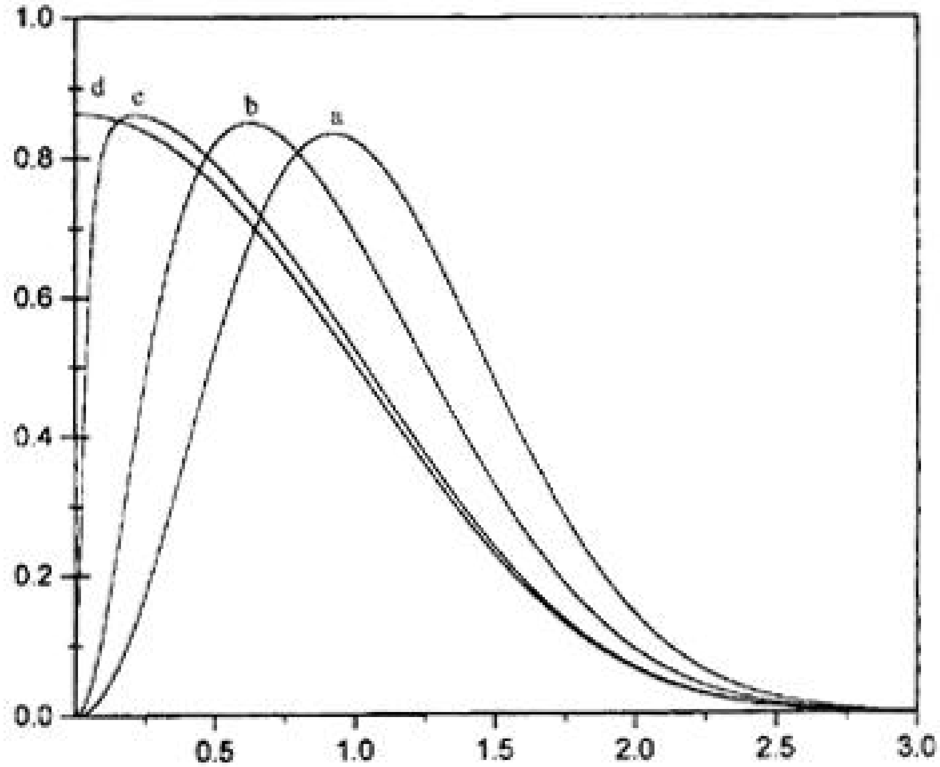

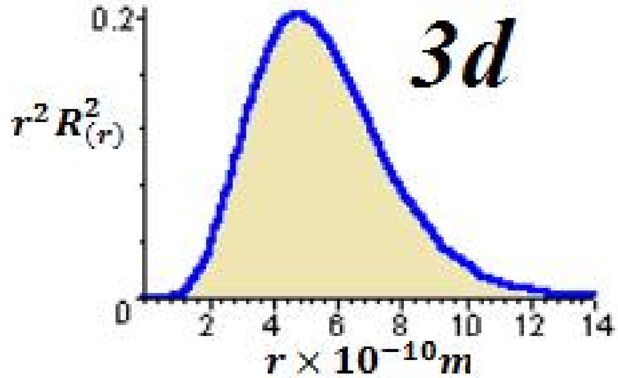

Hydrogen 3d Probability Density

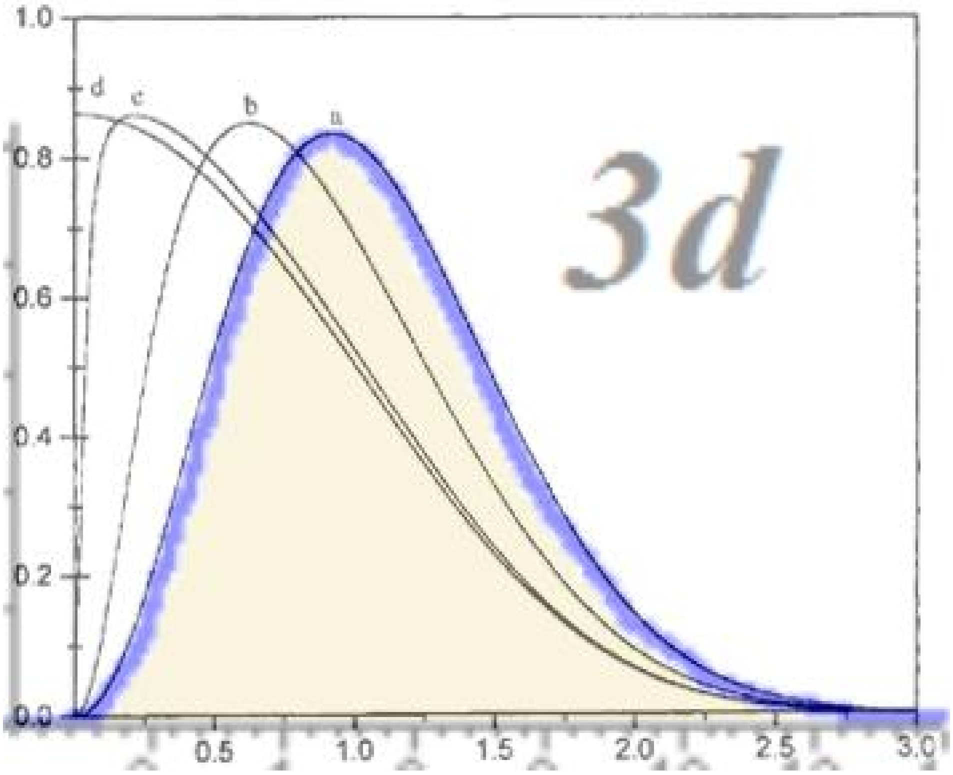

Super imposed graphs

Quantum simulation of Unruh radiation

Thermal behaviour of the matter-wave emission.

https://www.nature.com/articles/s41567-019-0537-1

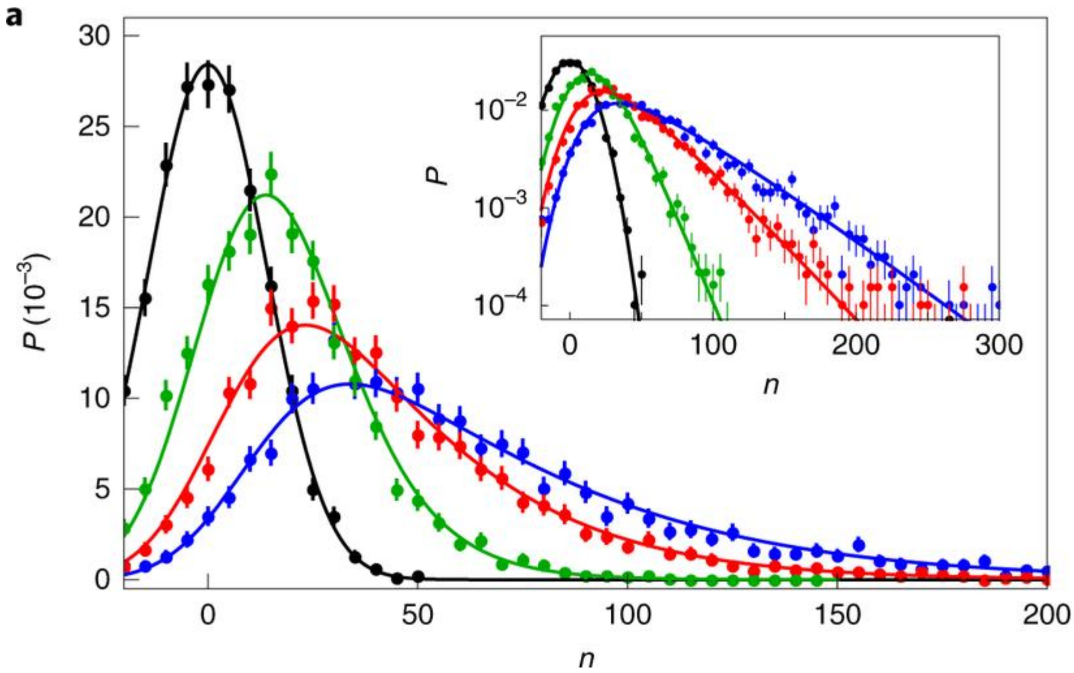

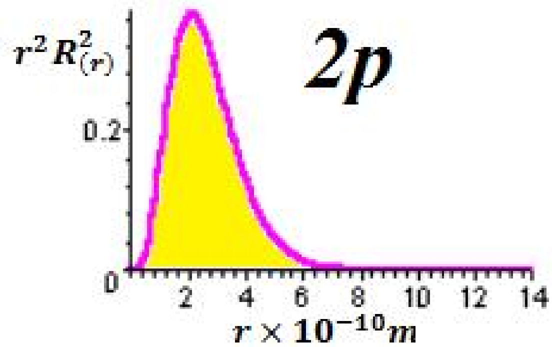

Hydrogen 2pProbability Density

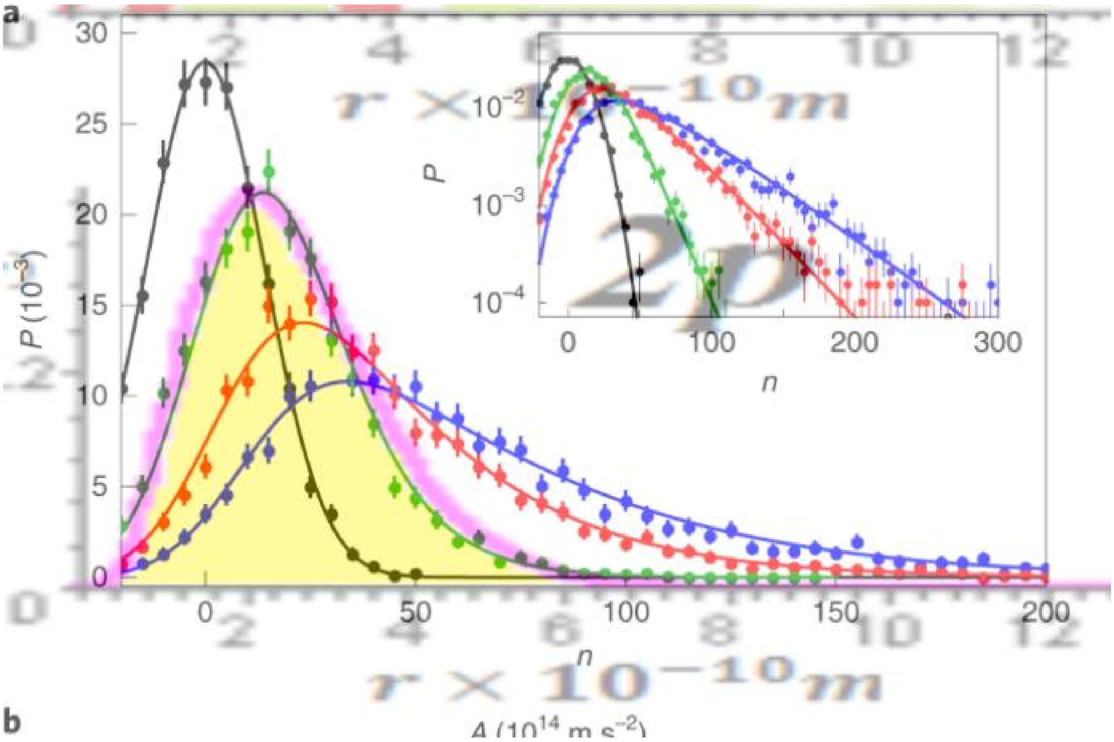

Super imposed graphs

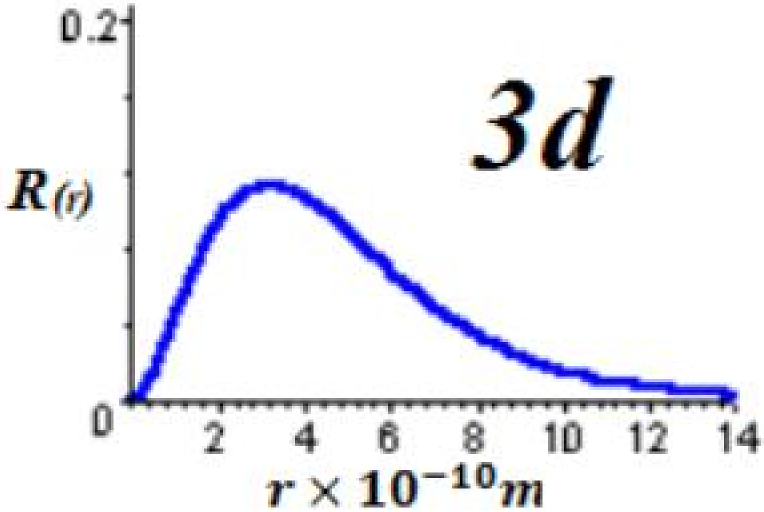

Hydrogen 3d Wave Function

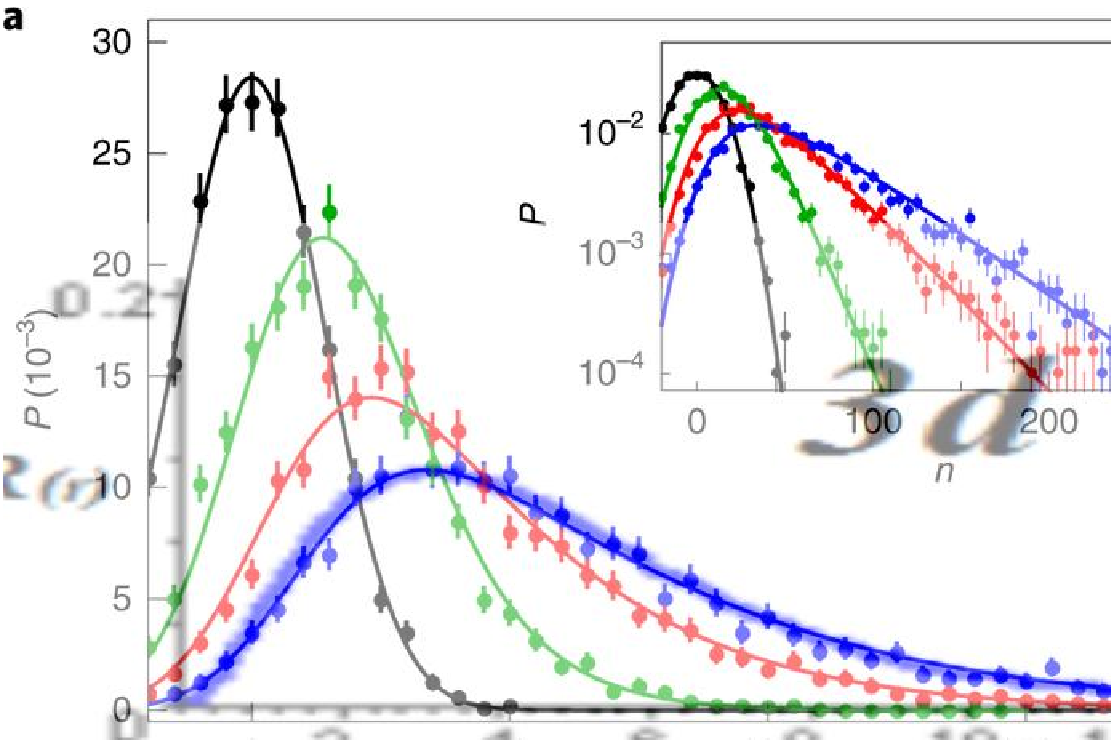

Super imposed graphs

Quantum metrology and estimation of Unruh effect

https://www.researchgate.net/figure/QFI-in-the-estimation-of-the-Unruh-temperature-T-as-a-function-of-the-energy-gap-O-for_fig1_268876335

QFI in the estimation of the Unruh temperature T as a function of the energy gap Ω for different interaction time Δ. The parameters related to the effective coupling parameter are fixed to satisfy . They are fixed with and κ = 0.02, respectively. The initial state parameter is given by θ = π/4 and the acceleration parameter is fixed with a = 0.4π.

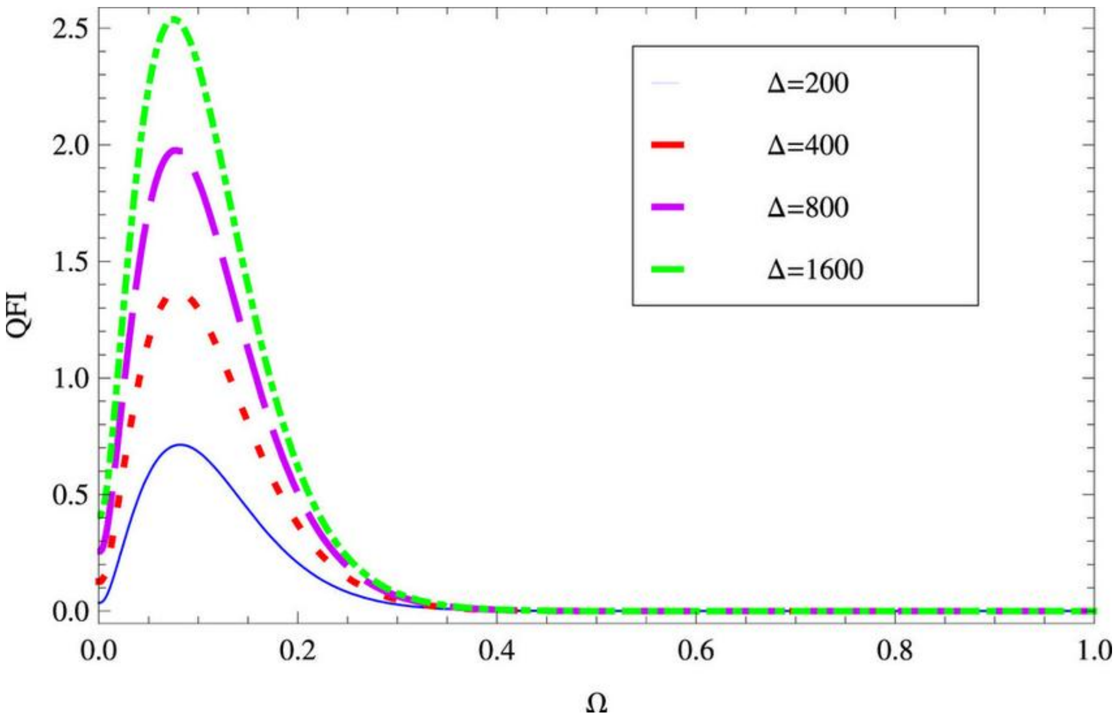

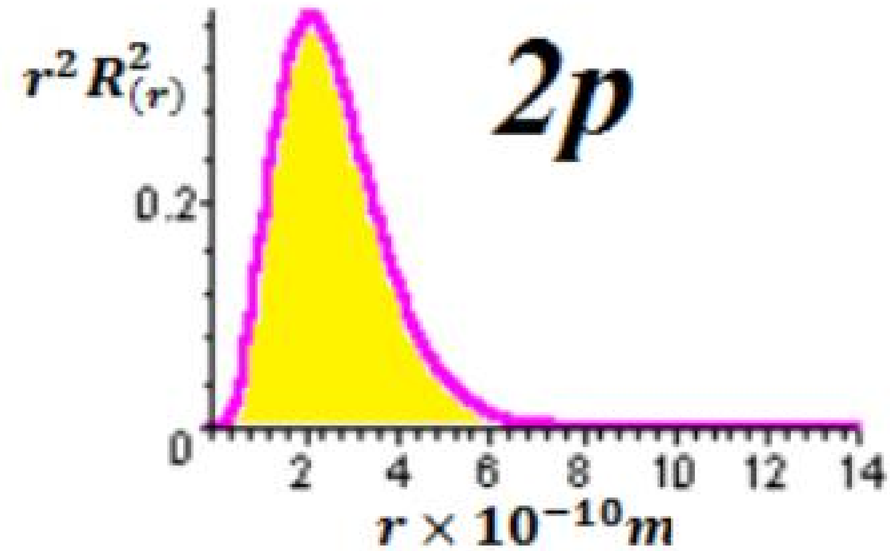

Hydrogen 2p Probability Density

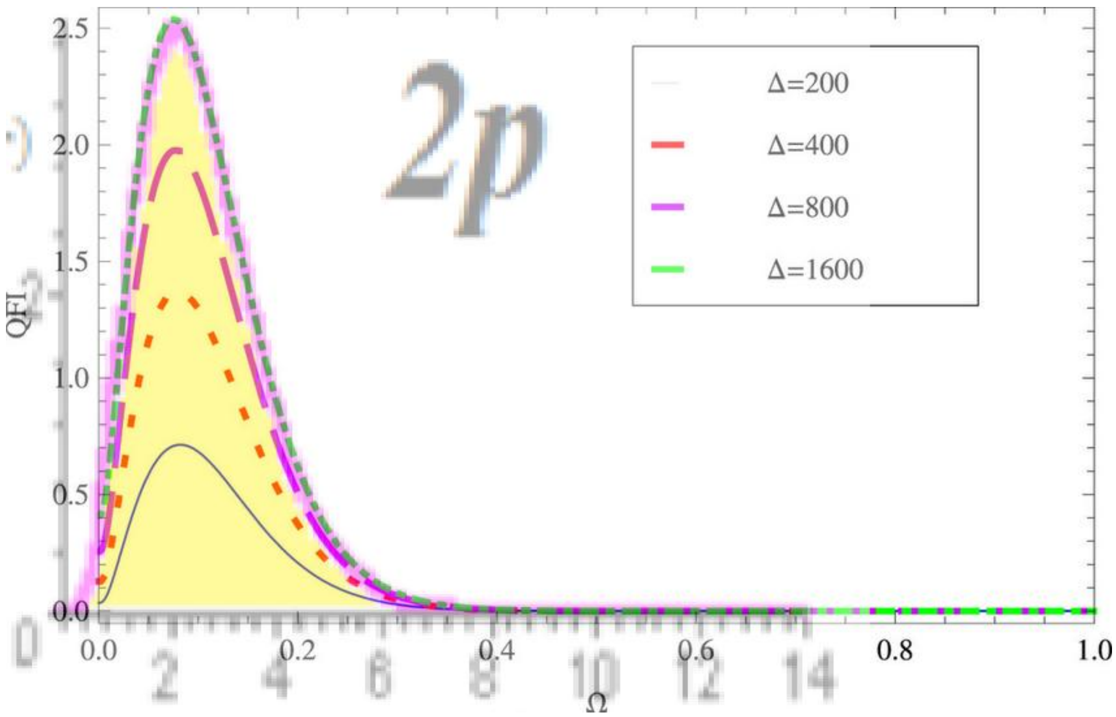

Super imposed graphs

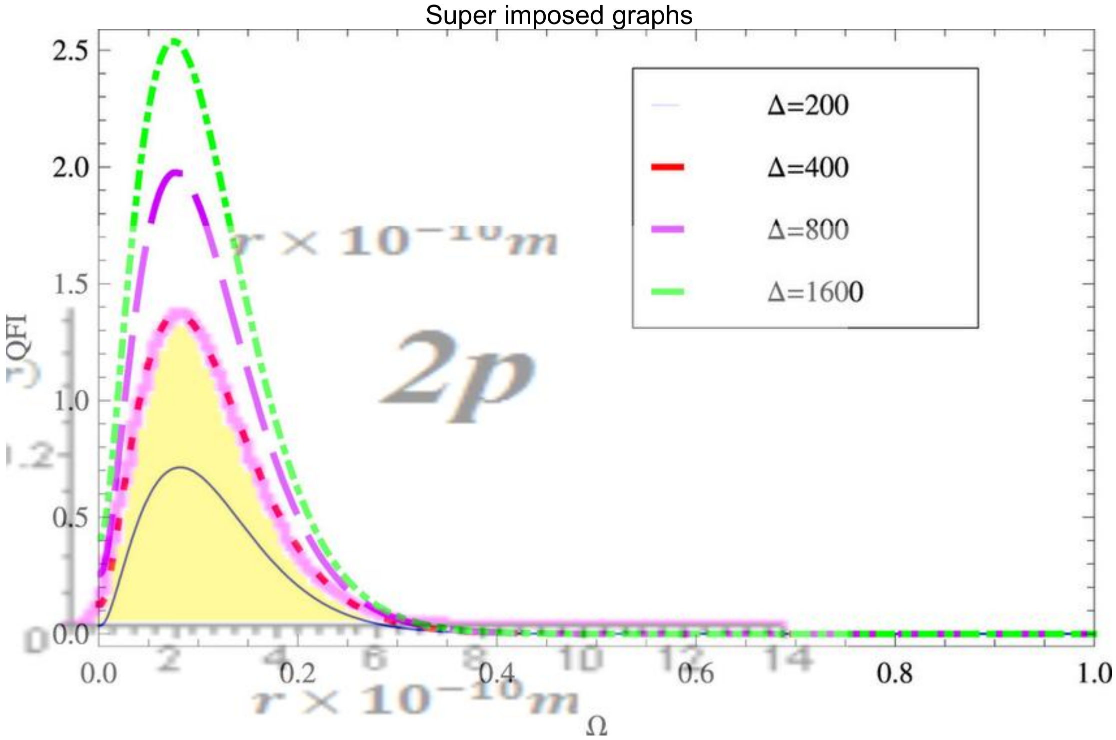

Super imposed graphs

What is the Maxwell-Boltzmann distribution?

https://www.khanacademy.org/science/physics/thermodynamics/temp-kinetic-theory-ideal-gas-law/a/what-is-the-maxwell-boltzmann-distribution

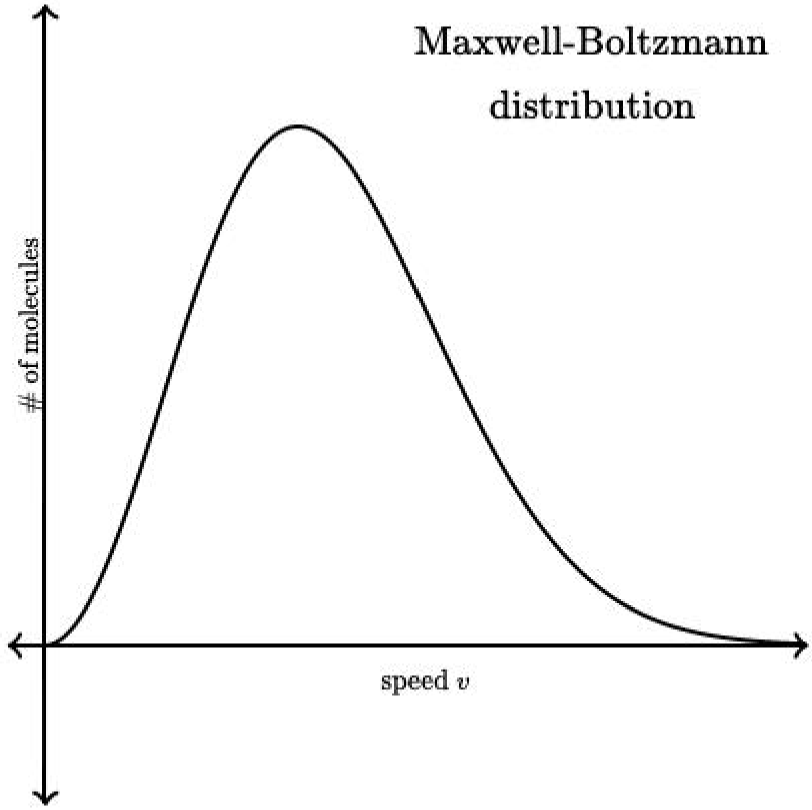

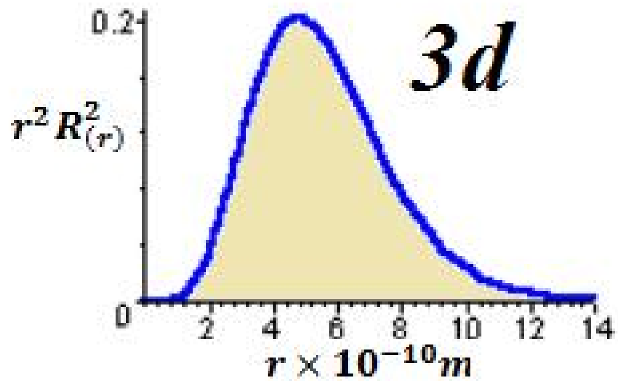

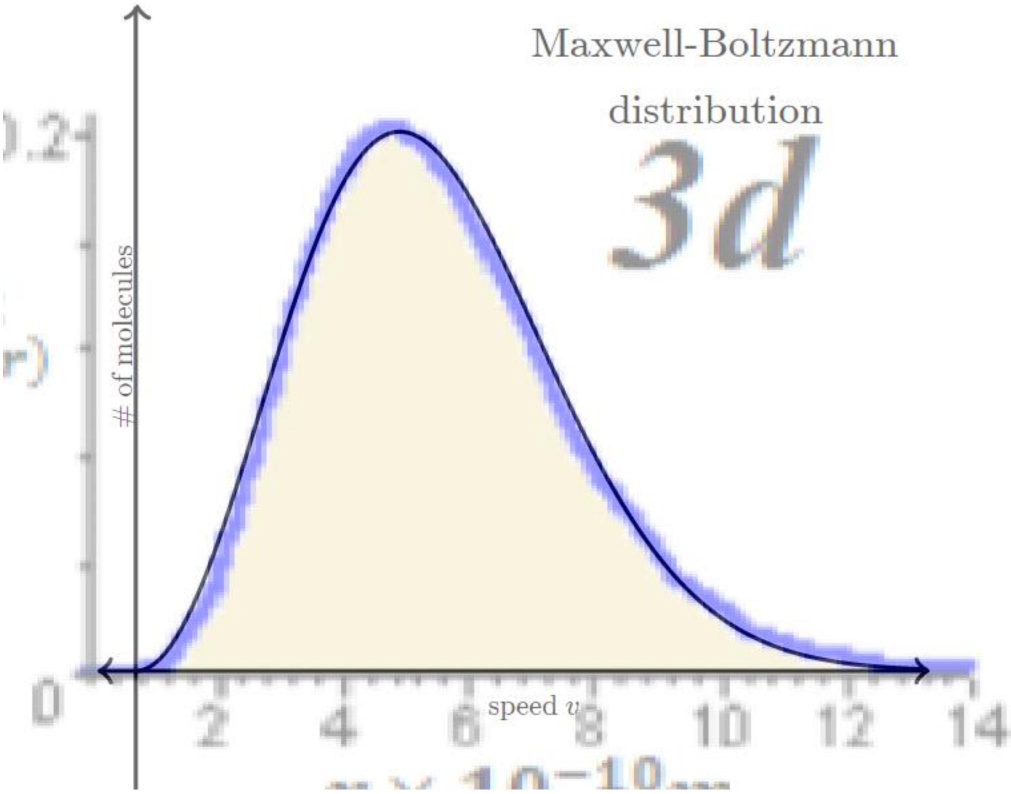

[The Wave Function of the Helium atom also has symmetries with Macro phenomenon:]

https://iopscience.iop.org/article/10.3847/1538-4357/aaec74

Photometric and Spectroscopic Properties of Type Ia Supernova 2018oh with Early Excess Emission from the *Kepler 2* Observations

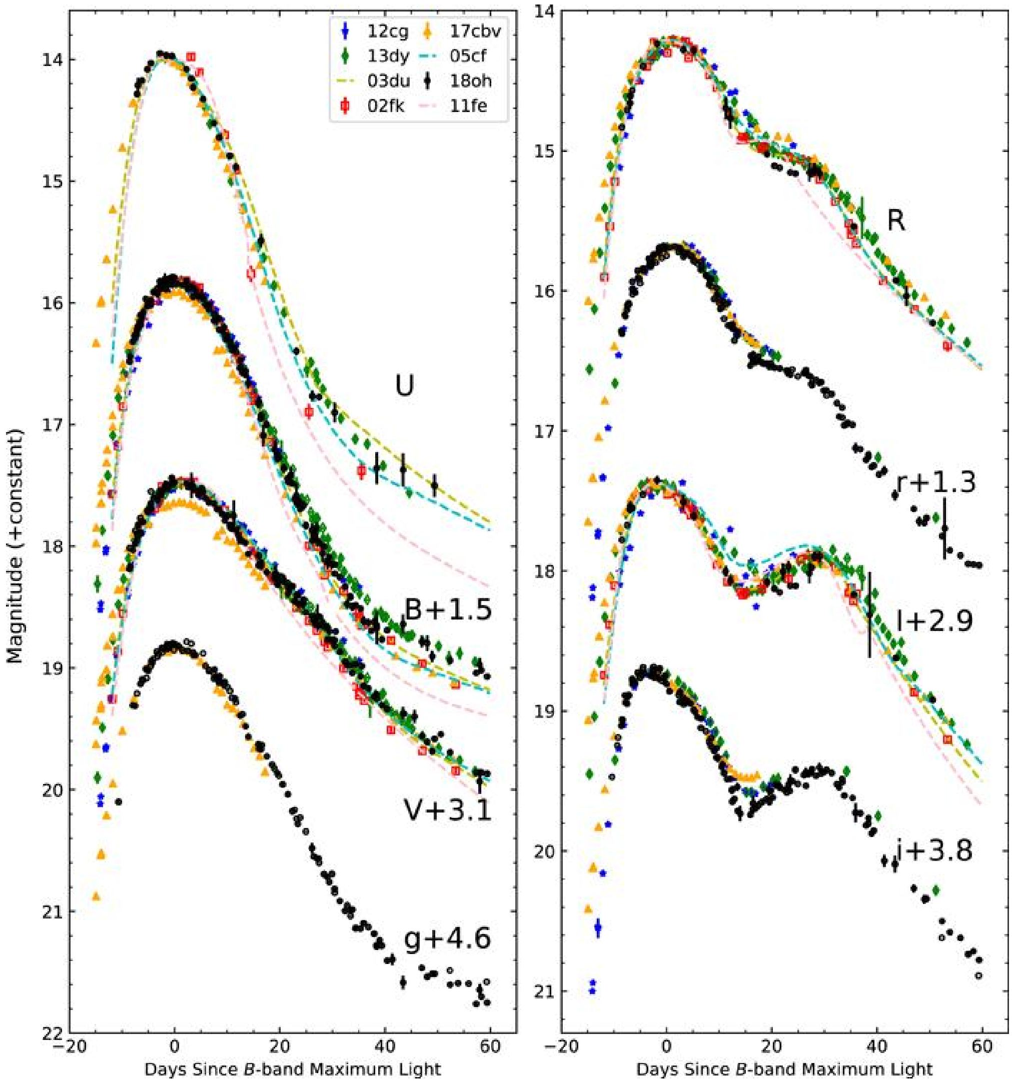

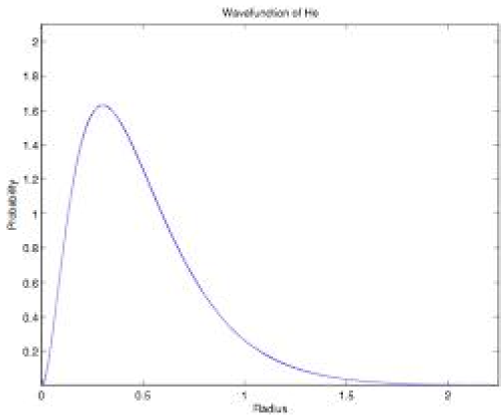

Helium wave function

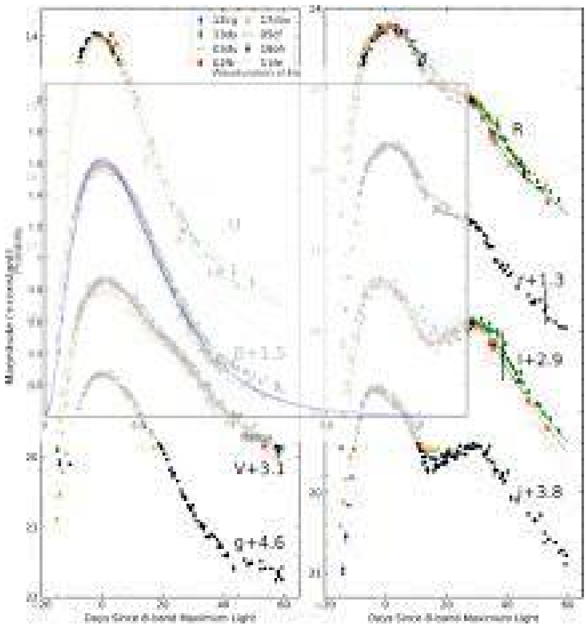

Super imposed graphs

https://www.nature.com/articles/s41550-019-0858-0
observational properties of thermonuclear supernovae

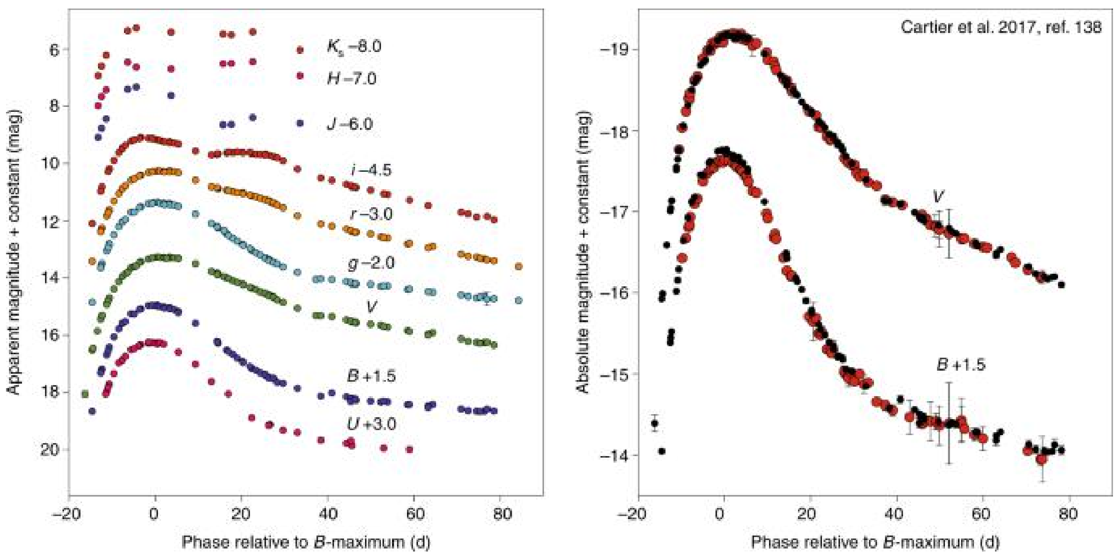

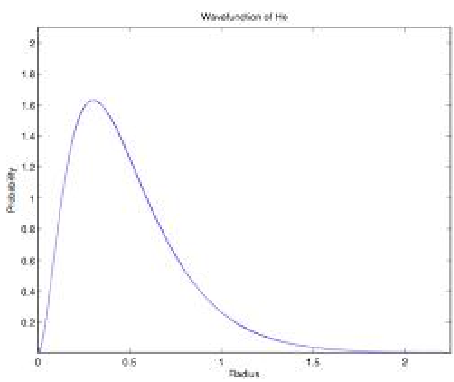

Helium Wave function

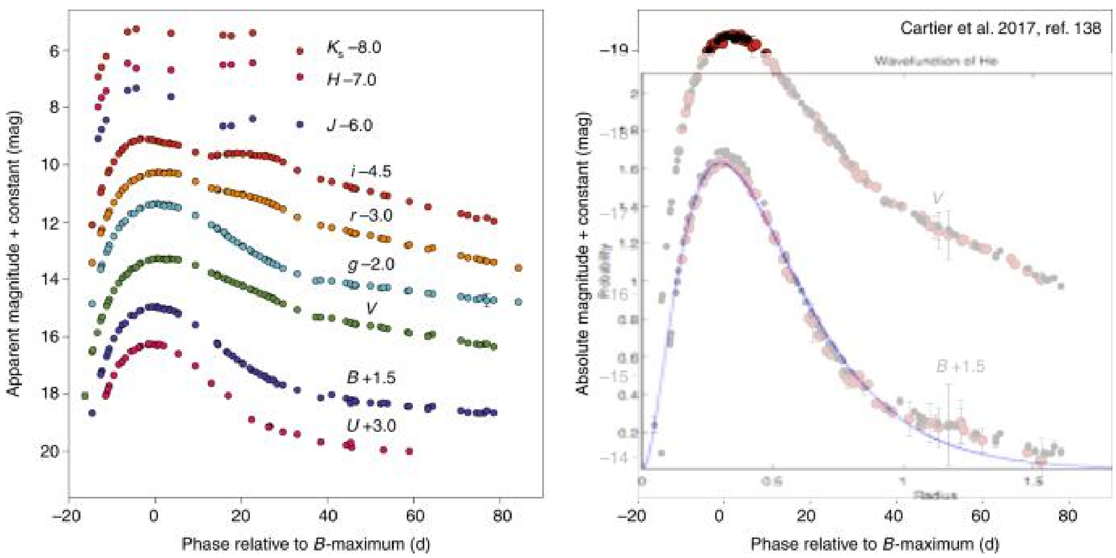

Super imposed graphs

Quasi-periodic oscillations around Kerr-MOG black holes

Radial profiles of frequencies of small harmonic oscillations ν_r, ν_θ and ν_ϕ of neutral particle around Kerr-MOG black hole having mass $M=10M_\odot$ measured by static distant observer

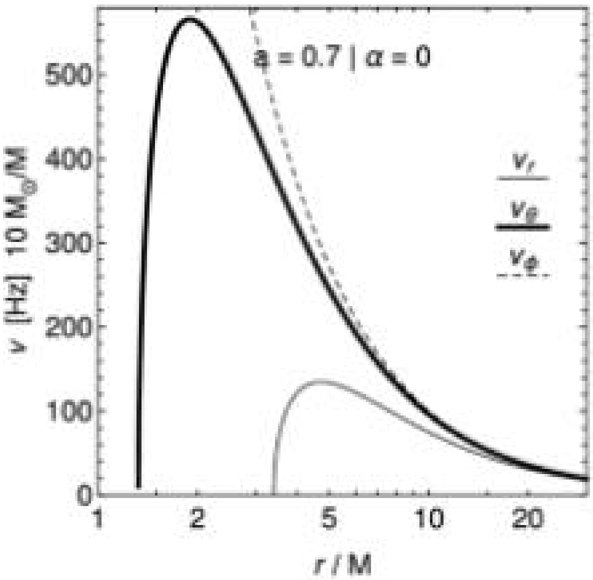

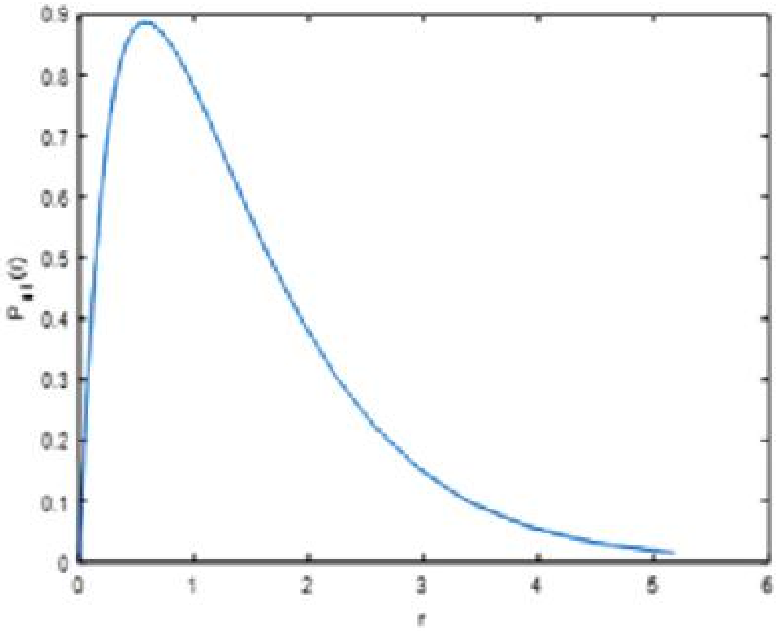

(a) $1s^2$

Helium Wave Function

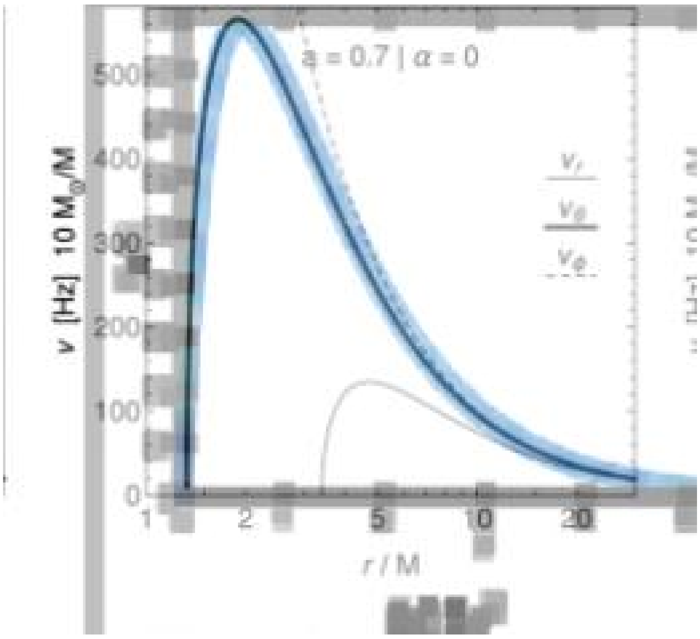

Super imposed graphs

https://www.researchgate.net/figure/This-graph-shows-the-current-mass-density-of-black-holes-as-a-function-of-their-initial_fig7_235497085

This graph shows the current mass density of black holes as a function of their initial mass mi. ρ0(m0) is the current number density of black holes of mass m0, so ρ0 = ρi (a 3 i /a 3 0). Because, for all practical purposes, m0 = mi, the area under the curve is the present matter density due to LQBH. If that density is equal to 0.22ρcrit, the LQBH will account for all dark matter. From this graph, we see that at present times, LQBH mass density is entirely dominated by black holes which had an initial mass of about 10 −5 mP. In this graph we have used β = 4 (the graph is not very sensitive to this choice) and Teq = 13% × 10 15 GeV (the numerical values of the graph vertical axis are sensitive to this value but location of the peak and the general shape of the graph are not).

Relative Contribution to Dark Matter Today

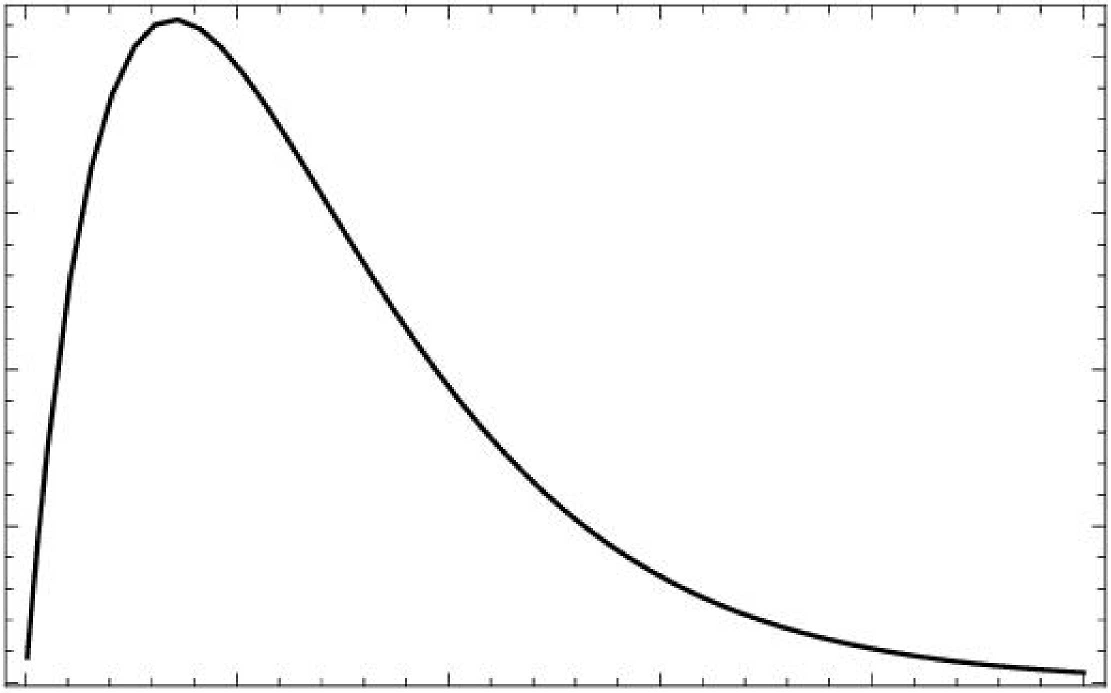

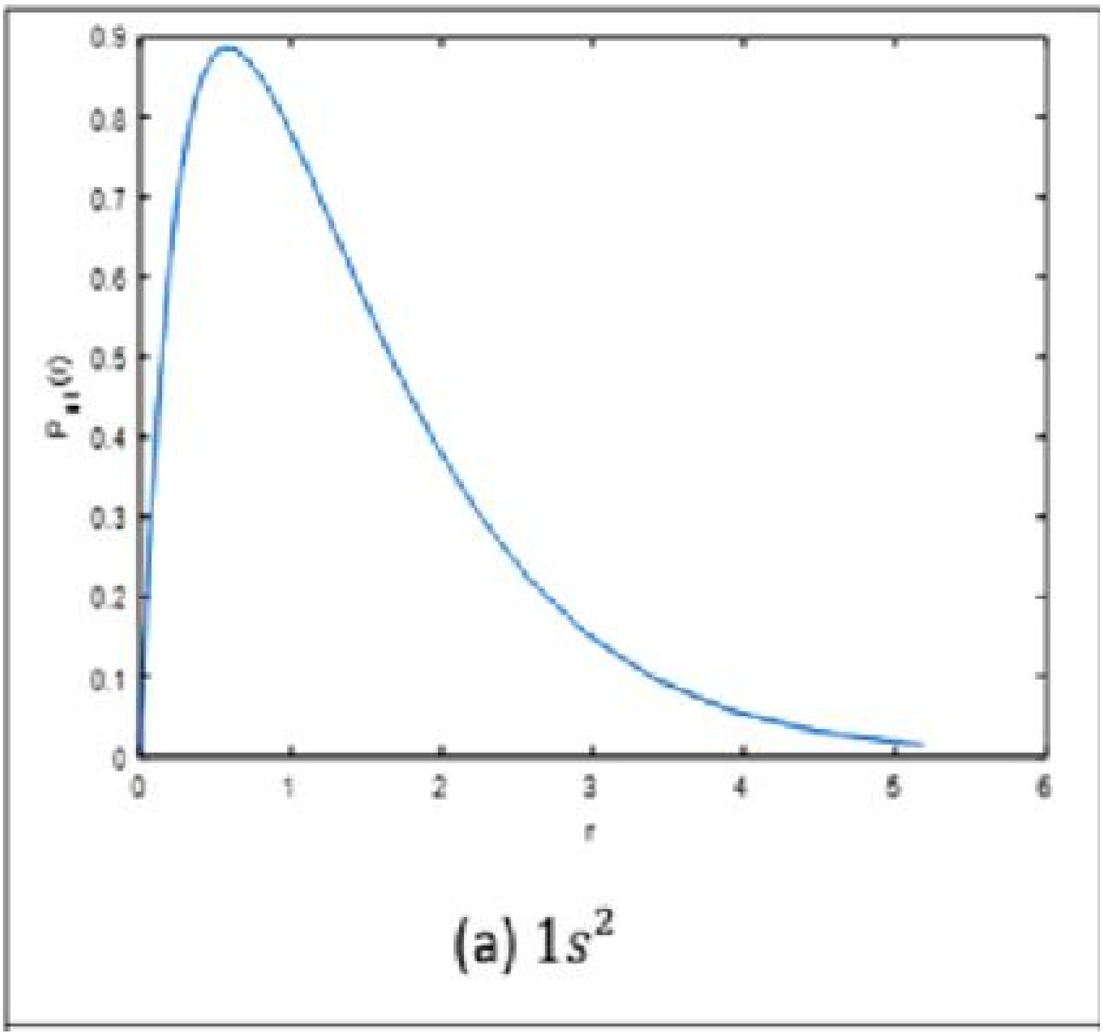

Helium Wave Function

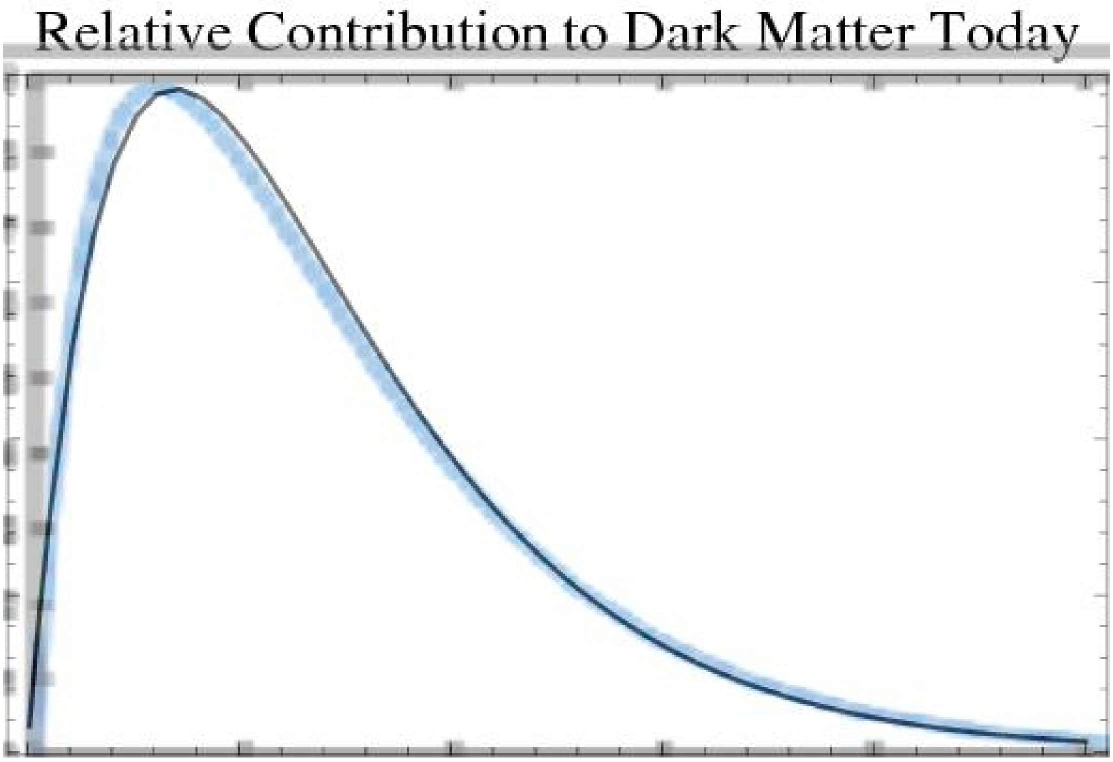

Super imposed graphs

https://www.nature.com/articles/s42005-019-0255-0

Searching for dark photon dark matter in LIGO O1 data

An example of dark photon dark matter signal power spectrum and corresponding detector sensitivity.

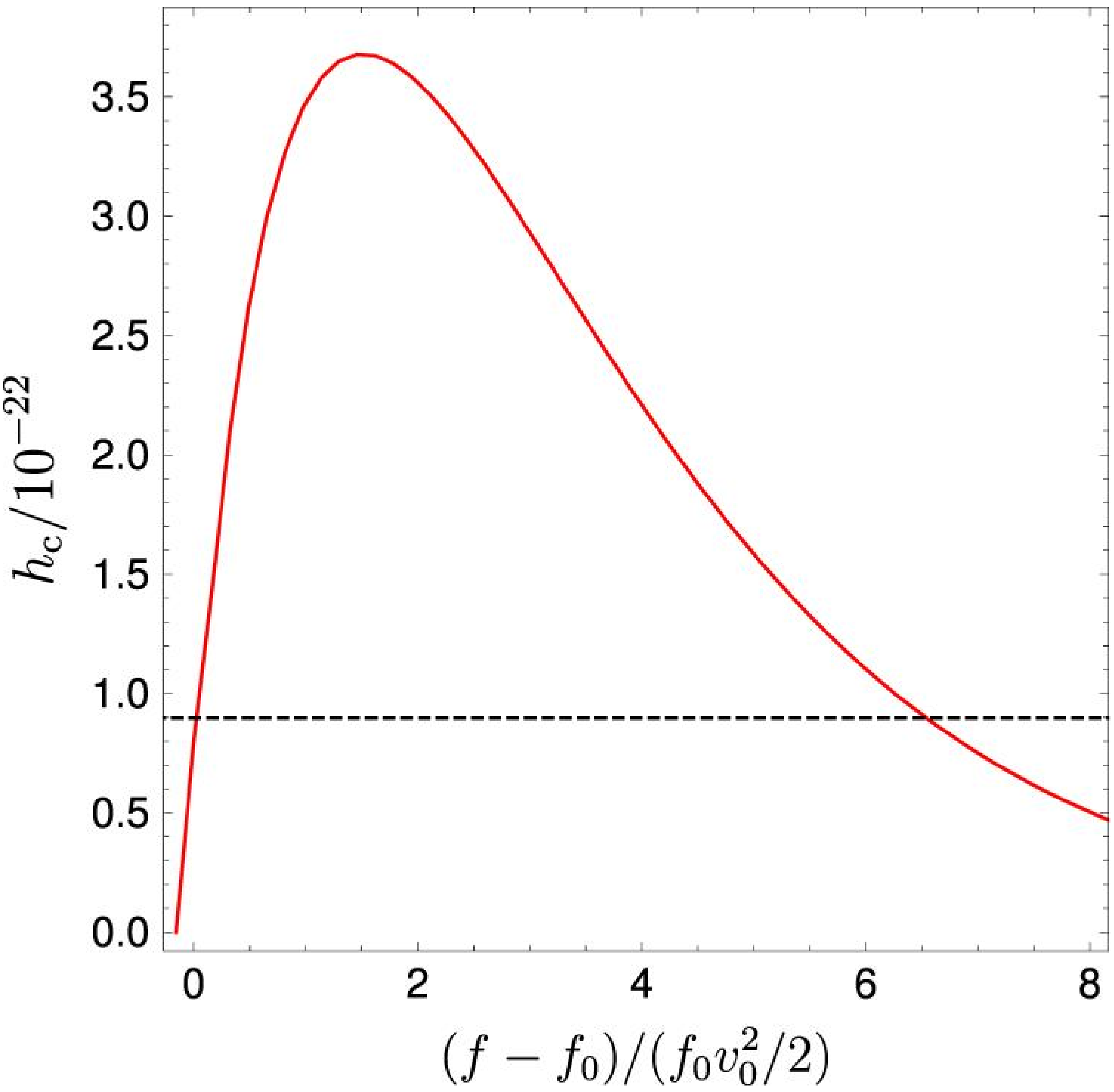

$h_c/10^{-22}$
0.0
0.5
1.0
1.5
2.0
2.5
3.0
3.5
0
2
4
6
8
$(f-f_0)/(f_0 v_0^2/2)$

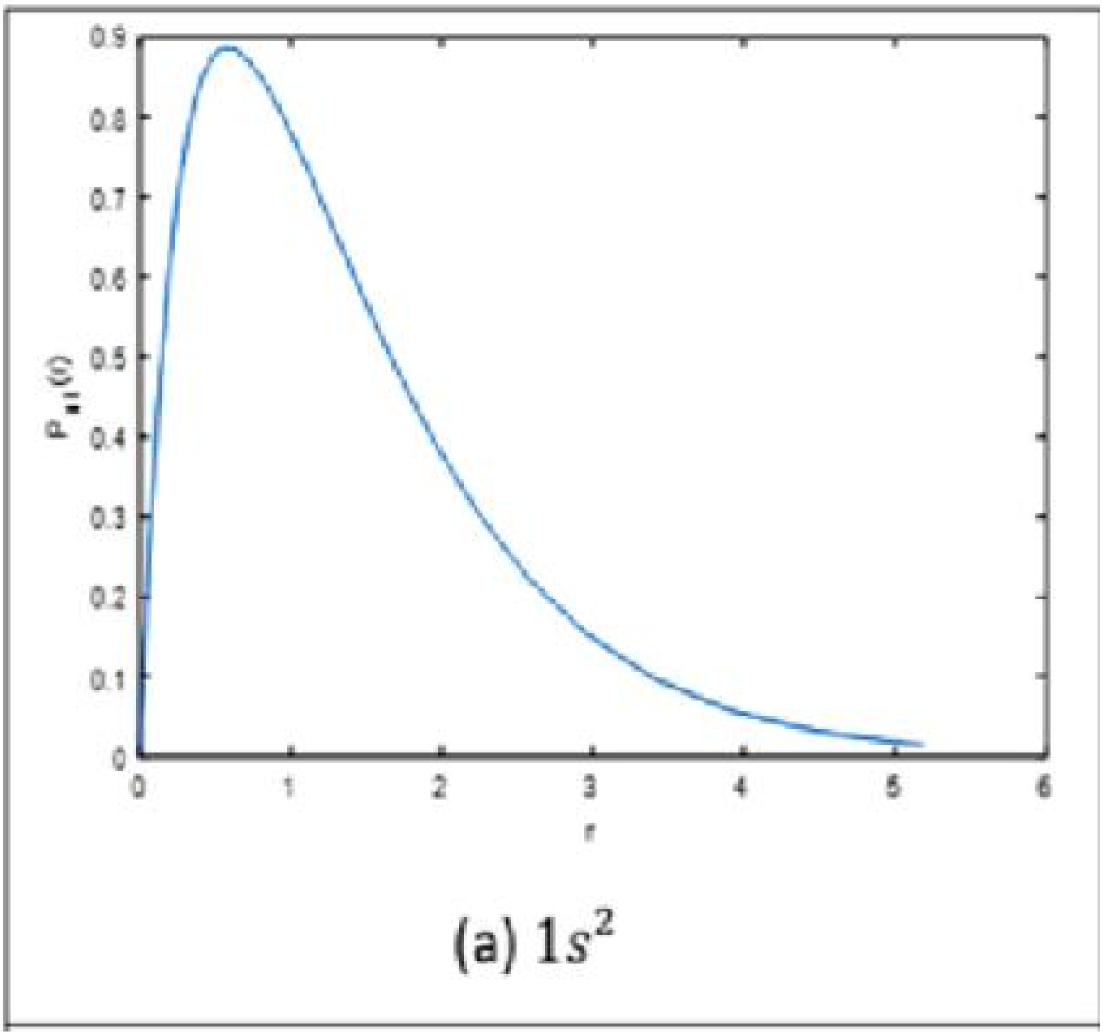

Helium wave function

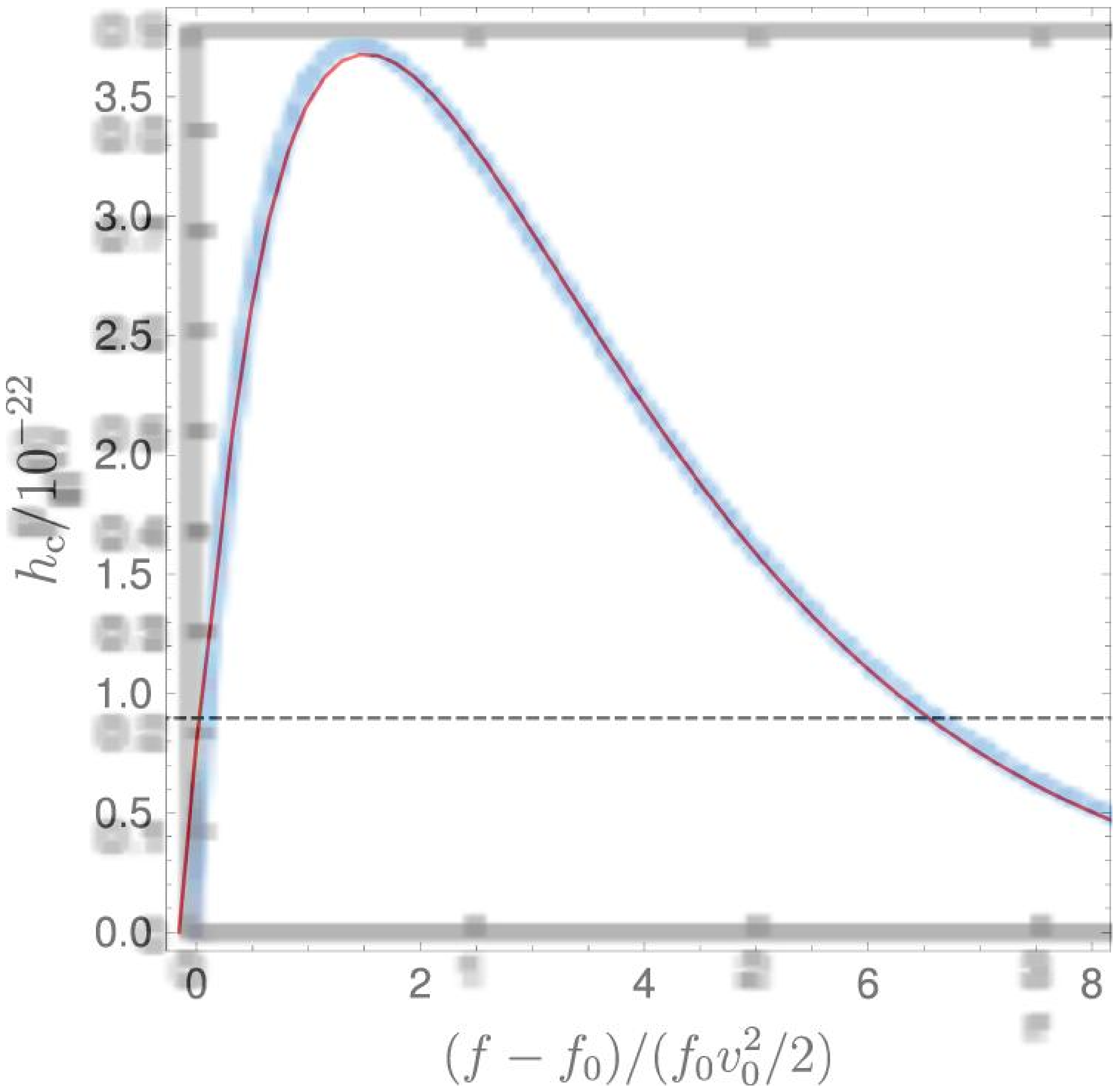

Super imposed graphs

Other interesting symmetries:

https://byjus.com/jee/superposition-of-waves/

What is Superposition of Waves

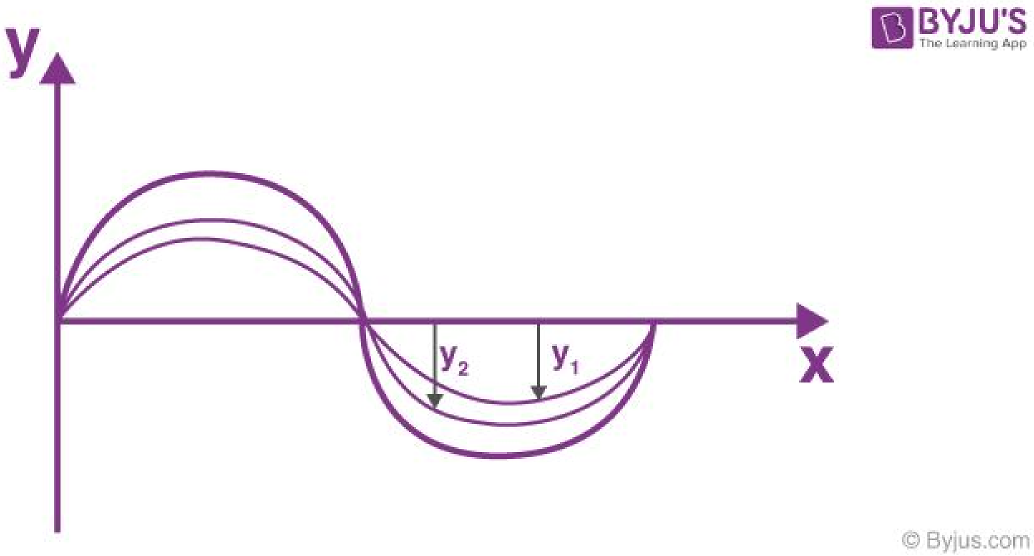

https://academics.uccs.edu/rtirado/PES_1060_Astro_2/Chaisson_8e_pdfs/26_LectureOutline.pdf

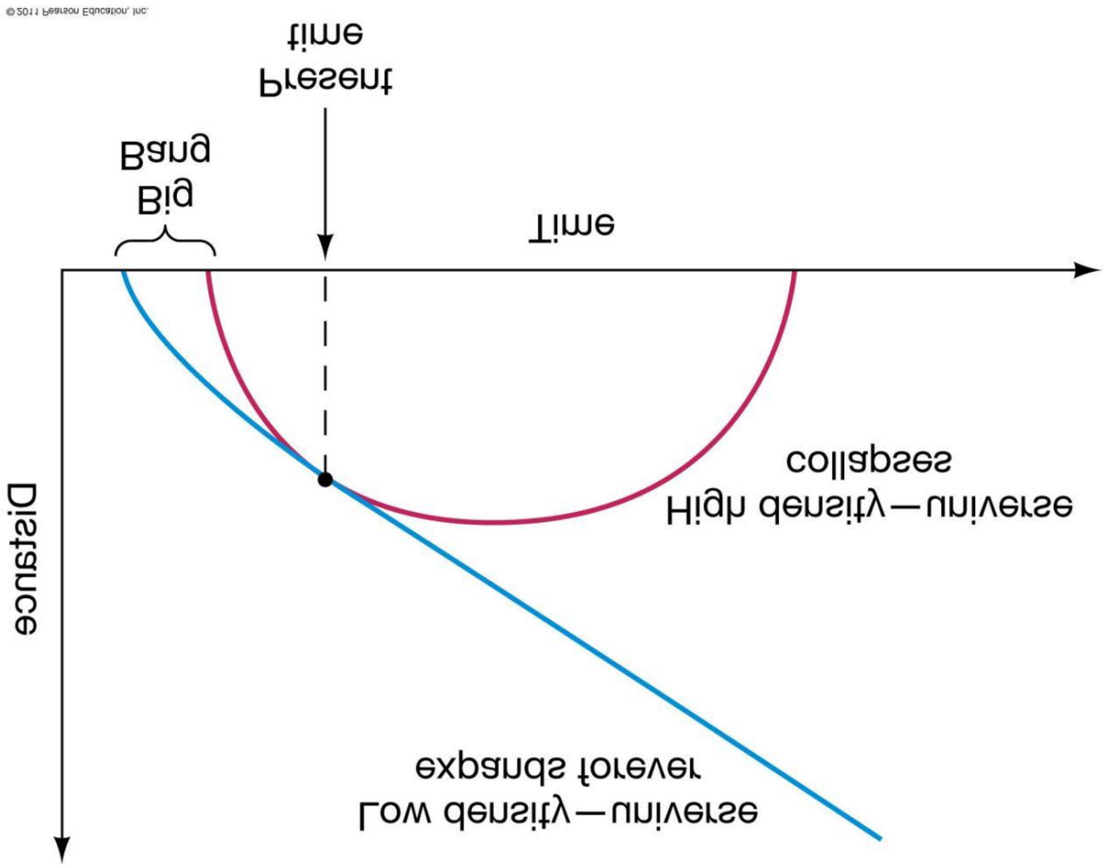

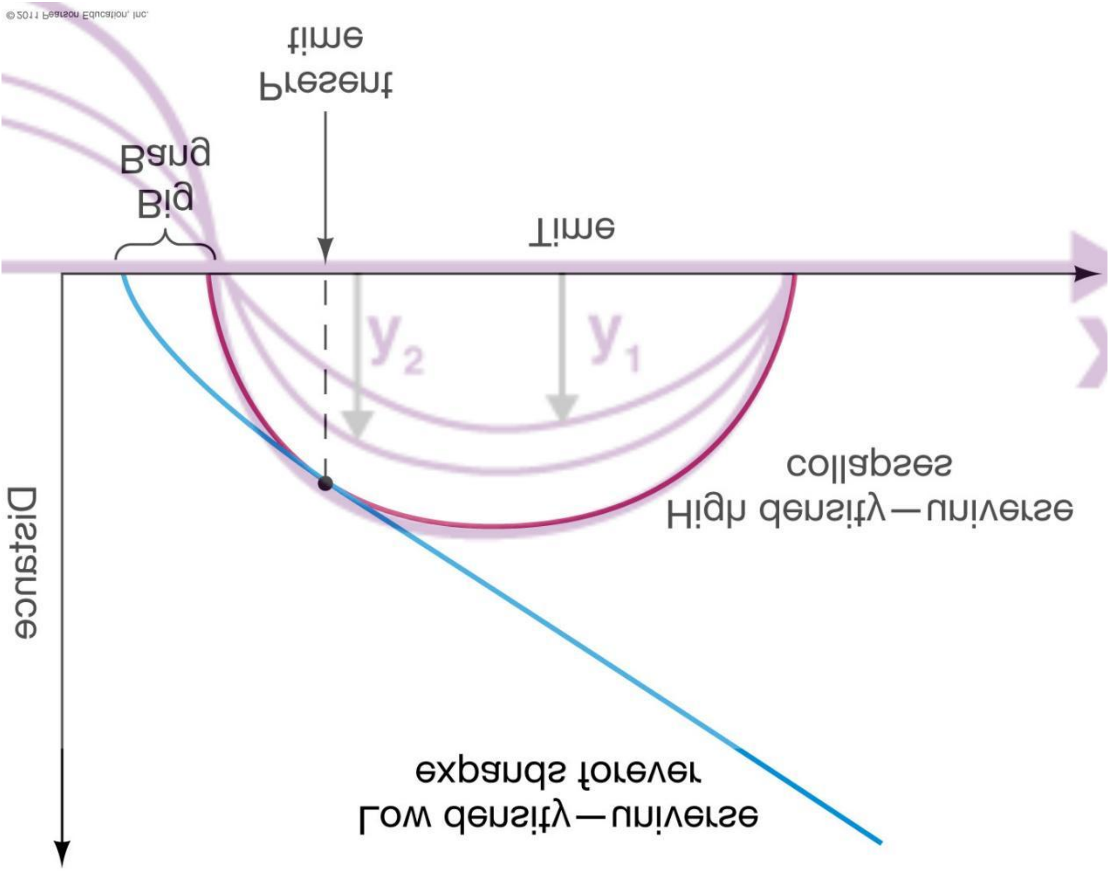

Super imposed graphs

This may mean the universe will eventually collapse if the two above graphs are related. It may also mean that before the big bang there was another big bang and thereafter the universe expanded and contracted up to the next big bang. When the universe contracts again it may create another big bang and the waves keep repeating much like the superposition of waves graph above.

https://www.nature.com/articles/417529a

Feshbach resonance bound-state energy and scattering length.

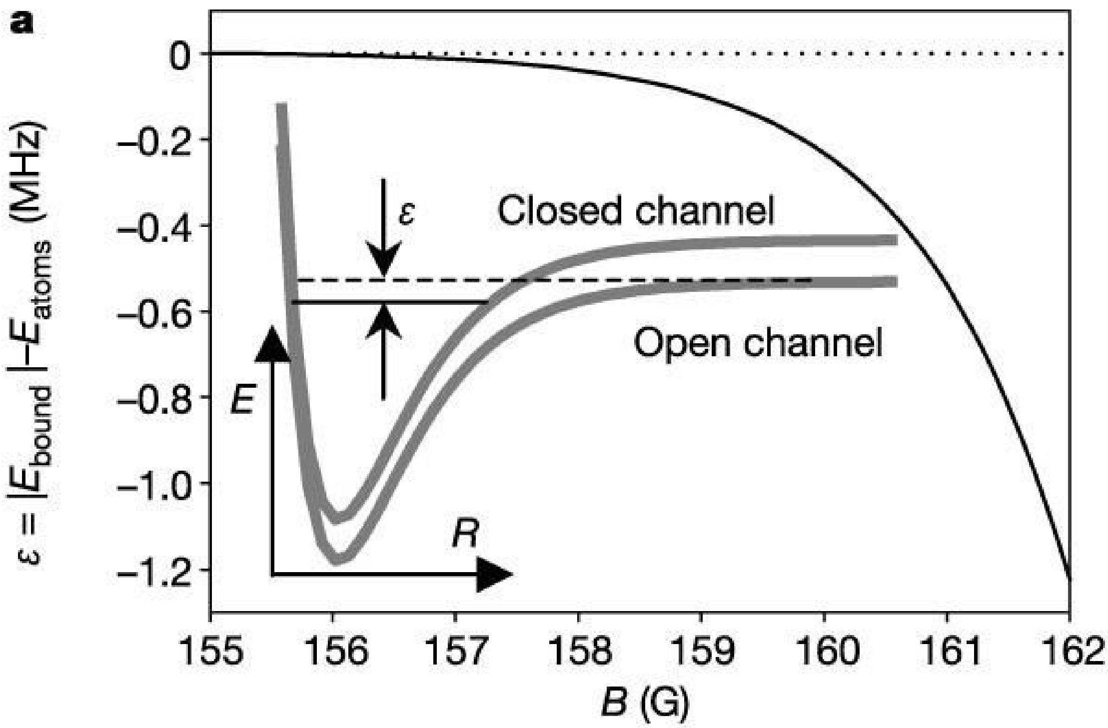

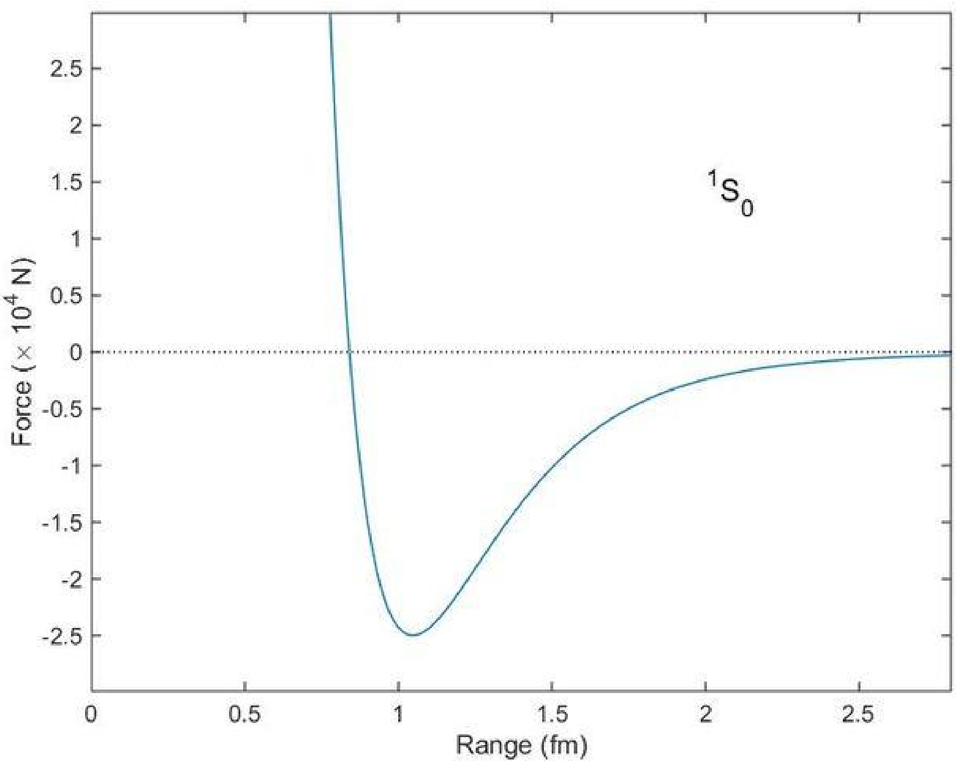

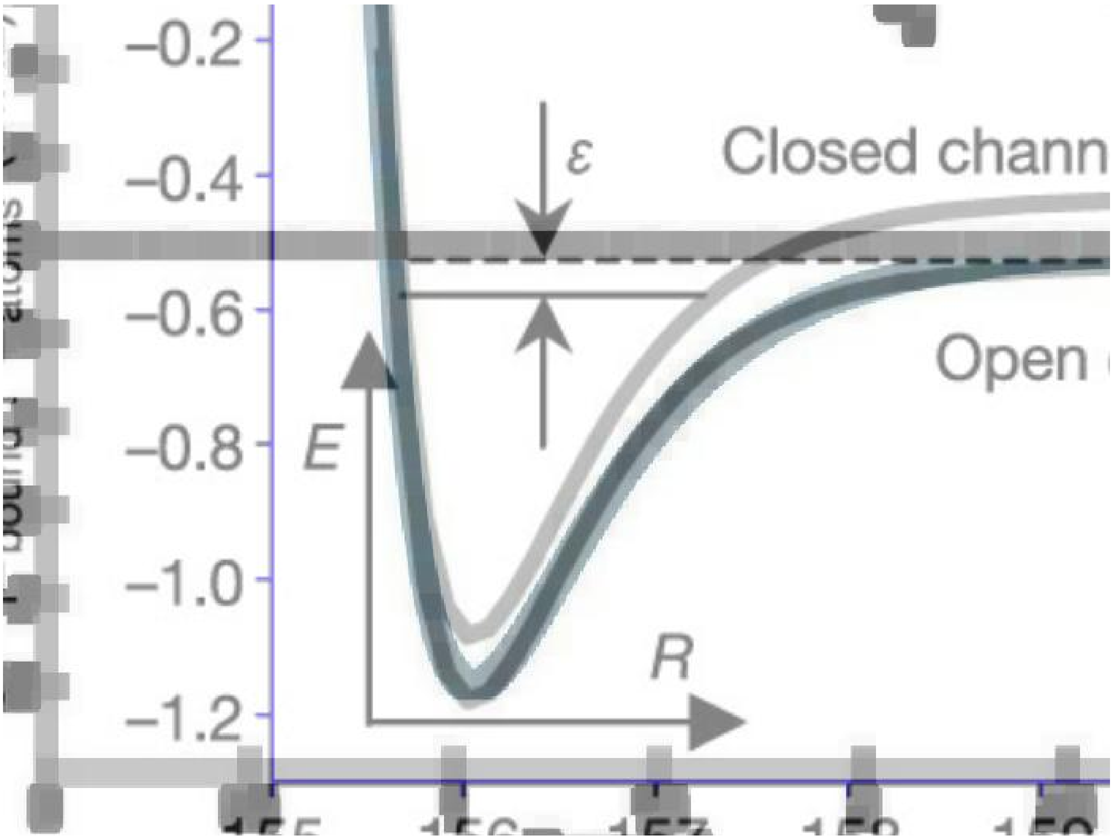

Super imposed graphs

Discussion:

Quantum mechanics behavior describes Macro phenomena such as macro cosmic phenomena, or Macro phenomena describes Quantum mechanic behavior, or both. Additionally, One Quantum mechanics system may also describe the behaviour of another quantum system.

These findings may further re-validate the observational data made by scientists such as the CMB graph and many other graphs of scientific phenomena. Model simulations that are graphed may be deemed correct if they have a similar shape, such as black hole physics as one example. We can use this discovery to fill in missing data of observational data that have graphs with partly similar shapes to wave functions or probability distributions of a quantum system. Furthermore, models may be created using computers to simulate a macro or quantum phenomenon and the output may be compared to an atoms wave function of probability distribution, and if the shapes are the same the model may be correct, otherwise they can be denied. One example of such a model may be of the evolution of the universe. Quantum computers may also be designed using the knowledge of this discovery. Current graphs that are similar in shape to a hydrogen atom's graph may also be made more precise due to uncertainties or measurement errors. Quantum gravity is another answer that may be discovered through the use of this discovery. There is the opportunity to find new relations between quantum graphs or macro graphs with other quantum systems or macro systems not shown in this paper which may lead to further discoveries. Furthermore, another atom's wave function or probability distribution may have an intimate relationship with other quantum or macro systems that are in or not in this paper. And lastly, new discoveries we cant even fathom right now could be made. I encourage the science community to advance humanity and make new discoveries.

Since the hydrogen atom is intimately related to macro phenomenon, it may be possible that the wave function and or the probability distribution of a single proton may also be related to macro phenomenon, hopefully for the singularity of a black hole, as one example. There are issues with determining such a wave function or probability distribution since the electron and proton results in a useful radius to generate a wave function. However if we find a way to isolate the proton and see how it deviates from the isolated location with each measurement, and account for that isolation, perhaps it may be possible. I do not know how such an experiment may occur but perhaps the following guesses may work. In one example, a magnetic field may be used to isolate the proton. In another example a qubit may be used where it is in a superposition, and the position is measured. Other examples may include using molecular hydrogen and putting one atom or both in a superposition. Another way may be to use quantum entanglement. If this measurement is possible, it may also be of use as a qubit. However these are just examples and may not work. I urge the science community to make new discoveries based on anything related to this paper. This may be an early scientific field and those who accept this discovery early and put in the effort to find something new may go down in history as a great scientist.

I have named this discovery Harsymmetry. Har means all/everything in Punjabi. It's also an abbreviation for Hydrogen Atom Radius. And Symmetry refers to the symmetries between the super imposed graphs.

References:

https://www.researchgate.net/figure/9-a-The-electronic-radial-wave-function-Rr-for-a-hydrogen-atom-b-The-probability_fig19_343017500
Hydrogen graphs used in analysis:
The electronic radial wave function R(r) for a hydrogen atom and the probability density for finding the electrons í µí± 2 í µí± (í µí±) 2 for a hydrogen atom (Adopted from ref. http://staff.mbi-berlin.de/hertel/physik3/chapter8/8.3html/01.htm)

https://www.scirp.org/html/11-7501495_40053.htm
Gravitational Force between the Black Hole & Light Particle in AGN

https://sci.esa.int/web/planck/-/51605-planck-s-gravitational-lensing-power-spectrum
Gravitational lensing power spectrum obtained from Planck data

https://iopscience.iop.org/article/10.1088/0004-637X/741/2/103
THE MASS DISTRIBUTION OF STELLAR-MASS BLACK HOLES

https://ned.ipac.caltech.edu/level5/Sept16/Bertone/Bertone4.html
The rotation curves for the galaxies M31, M101, and M81 (solid lines) obtained by Roberts and Rots in 1973. The rotation curve of the Milky Way Galaxy was included by the authors for comparison. From Ref. [260].

https://www.cosmos.esa.int/web/gaia/iow_20200716
Milky way rotation curve

http://roperld.com/science/GeneralRelativityMath.pdf
General Relativity Mathematics

https://www.researchgate.net/figure/Probability-distribution-of-galaxy-clusters-in-various-red-shift-ranges_fig3_363402503

Probability distribution of galaxy clusters in various red-shift ranges

https://en.wikipedia.org/wiki/Gravitational_microlensing
A typical microlensing light curve.

https://www.researchgate.net/figure/COBE-measurements-43-of-the-CMB-spectrum-error-bars-are-multiplied-by-200-in_fig1_51940305
COBE measurements [43] of the CMB spectrum (error bars are multiplied by 200), in agreement with a black-body spectrum of temperature T = 2.725K.

http://websites.umich.edu/~lowbrows/reflections/2006/dsnyder.19.html
If we plot the number of stars versus the energy with a histogram, we find a Maxwell-Boltzman distribution (Maxwell-Boltzman distributions are commonly found in large collections of interacting objects).

https://www.researchgate.net/figure/The-total-imposed-on-a-photon-during-its-motion-around-the-black-hole-versus-the_fig6_348739685
The total imposed on a photon during its motion around the black hole versus the radius˜rradius˜ radius˜r for different values of angular momentum. The other constants are taken as˜Mas˜ as˜M ≡ M/α = 2.5, α = 0.1, and b = 10.

https://link.springer.com/article/10.1140/epjc/s10052-019-6871-8/figures/1
Analysis of black hole thermodynamics with a new higher order generalized uncertainty principle

https://www.ligo.org/science/Publication-S5S6RD/index.php
RINGING OF THE COSMIC BELLS: A SEARCH FOR BLACK HOLE VIBRATIONS
We analyzed data from LIGO's fifth and sixth science runs (S5 and S6) and Virgo's science runs 2 and 3 (VSR2/3). In order to gauge the sensitivity of our search to GWs from perturbed IMBHs, we can plot the ringdown horizon distance as a function of black hole mass, for example for the LIGO detectors (H1, H2, and L1) during S5 as shown above. Horizon distances are comparable for data from S6-VSR2/3. The horizon distance shown here is the maximum distance to which we could see a perturbed black hole with a signal-to-noise ratio of 8.

https://iopscience.iop.org/article/10.3847/1538-4357/aab719
Distributions of nearest neighbor distances for gas-rich TF (orange) and NTF (blue) galaxies. Panel (a) shows the two distributions, whose difference is not statistically significant. These populations are further divided into galaxies whose nearest neighbors are within the same groups (b) and galaxies with neighbors outside of their groups (c).

https://astronomy.com/magazine/ask-astro/2014/04/remnant-radiation
The cosmic microwave background's “black body” curve

https://www.gw-openscience.org/s/events/GW150914/GW150914.html
Data release for event GW150914

https://phy.princeton.edu/sites/g/files/toruqf2261/files/resource-links/jacobson_jp1.pdf
Empirical velocity distributions for metal-poor stars in the RAVE-TGAS halo

https://www.researchgate.net/figure/The-probability-distribution-of-the-number-of-star-nearest-neighbors-for-a-r-s-s-3-s_fig2_255765312
The probability distribution of the number of (star) nearest- neighbors for (a) r s s 3 s 1⁄4 0.1 and (b) r s s 3 s 1⁄4 0.2 as the number of chain

https://www.researchgate.net/figure/Chain-mediated-effective-star-star-potential-as-obtained-by-inversion-of-the-OZ-equation_fig4_255765312
Chain-mediated effective star–star potential as obtained by inversion of the OZ equation in the limit r s s 3 s / 0 (see Ref. 27).

https://www.researchgate.net/figure/Various-cosmic-ray-source-supernova-remnants-distributions-are-available-in-the_fig10_258539610
Various cosmic ray source (supernova remnants) distributions are available in the literature. They are plotted here as a function of the Galactocentric distance r.

https://briankoberlein.com/blog/seeing-red/
Distribution of galaxies. The solid line of random distribution matches observation. The dotted lines of ejected quasars does not.

https://ned.ipac.caltech.edu/level5/Sept02/Saslaw/Saslaw1_4.html
The unnormalized frequency distribution of Hubble's galaxy counts compared to a random Gaussian distribution, after Bok (1934). The inset shows a recent fit of Bok's points to the distribution of Equation 27.24.

https://link.springer.com/article/10.1140/epjc/s10052-020-08623-2
Charged particle motion around non-singular black holes in conformal gravity in the presence of external magnetic field

https://www.zora.uzh.ch/id/eprint/163632/1/20070192.pdf

https://www.researchgate.net/figure/Potential-energy-and-total-energy-of-the-Keplerian-orbit-The-two-line-curves-show-the_fig1_344692919
Potential energy and total energy of the Keplerian orbit. The two line curves show the potential energy of Eq. (6) with and without the expansion term. The total energy of the Keplerian orbit crosses the bottom of the potential at r = r K .

https://www.researchgate.net/figure/The-effective-potential-V-m-of-an-extreme-Kerr-black-hole-for-a-test-particle-with-a_fig30_51933647
The effective potential V/μ of an extreme Kerr black hole for a test particle with a fixed orbital angular momentum as function of r/M.

https://www.semanticscholar.org/paper/Accelerated-expansion-of-the-Universe-in-the-of-Rezaei/e3ca26244fbf1deeaa0261761f0d91cf799307f8
Accelerated expansion of the Universe in the presence of dark matter pressure

https://www.gw-openscience.org/s/events/GW150914/GW150914.html
Data release for event GW150914

https://cds.cern.ch/record/2729754/plots
Supernova Neutrino Burst Detection with the Deep Underground Neutrino Experiment

https://iopscience.iop.org/article/10.1086/498208/pdf
Rotation curve of ngc 4448

https://www.researchgate.net/figure/Redshift-distribution-of-2MRS-galaxies-Blue-histogram-same-dN-ds-as-in-Fig-1-Curves_fig3_221666162
Redshift distribution of 2MRS galaxies. Blue histogram: same dN/ds as in Fig. 1. Curves: dN/ds predicted from different LF estimators. Black, continuous : Φ Sch. Red, continuos: Φ Spl. Black, dashed Φ V .

https://www.researchgate.net/figure/Normalized-redshift-distribution-of-GRBs-detectable-with-Swift-ie-with-observed_fig1_51962876
Normalized redshift distribution of GRBs detectable with Swift , i.e. with observed photon flux in excess to P lim = 0 . 4 ph s − 1 cm − 2 . The data show the observed redshift distribution

https://link.springer.com/article/10.1140/epjc/s10052-019-6630-x
Constraints on the matter density parameter in the flat DGP model, which are obtained from the lens redshift distribution of current SGL systems with and without the redshift evolution of lensing galaxies. Fitting results from recent observational Hubble parameter data (OHD) are also added for comparison
https://www.researchgate.net/figure/Observed-redshift-distribution-of-335-galaxy-clusters-in-the-ISCS-The-curve-a-fit-to_fig1_1922486
Observed redshift distribution of 335 galaxy clusters in the ISCS. The curve, a fit to the distribution, is used in the clustering analysis in §4.

https://www.americanscientist.org/article/why-do-galaxies-start-out-as-cosmic-pickles

https://indico.ictp.it/event/a04193/session/15/contribution/10/material/0/0.pdf
The power in individual modes is Rayleigh distributed around the mean
DISTRIBUTION OF MODE AMPLITUDES RELATIVE TO THE MEAN

https://www.physics.mcgill.ca/~soudal/docs/SNEWS_CASCA_poster.pdf
Neutrino energy MEV vs Event rate per 0.5 MEV

https://iopscience.iop.org/article/10.3847/1538-4357/abb9a6

Probing the Nature of High-redshift Weak Emission Line Quasars: A Young Quasar with a Starburst Host Galaxy

https://iopscience.iop.org/article/10.3847/1538-4357/aaec74
Photometric and Spectroscopic Properties of Type Ia Supernova 2018oh with Early Excess Emission from the *Kepler 2* Observations

https://www.nature.com/articles/s41550-019-0858-0
observational properties of thermonuclear supernovae

https://www.science.org/doi/10.1126/science.1075631
Age Estimates of Globular Clusters in the Milky Way: Constraints on Cosmology

https://arxiv.org/pdf/2110.13070.pdf
Spherical timelike orbits around Kerr black holes

https://www.semanticscholar.org/paper/Hawking-radiation-of-five-dimensional-charged-black-Miao-Xu/ee3d5dad12102723eecea76ff22ffb71828ce3eb

Hawking radiation of five-dimensional charged black holes with scalar fields

Figure 2: (Top) Plots of the power spectrum dE(ω)/(dtdω) with respect to frequency ω at l = 1, e = 1, and rh = 2 for q = −10,−5, and 8, respectively, from left to right. (Down) Plots of the power spectrum dE(ω)/(dtdω) with respect to frequency ω at l = 1, q = 1, and rh = 2 for e = 0, 2.8, and 3.5, respectively, from left to right.

https://www.researchgate.net/figure/Radial-distribution-in-the-Galactic-plane-of-the-CR-source-models-employed-in-this-work_fig1_316728846
Radial distribution in the Galactic plane of the CR source models employed in this work. In black, distributions from Ackermann et al. (2012): the pulsars (PSRs) distribution by Lorimer et al. (2006) used in the Sample Model, the alternative PSRs distribution by Yusifov & Küçük (2004), the OB stars distribution from Bronfman et al. (2000), and the SNRs distribution from Case & Bhattacharya (1998). In red the source models in the inner Galaxy introduced in our work: sources in the bulge (azimuthal average) following the distribution of the old stellar population as in model B from Robin et al. (2012), and sources in the central molecular zone (CMZ) following the distribution of molecular gas fromFerrì ere et al. (2007). The source distributions are independently normalized for display.

https://arxiv.org/pdf/1808.05114.pdf
A quantitative analysis of systematic differences in positions and proper motions of Gaia DR2 with respect to VLBI

https://royalsocietypublishing.org/doi/10.1098/rsta.2016.0271
The mechanism(s) of core-collapse supernovae

https://link.springer.com/article/10.1140/epjc/s10052-020-7692-5
Quasi-periodic oscillations around Kerr-MOG black holes

https://www.google.com/url?sa=i&url=https%3A%2F%2Fwww.preprints.org%2Fmanuscript%2F202112.0239%2Fv1%2Fdownload&psig=AOvVaw2Xb7Ik8c9kZriRImRq8eNe&ust=1664876952994000&source=images&cd=vfe&ved=2ahUKEwjrvqWM5MP6AhVYMjQIHV2zDQEQjRx6BAgAEAs

Figure 1. The Yukawa-like potential, complementary contribution to the inverse-square law, in
comoving scale, at several astronomical ranges (Own source).

https://digital.csic.es/bitstream/10261/269350/1/earthmatter.pdf
EARTH-STOPPING OF MILLICHARGED DARK MATTER

https://physicstoday.scitation.org/doi/10.1063/1.3120896
Introducing the black hole

https://www.researchgate.net/figure/Maxwellian-velocity-distribution-fg-of-the-collisions-velocities-of-the-aggregates_fig12_252340625
Maxwellian velocity distribution f(g) of the collisions velocities of the aggregates. Note, impact speeds of the range of mm s À1 up to cm s À1 are expected in Saturn's rings.

https://arxiv.org/pdf/1801.00133.pdf
A Model of the Collapse and Evaporation of Charged Black Holes
Figure 3: The plot of Hawking temperature against a0 − e0. All the units are Planck units.
Thermal behaviour of the matter-wave emission.

https://www.nature.com/articles/s41567-019-0537-1

https://www.researchgate.net/figure/QFI-in-the-estimation-of-the-Unruh-temperature-T-as-a-function-of-the-energy-gap-O-for_fig1_268876335
QFI in the estimation of the Unruh temperature T as a function of the energy gap Ω for different interaction time Δ. The parameters related to the effective coupling parameter are fixed to satisfy . They are fixed with and κ = 0.02, respectively. The initial state parameter is given by θ = π/4 and the acceleration parameter is fixed with a = 0.4π.

https://byjus.com/jee/superposition-of-waves/
What is Superposition of Waves

https://www.khanacademy.org/science/physics/thermodynamics/temp-kinetic-theory-ideal-gas-law/a/what-is-the-maxwell-boltzmann-distribution

https://www.researchgate.net/figure/This-graph-shows-the-current-mass-density-of-black-holes-as-a-function-of-their-initial_fig7_235497085
This graph shows the current mass density of black holes as a function of their initial mass mi. ρ0(m0) is the current number density of black holes of mass m0, so ρ0 = ρi (a 3 i /a 3 0). Because, for all practical purposes, m0 = mi, the area under the curve is the present matter density due to LQBH. If that density is equal to 0.22ρcrit, the LQBH will account for all dark matter. From

this graph, we see that at present times, LQBH mass density is entirely dominated by black holes which had an initial mass of about 10 −5 mP. In this graph we have used β = 4 (the graph is not very sensitive to this choice) and Teq = 13% × 10 15 GeV (the numerical values of the graph vertical axis are sensitive to this value but location of the peak and the general shape of the graph are not).

https://digitalcommons.lsu.edu/cgi/viewcontent.cgi?article=3761&context=physics_astronomy_pubs
Anomalies In The Cosmic Micr Anomalies In The Cosmic Microwave Background And Their Non- ound And Their NonGaussian Origin In Loop Quantum Cosmology

https://www.nature.com/articles/s42005-019-0255-0
Searching for dark photon dark matter in LIGO O1 data

https://phy.princeton.edu/sites/g/files/toruqf2261/files/resource-links/jacobson_jp1.pdf
Velocity Dependence of Dark Matter Electron Scattering
Dark matter velocity distributions f(|v|) in the heliocentric frame: [Fe/H] < −1.8 distribution (blue) and Standard Halo Model (yellow). (right) The function g(vmin) is plotted on a logarithmic scale with respect to minimum scattering velocity, using both velocity distributions

https://www.researchgate.net/figure/A-5800-K-Planck-distribution-function-divided-into-equal-100-nm-wavelength-intervals_fig2_236003842
A 5800 K Planck distribution function divided into equal 100 nm wavelength intervals.

https://link.springer.com/article/10.1007/s12043-019-1820-5
Radius of the proton

https://en.wikibooks.org/wiki/A-level_Physics_(Advancing_Physics)/Gravitational_Fields/Worked_Solutions
gravitational field strength against distance

https://iopscience.iop.org/article/10.1088/1402-4896/ab34c2

https://www.nature.com/articles/417529a
Feshbach resonance bound-state energy and scattering length.

https://www.scielo.br/j/bjp/a/t3fFWtyg4MHpmQTpxCbW6sD/?lang=en
Bose-Einstein condensation in a constant magnetic field

https://iopscience.iop.org/article/10.1088/1402-4896/ab34c2
Nonlinear oscillations of ultra-cold atomic clouds in a magneto-optical trap

https://iopscience.iop.org/article/10.1088/1361-6455/abd2d1
Absorption spectroscopy of the atomic beam under a 30° angle at the exit of the Zeeman slower. The resulting spectrum shows the longitudinal velocity

distribution and the effect of the slowing laser beam. Atoms exiting the oven with a velocity below $v_c \approx 390$ m s^{-1} are slowed down to below 50 m s^{-1}. The frequency axis is calibrated using a simultaneous spectroscopy measurement under an axis perpendicular to the atomic beam. The dashed curve is a fit to the thermal velocity distribution by a Maxwell–Boltzmann function at T_{oven} = 450 °C.

https://www.pnas.org/doi/10.1073/pnas.2017646117
The pressure as a function of specific volume at temperatures of 0.1 (crosses), 0.2 (squares), 0.32 (circles), 0.4 (stars), 0.5 (diamonds). This serves as a tool for detecting coexistence between two phases of different densities, as explained in the text. This particular result is for LJ boson 4He. (Inset) Same as the main graph but with a smaller PP *scale and only* T=0.32T=0.32*. Different symbols distinguish the superfluid phase (open), the normal phase (solid black), and the gas phase (gray).*

https://www.mdpi.com/2571-712X/2/2/19
The dependence of a quantity $\beta^{-1}(\bar{\omega})$ on the dimensionless frequency. As calculations show, in the frequency range under consideration (see table) there are only eight values of β^{-1} (red points), for which the quantization conditions (45) and (46) are satisfied. The blue dots denote such states for which the quantization conditions are not satisfied.

https://study.com/academy/lesson/newton-s-law-of-cooling.html
The plot of the temperature difference between the body and the surroundings with time gives the law of cooling graph.

https://chem.libretexts.org/Bookshelves/Physical_and_Theoretical_Chemistry_Textbook_Maps/Physical_Chemistry_(LibreTexts)/01%3A_The_Dawn_of_the_Quantum_Theory/1.01%3A_Blackbody_Radiation_Cannot_Be_Explained_Classically
Graphic representation of spectral distribution of blackbody radiation at different temperatures. The Stefan-Boltzmann's Law is observed as the increase in the emission amplitude with increasing temperature and the Wien's Displacement Law is observed as the shift to smaller wavelength with increasing temperature. (CC-BY 4.0; OpenStax)

https://www.semanticscholar.org/paper/Study-of-variation-of-temperature-of-black-holes-to-Mehta-Prasad/32908f5d6c7495fc2cabe7a4ce078c0b4d9671a9
Graph plotted between mass of different test of black holes and variation of temp. w. r. t. mass in XRBs.

https://link.springer.com/article/10.1140/epjc/s10052-015-3428-3
Electromagnetic fluxes from accretion disks gravitating around compact general relativistic objects, having different equations of state, with mass M=1.8M⊙M=1.8M⊙, and rotating at an angular velocity of $\Omega=5\times10^3 s^{-1}$

https://link.springer.com/article/10.1140/epjc/s10052-015-3636-x

Unfolded normalised distribution of the mass of C/AC/A R=1.2R=1.2 jets with 300<pT<400 GeV300<pT<400 GeV a before and b after splitting and filtering in an inclusive jet sample without pile-up (number of primary vertices NPV=1NPV=1). From [53], used under CC BY 4.0 and unchanged from original

https://www.researchgate.net/figure/Relative-velocity-distribution-eq-49-for-an-NFW-dark-matter-halo-only-The-dotted_fig8_242331467
Relative velocity distribution, eq. (4.9), for an NFW dark matter halo only. The dotted lines show a Maxwell-Boltzmann distribution with the same velocity dispersion: σ = 51.8km/s, 110.1km/s, 163.2km/s for r = 0.1kpc, 1kpc, 10kpc.

https://www.researchgate.net/figure/Radial-probability-density-distribution-of-interplanetary-matter-Upper-panel-a-is-the_fig1_253003364
Radial probability density distribution of interplanetary matter. Upper panel a) is the distribution of H with 3/4 of the nebular mass. Giant planets and the center of Kuiper Belt are all at the wave crests. Terrestrial planets are all at the first wave. Bottom panel b) is the distribution of He with 1/4 of the nebular mass and the first wave of H. Each terrestrial planet lies at a separate wave of He. It is interesting that the Kuiper Belt and Asteroid Belt lie in the sixth wave of H and He, and the widths of belts are consistent with wavelengths, respectively.

https://link.springer.com/article/10.1140/epjc/s10052-018-6273-3
Cascade analysis: best-fit energy distribution for the signal hypothesis (components stacked to illustrate the dark matter component), with the best fit parameters listed in Table 2. The fit is performed on un-binned data, but for visualization purposes a binning is applied in the figure

https://www.mdpi.com/2218-1997/7/8/264/htm
Figure 1. The distribution function f0(y)=n(y;∞).
It is remarkable that for y≪1

f0(y)∝1y12,

(76)
in striking contrast to the thermal Fermi–Dirac distribution function. The enhancement for small *y* indicates that this is a cold dark matter species.